

MODEL DEVELOPMENT FOR EVALUATING REMEDIATION OF  
CONTAMINATED SEDIMENTS: PCBs AND PBDEs AS CASES FOR  
HALOGENATED HYDROPHOBIC ORGANICS

A THESIS SUBMITTED TO  
THE GRADUATE SCHOOL OF NATURAL AND APPLIED SCIENCES  
OF  
MIDDLE EAST TECHNICAL UNIVERSITY

BY

FİLİZ KARAKAŞ

IN PARTIAL FULFILLMENT OF THE REQUIREMENTS  
FOR  
THE DEGREE OF DOCTOR OF PHILOSOPHY  
IN  
ENVIRONMENTAL ENGINEERING

MAY 2016



Approval of the thesis:

**MODEL DEVELOPMENT FOR EVALUATING REMEDIATION OF  
CONTAMINATED SEDIMENTS: PCBs AND PBDEs AS CASES FOR  
HALOGENATED HYDROPHOBIC ORGANICS**

submitted by **FİLİZ KARAKAŞ** in partial fulfillment of the requirements for the degree of **Doctor of Philosophy in Environmental Engineering Department, Middle East Technical University** by,

Prof. Dr. Gülbin Dural Ünver  
Dean, Graduate School of **Natural and Applied Sciences** \_\_\_\_\_

Prof. Dr. Kahraman Ünlü  
Head of Department, **Environmental Engineering** \_\_\_\_\_

Prof. Dr. İpek İmamoğlu  
Supervisor, **Environmental Engineering Dept., METU** \_\_\_\_\_

**Examining Committee Members:**

Assoc. Prof. Dr. Emre Alp  
Environmental Engineering Dept., METU \_\_\_\_\_

Prof. Dr. İpek İmamoğlu  
Environmental Engineering Dept., METU \_\_\_\_\_

Prof. Dr. Kevin R. Sowers  
Dept. of Marine Biotech. University of Maryland, BC \_\_\_\_\_

Prof. Dr. Ayşegül Aksoy  
Environmental Engineering Dept., METU \_\_\_\_\_

Assoc. Prof. Dr. Kadir Gedik  
Environmental Engineering Dept., Akdeniz Univ. \_\_\_\_\_

**Date:** \_\_\_\_\_

**I hereby declare that all information in this document has been obtained and presented in accordance with academic rules and ethical conduct. I also declare that, as required by these rules and conduct, I have fully cited and referenced all material and results that are not original to this work.**

Name, Last Name : FİLİZ KARAKAŞ

Signature :



## ABSTRACT

### MODEL DEVELOPMENT FOR EVALUATING REMEDIATION OF CONTAMINATED SEDIMENTS: PCBs AND PBDEs AS CASES FOR HALOGENATED HYDROPHOBIC ORGANICS

Karakaş, Filiz

Ph.D., Department of Environmental Engineering

Supervisor: Prof Dr. İpek İmamoğlu

May 2016, 349 pages

Understanding fate and transport (F&T) of halogenated hydrophobic organic compounds (HOCs) in sediments is a major concern and is imperative for their sound environmental management. This study aims to model the F&T of HOCs in sediments as individual compounds, and by taking into account anaerobic dehalogenation (AD). For this purpose, F&T of hydrophobic pollutant (FTHP) model is developed. As distinct from the literature, this model predicts future concentration of HOCs both as individual compounds and as total, by taking into account AD, as well as other relevant F&T mechanisms. AD rate constants ( $k_m$ ) of pathways are estimated by modifying a previously developed model as Anaerobic Dehalogenation Model. The range of  $k_m$  for PCBs and PBDEs estimated using laboratory studies of Baltimore Harbor contaminated sediments, USA, and of contaminated soil from Guangdong province, China, are between  $0.0001 - 0.129 \text{ d}^{-1}$  and  $0.001 - 0.024 \text{ d}^{-1}$ , respectively. The median of estimated  $k_m$  are found to be comparable to the few available rate constants published in the literature.

The FTHP model is applied to sediments of Lake Michigan and San Francisco Bay, USA, contaminated by PCBs and PBDEs, respectively. FTHP model calibration, validation, sensitivity and uncertainty analyses are performed for most of the congeners with satisfactory results. Goodness of fit results of model calibration is found to be comparable or better than those of similar models in the literature. For PCBs, future projection scenarios indicate reduction of toxicity – and the model is able to pinpoint which scenarios would better reduce toxicity, as individual toxic congener concentrations can be modeled. Similarly, for PBDEs, the bioaccumulation potential of sediments is found to be decreased through bioaugmentation. Total contaminant concentrations, however, can only be reduced by dredging. On the other hand, predicting bioremediation with FTHP model enables the user to evaluate toxicity changes through the time course of bioremediation, as toxic congeners are produced/reduced via individual AD reactions. Overall, systematic identification and quantification of AD pathways coupled with congener specific modeling can aid remediation efforts such that congener specific monitoring/enhancement of bioremediation could be possible for sediment-bound HOCs.

**Keywords:** Hydrophobic organic pollutants, sediment, anaerobic dehalogenation rate constant, bioaugmentation, toxicity, fate and transport processes.

## ÖZ

### **KİRLENMİŞ SEDİMANLARIN TEMİZLENMESİNDE KULLANILMAK ÜZERE BİR MODEL GELİŞTİRİLMESİ: HALOJENLİ HİDROFOBİK KİMYASALLARA ÖRNEK OLARAK PCBLER VE PBDELER**

Karakaş, Filiz

Doktora, Çevre Mühendisliği Bölümü

Tez Yöneticisi : Prof. Dr. İpek İmamoğlu

Mayıs 2016, 349 sayfa

Hidrofobik organik kirleticilerin (HOKlar) taşınımı ve akıbetini anlamak çevre yönetimi açısından büyük önem taşımaktadır. Bu çalışma, HOKları ayrı ayrı bileşik olarak ve anaerobik dehalojenasyonunu da ele alarak sedimandaki taşınım ve akıbetlerini (F&T) belirleyen mekanizmalarını modellemeyi hedeflemektedir. Bu amaçla, hidrofobik kirletici taşınım ve akıbet (FTHP) modeli geliştirilmiştir. Literatürden farklı olarak bu model, ayrı ayrı bileşiklerin dehalojenasyon reaksiyonlarını, taşınım ve akıbetlerini belirleyen mekanizmalarla birlikte dikkate alarak her bir bileşiğin ve toplamlarının gelecekteki derişimlerini tahmin etmeyi hedeflemektedir. Anaerobik dehalojenasyon hız sabitlerini ( $k_m$ ) tahmin etmek için daha önce geliştirilen model modifiye edilerek Anaerobik Dehalojenasyon modeli geliştirilmiştir. Hız sabitleri  $0.0001 - 0.129 d^{-1}$  ve  $0.001 - 0.024 d^{-1}$  arasında olarak PCBlerle kirlenmiş Baltimore Limanı'ndan alınan laboratuvar sedimanları ve PBDElerle kirlenmiş Çin Guangdong'dan alınan toprak verileri ile tahmin edilmiştir. Bu değerlerin medyanlarının literatürdeki az sayıda çalışmada verilenlerle karşılaştırılabilir olduğu belirlenmiştir.

FTHP modeli PCBlerle kirlenmiş Michigan Gölü'ndeki ve PBDElerle kirlenmiş San Fransisco Körfezi'ndeki sedimanlara uygulanmıştır. Kalibrasyon, validasyon, duyarlılık ve belirsizlik analizleri modelin başarılı bir şekilde uygulandığını göstermiştir. Model kalibrasyonu uyum verileri literatürdeki benzer modellerle karşılaştırılabilir veya daha iyi bulunmuştur. Oluşturulan gelecekle ilgili senaryolarda, biyoaugmentasyon yöntemiyle toksisitenin azaldığı görülmüş – tekil toksik bileşiklerin derişimleri modellenebildiğinden, senaryolardan hangisinin daha iyi toksisite azalmasını sağlayacağı belirlenebilmiştir. Benzer şekilde PBDEler için, sediman biyobirikim potansiyelinin biyoaugmentasyon ile düşürülebileceği bulunmuştur. Ancak, toplam kirletici miktarı sadece sedimanın çıkarılması senaryosuyla gerçekleşebilir. Diğer yandan, biyoremediasyonun FTHP modeli ile toksik bileşiklerin tekil reaksiyonlarının ele alınarak tahmin edilmesi, iyileştirme sürecinde kullanıcının toksisite deęişimlerini zamana baęlı olarak deęerlendirebilmesini sağlamaktadır. Genel olarak anaerobik dehalojenasyon reaksiyonlarının sistematik olarak tanımlanması ve kantifiye edilmesi, ve de bu tip taşınım ve akıbet modellerinde kullanılması sedimanların temizlenmesine katkı sağlayabilir. Böylece, hidrofobik kirleticilerle kirlenmiş sedimanlar gözleme aşamalarında ve de biyoremediasyonun iyileştirilmesinde kullanılabilir.

**Anahtar Kelimeler:** Hidrofobik organik kirleticiler, Sediman, Anaerobik dehalojenasyon hız sabiti, Biyoaugmentasyon, Toksisite, Taşınım ve akıbet mekanizmaları.

*To My Family*

## ACKNOWLEDGEMENTS

I would like to thank firstly to my supervisor Prof. Dr. İpek İmamoglu for her advices, discussions, and positive attitude throughout this research. I would like to thank to my PhD Dissertation Monitoring Committee Members, Prof. Dr. Ayşegül Aksoy and Prof. Dr. Kevin Sowers for their comments and recommendations that greatly improved this research. I also thank to my other dissertation members Assoc. Prof. Dr. Kadir Gedik and Assoc. Prof. Dr. Emre Alp for their valuable recommendations.

I would like to thank to my friend, Hale Demirtepe for her friendship in challenging time. I am really going to miss our break time and discussions on scientific issues, life and how a feeling to be a PhD candidate. I would also like to express my thanks to my friend Ece Kendir and my office mates, Cansu Dönmezoğlu, Hazal Aksu and Debebe Fanta to feel me happy with their friendships. I would like to express my gratitude to Dr. Fadime Kara Murdoch for her help and support in my laboratory studies I worked in the projects in the first years of my PhD.

My deepest thanks go to my family, especially my parents, Döndü and Cafer Demircioğlu for her and his endless loves and warm hearts I always feel, and to my parent in-laws, Mehmet Ali and Yıldız Karakaş. Unfortunately, we did not have much time to spend with my mother in law, but I thank to her for growing such a kind and valuable man, my husband. My parents are always near me during the most challenging times. I specially thank to my older sister, Tevhide Demircioğlu who is the only person loving me like my mother and also to my little sister, Sevda Demircioğlu for her close friendship, enjoyable times we share, and her help throughout this research academically and commonly. They and my mother always helped me, by cooking meals, preparing my study area and cleaning my home for me. Another of my thanks goes to my sister, Figen Bozkurt, my older brother, Ersin

Demirciođlu and my brother Sercan Kargı for their loves with their smiling faces and warm hearths.

During this research, my two nephews were born, Jr. Cafer Demirciođlu and Ege Bozkurt. They are the gifts to me and they always put a smile on my face when I see them in these challenging times. I also feel happy by playing and spending time with three lovely kids I called “minikler”; Eren Özkan, Emre Anıl and İrem Özkan. I would like to thank deeply to my older brother Ahmet Anıl for sharing his life experience and giving advice about the life with his calm voice, and to my older sister Duygu Anıl for her friendship, enjoyable times we spent in zumba and guidance in academic life. I also want to thank to my older brother Celalettin Özkan and my older sister İlknur Özkan for their loves. I always think that I am very lucky to have such a big family.

Lastly, I am especially grateful to my husband, Kıvanç Karakaş for his endless love, support and patience. I owe him much more than words can express. He has always believed me and encouraged me to complete this thesis and make it the best one. We have progressed in science and art together. He presents me such a lovely life that is filled with his love. Thanks to God for letting me know him in my life.

## TABLE OF CONTENTS

ABSTRACT .....	v
ÖZ.....	vii
ACKNOWLEDGEMENTS .....	x
TABLE OF CONTENTS .....	xii
LIST OF TABLES .....	xvi
LIST OF FIGURES.....	xxi
CHAPTERS	
1. INTRODUCTION.....	1
2. LITERATURE REVIEW.....	7
2.1 HALOGENATED HYDROPHOBIC ORGANIC COMPOUNDS (HOCs).....	7
2.1.1 Polychlorinated Biphenyls (PCBs).....	8
2.1.2 Polybrominated Diphenyl Ethers (PBDEs).....	14
2.1.3 Toxicity Evaluations .....	19
2.2 FATE OF PCBs AND PBDEs IN THE ENVIRONMENT.....	20
2.2.1 Fate Mechanisms in the Environment.....	20
2.2.2 Fate of PCBs.....	32
2.2.3 Fate of PBDEs.....	33
2.3 MODELING .....	34
2.3.1 Fate and Transport Models.....	35
2.3.2 Models for Degradation Pathway Identification of PCBs and PBDEs ..	50
3. MATERIALS AND METHODS .....	55
3.1 DESCRIPTION OF TERMINOLOGY .....	56
3.2 ANAEROBIC DEHALOGENATION MODEL .....	58
3.2.1 Description of Model .....	58
3.2.2 Computer Program .....	64



3.2.3	Preparation of Dehalogenation Pathways as Input for ADM.....	76
3.3	FATE AND TRANSPORT (F&T) MODEL.....	77
3.3.1	Conceptual Model.....	77
3.3.2	Selection of A Model Equation.....	79
3.3.3	Model Assumptions.....	84
3.3.4	Description of the FTHP model.....	84
3.3.5	FTHP Model Computer Program.....	86
3.3.6	Estimation of Model Parameters.....	103
3.3.7	Model Stability and Accuracy.....	106
3.3.8	Model Calibration, Validation, Sensitivity and Uncertainty Analyses	108
3.4	PCB DATA.....	111
3.4.1	Microcosm PCB Data: Baltimore Harbor Sediments, USA.....	112
3.4.2	FTHP model PCB Data: Lake Michigan Sediments, USA.....	117
3.5	PBDE DATA.....	139
3.5.1	Laboratory PBDE Data: Contaminated Soil, China.....	139
3.5.2	Environmental PBDE Data: San Francisco Bay, USA.....	141
4.	VERIFICATION OF MODELS.....	157
4.1	ARTIFICIAL DATA SET.....	157
4.2	ADM VERIFICATION.....	161
4.2.1	Example Run.....	161
4.3	FTHP MODEL CODE VERIFICATION.....	165
4.3.1	Example Run.....	165
5.	ESTIMATION OF BIODEGRADATION RATE CONSTANTS OF PCB DECHLORINATION REACTIONS USING AN ANAEROBIC DEHALOGENATION MODEL.....	171
5.1	INTRODUCTION.....	171
5.2	METHODOLOGY.....	173
5.2.1	Baltimore Harbor (BH) Microcosm Data Set.....	173
5.2.2	Anaerobic Dehalogenation Model (ADM).....	174
5.3	RESULTS AND DISCUSSION.....	175

5.3.1	Analysis of ADM Results for All Dechlorination Activities .....	175
5.3.2	Evaluation of $k_m$ values in DA 18 .....	181
5.4	CONCLUSIONS .....	184
6.	PREDICTION OF BIODEGRADATION RATE CONSTANTS OF PBDE CONGENERS USING AN ANAEROBIC DEHALOGENATION MODEL .....	187
6.1	INTRODUCTION.....	187
6.2	METHODS AND MATERIALS.....	189
6.2.1	Soil Data Set.....	189
6.2.2	Anaerobic Dehalogenation Model (ADM) .....	189
6.3	RESULTS AND DISCUSSION.....	191
6.4	CONCLUSIONS .....	194
7.	MODELING BIODEGRADATION OF PCBS IN SEDIMENT CONSIDERING FATE AND TRANSPORT MECHANISMS .....	197
7.1	INTRODUCTION.....	197
7.2	METHODOLOGY.....	199
7.2.1	Fate and Transport of Hydrophobic Pollutant (FTHP) model .....	201
7.2.2	Lake Michigan (LM) Sediment Data Set .....	203
7.3	RESULTS AND DISCUSSIONS .....	206
7.3.1	Testing of the FTHP Model .....	206
7.3.2	FTHP Model Future Prediction Results .....	215
7.4	CONCLUSIONS .....	221
8.	MODELING BIODEGRADATION OF PBDES IN SEDIMENTS USING A FATE AND TRANSPORT MODEL.....	223
8.1	INTRODUCTION.....	223
8.2	METHODOLOGY.....	225
8.2.1	Fate and Transport of Hydrophobic Pollutant (FTHP) model .....	227
8.2.2	Environmental PBDE Data: San Francisco Bay, USA .....	229
8.3	RESULTS AND DISCUSSIONS .....	233
8.3.1	Testing of the FTHP Model .....	233
8.3.2	FTHP Model Future Prediction Results .....	241

8.4	CONCLUSIONS .....	246
9.	OVERVIEW .....	247
10.	RECOMMENDATIONS .....	251
11.	REFERENCES.....	253
APPENDICES		
APPENDIX A	LIST OF CONGENERS.....	269
APPENDIX B	LIST AND NAMES OF MOST COMMONLY STUDIED PBDE CONGENERS .....	271
APPENDIX C	MASS BALANCE EQUATIONS AND MECHANISMS OF THE MODELS REVIEWED IN THE LITERATURE .....	273
APPENDIX D	INPUT AND OUTPUT OF THE PATHWAY FUNCTION FOR PCBs AND PBDEs .....	279
APPENDIX E	RESULTS OF ADM FOR BH SEDIMENT MICROCOSMS CONTAMINATED BY PCBs .....	293
APPENDIX F	RESULTS OF FTHP MODEL FOR LAKE MICHIGAN SEDIMENTS CONTAMINATED BY PCBs.....	307
APPENDIX G	RESULTS OF FTHP MODEL FOR SAN FRANCISCO BAY SEDIMENTS CONTAMINATED BY PBDEs .....	327
	CURRICULUM VITAE .....	347

## LIST OF TABLES

### TABLES

Table 2.1 Physicochemical properties of Aroclor mixtures at 20-25°C (Mackay et al., 2006).....	12
Table 2.2 Physicochemical properties of PCB homologs at 20-25°C (Mackay et al., 2006).....	12
Table 2.3 Physicochemical properties of dioxin-like PCB congeners (WHO, 2003)	13
Table 2.4 Physicochemical properties of technical PBDE mixtures (ATSDR, 2004)	17
Table 2.5 Physicochemical properties of PBDE congeners(ATSDR, 2004) .....	18
Table 2.6 Toxic equivalency factors for coplanar and mono- and di- <i>ortho</i> -substituted PCBs.....	20
Table 2.7 Comparison of microbial dechlorination activities (Bedard, 2003) as tabulated by Bzdusek (2005).....	24
Table 2.8 Dechlorination activities and corresponding microorganism or strain (Sowers & May, 2013). .....	26
Table 2.9 Overview of PBDE debromination studies .....	28
Table 2.10 Models used in various media contaminated by halogenated compounds (e.g. PCBs, PBDEs, PCE, TCE).....	37
Table 2.11 Transformation Rate and Constant Estimations in WASP4 Model .....	49
Table 3.1 Amount of reaction estimated by ADM.....	62
Table 3.2 Concentration of congeners after reaction 1 and 2.....	63
Table 3.3 Descriptions of items used in ADM flow chart .....	69
Table 3.4 An overview of model equations in the literature .....	81
Table 3.5 Descriptions of items used in FTHP flow chart .....	90
Table 3.6 Input Parameters needed for the model.....	103
Table 3.7 Equation of Distribution Used for MC in uncertainty analysis.....	110

Table 3.8 IUPAC numbers of PCB congeners analyzed in microcosm sediments (Fagervold et al., 2007, 2011) .....	117
Table 3.9 History of PCB contamination in Lake Michigan Basin (Rossmann, 2006) .....	119
Table 3.10 Sediment samples collected from Segment 49 .....	123
Table 3.11 Concentration of individual PCB congeners in 10 sediment samples (ng/L) (USEPA, 2015) .....	126
Table 3.12 Descriptive statistics of PCB congener concentrations (ng/L) in the water column at the north region .....	131
Table 3.13 Descriptive statistics of PCB congener concentrations (ng/L) in the water column at the south region .....	132
Table 3.14 Descriptive statistics of TSS Data.....	133
Table 3.15 Volume and Area of Sediment Layer and Water Column (Rossmann, 2006) .....	134
Table 3.16 Water and sediment properties measured in LMMBP (Rossmann, 2006) .....	134
Table 3.17 Molecular weight, solubility and $K_{ow}$ of congeners (Mackay et al., 2006) .....	135
Table 3.18 Settling, Resuspension and Burial Velocities (Rossmann, 2006).....	137
Table 3.19 Molecular Diffusion Coefficient of Congeners (Schneider, 2005).....	137
Table 3.20 Molecular Diffusion used in the FTHP model.....	138
Table 3.21 Concentration of individual PBDE congeners in 9 sediment samples (ng/L) (SFEI, 2015).....	147
Table 3.22 Concentration of congeners in water column and in 9/13/2011 .....	149
Table 3.23 Descriptive statistics of TSS Data.....	150
Table 3.24 Depth and Area of Sediment Layer and Water Column .....	151
Table 3.25 Water and Sediment Properties.....	151
Table 3.26 Solubility and $K_{ow}$ of PBDE congeners (Mackay, 2006).....	152
Table 3.27 Molecular diffusion coefficient of PBDE congeners (Blauenstein, 2007) .....	155
Table 3.28 Molecular Diffusion used in the FTHP model.....	156

Table 4.1 Abundance of seven congeners in the original Aroclor 1260 and after dechlorination.....	158
Table 4.2 Doubly Flanked <i>para</i> Removal.....	158
Table 4.3 Abundance of All Coeluting Congeners After Dechlorination.....	160
Table 4.4 Model Input.....	161
Table 4.5 Initial and final concentration of coeluting congeners by the model and in the data set.....	162
Table 4.6 Calculation of $k_m$ values for Artificial data by excel.....	164
Table 4.7 Model $k_m$ results.....	164
Table 4.8 Model Input Information for numbers of congeners, paths and time.....	165
Table 4.9 Model Input Information for biodegradation rate constants.....	165
Table 4.10 Model Input Information.....	166
Table 4.11 Model Input Information belonging to water column, sediment layer and system properties.....	166
Table 4.12 Calculation of contaminant partitioning coefficients in the sediment (Kds).....	167
Table 4.13 Calculation of contaminant partitioning coefficients in the water (K <sub>dw</sub> ).....	167
Table 4.14 Calculation of fractions of contaminant (unitless).....	167
Table 4.15 Estimation of diffusion mass-transfer coefficient at the sediment-water interface.....	168
Table 4.16 Estimation of resuspension velocity ( $v_r$ ).....	168
Table 4.17 Calculations in biodegradation term.....	169
Table 5.1 Dechlorination activities and $k_m$ values estimated by ADM.....	179
Table 5.2 Goodness of fit results ( $R^2$ and $R^2_{\text{reac}}$ ) for each sample run for each time interval.....	180
Table 5.3 List of all dechlorination pathways for the best performing dechlorination activities, DA18, DA23, DA24 and DA25.....	181
Table 5.4 Comparison of $k_m$ values with the values in the literature.....	184
Table 6.1 DAs and $k_m$ values estimated by ADM.....	192
Table 6.2 Goodness of fit results ( $R^2$ and $R^2_{\text{reac}}$ ) for each sample run and each time interval.....	193

Table 6.3 Degradation rate constants of eight debromination pathways according to the DAs .....	194
Table 7.1 Concentration of individual PCB congeners in 10 sediment samples (ng/L) (USEPA, 2015) .....	205
Table 7.2 Results of the goodness of fit parameters for calibration and validation.	211
Table 7.3 Distribution of parameters assumed for uncertainty analysis .....	214
Table 7.4 RSD of Future Prediction Calculated for 1000 times in Uncertainty Analysis .....	214
Table 7.5 Future scenarios .....	216
Table 8.1 Concentration of individual PBDE congeners in 9 sediment samples (ng/L) (SFEI, 2015).....	231
Table 8.2 Maximum and median $k_m$ values of 8 pathways in corresponding Das by ADM .....	235
Table 8.3 Cases for use of $k_m$ values during calibration of FTHP model .....	236
Table 8.4 Results of the goodness of fit parameters for calibration and validation.	237
Table 8.5 Future scenarios .....	242
Table 8.6 $k_m$ values used for the other pathways which are not available ( $d^{-1}$ ) .....	243
Table A. 1 List of PCB congeners .....	269
Table A. 2 List of most commonly studied PBDE congeners (USEPA, 2010).....	270
Table B. 1 Technical flame-retardant (Penta- Octa- and Deca-PBDEs) compositions (% , w/w) (La Guardia et al., 2006) .....	271
Table C.1 Recovery Model (Boyer et al., 1994 and Ruiz et al., 2000).....	273
Table C.2 TOXIWASP Model (Ambrose et al., 1983).....	274
Table C.3 LM-2 Model .....	275
Table C.4 PMHR Model (Farley et al., 1999).....	276
Table C.5 WASP4 Model (Ambrose et al., 1988) .....	277
Table C.6 Mass Balance Equations for surface sediment layer .....	278
Table D.1 Input of the Pathway Function for PCBs .....	279
Table D.2 Output of the Pathway Function for PCBs.....	283
Table D.3 Input of the Pathway Function for PBDEs.....	289
Table D.4 Output of the Pathway Function for PBDEs .....	292
Table E.1 Numbers of samples and shuffles in each sample run by ADM .....	294

Table F.1 $k_m$ values estimated by ADM for DA18, DA25, DA19, DA13 and DA20 .....	307
Table F.2 Trials for calibration of PCB congeners in Lake Michigan sediment .....	310
Table F.3 Min, Max, Mean and Variance of 7 Parameters for Uncertainty Analysis .....	322
Table G.1 Trials for calibration of PBDE congeners in Lake Michigan sediment ..	328
Table G.2 Min, Max, Mean and Variance of 7 Parameters for Uncertainty Analysis .....	340
Table G.3 $k_m$ values for possible pathways used for the last scenario .....	345



## LIST OF FIGURES

### FIGURES

Figure 2.1 General PCB structure .....	8
Figure 2.2 General PBDE structure .....	14
Figure 2.3 Sediment zones and fate processes of the pollutant in the bed sediment (Allan & Stegemann, 2007) .....	22
Figure 3.1 Interrelationship between ADM and FTHP models .....	56
Figure 3.2 Description of ADM .....	65
Figure 3.3 An example dechlorination pathway, output of the <b>FindPathways</b> function A. Structural depiction, B. Depiction in the model.....	66
Figure 3.4 ADM Flowchart.....	68
Figure 3.5 Input File: Sample and Predicted Profiles .....	72
Figure 3.6 Input File: Pathways pertaining to each DA.....	73
Figure 3.7 Output File of ADM .....	74
Figure 3.8 Conceptual Model (HHOCs: Halogenated HOCs).....	78
Figure 3.9 Flowchart of the FTHP Model.....	89
Figure 3.10 Steps of FTHP model development and application .....	92
Figure 3.11 Input File-1 .....	96
Figure 3.12 Input File-2 .....	97
Figure 3.13 Input-3 for Calibration and Validation .....	98
Figure 3.14 Uncertainty File-1 for Values in Input file 1 .....	99
Figure 3.15 Uncertainty File-2 for Values in Input file 2 .....	100
Figure 3.16 Output File-Out1.....	101
Figure 3.17 Outputfile-Out2 for Calibration and Validation .....	102
Figure 3.18 Solid Mass Balance in Sediment .....	104
Figure 3.19 Uses of PCB Data Sets .....	111
Figure 3.20 BH Microcosm Data (Fagervold et al., 2007, 2011) .....	113

Figure 3.21 BH (SF1+DEH10) Microcosm Data (Fagervold et al., 2007, 2011)....	114
Figure 3.22 BH (o17+DF1) Microcosm Data (Fagervold et al., 2007, 2011) .....	115
Figure 3.23 BH (SF1+DEH10+o17+DF1) Microcosm Data (Fagervold et al., 2007, 2011).....	116
Figure 3.24 Segmentation of the water column (Left) and surficial sediments (Right) used in LM2-Toxic Model (Rossmann, 2006) .....	120
Figure 3.25 Distribution of total PCBs (ng/L) in 1994-1995 Lake Michigan water column (Left) and surficial sediments (Right) (Zhang, 2006, part1ch5) .....	121
Figure 3.26 Surface sediment samples collected in Segment 49 .....	122
Figure 3.27 Water column sampling locations in Segment 37 .....	124
Figure 3.28 Samples at South and North used for calibration and validation in segment 49, respectively.....	127
Figure 3.29 Time Variation of Total PCBs PCBs in Lake Michigan water column (ng/L) (a) between 1975 and 1995 (b) between 1986 and 1995 (Rossmann, 2006)	129
Figure 3.30 Distribution of Total Concentration of Congeners Through Time .....	130
Figure 3.31 TSS Concentration.....	133
Figure 3.32 Total PCB concentration versus depth in Lake Michigan - $\Sigma_{39}$ PCBs (USEPA, 2006).....	136
Figure 3.33 Molecular Diffusion vs. No of Cl on biphenyl structure .....	138
Figure 3.34 Uses of PBDE Data Sets .....	139
Figure 3.35 Microcosm PBDE data (Song et al., 2015).....	140
Figure 3.36 Segmentation (Oram et al., 2008a) .....	142
Figure 3.37 Distribution of BDE 47 (Left) and BDE209 (Right) (ng/g) in 2012 in San Francisco Bay Surficial Sediment (Sutton et. al, 2015) .....	144
Figure 3.38 Distribution of Total PBDEs (ng/g) between 2002-2014 in San Francisco Bay Surficial Sediment (Sutton et. al, 2015).....	144
Figure 3.39 Sampling Points of PBDEs in Surface Sediment and water column ....	145
Figure 3.40 TSS Concentration .....	150
Figure 3.41 Total PBDE Concentration in sediment from Adviso Wetland Core (Grenier and Davis, 2011) (Yee et al., 2011) .....	154
Figure 3.42 Molecular Diffusion vs. No of Br in diphenyl ether structure .....	156
Figure 4.1 Application of artificial anaerobic dechlorination on data set .....	159

Figure 4.2 Anaerobic dechlorination pathways depicted with coeluting congeners	160
Figure 4.3 Measured vs. ADM predicted data plot	162
Figure 4.4 Comparison of concentrations estimated by FTHP model in MatLAB and MS Excel	170
Figure 5.1 Distribution of $k_m$ values modeled by ADM for DA 18	182
Figure 7.1 FTHP model development for and application to Lake Michigan Sediments	200
Figure 7.2 PCB Conceptual Model	203
Figure 7.3 Samples at South and North used for calibration and validation in segment 49, respectively	204
Figure 7.4 FTHP model calibration plots (time vs. sediment PCB concentration)	209
Figure 7.5 PCB concentration in Lake Michigan surface sediment from PCB validation of the FTHP model	210
Figure 7.6 Future prediction concentrations in surface sediment	219
Figure 7.7 TEQ temporal changes in surface sediment	220
Figure 8.1 FTHP model development for and application to Lake Michigan Sediments	226
Figure 8.2 PBDE Conceptual Model	228
Figure 8.3 Surface sediment and water column sampling points for PBDE data used	230
Figure 8.4 PBDE concentration in San Francisco sediment from PBDE calibration of the FTHP model	238
Figure 8.5 PBDE concentration in San Francisco sediment from PBDE validation of the FTHP model	239
Figure 8.6 Possible pathways of debromination in the literature considering congeners measured in San Francisco Bay sediments	243
Figure 8.7 Future prediction concentrations in surface sediment	245
Figure E.1 Comparison of scatter plot of (first row) the PCB profiles of Data set 1.BH for days, $t_0$ vs. $t_{100}$ , $t_{100}$ vs. $t_{200}$ and $t_{200}$ vs. $t_{300}$ and (second row) prediction profiles at days 100, 200 and 300 for DA 18 (Activity of DEH10) by ADM	295
Figure E.2 Comparison of scatter plot of (first row) the PCB profiles of Data set 2.BH for days, $t_0$ vs. $t_{100}$ , $t_{100}$ vs. $t_{200}$ and $t_{200}$ vs. $t_{300}$ , (second row) prediction profiles	

at days 100 and 300 for DA 18 (Activity of DEH10) by ADM and (third row) prediction profiles at days 100, 200 and 300 for DA 23 (Activity of DEH10+SF1) by ADM.....	000296
Figure E.3 Comparison of scatter plot of (first row) the PCB profiles of Data set 3.BH for days , t0 vs. t100, t100 vs. t200 and t200 vs. t300, (second row) prediction profiles at days 100, 200 and 300 for DA 18 (Activity of DEH10) by ADM and (third row) prediction profiles at days 100, 200 and 300 for DA 24 (Activity of o17+DF1) by ADM.....	297
Figure E.4 Comparison of scatter plot of (first row) the PCB profiles of Data set 4.BH for days , t0 vs. t100, t100 vs. t200 and t200 vs. t300, (second row) prediction profiles at days 100, 200 and 300 for DA 18 (Activity of DEH10) by ADM and (third row) prediction profiles at days 100, 200 and 300 for DA 25 (Activity of Deh10+SF1+o17+DF1) by ADM .....	298
Figure E.5 PCB congener profiles of Data Set 1.BH: Graph above is measured day 100 vs. 100, Graph below is day 200 measured vs. predicted by the model for D. Act. 18 .....	299
Figure E.6 PCB congener profiles of Data Set 3.BH: Graph above is measured day 100 vs. 200, Graph below is day 200 measured vs. predicted by the model for D. Act. 18 .....	300
Figure E.7 PCB congener profiles of Data Set 4.BH: Graph above is measured day 100 vs. 200, Graph below is day 200 measured vs. predicted by the model for DA 18 .....	300
Figure E.8 PCB congener profiles of Data Set 2.BH: Graph above is measured day 0 vs. 100, Graph below is day 100 measured vs. predicted by the model for DA 23 .....	301
Figure E.9 PCB congener profiles of Data Set 2.BH: Graph above is measured day 100 vs. 200, Graph below is day 200 measured vs. predicted by the model for DA 23 .....	302
Figure E.10 PCB congener profiles of Data Set 3.BH: Graph above is measured day 100 vs. 200, Graph below is day 200 measured vs. predicted by the model for DA 24 .....	303

Figure E.11 PCB congener profiles of Data Set 4.BH: Graph above is measured day 0 vs. 100, Graph below is day 100 measured vs. predicted by the model for DA 25 .....	304
Figure E.12 PCB congener profiles of Data Set 4.BH: Graph above is measured day 100 vs. 200, Graph below is day 200 measured vs. predicted by the model for DA 25 .....	305
Figure F.1 Sensitivity Analysis of PCB congeners in Lake Michigan sediment: TSS Comparison .....	311
Figure F.2 Sensitivity Analysis of PCB congeners in Lake Michigan sediment: vb Comparison .....	312
Figure F.3 Sensitivity Analysis of PCB congeners in Lake Michigan sediment: vs Comparison .....	313
Figure F.4 Sensitivity Analysis of PCB congeners in Lake Michigan sediment: Cs Comparison .....	314
Figure F.5 Sensitivity Analysis of PCB congeners in Lake Michigan sediment: Cw Comparison .....	315
Figure F.6 Sensitivity Analysis of PCB congeners in Lake Michigan sediment: DA18 Comparison .....	316
Figure F.7 Sensitivity Analysis of PCB congeners in Lake Michigan sediment: Diffusion Comparison.....	317
Figure F.8 Sensitivity Analysis of PCB congeners in Lake Michigan sediment: focs Comparison .....	318
Figure F.9 Sensitivity Analysis of PCB congeners in Lake Michigan sediment: focw Comparison .....	319
Figure F.10 Sensitivity Analysis of PCB congeners in Lake Michigan sediment: Kow Comparison .....	320
Figure F.11 Probability Graph for Normal Distribution of Uncertainty Analysis of Lake Michigan at 20.year.....	323
Figure F.12 Probability Graph for Lognormal Distribution of Uncertainty Analysis of Lake Michigan at 20.year.....	324
Figure F.13 Mean and Standard Deviation of Output Concentration of Each Congener for 1000 runs by MC Simulation .....	325

Figure G.1 Sensitivity Analysis of PBDE congeners in SF Bay sediment: $C_s$ Comparison .....	330
Figure G.2 Sensitivity Analysis of PBDE congeners in SF Bay sediment: $C_w$ Comparison .....	331
Figure G.3 Sensitivity Analysis of PBDE congeners in SF Bay sediment: $k_m$ Comparison .....	332
Figure G.4 Sensitivity Analysis of PBDE congeners in SF Bay sediment: $D_m$ Comparison .....	333
Figure G.5 Sensitivity Analysis of PBDE congeners in SF Bay sediment: $f_{ocs}$ Comparison .....	334
Figure G.6 Sensitivity Analysis of PBDE congeners in SF Bay sediment: $f_{ocw}$ Comparison .....	335
Figure G.7 Sensitivity Analysis of PBDE congeners in SF Bay sediment: $K_{ow}$ Comparison .....	336
Figure G.8 Sensitivity Analysis of PBDE congeners in SF Bay sediment: TSS Comparison .....	337
Figure G.9 Sensitivity Analysis of PBDE congeners in SF Bay sediment: $v_b$ Comparison .....	338
Figure G.10 Sensitivity Analysis of PBDE congeners in SF Bay sediment: $v_s$ Comparison .....	339
Figure G.11 Probability Graph for Normal Distribution of Uncertainty Analysis of Lake Michigan at 20.year.....	342
Figure G.12 Probability Graph for Lognormal Distribution of Uncertainty Analysis of Lake Michigan at 20.year.....	343
Figure G.13 Mean and Standard Deviation of Output Concentration of Each Congener for 1000 runs by MC Simulation.....	344

## LIST OF ABBREVIATIONS

ADM: Anaerobic Dechlorination Module

Avg: Average

BC: Black Carbon

BH: Baltimore Harbor

BIC: Biotic Carbon

Br: Bromine

CB: Chlorobiphenyl

Cl: Chlorine

DA: Dehalogenation Activity, Dechlorination/Debromination Activity

dw: dry weight

DOC: Dissolved Organic Carbon

F&T: Fate and transport

FTHP: Fate and Transport of Hydrophobic Pollutants

HOCs: Hydrophobic Organic Chemicals

PMHR: PCB Model for Hudson River

LM: Lake Michigan

LMMBP: Lake Michigan Mass Balance Project

MCL: Maximum Contaminant Level for drinking water

OM: Organic Matter

PCBs: Polychlorinated Biphenyls

PBDEs: Polybrominated Diphenyl Ethers

PCE: Tetrachloroethylene

PDC: Particulate detrital carbon

POC: Particulate Organic Carbon (Biotic Carbon + Particulate detrital carbon)

RK4: Runge Kutta 4<sup>th</sup> order

RSD: Relative standard deviation

SD: Standard deviation

SF: San Francisco

SOM: Sediment Organic Matter

TCE: Trichloroethylene

TOC: Total Organic Carbon (Particulate Organic Carbon + Dissolved Organic Carbon)



## LIST OF NOTATIONS

Items	Unit	Descriptions
Avg	mole ‰	Average of predicted profiles estimated for each shuffle
$A_w$ and $A_m$	$m^2$	Surface areas of water and surface sediment, respectively
$C_d(i)$	mole ‰	Concentration of daughter congener at initial time, $t_i$
$C_d(f)$	mole ‰	Concentration of daughter congener at final time, $t_f$
$C_m(i)$	mole ‰	Concentration of mother congener at initial time, $t_i$
$C_m(f)$	mole ‰	Concentration of mother congener at final time, $t_f$
$c_m^i$	ng/L	Concentration of contaminant $i$ in surface sediment
$c_s^i(0)$	ng/L	$i^{\text{th}}$ contaminant concentration at the top of the deep contaminated layer
Cmtnew	ng/L	Concentration of each congener calculated in each time step of FTHP model
$c_w^i$	ng/L	Concentration of contaminant $i$ in water column
costheta	-	Cosine theta ( $\cos \theta$ ), indicator of the similarity between two data using angular profile of predicted and measured data
DA	-	Dechlorination activity
DL	mole ‰	Detection limit
$D_m$	$cm^2/sec$	Molecular diffusion coefficient
$D_s$	$cm^2/sec$	Molecular diffusivity
$F_{dp}$	-	Ratio of contaminant concentration in the sediment pore water to contaminant concentration in total sediment
$F_{dw}$	-	Fraction of contaminant in dissolved forms in water
$F_{pw}$	-	Fraction of contaminant in particulate form in water
$f_{oc}$	g-orgC/g	Fraction of organic carbon in solid
it	-	Counter to check the number of shuffles (from 0 to 150)
$K_d$	L/kg	Solid-water distribution coefficient
$k_1, k_2, k_3$ and $k_4$		Calculated terms in RK4.
$k_m, k_{val}$	$d^{-1}$	Biodegradation rate constant of a dehalogenation pathway estimated for mixed surficial sediment
$K_{ow}$	-	Octanol-water partitioning coefficient
$m \rightarrow d$		A dehalogenation pathway indicating replacement of chlorine from the mother congener, $m$ , with hydrogen, to produce the daughter congener
Median	mole ‰	Median of predicted profiles estimated for each shuffle
pathorder	-	Order of each pathway in the shuffles

Items	Unit	Descriptions
$R^2$	-	Multiple correlation coefficient of all congeners modeled
$R^2_{\text{reac}}, RR^2$	-	Multiple correlation coefficient of only reactive congeners modeled
S	-	Objective function calculated during each run
$S_{\text{initial}}$	-	The initial value of the objective function – calculated at initial time before any calculations made on mother/daughter congener concentrations
$S_{\text{min}}$	-	The smallest S obtained during model run
Sol	mg/L	Solubility of the congeners
$S_{\text{previous}}$	-	Objective function calculated during previous run
$S_w$	$\text{g/m}^3$	Total suspended solid concentration
t	day	Time, day
$t_i$	day	Initial time
$t_f$	day	Final time
$\Delta t$	day	Time step
$v_b$	m/day	Burial velocity
$v_d$	m/day	Diffusion mass-transfer coefficient at the sediment, water and deep sediment interface
$V_m$	$\text{m}^3$	Volume of mixed sediment
$v_r$	m/day	Resuspension velocity of sediments
$v_s$	m/day	Settling velocity of particulate matter
$x_j$	mole ‰	Congener profile of microorganism PCB data measured at day e.g. T=100 day
$\hat{y}_j$	mole ‰	Predicted congener profile (either from Frame et. Al (1996) or microcosm PCB data at t=0 d) altered according to a dechlorination activity
$\sum_{j=1}^m$	-	Summation of m number of congeners

## CHAPTER 1

### INTRODUCTION

Hydrophobic organic compounds (HOCs) are named because of their low water solubility, high octanol-water partitioning coefficient ( $K_{ow}$ ) with high sorption capacity to organic carbon. After these chemicals are released into the environment intentionally or unintentionally, they can be easily bioaccumulated and persist in fatty tissues of living organisms as a result of these properties (USEPA, 2010). HOCs strongly bind to the solid phase owing to these properties. Therefore, they are accumulated on suspended particulate matter and either transported with them, or settle and become part of the sediments. Contaminated sediments become a legacy from past pollution that can continue to negatively impact the environment even years after pollutant loads have been controlled. Understanding fate and transport of HOCs in sediments is of major concern and is imperative for sound environmental management of HOCs. In this study, fate and transport of halogenated HOCs in sediments are investigated. Two groups of pollutants, namely, polychlorinated biphenyls (PCBs) and polybrominated diethers (PBDEs) are studied as cases.

PCBs are a class of persistent organic pollutants (POPs). These chemicals had a widespread use in many industries such as heat exchange fluids, dielectric fluids in electric transformers and capacitors, and as additives in paint, carbonless copy paper, and plastics (POPs, 2008). Historically, about 1.7 million tons of PCBs was globally produced between 1930 and 1993 (Breivik et al., 2007). Despite prohibition of commercial production of PCBs firstly in 1977 in the USA, and lastly in 1993 in Russia (Breivik et al., 2002), PCBs are still available in old transformers, capacitors, heat exchangers, etc. PCBs are internationally regulated as part of the original twelve POPs

under the Stockholm Convention, which necessitates elimination of the use of equipment containing PCBs by 2025 and management of wastes containing PCBs by 2028. They are released into the environment after being sold/used as formulations composed of about 150 PCB congeners (Frame et al., 1996). Polybrominated diphenyl ethers (PBDEs) are a group of flame retardants. These chemicals have been used widely in building materials, electronics, furnishings, motor vehicles, airplanes, plastics, polyurethane foams and textiles (ATSDR, 2004). The first commercial productions of PBDEs began in the 1970s in Germany (ATSDR, 2004). PBDEs are regulated internationally by the Stockholm Convention, as a part of the new generation POPs. Although production of tetra-, penta-, hexa- and hepta- PBDE congeners are banned by the Convention, production of PBDEs still continues around the globe and pose a threat to the environment due to their bioaccumulative property and persistence (POPs, 2008). PBDE mixtures sold/used typically contain 22 congeners. (La Guardia et al., 2006).

When the compound to be modeled is not a single chemical (e.g. trichloroethylene - TCE) but a family of chemicals (e.g. about 150 PCB congeners in a commercial formulation), this presents an added challenge in modeling. Physicochemical properties of the congeners differ from one another having an impact on the fate mechanisms affecting their distribution in the environment. For example, when one congener can be biodegraded anaerobically, the same rate or extent may not be said for another congener of the same PCB family. In addition, congeners in a family do not possess the same toxicity (Van den Berg et al., 2006) or bioaccumulative effect (Hale et al., 2003) on organisms. This variation among congeners become especially prominent when a biotic fate mechanism, namely, anaerobic dehalogenation of HOCs are considered. Anaerobic dehalogenation of PCBs and PBDEs are shown by laboratory (Brown et al., 1984; Tokarz et al., 2008) and environmental (Siebielska & Sidelko, 2015; Zanaroli et al., 2012) studies to be an important fate mechanism affecting their distribution in contaminated sediments.

Fate and transport (F&T) models are valuable in predicting the remediation outcome and frequently used for better environmental management of sites contaminated with various chemicals. In the literature, numerous studies exist for modeling of PCBs as total-PCBs, homologs or individual congeners (Connolly et al., 2000; Davis, 2004; Farley et al., 1999; Shen et al., 2012; Zhang et al., 2008, 2009) or as total maximum daily load (TMDL) of PCBs (LimnoTech, 2007; Shen, 2011; Shen et al., 2012). There are also, although much less in number, studies about modeling of PBDEs (Davis, 2004; Rowe, 2009). According to our literature review, it is seen that there are a number of F&T models that run on an individual PCB and PBDE congener basis (Davis, 2004; Oram et al., 2008b; Rowe, 2009; Shen, 2011; Shen et al., 2012; Zhang et al., 2008). Following simulation, however, the output is evaluated for total PCBs or PBDEs (Zhang et al., 2008, 2009). Biodegradation is typically either assumed to be negligible or as a first order decay reaction, with a generic reaction rate constant. The study by Davis (2004) runs the model with a general degradation term for each congener, however it neither differentiates between biological/chemical degradation, nor takes products of degradation into account.

Our literature review indicates that there is no model that runs on an individual congener basis, considering biodegradation of these compounds with their relevant products, and other F&T processes together. In other words, such models have not been developed before. The main reason for this can be that degradation pathways of individual congeners have only been studied in the last decade or two. Mechanisms of individual congeners in the environment have gained importance only recently. Up to now, change in amount of total congeners were of concern, even if individual congeners were modeled. Consequently, biodegradation of these compounds with their relevant products was not considered in these models. According to our literature review, physicochemical properties of the congeners differentiate from one another having an impact on the fate mechanisms affecting their distribution in the environment. Additionally, all these compounds are not toxic and bioaccumulative, but they can degrade to toxic or bioaccumulative ones by anaerobic dehalogenation reactions. Therefore, investigation of individual congeners by such models is

important. Hence this study aims to develop a F&T model for contaminated sediments that takes into account anaerobic dehalogenation of congeners. Accordingly, our considerations by the model are (i) to evaluate the reduction of toxic and/or bioaccumulative congeners, and (ii) to decrease amount of higher homolog groups in a contaminated site. The specific aims are;

1. To estimate anaerobic dehalogenation reactions and their rate constants to be used as input in the fate and transport model. This aim is carried out by modifying a previously developed model to yield a generic anaerobic dehalogenation model (ADM), which identifies anaerobic dehalogenation pathways, estimates rate constants for dehalogenation reactions, by using laboratory sediment dehalogenation data as input.
2. To develop a congener specific F&T model by incorporating biodegradation into an existing model to consider biodegradation reactions of individual contaminants, taking into account reactants and products, as well as all relevant F&T mechanisms,
3. To apply the developed model on environmental HOC data (i.e. PCB and PBDE contaminated sediment data) and evaluate the effectiveness of various remediation scenarios.

One advantage of such models is that they can aid in the investigation of effective remediation strategies and better management of the environment. In other words, comprehensive remedial strategies such as monitored natural attenuation, bioaugmentation/biostimulation or dredging can be assessed by this model for better management of contaminated sites. Furthermore, such models using biodegradation of individual congeners and considering their products in contaminated sediment can help decrease the toxicity of sediments for elimination or reducing the risk to aquatic organisms and humans. Additionally, these models can help understand the fate mechanisms especially biodegradation of HOCs such as PBDEs which include a very limited number of studies about their behavior and fate. Remedial strategies then, can be developed. New chemicals are synthesized every day for a multitude of purposes,

therefore the F&T of new compounds can also be evaluated using the developed model.

This dissertation is organized as a collection of manuscripts of which portions have either already been submitted for publication, or will be submitted. Other than these, the dissertation also includes a comprehensive literature review section and methodology section presenting the details of the development of the model and laboratory and environmental HOC data sets used to test the model. Some repetition may appear in the introduction and methodology sections of the relevant topics.





## CHAPTER 2

### LITERATURE REVIEW

#### 2.1 Halogenated Hydrophobic Organic Compounds (HOCs)

HOCs are called hydrophobic because of their low water solubility, high sorption capacity to organic carbon and high octanol-water partitioning coefficient ( $K_{ow}$ ). These chemicals can be bioaccumulated in fatty tissues of animals and humans as a result of these properties (USEPA, 2010). HOCs strongly bind to the solid phase owing to these properties. Therefore, they are accumulated on suspended particulate matter and either transported with them, or settle and become part of the sediments.

Petrovic et al. (2007) proposed a criterion for selection of compounds to be monitored in sediments, where he states that  $\log K_{ow}$  should be higher than 5 for monitoring in sediments, should be lower than 3 for monitoring in water and values between 3 and 5 depends on the degree of contamination and are optional. In short, the higher  $\log K_{ow}$  is, the higher affinity towards sediment and suspended matter. For example, hexachlorobenzene (HCB) and atrazine should be monitored in sediment and water, due to the high sorption capacity and high water solubility, respectively (Petrovic et al., 2007).

Halogenated HOCs such as DDT, PCBs, PBDEs are typically persistent for decades in the environment. Halogenated HOCs were mostly produced due to their chemical and physical stability for agricultural (e.g. DDT) or industrial (e.g. PCBs) use. Because of their exceptional properties, these chemicals had widespread use in these sectors. However, after their abundant use and discharge, their toxic, persistent and bioaccumulative properties were discovered in the environment and in biota. Although

they tend to persist for decades, they can be affected by physicochemical and biological degradation mechanisms in the environment. By this way, their partitioning into different media (water, air, soil, sediment, biota) is also affected. Therefore, any site contaminated with these chemicals should be investigated by using fate and transport models in order to develop effective remediation strategies for the region. PCBs and PBDEs are selected in this study to represent Halogenated HOCs.

### 2.1.1 Polychlorinated Biphenyls (PCBs)

Polychlorinated biphenyls (PCBs) are a class of persistent organic pollutants, internationally regulated by the Stockholm Convention (POPs, 2008). They consist of two phenyl rings, 12 carbons and 10 atoms which can be either chlorine or hydrogen ( $C_{12}H_{10-n}Cl_n$ ) (Figure 2.1). Positions 2, 2', 6, and 6' are defined as *ortho*, positions 3, 3', 5, and 5' are defined as *meta* and positions 4 and 4' are defined as *para* positions. According to position (*meta*, *para* and *ortho*) and number of chlorine in the biphenyl structure, theoretically, 209 PCB compounds are available, each of which is called congener. PCB congeners including same number of chlorine are called homologs. In in homologs, PCB congeners having different positions are recognized as isomers. Additionally, PCB congeners are also named according to the configuration of chlorines, such that **singly flanked**: presence of other chlorines in either of the adjacent positions, **doubly flanked**: presence of chlorine in both adjacent positions and **unflanked**: absence of chlorine in any of the adjacent positions.

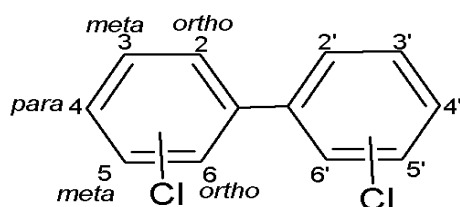


Figure 2.1 General PCB structure

Ballschmiter and Zell (1980), following the “International Union of Pure and Applied Chemistry” (IUPAC) rules, named 209 congeners by numbering them. They are called as “Ballschmiter”, “BZ” or “IUPAC” numbers from 1 to 209. Imamoglu (2001) states that another notation with a hyphen representing separation of rings is commonly used since it makes structure of the congener more explicit when compared to the IUPAC numbering. As an example, 22’55’ is referred to as congener 52 in IUPAC numbering, where it is written as 25-25 in the latter way of depicting congeners. The complete list of congeners considering the numbering and structure of PCBs is provided in Appendix A. The congener list used here is taken from Frame et al. (1996). This nomenclature differs from USEPA (2015) for three congeners 107, 108 and 109. The structure of congeners 107, 108 and 109 are : 234-35, 2346-3 and 235-34, respectively, as given in Frame et al. (1996) while they are 235-34, 234-35 and 2346-3, respectively in USEPA (2003).

The congeners including both non-*ortho* and mono-*ortho* substituted PCBs can rotate freely on carbon-carbon central biphenyl bond because of no steric hindrance associated with *ortho* chlorines. Due to free rotation, the congeners are oriented in the same plane, which are called planar or coplanar configuration (dihedral angle=0°). Other configuration is nonplanar in which two benzene rings are in a perpendicular plane (dihedral angle=90°) (ATSDR, 2004). For example, congener 77 (34-34) is a non-*ortho* substituted planar congener and congener 153 (245-245) is a di-*ortho* substituted nonplanar congener. The planar and coplanar congeners are also dioxin-like compounds since they are biochemically active and the most toxic (Karcher, 2005) and the toxicity decreases substantially as *ortho* positions increase. The details about toxicity is mentioned in section 2.1.3.

PCBs were sold as mixtures under different trade names in various countries such as Aroclors (A1016, 1260, 1254, 1242, etc.) in USA, Clophen (Clophen A60, A30, etc.) in Germany, Kanechlors in Japan, etc. (UNEP, 1999). In Aroclor, first two digits

explains carbon number and last two digits expresses approximate chlorine content by weight percent. Aroclor mixtures and the contents of congeners are presented in detail by Frame et al. (1996).

PCBs were commercially successful due to their chemical and thermal stability. Therefore, these chemicals had a widespread use in many industries such as heat exchange fluids, dielectric fluids in electric transformers and capacitors, and as additives in paint, carbonless copy paper, and plastics (POPs, 2008). Global production of about 1.7 million tons of PCBs is recorded from 1930 until 1993 (Breivik et al., 2007). Despite prohibition of commercial production of PCBs firstly in 1977 in USA, and lastly in 1993 in Russia (Breivik et al., 2002), PCBs are still available in old transformers, capacitors and heat exchangers. Another important point for PCBs is that after discharge of PCBs into the environment directly or unintentionally, it creates widespread pollution in the environment, and then has the potential to cause adverse effects on human and animals due to bioaccumulative, persistence and toxic properties. PCBs are among the Persistent Organic Pollutants (POPs) list of the Stockholm Convention, which deals with elimination of the use of equipment containing PCBs by 2025 and management of wastes containing PCBs by 2028. The Convention is implemented by the countries ratifying it. Turkey ratified the Convention in 2010.

### *Physicochemical Properties of PCBs*

PCBs were produced as mixtures including various congeners with a variety of number of chlorines, and because of that, they were released into the environment as such. Therefore, physicochemical properties of mixtures are also important to understand the fate and behavior of PCBs in the environment. Table 2.1 shows physicochemical properties of Aroclor mixture as an example. As chlorine content of mixture increase, water solubility, vapor pressure decrease and octanol water partitioning increase. The physiochemical properties of homolog groups and individual congeners are given in Table 2.2 and Table 2.3, respectively. Vapor pressure and Henry's constant indicate tendency of volatilization of a compound/mixture. By this way, the affinity of the

chemicals towards the air phase can be estimated. PCBs are categorized as semivolatile organic compounds (ATSDR, 2004).

Water solubility and octanol water partitioning can be indicators for hydrophobicity which is important for bioavailability of the compound (Henry & DeVito, 2003). PCB congeners having high number of chlorines have lower water solubility, hence may not be of interest for monitoring in the water phase. When  $\log K_{ow}$  increases, sorption to solid phases and bioaccumulation in organisms increase for a compound. As can be seen from Table 2.2 and Table 2.3, highly chlorinated PCBs have high  $\log K_{ow}$  and high hydrophobicity. Therefore, higher chlorinated congeners are sorbed to particulate matter in aquatic environment and settle down to become part of the sediments (Lick, 2009). Hence, higher chlorinated PCBs with higher  $K_{ow}$  values indicate less bioavailability when compared to lower chlorinated congeners with lower  $K_{ow}$  values (Henry & DeVito, 2003).

Highly chlorinated and fewer *ortho* substituted PCB congeners have less volatility, less water solubility, more sorption capacity and are more willing to take part in anaerobic dechlorination processes especially in buried sediments (Henry & DeVito, 2003). Therefore these congeners are likely to be much more in soils and sediments, less in water and in the atmosphere, and highly bioaccumulative (Henry & DeVito, 2003).

Table 2.1 Physicochemical properties of Aroclor mixtures at 20-25°C (Mackay et al., 2006)

Mixtures	Molecular Weight (g/mole)	% Cl	Avg. No. of Cl/molecule	Water Solubility (g/m <sup>3</sup> )	Vapor pressure (Pa)	Henry's law constant (Pa m <sup>3</sup> /mol)	logKow
Aroclor1232	221	31.4-32.5	2.04	1.45	0.54	82-270	4.5-5.2
Aroclor1242	261	42	3.1	0.1-0.75	0.05-0.13	45-130	4.5-5.8
Aroclor1248	288	48	3.9	0.1-0.5	0.0085-0.11	5-300	5.8-6.3
Aroclor1254	327	54	4.96	0.01-0.30	0.008-0.02	20-260	6.1-6.8
Aroclor1260	372	60	6.3	0.003-0.08	0.0002-0.012	20-60	6.3-6.8

Table 2.2 Physicochemical properties of PCB homologs at 20-25°C (Mackay et al., 2006)

Homologs	Water Solubility (g/m <sup>3</sup> )	Vapor pressure (Pa)	Henry's law constant (Pa m <sup>3</sup> /mol)	logKow
Dichloro-	0.060-2.0	0.008-0.60	17.0-92.21	4.9-5.30
Trichloro-	0.015-0.40	0.003-0.22	24.29-92.21	5.5-5.90
Tetrachloro-	0.0043-0.010	0.002	1.72-47.59	5.6-6.50
Pentachloro-	0.004-0.020	0.0023-0.051	24.8-151.4	6.2-6.50
Hexachloro-	0.0004-0.0007	0.0007-0.012	11.9-818	6.7-7.30
Heptachloro-	0.000045-0.0002	0.00025	5.4	6.7-7.0
Octachloro-	0.0002-0.0003	0.0006	38.08	7.1
Nonachloro-	0.00018-0.0012	-	-	7.2-8.16
Decachloro-	0.000761	0.00003	20.84	8.26

Table 2.3 Physicochemical properties of dioxin-like PCB congeners (WHO, 2003)

IUPAC No	Structure	Homolog Group	Molar Mass (g/mol)	Water solubility (mg/litre at 25 °C)	logKow	Vapour pressure (mmHg at 25 °C)	Henry's law constant (atm·m <sup>3</sup> /mol at 25 °C)
77	3,3',4,4'	tetrachlorobiphenyls	292	0.175	6.04- 6.63	4.4 × 10 <sup>-7</sup>	0.43 × 10 <sup>-4</sup> 0.94 × 10 <sup>-4</sup> 0.83 × 10 <sup>-4</sup>
81	3,4,4',5	pentachlorobiphenyls	326.4				
105	2,3,3',4,4'	pentachlorobiphenyls	326.4	0.0034	6.98	6.531 × 10 <sup>-6</sup>	8.25 × 10 <sup>-4</sup>
118	2,3',4,4',5	pentachlorobiphenyls	326.4	0.0134(20 °C)	7.12	8.974 × 10 <sup>-6</sup>	2.88 × 10 <sup>-4</sup>
126	3,3',4,4',5	pentachlorobiphenyls	326.4				
138	2,2',3,4,4',5	hexachlorobiphenyls	360.9	0.0159(calc.)	6.50-- 7.44(calc.)	4 × 10 <sup>-6</sup>	1.07 × 10 <sup>-4</sup> 0.21 × 10 <sup>-4</sup>
153	2,2',4,4',5,5'	hexachlorobiphenyls	360.9	0.00091 0.00086	8.35 6.72	3.80 × 10 <sup>-7</sup>	2.78 × 10 <sup>-4</sup> 1.32 × 10 <sup>-4</sup> 1.31 × 10 <sup>-4</sup>
156	2,3,3',4,4',5	hexachlorobiphenyls	360.9	0.00533	7.6	1.61 × 10 <sup>-6</sup>	1.43 × 10 <sup>-4</sup>
163	2,3,3',4',5,6	hexachlorobiphenyls	360.9	0.001195	7.2	5.81 × 10 <sup>-7</sup>	0.15 × 10 <sup>-4</sup>
169	3,3',4,4',5,5'	hexachlorobiphenyls	360.9	0.000036-- 0.01230(calc.)	7.408	4.02 × 10 <sup>-7</sup>	0.15 × 10 <sup>-4</sup> 0.59 × 10 <sup>-4</sup>
180	2,2',3,4,4',5,5'	heptachlorobiphenyls	395.3	0.00031-- 0.00656(calc.)	6.70- 7.21(calc.)	9.77 × 10 <sup>-7</sup>	1.07 × 10 <sup>-4</sup> 0.32 × 10 <sup>-4</sup>

### 2.1.2 Polybrominated Diphenyl Ethers (PBDEs)

Polybrominated diphenyl ethers (PBDEs) are a group of flame retardants. They consist of diphenyl ether, 12 carbons, 1 oxygen and 10 atoms which can be either bromine or hydrogen (PBDE = C<sub>12</sub>H<sub>(10-x)</sub>Br<sub>x</sub>O and x=m+n) (Figure 2.2). As in PCBs, possible 209 structures, which are called as congeners, are available.

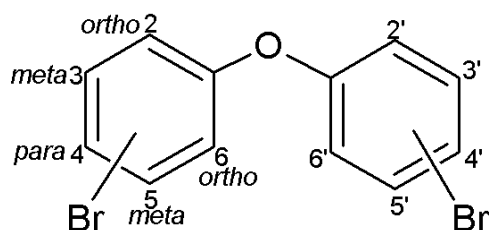


Figure 2.2 General PBDE structure

As in PCBs, PBDEs are also named by the numbering system by Ballschmiter and Zell (1980) and follow IUPAC rules. Therefore, the congener list given for PCBs in Appendix A is also the same for PBDEs (Table A.2). The nonhalogenated substitution in *ortho* position indicates the planar or near planar configuration (dihedral angle=0°) which enables benzene rings to rotate around the bond connecting them. Therefore, it is called coplanar like in PCBs. In contrast, when bromines are substituted in the *ortho* position, a nonplanar configuration (dihedral angle=90°) is formed, since steric hindrance prevents rotation.

The first commercial productions of PBDEs began in the 1970s in Germany (ATSDR, 2004). The production of tetra-, penta-, hexa- and hepta- PBDE congeners are banned by the Stockholm Convention due to their toxicity and persistence (POPs, 2008). According to the study of Hale et al. (2003), 33965 tons of PBDE commercial products (penta, octa and deca PBDE mixtures) were used in North America, which is about 50% of global demand in 1999. The study also shows that 97.5% production of penta mixture was produced in North America according to a 1999 survey.



PBDEs have been used as flame retardants widely in building materials, electronics, furnishings, motor vehicles, airplanes, plastics, polyurethane foams and textiles (ATSDR, 2004). They were produced as mixtures. However, the number of PBDE congeners used commercially in mixtures are much less than those used for PCBs (ATSDR, 2004). The most commonly studied congeners/mixtures are given in Appendix B. Three classes of mixtures were produced according to the average bromine numbers attached to the phenyl rings; penta-, octa-, and deca-BDEs. In the US, DE-60F, DE-61, DE-62, and DE-71 for pentaBDE mixtures; DE-79 for octaBDE mixtures; and DE 83R, Saytex 102E for decaBDE mixtures were produced (La Guardia et al., 2006). The mixtures and the contents of congeners are indicated in Table B.1. Three homolog groups have generally been included in these mixtures; penta-, octa- and decabromodiphenyl ethers. The major congener in decaBDEs is BDE-209. Tokarz et al., (2008) reports that the production of more than 80% of PBDEs by mass was BDE-209.

DecaBDE mixture includes 82% of these bromodiphenyl ethers produced. This mixture is used for electronic enclosures, such as television cabinets. OctaBDE mixture is used in plastics for business equipment. PentaBDE mixture is used in foam for cushioning in upholstery (ATSDR, 2004). These mixtures (especially octa and deca BDE mixtures) were produced by European countries and Japan under various trade names (ATSDR, 2004). The mixtures of pentaBDEs and octaBDEs were banned (POPs, 2008), but there is no law or framework for decaBDEs.

#### *Physicochemical Properties of PBDEs*

The information about physicochemical properties regarding water solubility, volatility and partitioning coefficients is presented for mixtures and individual congeners in Table 2.4 and Table 2.5, respectively.

PBDE mixtures contain congeners of various numbers of bromines. For example, pentaBDE mixture includes tetrabromodiphenyl ether (24–38%) and pentabromodiphenyl ether (50–62%) homologs with small amounts of hexabromodiphenyl ether (4–8%) and trace amounts of tribromodiphenyl ether (0–1%) homologs. While the octaBDE mixture consists of hexa-, hepta-, octa-, and nonabrominated diphenyl ether homologs with trace amounts of decabromodiphenyl ether (i.e., BDE 209), the decaBDE is a mixture of 97% BDE 209 congener with 3% nona- and octaBDE homolog impurities (ATSDR, 2004).

Physicochemical properties are presented in Table 2.5 for congeners that are abundant in original mixtures and hence probably more available in the environment. PBDEs are semivolatile organic compounds like PCBs. Lower brominated congeners that are associated with higher vapor pressure and Henry's constant (Table 2.5) have more of a tendency towards escaping into the gas phase. As can be seen from Table 2.5, the higher the number of bromine substitutions, the lower the water solubility and higher the  $\log K_{ow}$ . This indicates high hydrophobicity and higher tendency of sorption of higher brominated congeners to solid phase.

Table 2.4 Physicochemical properties of technical PBDE mixtures (ATSDR, 2004)

Property	Pentabromodiphenyl ether	Octabromodiphenyl ether	Decabromodiphenyl ether
Molecular weight, g/mole		Mixture	959.22
Physical state	Highly viscous liquid 13.3 µg/L (commercial); 2.4 µg/L (pentabromodiphenyl ether component); 10.9 µg/L (tetrabromodiphenyl ether component)	Powder	Powder
Water solubility		<1 ppb at 25 °C (commercial); 1.98 µg/L (heptabromodiphenyl ether component)	<0.1 µg/L
Vapor Pressure	2.2x10 <sup>-7</sup> –5.5x10 <sup>-7</sup> mm Hg at 25 °C; 3.5x10 <sup>-7</sup> mm Hg	9.0x10 <sup>-10</sup> –1.7x10 <sup>-9</sup> mmHg at 25 °C; 4.9x10 <sup>-8</sup> mm Hg at 21 °C	3.2x10 <sup>-8</sup> mm Hg; 3.47x10 <sup>-8</sup> mm Hg
Henry's Law constant (atm-m <sup>3</sup> /mole)	1.2x10 <sup>-5</sup> ; 1.2x10 <sup>-6</sup> ; 3.5x10 <sup>-6</sup>	7.5x10 <sup>-8</sup> ; 2.6x10 <sup>-7</sup>	1.62x10 <sup>-6</sup> ; 1.93x10 <sup>-8</sup> ; 1.2x10 <sup>-8</sup> ; 4.4x10 <sup>-8</sup>
logKow	6.64–6.97 6.57	6.29	6.265

Table 2.5 Physicochemical properties of PBDE congeners(ATSDR, 2004)

Congener	Vapor pressure (mm Hg)	Water solubility (µg/L)	Henry's Law constant (atm m <sup>3</sup> /mol)	logKow
<b>BDE-3</b>	1.94x10 <sup>-3</sup>	—	—	—
<b>BDE-15</b>	1.30x10 <sup>-4</sup>	130	2.07254x10 <sup>-4</sup>	—
<b>BDE-17</b>	—	—	—	5.74
<b>BDE-28</b>	1.64x10 <sup>-5</sup>	70	5.03331x10 <sup>-5</sup>	5.94
<b>BDE-47</b>	1.40x10 <sup>-6</sup>	15	1.48038x10 <sup>-5</sup>	6.81
<b>BDE-66</b>	9.15x10 <sup>-7</sup>	18	4.93461x10 <sup>-6</sup>	—
<b>BDE-77</b>	5.09x10 <sup>-7</sup>	6	1.18431x10 <sup>-5</sup>	—
<b>BDE-85</b>	7.40x10 <sup>-8</sup>	6	1.08562x10 <sup>-6</sup>	—
<b>BDE-99</b>	1.32x10 <sup>-7</sup>	9	2.26992x10 <sup>-6</sup>	7.32
<b>BDE-100</b>	2.15x10 <sup>-7</sup>	40	6.80977x10 <sup>-7</sup>	7.24
<b>BDE-138</b>	1.19x10 <sup>-8</sup>	—	—	—
<b>BDE-153</b>	1.57x10 <sup>-8</sup>	1	6.61238x10 <sup>-7</sup>	7.9
<b>BDE-154</b>	2.85x10 <sup>-8</sup>	1	2.36862x10 <sup>-6</sup>	7.82
<b>BDE-183</b>	3.51x10 <sup>-9</sup>	2	7.30323x10 <sup>-8</sup>	8.27
<b>BDE-190</b>	2.12x10 <sup>-9</sup>	—	—	—

### 2.1.3 Toxicity Evaluations

Toxic compounds are persistent and bioaccumulated in fatty tissues of animals and humans because of their hydrophobic property and resistance toward metabolism (USEPA, 2010). In the literature, toxicity information is available for PCB congeners, and but not for PBDEs. Therefore, toxicity evaluations can only be made for PCB congeners.

Concentration of a compound is not used to evaluate the toxicity in a site for site characterization, risk assessment and cleanup level development (USEPA, 2013). Instead, the total toxic equivalent (TEQ) is used, which is calculated by multiplying the concentration of each compound with its toxic equivalency factors (TEFs) (Van den Berg et al., 2006). TEFs for dioxin and dioxin-like compounds are used as a relative toxicity measure (USEPA, 2013). 2,3,7,8-tetrachlorodibenzo-p-dioxin (2,3,7,8-TCDD), is considered as the most toxic compound. Hence, toxicity of PCB congeners is based on the configuration of this congener. PCB congeners getting closer to the configuration of 2,3,7,8-TCDD are defined as “dioxin-like congeners”. Dioxin-like congeners have two *para*, at least two *meta* positions with no more than one *ortho* chlorine substitution (Bedard, 2003). The coplanar congeners which are without *ortho* substituted chlorines, are biochemically active and the most toxic (Karcher, 2005) while toxicity decreases substantially as the number of chlorines in positions *ortho* positions increase.

TEF values for dioxin-like PCB congeners are presented in Table 2.6. In the table, the values prepared in 1994 (third column) and 2005 (forth column) are listed. As can be seen from the table, while TEF values of mono-*ortho* substituted PCBs decrease from 1997 to 2005, the values of di-*ortho* substituted PCBs are absent and there is no increase/decrease rule for non-*ortho* substituted PCBs. In our study, TEF values updated in 2005 will be used. Accordingly, the most toxic congeners are PCB 77, PCB 126, PCB 169 and followed by others. When all Aroclor mixtures in Frame et al (1999) are reviewed, it is seen that the most toxic three congeners are only present in trace

amounts (0-0.52% by weight). For mono *ortho* substituted congeners, all congeners except for 118 and 105 are found in trace amounts in highly chlorinated A1254 and A1260, while they are not detected in lower chlorinated mixtures (e.g. A1242). PCB 118, PCB 105 and di-*ortho* substituted congeners PCB 170 and PCB 180 are found in high proportions in highly chlorinated A1254 and A1260.

Table 2.6 Toxic equivalency factors for coplanar and mono- and di-*ortho*-substituted PCBs

Congener Structure	IUPAC #	TEF values	
		WHO 1994 <sup>a</sup>	WHO 2005 <sup>b</sup>
non- <i>ortho</i> substituted PCBs			
3,3',4,4'-TetraCB	PCB 77	0.0005	0.0001
3,4,4',5-TetraCB	PCB 81	-	0.0003
3,3',4,4',5-PentaCB	PCB 126	0.1	0.1
3,3',4,4',5,5'-HexaCB	PCB169	0.01	0.3
mono- <i>ortho</i> substituted PCBs			
2,3,3',4,4'-PentaCB	PCB 105	0.0001	0.00003
2,3,4,4',5-PentaCB	PCB 114	0.0005	0.00003
2,3',4,4',5-PentaCB	PCB 118	0.0001	0.00003
2',3,4,4',5-PentaCB	PCB 123	0.0001	0.00003
2,3,3',4,4',5-HexaCB	PCB 156	0.0005	0.00003
2,3,3',4,4',5'-HexaCB	PCB 157	0.0005	0.00003
2,3',4,4',5,5'-HexaCB	PCB 167	0.00001	0.00003
2,3,3',4,4',5,5'- HeptaCB	PCB 189	0.0001	0.00003
di- <i>ortho</i> substituted PCBs			
2,2',3,3',4,4',5-HpCB	PCB 170	0.0001	-
2,2',3,4,4',5,5'-HpCB	PCB 180	0.00001	-

<sup>a</sup>:Ahlborg et al., 1994 <sup>b</sup>:Van den Berg et al., 2006

## 2.2 Fate of PCBs and PBDEs in the Environment

### 2.2.1 Fate Mechanisms in the Environment

The focus of this study is HOCs (PCBs and PBDEs being used as model compounds), therefore solid phase (i.e. sediment) is the major component during the explanation of the fate mechanisms. Sediments are defined as open and dynamic biogeochemical

systems (NRCC, 2002). In Tandlich (2003), soil is classified in three parts: organic, inorganic (mineral) and living components. Minerals include silicates (silicon and oxygen) which are abundant in the Earth's crust. Minerals are categorized according to sizes; coarse minerals are classified as the sand fraction (quartz and feldspars having diameters greater than 0.05 mm) (NRCC, 2002), and finer minerals are classified as silt (having diameter between 0.002 and 0.05mm) and clay (alluminosilicate having diameter smaller than 0.002 mm) fractions. Organic phases are essentially composed of detrital materials of plants and animals or their degradation products, and geologic forms of organic matter (OM) such as kerogen, coal, soot, charcoal, black carbon (BC) (NRCC, 2002), and humic acids. Sediments have the tendency to accumulate carbon over time due to anaerobic conditions (NRCC, 2002). Sorption is controlled by organic carbon content of suspended solids or sediment. Transport and fate of HOCs such as PCBs are strongly influenced by sorption to organic carbon and interactions between the water column and sediments. Humic acids have lower sorption capacity for HOCs than the more dense carbon forms (NRCC, 2002). Additionally, HOCs more strongly sorb to BC than all other forms of OMs in sediment. Greene et al. (2013) state that sorption to BC decreases PCBs partitioning into the water column.

Sediment zones and fate processes of a pollutant in the bed sediment are depicted in Figure 2.3. Most HOCs such as PCBs and PBDEs, when sorbed to particulate matter in aquatic environments end up in sediments (Lick, 2009), which results in contamination of sediments. Although HOCs (PCBs and PBDEs) are mainly bound to sediments, they can also be released into the water column under certain circumstances. When they are released from sediment to water in contact with sediment, two types of release processes are considered (1) physicochemical and (2) biological (NRCC, 2002). The physicochemical processes happen when water saturation of the sediment, water chemistry and sediment surface properties are changed. NRCC (2002) indicates that the rates of release change from minutes to hours or years, depending on the properties of the contaminant, solid phase and water. The diffusion transport and desorption processes are considered for this release. The biological release processes (NRCC, 2002) that include desorption of the contaminant

from sediment or solid by biological processes such as digestive tract, biological transformation of the chemical and bioturbation that changes the physical and chemical properties of the sediment and bioavailability of the contaminant.

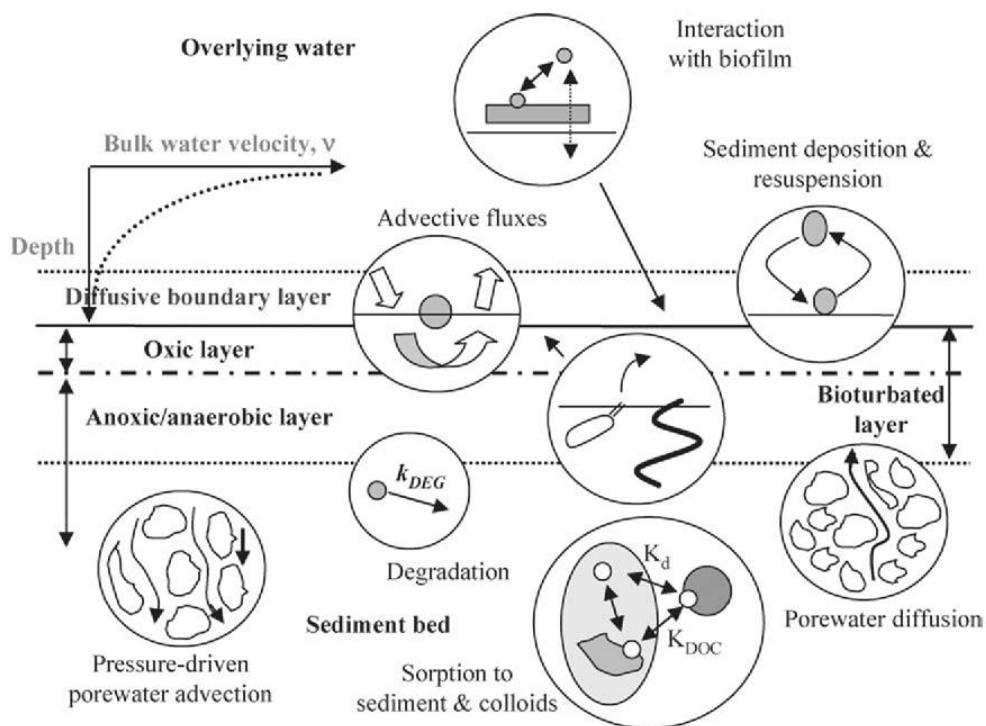


Figure 2.3 Sediment zones and fate processes of the pollutant in the bed sediment (Allan & Stegemann, 2007)

Our literature review indicated that environmental mechanisms affecting the fate and behavior of PCBs and PBDEs in bed sediment are partitioning between freely dissolved, dissolved organic carbon (DOC) and particulate organic carbon (POC), degradation (i.e. anaerobic dehalogenation), settling, resuspension at the interfaces between water column and surface sediment, diffusion exchange at the interfaces between water column and surface sediment and pore water as well as burial to deeper sediment. They are briefly described in the next sections.



### **2.2.1.1 Anaerobic Dehalogenation in Sediment**

#### **Anaerobic Dechlorination of PCBs**

PCB dechlorination is the replacement of one or more chlorines with a hydrogen in the PCB structure resulting in the production of less chlorinated congeners (Sowers & May, 2013). Various halorespiring bacteria are responsible for performing anaerobic dechlorination (Zanaroli et al., 2010).

Abramowicz (1995) states that the anaerobic microorganisms attack highly chlorinated congeners, resulting in *para* and *meta* chlorine removals. Anaerobic dechlorination of PCBs by microorganisms was first demonstrated in the 1980s (Bedard et al., 1986; Brown et al., 1987). Brown et al. (1984) firstly discussed microbial degradation of PCBs comparing original Aroclor 1242 profiles with data from upper Hudson River sediments. Then, various PCB dechlorination processes were identified by numerous studies regarding congener selectivity of microorganisms, targeted positions and dechlorination products (Bedard, 2003; Sowers & May, 2013). Bedard and colleagues (2003) defined these pathways based on contaminated sites such as Activity H, H', Q, N, etc. Table 2.7 summarizes the dechlorination activities including *para* and *meta* chlorine removal regarding configuration; flanked, doubly flanked and unflanked. *Ortho* chlorine removal is observed in the laboratory studies, but it was not observed in the environment (May et al., 2006).

Table 2.7 Comparison of microbial dechlorination activities (Bedard, 2003) as tabulated by Bzdusek (2005).

Dechlorination Activity	Targeted Chlorine	Homolog Substrate Range	Reactive chlorophenyl groups <sup>a</sup>	Primary chlorophenyl products
<b>P</b>	Flanked <i>para</i>	4-6	<u>34</u> , <u>234</u> , <u>245</u> , <u>2345</u> , <u>23456</u>	(23), 25, 235, 2356
<b>H</b>	Flanked <i>para</i> <sup>b</sup>	4-7	<u>34</u> , <u>234</u> , <u>245</u> , <u>2345</u>	3, 24, 25, 235
<b>H'</b>	Flanked <i>para</i> <sup>b,c</sup>	3-5	<u>23</u> , <u>34</u> , <u>234</u> , <u>245</u> , <u>2345</u>	2, 3, 24, 25, 235
<b>N</b>	Flanked <i>meta</i>	5-9	<u>234</u> , <u>236</u> , <u>245</u> , <u>2345</u> , <u>2346</u> , <u>23456</u>	24, 25, 26, 246
<b>M</b>	Flanked and unflanked <i>meta</i>	2-4	<u>3</u> , <u>23</u> , <u>25</u> , <u>34</u> , <u>234</u> , <u>236</u>	2, 4, 24, 26
<b>Q</b>	Flanked and unflanked <i>para</i> <sup>b,c</sup>	2-4	<u>4</u> , <u>23</u> , <u>24</u> , <u>34</u> , <u>234</u> , <u>245</u> , <u>246</u>	2, 3, 25, 26
<b>LP</b>	Flanked and unflanked <i>para</i> <sup>d</sup>	3-6	<u>24</u> , <u>245</u> , <u>246</u>	2, 25, 26

<sup>a</sup>The targeted chlorine(s) for each chlorophenyl group is (are) underlined.

<sup>b</sup>The doubly flanked *meta* chlorine of 234-chlorophenyl groups is also targeted.

<sup>c</sup>The *meta* chlorine of 23-chlorophenyl groups is also targeted.

<sup>d</sup>The substrate range of this dechlorination process has not been completely characterized.

Another classification of anaerobic dechlorination of PCBs is based on a microorganism or group of microorganisms. Sowers and May (2013) summarize dechlorination activities and corresponding microorganisms or strains in a table (Table 2.8). The microorganisms or groups are o-17, DF1, SF-1, *Dehalococcoides mccartyi* 195 and *Dehalococcoides spp.*, CBDB1 and DEH-10. Dechlorination activities for each strain is categorized by the positions of the target chlorines. However, they have some constraints. In o-17 culture, for example, dechlorination of 2,3,5,6- PCB is restricted in the presence of A1260 and 2,4,6-PCB can not be dechlorinated by o-17. In the study of May et al. (2006), o-17 culture did not dechlorinate *ortho* chlorines flanked with a *meta* chlorine when doubly flanked *meta* chlorines are available. Additionally, they can only dechlorinate doubly flanked *meta* chlorines before *ortho*. As a constraint for DF-1, they can only dechlorinate doubly flanked chlorines. (Wu et al., 2002). Chlorine configurations of 3, 4, 23, 24, 25, 34, 35, 235, 236, 246, 2356, and 245–245 are not dechlorinated (Wu et al., 2000). A constraint for DEH-10 is that DEH-

10 can dechlorinate doubly flanked chlorine in 234 substituted congeners and *para* flanked *meta* chlorines in the absence of doubly flanked chlorines (Fagervold et al., 2007). Adrian et al. (2009) point out that CBDB1 can decrease and remove dioxin-like PCBs called as two *meta* and two *para* chlorines and no more than one *ortho* chlorine. However, they can not dechlorinate the following congeners: 2356-245, 2356-34, 2356-25, 236-25, 236-34, 235-236, 236-236-CB.

In the literature, first order kinetic model was commonly used to estimate dechlorination rates of PCB congeners (Cho et al., 2003; Siebielska & Sidelko, 2015). However, there is also a study estimating dechlorination rate considering number of microorganisms. Lombard et al. (2014) stated that dechlorination rate is dependent on number of microorganisms rather than concentration of congeners and dechlorination activity can be observed even at low concentrations (e.g. 1 ng/L). The study of Lombard et al. (2014) investigated rates of congener 61 to congener 23 by DF1 in the pore water considering environmentally relevant concentration (1 to 500 ng/L) of contaminant and concentration of cells ( $>10^6$  cells/mL). The result of this study indicated that bioaugmenting with densities of  $10^5$ -  $10^6$  cells/mL can increase the rates of dechlorination. Additionally, if concentration of congeners in pore water, which is the bioavailable portion of the contaminant is known, dechlorination rates can be estimated. They then, can be used for remediation studies. As a result, two types of studies observed the first order relationship between rate and contaminant concentration, however rates vary. The variation is explained by number and types of microorganisms as well as concentration of congeners in pore water which is not reported by Cho et al. (2003) or Siebielska and Sidelko (2015).

Table 2.8 Dechlorination activities and corresponding microorganism or strain (Sowers & May, 2013).

Microorganism or group	Dechlorination activities	Examples of dechlorination pathways	References
o-17	Flanked <i>ortho/meta</i>	2356- (#65) → 235- (#23) → 35- (#14)	(Cutter et al., 2001; May et al., 2006)
DF-1	Doubly flanked <i>meta/para</i>	234- (#21) → 24- (#7) 345- (#38) → 35-(#14)	(Wu et al., 2002)
Dehalococcoides sp. DEH-10	Doubly flanked <i>meta/para</i> <i>Para</i> flanked <i>meta</i>	234-236 (#132) → 236-24- (#91) → 24-26- (#51)	(Fagervold et al., 2007)
SF-1	Doubly flanked <i>meta</i> <i>Ortho</i> flanked <i>meta</i>	2345-24 (#137) → 245-24 / 235-24 (#99/90)	(Fagervold et al., 2007)
Dehalococcoides sp CBDB1	Doubly and singly flanked <i>para</i> Doubly flanked <i>meta</i>	34- → 3-	(Adrian et al., 2009)
Dehalococcoides mccartyi 195	Doubly flanked <i>meta/para</i>	23456- (#116) → 2356- (#65) / 2346- (#62) → 246- (#30)	(Fennell et al., 2004)

### *Anaerobic Debromination of PBDEs*

Anaerobic debromination of PBDEs is the replacement of bromine atoms with hydrogen by the action of anaerobic microorganisms. Products of debromination reactions result in the accumulation of less brominated PBDEs in humans and the environment (Tokarz et al., 2008). Therefore, anaerobic debromination of PBDEs has been investigated and evaluated in the last decade (Ding et al., 2013; Huang et al., 2014; Robrock et al., 2008; Tokarz et al., 2008). These studies examined debromination pathways of PBDEs by different microorganisms and/or microbial groups. Additionally, some of these studies examined debromination pathways in terms of bromine configuration with different products. For example, Tokarz et al. (2008) and Huang et al. (2014) noted that removal of *ortho* bromine is also possible along with removal of *para* and *meta* bromines while Ding et al. (2013) and Robrock et al. (2008) indicated preferential removal of *para* and *meta* bromines. Various products were observed in these studies. For example, Tokarz et al. (2008) observed BDE 17 and BDE 28 as final product of BDE 209 debromination. Similarly, Robrock et al. (2008) indicated BDE 17 as major product in the debromination pathway of seven environmentally relevant PBDE congeners (196, 203, 197, 183, 153, 99 and 47). In contrast, different products were revealed in the studies of Huang et al. (2014): BDEs 71 and 3, and Ding et al. (2013): BDEs 4, 18, 19, 44 52, and 59. An overall summary of these studies including microorganisms, pathways, electron donor, and acceptors are given in Table 2.9 and briefly discussed in this section.

Table 2.9 Overview of PBDE debromination studies

Study	Media	Microorganism	Configuration
Tokarz et al., 2008	Sediment microcosms	Some halorespiring bacteria	Removal of <i>para</i> and <i>meta</i> bromines
		Example to pathways identified 209→207→197→184→154→99→47→28	
Robrock et al., 2008	Medium prepared in lab	ANAS195, Dehalobacter restrictus PER-K23 and Desulfitobacterium hafniense PCP-1	Removal of <i>para</i> and <i>meta</i> bromines.
		Example to pathways identified 203→183→153→99→47→17	
Ding et al., 2013	Medium prepared in lab	Acetobacterium sp. Strain AG aand culture G derived from octa-BDE-debrominating microorganisms	<i>para</i> -dominant debromination pattern
		Example to pathways identified 183→154→103→53→19	
Huang et al., 2014	Sediment samples in lab medium	Anaerobic microorganisms	<i>Para</i> , <i>meta</i> and <i>ortho</i> removal
		Example to pathways identified 209→207→196→183→154→100→47→28→15→3	

BDE 209 can be degraded under anaerobic conditions, but a long time is needed. Huang et al (2014) demonstrated enhanced debromination of congener BDE 209 to product BDE 3 with various factors such as the addition of rhamnolipid, surfactin, vitamin B12, zero-valent iron, acetate, lactate, and pyruvate. One of the findings was that the addition of electron donors (acetate, lactate, and pyruvate) increases the degradation rate of BDE 209. Tokarz et al. (2008) studied debromination pathways of BDE 209 to final products BDE 17 and BDE 28 in sediment under anaerobic conditions. The removal of *ortho* bromine as well as removal of *para* and *meta* bromines was observed.

If two issues become clear about debromination of PBDEs, the efficiency of biodegradation in contaminated sites can be enhanced. Firstly, there is no clarification of a dominant set of pathways for PBDEs in the environment - there is a need to investigate debromination pathways in accordance with different regiospecificity in different environments (Rodenburg et al., 2014). Secondly, anaerobic debromination of PBDEs was investigated under laboratory conditions in the studies and rates of debromination of PBDEs were increased with the addition of halogenated electron acceptors. However, the environmental microorganisms with the ability to debrominate PBDEs are not always present with other contaminants (electron acceptors) in contaminated sites (Huang et al., 2014). Furthermore, these microorganisms have not been identified. Therefore, these microorganisms should be identified to enhance the efficiency of biodegradation in the environment. By this way, remedial strategies can be developed in contaminated sites for natural attenuation, bioaugmentation and/or biostimulation.

#### **2.2.1.2 Settling**

Settling is an important process for HOCs. Since these compounds are hydrophobic, they tend to move to sediment by partitioning solid phase in water. Hence, sorption mechanism is important in settling process. Sorption is defined as the partitioning of HOCs among freely dissolved, DOC bound and those attached to solid phase that exists in water column and sediment (Farley et al., 1999). Sorption mechanism is controlled by organic carbon content of suspended solids or sediment. Transport and fate of HOCs are strongly influenced by sorption to organic carbon and interactions between the water column and sediments. Farley et al. (1999) states that sorption of PCBs is defined by fraction of organic carbon ( $f_{oc}$ ) which is equal to particulate organic carbon over average suspended solid concentration or sediment concentration. Connolly et al. (2000) simulated sediment as two parts: cohesive and non-cohesive according to particle size and textures. PCB concentrations were evaluated separately in both types of sediments due to their different sorption capacities. Parsons et al. (2007) discuss sorption of HOCs to sediment organic matter (SOM) and black carbon

(BC) which is formed in the environment by combustion of biomass and fossil fuel, and includes nearly 1-15% of total organic carbon content. They indicate that HOCs more strongly sorb to BC than all other forms of SOMs. Additionally, Parsons et al. (2007) evaluated some studies in the literature and state that sorption of HOCs to BC shows nonlinear sorption behavior (or conforms to the non-linear sorption model), whereas sorption to SOMs are observed to follow the linear sorption model.

### **2.2.1.3 Resuspension**

Resuspension occurs due to bioturbation and/or current. The resuspension of the sediment is considered when shear stress is greater than the critical shear stress, and deposition is considered when shear stress is smaller than the critical shear stress of deposition (Shen et al., 2012). When PCBs are sorbed or attached to solid phase (suspended solids/POC) in the water column, they can be deposited to sediment and reversibly they will be resuspended to water column from sediment. In the literature, deposition and resuspension of POC bound chemicals are evaluated considering different carbon sources. Farley et al. (1999) studied in Hudson River and sediment, and state that the continuous exchange of PCBs is due to settling of phytoplankton and other suspended solids and resuspension of SOM rather than pore water diffusion of dissolved and DOC bound contaminant. LimnoTech (2007) simulated PCBs sorbed to POC which are divided into two parts: biotic (algal) carbon and particulate detrital carbon. In the model, PCBs sorbed to particulate detrital carbon are settled or were resuspended at the interface, but PCBs sorbed to biotic (algal) carbon are only deposited through sedimentation.

### **2.2.1.4 Diffusion Exchange**

The diffusion exchange is determined for water-sediment interface and sediment-deeper sediment exchange. In water-sediment interface, pore water column exchange depends on hydrodynamic structure such as current, wave at the water-sediment interface and bioturbation (Farley et al., 1999). When water flow through sediment,



bioturbation is out of consideration, molecular diffusion of the compound is dominant (Allan & Stegemann, 2007). Diffusion of PCBs can occur for both the freely dissolved and DOC-bound phases (LimnoTech, 2007).

#### **2.2.1.5 Burial**

POC bound HOCs in deep sediment are no longer available for resuspension. A burial rate between the top and bottom sediment layers is defined by the models.

#### **2.2.1.6 Sorption/Desorption**

Sorption and desorption are important mechanisms affecting HOCs. In fact, Zhang et. al (2008) argue that the F&T models of PCBs are controlled by sorption to organic carbon in aquatic environment. Similarly, Shen et. al (2012) state that F&T models depend on movement of organic carbon because of the strong sorption capacity of PCBs to organic carbon. The flux of chemicals between sediments and the overlying water is mainly because of sediment erosion/deposition, molecular diffusion, bioturbation and groundwater flow. These processes are affected by sorption (Lick, 2009). Another issue about sorption is whether it is long or short term. Thomann and DiToro (1984) and Chapra (1997) stated that sorption is a fast reaction. However, Lick (2009) pointed out that some early studies on sorption were done in very short term, hours to a few days, but long term studies indicated that sorption kinetics were slower, from days to months (Lick, 2009). Parsons et al. (2007) indicated that the desorption rate from sediment is important for the bioaccumulation of contaminants in terms of bioavailable contaminant and the amount of organic carbon does not have a relation with the desorption rate in the sediment.

#### **2.2.1.7 Bioaccumulation**

Bioaccumulation is total accumulation of contaminants in the tissue of an organism through food or from water. Bioaccumulation is considered for the benthic organisms

living in the sediment. Bioavailability of the contaminants in sediments focuses on the factors that affect the fraction of total contaminant levels which are available for human or ecological receptors (NRCC, 2002). The bioavailability of contaminant for partitioning is expressed by biota-sediment accumulation factor (BSAF) which is the concentration in the tissue over concentration in sediment. It is used to determine the distribution of OM and to evaluate the bioavailability of contaminant. BSAF is dependent on properties of organics and solids, and lipid content of the organisms (NRCC, 2002).

### **2.2.2 Fate of PCBs**

Although PCBs are chemically stable in the environment, they can be affected by various partitioning and transformation mechanisms such as physicochemical weathering and biological degradation. While physicochemical weathering has an effect only on the distribution of the congeners in the environment without changing the structure, biological processes change the structure and may even lead to mineralization of the contaminant.

Physicochemical weathering includes processes such as sorption, volatilization, atmospheric transport, wet and dry deposition, etc. PCBs which are semi volatile compounds, tend to move among environmental compartments (air, water, soil, sediment) (Gouin et al., 2000). The fate of PCBs is related to the degree of chlorine. Less chlorinated congeners tend to be more mobile (Johnson et al., 2005). Therefore, lightly chlorinated congeners can be transported in the aqueous or gaseous phase. Those that are *ortho*-rich, on the other hand, can be volatilized more easily when compared to non-*ortho* congeners (Johnson et al., 2005). Upon release into the aquatic environment, PCBs adsorbed strongly to soil, with generally increasing adsorption as the degree of chlorination increases. If released to water and air, the important fate processes are adsorption to suspended matter and sediment and association with particulate matter after presence in the gaseous phase, respectively. Sorption to the

particulate phase will increase as the degree of chlorination of the PCB increases. PCBs are removed from the atmosphere by wet and dry deposition.

Another mechanism undergone by PCBs is anaerobic dechlorination. These substances are more willing to sorp to particle in water column and then settle and accumulate in sediment. In the sediment, these chemicals can be dechlorinated by anaerobic microorganisms (Fagervold et al., 2005). Especially, highly chlorinated congeners are more likely to be available in soils and sediments (Henry & DeVito, 2003).

### **2.2.3 Fate of PBDEs**

PBDEs can be released into the environment during their initial synthesis, incorporation into polymers or related finished products, during use of said products (Hale et al., 2003). Furthermore, their release can result from incineration of municipal waste, deposition to landfills, discharge to municipal sewage-treatment plants, or emission directly to the atmosphere as particulate matter (ATSDR, 2004). They can be adsorbed to particulate matter (dust) in indoor environment where they are produced (Lassen et al., 1999). When released to the environment, PBDEs are associated with soil or sediment due to their comparatively low volatility and aqueous solubility of the PBDEs (Hale et al., 2003). They generally do not undergo long-range transport, but some congeners in pentaBDE commercial mixtures, for example, 2,2',4,4'-tetrabromodiphenyl ether (BDE 47) and 2,2',4,4',5-pentabromodiphenyl ether (BDE 99), were observed in the Arctic regions (USEPA, 2010). This is probably due to transportation of these lower brominated congeners with dust particles to remote areas instead of transport in vapor phase (USEPA, 2010). If PBDEs find their way to sewage treatment plants, they can be concentrated in sewage sludges owing to the high organic content of sludge (Hale et al., 2003). Sediments and soils are sinks for PBDEs. These chemicals tend to deposit into sediments because of their persistence, low water solubility and high sorption capacity (De Wit, 2002).

The most important biotic and abiotic processes for the breakdown of PBDEs are biodegradation and photolysis, respectively (USEPA, 2010). Like PCBs, fate of PBDEs is affected by the physicochemical weathering processes such as sorption, volatilization, atmospheric transport, and wet and dry deposition, etc. (ATSDR, 2004). When the fate of PBDEs is investigated in water, for example, PBDEs much like PCBs, can be sorbed strongly to suspended solids and sediment, and bioconcentrated in aquatic organisms. Leaching into groundwater is not likely to occur. In the water column, they are not likely to be dominant due to their low water solubility. Since PBDEs have low volatility, their volatilization from soil or from sediment through the water column into air is not a dominant process (ATSDR, 2004). Photolysis is a probable transformation process for PBDEs. According to ATSDR (2004), information on the transformation and degradation of PBDEs in soil is limited. The extent to which PBDEs undergo direct photolysis in soils and sediment is unknown.

### **2.3 Modeling**

As a general term, models consider a process in a simpler form or representation of small versions of the real thing (Dunnivant & Anders, 2006). During modeling of a pollutant, mathematical models are important to explain its movement in the past and future. For mathematical modeling of pollutants, Schnoor (1996) indicated three scopes “(i) to gain better understanding of the fate and transport of chemicals by quantifying their reactions, speciation, and movement, (ii) to determine chemical exposure concentrations to aquatic organisms and/or humans in the past, present, or future and (iii) to predict future conditions under various loading scenarios or management action alternatives”. The movement of the pollutant is predicted by using fate and transport (F&T) processes. General mass balance approach for the fate and transport models is given below (Schnoor, 1996) in equation 2.1. Transport of the compound is defined by input and output in the equation, which include diffusion, dispersion and/or advection. The reaction term in the equation can be described by any

chemical reaction such as redox, reversible/irreversible reactions, precipitation, dissolution, hydrolysis, and/or biological transformation reactions (Schnoor, 1996).

$$\text{Accumulation with in Control Volume} = \text{Input} - \text{Output} \pm \text{Reaction} \quad 2.1$$

Models differentiate from each other according to fate mechanisms or contaminated media considered, assumptions, as well as numerical methods used to solve the model equations. Under this scope, various F&T models in the literature are reviewed in Section 2.3.1. After this review, the pathway quantification studies are examined in Section 2.3.2. to identify the pathways between congeners which are then used in the degradation term of the F&T model developed in this study.

### **2.3.1 Fate and Transport Models**

Various fate and transport models were reviewed in the literature and a list of models, as could be found in the literature, are given in Table 2.10. The models in Table 2.10 are compared in terms of (i) contaminant: total PCBs/PBDEs or individual congeners, and other chemicals, (ii) media modeled, (iii) mechanisms considered for transport and fate of contaminant, (iv) how degradation is handled in the model.

Firstly, models are compared for contaminants modeled. In Table 2.10, apart from PCBs and PBDEs, the models including other chlorinated compounds such as PCE and TCE are also reviewed since soil is porous media like sediment and TCE/PCE like PCBs/PBDEs can be biologically degraded to products. In the literature, numerous studies exist for modeling of PCBs in terms of total-PCBs, PCBs as homologs or individual congeners (Connolly et al., 2000; Farley et al., 1999; Shen et al., 2012; Zhang et al., 2008). Additionally, there are however much less number of studies about modeling of PBDEs (Davis, 2004; Rowe, 2009). As distinct from these studies, total maximum daily load (TMDL) of PCBs was also studied by using F&T models

(LimnoTech, 2007; Shen, 2011; Shen et al., 2012). In the literature, it is seen that some F&T models work for individual PCB and PBDE congeners (Davis, 2004; Oram et al., 2008b; Rowe, 2009; Shen, 2011; Shen et al., 2012; Zhang et al., 2008). However, after simulation, the output of the model is evaluated for total PCBs or PBDEs. There are other studies on modeling degradation of PCE, TCE, DCE and their reactions between them. Furthermore, the models for other chemicals indicated in Table 2.10 are also reviewed.

Secondly, models are examined for the media modeled. The literature review indicates that the transport and fate mechanisms of these models differentiate from each other depending on the media modeled. Therefore, media is an important parameter for model development. The reviewed models are built upon soil, sediment, water or combinations of these media with water (Table 2.10). As different from other studies which mention one sediment compartment, Ambrose (1983), Shen et al. (2012) and Boyer et al. (1994) use two sediment layers; surface and deep sediment.

The third one is for fate and transport mechanisms used in the models. Several modeling studies evaluating fate mechanisms are carried out for anaerobic dechlorination, metabolism, photolysis, hydrolysis, dechlorination with zero-valent iron, organic matter mineralisation, acid/base dissociation, redox, sorption, dissolution/precipitation, speciation, complexation, dissolution/precipitation, acid/base dissociation. It is demonstrated in Table 2.10 that the common ones for sediment are microbial degradation, especially for PCBs. Sorption/desorption is another important fate mechanism. It is dealt in the mass balance equation as partitioning coefficient (e.g. Boyer et al. (1994), Zhang et al. (2008)) or as a sorption/desorption term when only dissolved or particulate phase is modeled (e.g. Ambrose et al. (1983, 1988)). Studies investigate the partitioning of the contaminant to suspended solids, dissolved, freely dissolved or biosorped phase. As a different study, Farley et al. (1999) investigate the effect of phytoplankton on PCBs since phytoplankton controls the partitioning of PCBs to suspended solids in the water.

Table 2.10 Models used in various media contaminated by halogenated compounds (e.g. PCBs, PBDEs, PCE, TCE)

Model	Contaminant	Media	Transport/Fate Mechanisms	References
	t-PCB	Water, surface sediment	Transport:diffusion (w <sup>a</sup> ), resuspension (w), volatilization (w), deposition to sediment, advection, dispersion applied to sediment particle and particulate PCBs (s <sup>b</sup> )	Connolly et al. (2000), Russell et al. (2006)
	(2,3,7,8-TCDD) and homolog-PCB groups	Surface sediment, water	Transport: tidal dispersion (w), volatilization (w), tributary/external input(w), settling, resuspension, diffusive exchange between water and pore water, burial(s) Fate: Anaerobic dechlorination	Farley et al. (1999)
	TMDL homolog PCBs or congeners	River water, surface and deep sediments	Transport: Settling, diffusion, volatilization (w)	Shen (2011), Shen et al. (2012)
	PCB/PBDE congeners	Water, sediment	Transport:External loads(w), settling, resuspension, burial(s), diffusion Fate: first order degradation	Rowe (2009)
	PBDE homologs	Air, water, sediment	Transport:Depositon(air), settling, resuspension, burial (s), (bi-directionsl) diffusion Fate: aerobic and anaerobic biodegradation, direct photolysis, reaction with OH radicals	Bogdal et al. (2010)
	PCB/PBDE congeners	Water, sediment	Transport: External load(w), volatilization (w), settling, resuspension, diffusion, burial(s) Fate: Degradation including metabolism, photolysis, and hydrolysis.	Oram et al. (2008a) Davis (2004)
	PCB individual congeners	Water	Transport: Evaporation Fate: Biosorption and biodegradation	Dercova et al. (1998;1999);
	PCB individual congeners	Water	Fate: Degradation, Abiotic processes such as adsorption and volatilization	Commandeur et al. (1995)

Table 2.10 (*continued*)

<b>Model</b>	<b>Contaminant</b>	<b>Media</b>	<b>Transport/Fate Mechanisms</b>	<b>References</b>
LM2 Model	Total of 54 PCB congeners	Water, sediment	Transport: Diffusion, resuspension, settling, burial(s) Fate: Volatilization(w)	Zhang et al. (2008)
	PCDD, PCDF and PCB congeners	Water, soil, sediment	Fate: Biodegradation and photolysis	Sinkkonen et al. (2000)
MICHTOX	<sup>c</sup>	Water, sediment	Transport: Diffusion, resuspension, settling, burial(s) Fate: Volatilization(w)	Endicott et al. (2006)
	TCE	Aquifer, groundwater	Transport: Advection, dispersion Fate: microbial degradation	Chen-Charpentier & Kojouharov, (2008)
	TCE, DCE, VC	Aquifer, groundwater	Fate: Dechlorination with zero-valent iron, sorption, desorption	Schafer et al. (2003)
	TCE	Subsoil and groundwater	Transport: Advection, dispersion Fate: Microbial degradation, sorption	Travis and Rosenberg (1997)
	PCE, TCE, DCE, Ethylene, Ethane	Aquifer, groundwater	Transport: Advection, dispersion Fate: Biological/Chemical reactions, adsorption	Xu et al. (2012)
	PCE, TCE, DCE, VC	Subsoil and groundwater	Fate: Biodegradation	Yu and Semprini (2004)
	Any chemicals	Soil, groundwater, surface water	Advective-dispersive transport model with non-linear reaction term	Chamkha (2007)
Recovery	<sup>d</sup>	Water, surface and deep sediments	Transport: Diffusion, resuspension, settling, burial(s), volatilization(w), external loads (w) Fate: Photolysis, hydrolysis, microbial degradation	Boyer et al. (1994)



Table 2.10 (continued)

Model	Contaminant	Media	Transport/Fate Mechanisms	References
TOXIWASP	<sup>e</sup>	Water, surface and deep sediments	Transport: External loads(w), volatilization(w), settling, resuspension, burial, dispersion, diffusion Fate: Degradation(hydrolysis, photolysis, microbial degradation)	Ambrose (1983)
WASP4	<sup>f</sup>	Water, sediment	Transport: External loads(w), volatilization(w), settling, resuspension, burial, dispersion, diffusion Fate: Degradation(hydrolysis, photolysis, microbial degradation)	Ambrose et al. (1988)
CANDY		sediment	Transport: Diffusion, burial, bioirrigation Fate: Slow organic matter mineralisation kinetics, equilibrium reactions	Mucci et al. (2003) as cited by Allan by Stegemann (2007)
MEDIA	Metals	sediment	Transport: Advection, diffusion, bioturbation Fate: Organic matter mineralisation, acid/base dissociation, redox, dissolution/precipitation, sorption	Meysman et al. (2003) as cited by Allan by Allan and Stegemann (2007)
HYTEC	Ions, organics, colloids	sediment	Transport: Advection, colloidal movement Fate: Speciation, complexation, dissolution/precipitation, acid/base dissociation	Van der Lee et al. (2003) as cited by Allan by Allan and Stegemann (2007)
TRANSCAP-1D	Arsenic	sediment	Transport: Diffusion, advection, bioirrigation Fate: Sorption	Locat et al. (2003) as cited by Allan by Allan and Stegemann (2007)
D.S.D 1D	Silica	sediment	Transport: porewater diffusion, sorption, Fate: First order degradation rates	House et al. (2000) as cited by Allan by Allan and Stegemann (2007)
Capping Design	PAHs, PCBs	sediment	Transport: Advection, diffusion, biodiffusion Fate: Degradation, sorption	Palermo et al. (1998) as cited by Allan by Allan and Stegemann (2007)

<sup>a</sup>Mechanisms only in water, <sup>b</sup>Mechanisms only in sediment, <sup>c</sup>Toxic Chemicals: Organics (congener or total PCBs) and Metals, <sup>d</sup>: Chlordane, DDT, Dieldrin, Lindane, Aroclors 1242, 1248, 1254 and 1260, Benzene, Chlorobenzene, Ethyl Benzene, Pentachlorophenol, Phenol, Toluene, Anthracene, Benzo(a)pyrene, Naphthalene, Chloroform and Compound Not Listed. <sup>e</sup>Toxic Chemicals: Organics and Metals, <sup>f</sup>Toxic Chemicals: ionized and nonionized organics and Metals

In the literature, modeling studies attempt to evaluate various transport mechanisms such as the diffusion, pore diffusion, bio-diffusion, burial, advection, colloidal movement, bioturbation, bioirrigation, resuspension, and/or settling. These models are simulated in one, two, and/or three dimensional transport modeling. As different from other studies, Farley et al. (1999), Russell et al. (2006) and Connolly et al. (2000) perform hydrodynamic transport (including the physical properties of the river or water such as freshwater flows, tidal motion, salinity and density-driven currents), sediment transport, chemical fate modeling and bioaccumulation in river water, sediment and fish. Additionally, Connolly et al. (2000) dealt with different transportation tendencies of PCBs on cohesive and non-cohesive sediments in upper Hudson River. The studies reviewed identify settling, resuspension, burial and diffusion as the major transport processes for a pollutant bound onto sediment.

The last review item is regarding handling the degradation term. In some studies, details about type of degradation is not given (Table 2.10). In other studies, microbial degradation is defined as the dominant process for sediment among hydrolysis and photolysis. Typically, biodegradation is handled for total concentration, dissolved or particulate phase in degradation term of mass balance equation. A number of studies consider the use of empirical equations for calculation of reaction rates (Commandeur et al., 1995; Dercova et al., 1999; Dercova et al., 1998) in biodegradation term including estimations of half lives of some congeners (Sinkkonen & Paasivirta, 2000), and biosorption rate (Dercova et al., 1999). In the studies considering PCBs/PBDEs as individual congeners (Table 2.10), biodegradation rate is either neglected or is assumed mostly as first order degradation rate. However, rate constant is not assumed or considered together with the effects of degraded products except for studies on PCE and TCE (Chen-Charpentier & Kojouharov, 2008; Travis & Rosenberg, 1997; Xu et al., 2012).

In the studies of PCE and TCE contaminated media, the effects of degraded products are considered during remediation of subsurface and groundwater contamination

(Chen-Charpentier & Kojouharov, 2008; Travis & Rosenberg, 1997; Xu et al., 2012). Xu et al. (2012) studied that PCE and daughters can be dechlorinated by a combination of zero-valent iron (ZVI) and anaerobic microbial communities (FeMB) in contaminated groundwater and subsurface soil. Five component transport model (PCE→TCE→1,1DCE→ethylene→ethane) in three dimensions is used to simulate mother-daughter kinetic chain reactions. Additionally, Schafer et al. (2003) decreased TCE to its daughter products by ZVI. Yu and Samprini (2004) dealt with kinetic reaction equations for bioaugmentation with dechlorination cultures to completely transform PCE and TCE to ethylene by reductive dechlorination. There are also other methods regarding TCE dechlorination which includes co-metabolism (Chen-Charpentier & Kojouharov, 2008). All these models for PCE and TCE indicate that transport and fate processes include the effects of degraded products (TCE, DCE, ethylene or ethane) in a model.

Some of the studies discussed above are explained in detail in terms of mass balance equations and use of parameters and their estimation. From models reviewed, five models are selected for this detailed evaluation since such information is readily available in the corresponding sources; Recovery, WASP4, TOXIWASP, LM2 and PCB Model for Hudson River (PMHR) models). Moreover, two equations discussed in Chapra (1997) and Thomann and DiToro (1984) are also evaluated here with MICHTOX model and mass balance for surface sediment in Qi (2003). In these approaches, either mechanisms different from the mentioned models or model equations and some information on different equations to the same mechanisms are examined. The equation and details about these models are tabulated in Appendix Table C.1, C.2, C.3, C.4, C.5 and C.6. The models and equations reviewed are described and compared below with respect to media, processes, parameter estimations, dimensions, and assumptions made in the models as well as numeric solutions.

### 2.3.1.1 Media

All models are applied to sediment and water. It is seen that some models can be applied to various water environments such as rivers, harbors, estuaries and lakes (Recovery, WASP4 and TOXIWASP) while others can be applied to lakes and rivers (LM2 and PMHR models). Modeling of both surface and deep sediment are explored in Recovery and TOXIWASP while only surface sediment is evaluated in other models.

### 2.3.1.2 Transport Processes and Reactions

Transport processes considered in five models for surface sediment are pore water diffusion, burial, settling and resuspension. Also bioturbation effect on mechanisms between overlying water and surface sediment is added by Recovery model. When all mechanisms are reviewed in Recovery Model and equation in Chapra (1997), it is seen that they are the same. When reaction terms are compared for these models, common reactions in all models are biodegradation and sorption. However, other transformation terms such as hydrolysis, oxidation, photolysis and/or volatilization are also considered by TOXIWASP, LM2 and WASP4. Additionally, LM2 and PMHR models include bioaccumulation.

**Sorption:** Models allow for two phase- or three phase- sorption of the contaminant. Recovery model allows for two phase- sorption (particulate and dissolved). Recovery model assumes weight fraction of organic carbon in the solid matter. However, in TOXIWASP model, partitioning is applied for three phases; sorbed to particulate, biota and dissolved phases. LM2 model simulates three organic carbon states: biotic carbon (BIC), particulate detrital carbon (PDC), and dissolved organic carbon (DOC). Sum of BIC and PDC represents particulate organic carbon ( $POC = BIC + PDC$ ). When BIC which is in live phytoplankton biomass settles to sediment, it converts to PDC derived from phytoplankton decomposition, zooplankton excretion, and allochthonous sources (Zhang et al., 2008). Therefore, only partitioning of PDC and

DOC of contaminant is evaluated in surficial sediment. While PCB modeling is done for 4 phases (sorbed to PDC, BIC, DOC, and dissolved) in water, three phases (except BIC) are considered in sediment due to conversion of BIC to PDC in sediment. Farley et al. (1999) consider the partitioning of PCBs between three phases: solid bound, DOC bound and freely dissolved phases. WASP4 allows partitioning of the contaminant to 3 types of solids during one simulation. Three solid types are descriptive solids concentration field, descriptive solids concentration field with specified solids transport rates and simulated total solids. Therefore, five phases (DOC bound, freely dissolved and bound to 3 types of solids) are included. Environmental parameters affecting partitioning are sediment concentrations (suspended and benthic sediments), organic carbon fraction (suspended and benthic sediments) and dissolved organic carbon concentration.

**Settling/Resuspension/Burial:** All reviewed models including total, particulate and/or dissolved phases of the contaminant were evaluated for settling, resuspension and burial processes. For settling process, the contaminant in particulate phase is considered in all models. For resuspension process, while total contaminant in the sediment is modeled by Recovery model and Chapra (1997), particulate phase of the contaminant in the sediment is evaluated by other models. For the burial process, particulate phase of the contaminant in the sediment is considered in PMHR and TOXIWASP while total contaminant in the sediment is used for Recovery, Chapra (1997) and Thomann and DiToro (1984). The partition in burial process in LM2 and WASP4 is not discussed since general mass balance equation applied to water column and benthos is given (Appendix C Table C.5).

**Diffusion:** Mass balance equations of the models indicated that the models are set for pore water diffusion, diffusion through mixed and/or deep sediment, diffusion/dispersion process. Accordingly, Recovery model investigate the fate of the contaminant by diffusion through mixed and deep sediment while LM2, WASP4, TOXIWASP and PMHR models take into account only diffusion in surficial sediment.

They consider DOC bound and dissolved phases separately for diffusion process while both are taken as one phase in the Recovery model. In TOXIWASP model, pore water diffusion is controlled by vertical concentration gradient and vertical diffusion coefficient contaminant. Pore water diffusion acts on contaminant in dissolved phase between overlying water and surface sediment (Ambrose et al., 1983). Diffusion/Dispersion process in LM2 is the same as in WASP4. As different from in LM2, WASP4 also evaluates pore water diffusion. On the other hand, Qi (2003) specifies mass balance for dissolved form of the contaminant in the pore water while other models consist of mass balance of total contaminant (sum of dissolved plus particulate forms).

**Degradation:** Degradation is handled in Recovery, TOXIWASP, PMHR, Chapra (1997), Tomann and DiToro (1984), and WASP. They consider photolysis, hydrolysis and biodegradation (Appendix C). They are evaluated as first or second order decay. Total, particulate and/or dissolved phases of the contaminant were considered for the degradation term. Details about this task is not given for all models. Models including details are only explained here. For Recovery model, first-order decay is used and equations are defined for the water phase. During model development for degradation in deep sediments, total concentration (dissolved and particulate) of the contaminant is used in the model. However, estimation of decay coefficients is not explained. In TOXIWASP, second order degradation is considered and the model equation shows that three phases can be utilized and degraded by microorganisms using different rate constants for each phase. In PMHR, model considers only dissolved contaminant (and not DOC or particulate) while calculating degradation. On the other hand, Farley et al. (1999) state that aerobic degradation and anaerobic dechlorination are not significant processes which affect fate of PCBs in the Lower Hudson River. Therefore, degradation rate constants are assumed as negligible in their model. Chapra (1997) handles degradation by a rate constant for total amount of contaminant while Thomann and DiToro (1984) express two different rate constants for two phases: particulate and dissolved (Appendix C Table C.6). WASP model summarizes environmental and chemical properties affecting biodegradation rate constants. Accordingly,

environmental parameters affecting biodegradation are water column temperature and active bacterial populations (in suspended and benthic sediments). In LM2, partitioning of organic carbon is estimated. Fraction of contaminant is then calculated.

### **2.3.1.3 Carbon Mass Balance**

In carbon mass balance, distribution of organic carbon is evaluated in the modeling region depending on time. For example, LM2 model conducts a carbon mass balance. The rates such as settling, resuspension, decay rates affect the organic carbon fraction (Zhang et al 2006, part 4 Ch3). Therefore, organic carbon is also considered as a variable. In contrast to LM2 model, the effect of carbon is evaluated by partitioning coefficient in the mass balance equation of contaminant in Recovery, TOXIWASP, and PMHR models. In Recovery model, solid mass balance is performed to estimate settling, resuspension or burial velocity under steady state conditions. TOXIWASP has a mass balance for change of solid in water and sediment since partitioning of PCBs to solid impacts their fate.

### **2.3.1.4 Estimation of Parameters**

Since sediment properties are highly variable and are difficult to measure, semi empirical approximations and even parameterizations of some transport processes are used in some circumstances (Lick, 2009). Lick (2009) states that significant processes and parameters should be evaluated independently in order to minimize non uniqueness of solutions. Therefore, each process of deposition/erosion, molecular diffusion, and diffusion is evaluated separately by means of the mass balance approach. Estimations of common processes which are sorption, settling, resuspension, diffusion, burial and degradation parameters of models discussed above, are explained in this section.

**Sorption:** The partitioning coefficients are important parameters to be estimated in the mass balance equation. The estimation of the partitioning coefficients and number of

phases are discussed here for each model. In Recovery model, as discussed in previous section, corresponding parameters are dissolved and particulate fractions of contaminants in water and pore water to be used in diffusion and settling mechanisms, respectively. These fractions are estimated by the equations in Appendix C Table C.1. In TOXIWASP model, dissolved fraction of contaminant in the water, and sorbed fraction of contaminant on sediment and onto biological phase are the parameters formulized in Appendix C Table C.2. In LM2 model, the equations for both three and two phase partitioning to be used for total PCB are considered (Appendix C Table C.3). In LM2, two phase partitioning is selected. In WASP4 model, the partitioning coefficients for solids and DOC is calculated from linear form of Freundlich isotherms. The empirical equations are given in Appendix C Table C.5. If  $K_{oc}$  values are not known,  $K_{oc}$  is estimated from the equation correlating with  $K_{ow}$  (Appendix C Table C.5). The model states that solid concentration should be used in the estimation of the solid partitioning coefficient which can be seen in Appendix C Table C.5. The DOC bound, solid bound and dissolved fractions are estimated by considering total concentration in phases and from equations in Appendix C Table C.5.

**Settling/Resuspension/Burial:** Lick (2009) expresses the definition of erosion (resuspension) rate as “total flux of sediment from sediment bed into the overlying water in the absence of deposition”. Particles in suspension have movement horizontally due to gravitational and turbulent forces (Lick, 2009). The estimation of settling, burial and resuspension velocities in the models is discussed here. The settling velocity is estimated by measuring directly or predicting from literature as considering textures of sediment, and using solid/carbon mass balance. Resuspension is calculated by solid/carbon mass balance while burial is estimated by solid/carbon mass balance or analysis of the box cores for each sampling location (Zhang et al., 2008).

The settling velocity or one of the aforementioned velocities is calculated by solid mass balance in Recovery model and Chapra (1997) provided that other two velocities are known (Table C.1). This is done for settling velocity in WASP4 that movement of



sediment in the bed is assumed by using one of two options, constant bed and variable bed volume options. The constant bed volume option explains that bed sediment volumes remain constant and sediment concentration of the bed changes according to net flux of sediment. This is expressed by sedimentation velocity and the flux equations for upper and lower beds are given in Table C.5. The variable bed volume option is that the sediment concentration is constant and the bed volume changes according to deposition and scour. Second option is also considered for TOXIWASP model.

In LM2, burial velocity is also estimated from the analysis of the box cores for each sampling location (Zhang et al., 2008). Then, resuspension rate is calculated from the equation done for mass balance of PDC for sediment iteratively by settling velocity (Appendix C Table C.3). However, this equation is used for the water depth greater than 100 m since non-wave-induced resuspension that included bottom current-induced resuspension and resuspension caused by bioturbation only (Zhang et al., 2008). For water depth less than 100m, an empirical wave induced resuspension equation developed by LM2 model project is used due to manipulation in application of first equation. Moreover, burial velocity is estimated by using mass balance equation for solids in the water and the sediment.

$$v_b = \frac{Q m_{in} - m}{A (1 - \phi)\rho} \quad 2.2$$

where  $v_b$ : burial velocity (m/yr),  $Q$ : flow rate (m<sup>3</sup>/yr),  $m_{in}$ : inflow suspended soil concentration to water (g/m<sup>3</sup>),  $m$ : suspended soil concentration in water(g/m<sup>3</sup>),  $\phi$ :porosity,  $\rho$ :bulk density (g/m<sup>3</sup>) and  $A$ : Area of water column (m<sup>2</sup>). When burial velocity is measured, resuspension velocity can be estimated from mass balance for solids in the sediment layer under steady state condition. The equation is:

$$v_r = v_s \frac{m}{(1 - \phi)\rho} - v_b \quad 2.3$$

where  $v_r$ : resuspension velocity (m/yr) and  $v_s$ : settling velocity (m/yr).

### **Diffusion/Dispersion:**

Diffusion/Dispersion is estimated by using mass transfer coefficient for diffusive sediment-water exchange in the equation for Recovery model (Table C.1), vertical dispersion coefficient and characteristic mixing length for TOXIWASP (Table C.2). On the other hand, LM2 model assumes that only vertical exchanges exist in the sediment layer. Then the bulk dispersion/diffusion coefficient is estimated by using equation in Table C.3. The mixing coefficient is estimated by using a thermal balance model (Table C.3) at the interfaces. While burial and resuspension mechanisms in Chapra's equation are responsible for dissolved and particulate phases, diffusion is relevant only for the dissolved phase.

### **Degradation:**

The estimation of degradation rate constant and its relationship with the contaminant partitioning to particulate and dissolved phases are investigated in the selected models. Recovery and LM2 models do not discuss estimation of biodegradation parameters and use first order degradation. TOXIWASP model using second order degradation estimates the rate constant by Monod equation which is given in Table C.2.

In WASP4 model, the relationship between order of rate constant and rate is expressed for any contaminant. It is given in Table 2.11. For kinetic reactions, Level 1 of kinetic reactions expresses the first order decay. Rate constant is estimated from half-life equations if half-lives are provided. Level 2 also includes first order decay, but it is used when spatial change is considered in environmental conditions. Level 3 additionally evaluates time variation. Degradation rate constant is based on second order and its overall is first order rate constant. Level 4 computes the simulation of transport products by defining appropriate yield coefficient (Table 2.11). Accordingly, Level 3 seems appropriate for the degradation of the individual PCB/PBDE congeners provided that some parameters such as yield coefficient are available.

Table 2.11 Transformation Rate and Constant Estimations in WASP4 Model

Complexity Levels	Complexity Explanation*
1	$S_{k1} = -\sum K_i C_1$ and $K_i = 0.693/T_{Hi}$
2	$S_{kc} = -K_{Tc}(x)C_1$
3	$S_{kc} = K_{Tc}C_1$ and $K_{Tc} = \sum_i \sum_j \sum_k k_{ijk} [E]_k f_{ijc}$
4	$S_{kc1} = \sum_c \sum_k K_{kc} C_c Y_{kc1} \quad c=2,3$  $S_{kc2} = \sum_c \sum_k K_{kc} C_c Y_{kc2} \quad c=1,3$  $S_{kc3} = \sum_c \sum_k K_{kc} C_c Y_{kc3} \quad c=1,2$

\*  $C_1$ : chemical concentration, mg/L,  $K_i$ : first order decay constants,  $\text{day}^{-1}$ , including:  $K_{HN}$ ,  $K_{HOH}$ =neutral, acid, and base catalyzed hydrolysis constants,  $\text{day}^{-1}$ ,  $K_{BW}$ ,  $K_{BS}$ : water column and benthic biodegradation constants,  $\text{day}^{-1}$ ,  $K_F$ : photolysis constant,  $\text{day}^{-1}$ ,  $K_O$ :oxidation constant,  $\text{day}^{-1}$ ,  $K_V$ : volatilization constant,  $\text{day}^{-1}$ ,  $K_E$ :extra constant,  $\text{day}^{-1}$ ,  $T_{Hi}$ : half lives, days,  $T_{HBW}$ - $T_{HBS}$ : water column and benthic biodegradation half lives, days where,  $K_{Tc}(x)$ : spatially variable lumped first order decay rate constant for chemical “c”,  $\text{day}^{-1}$

### 2.3.1.5 Numerical Solutions

TOXIWASP and LM2 models are developed by adaptation of transport framework of Water Analysis Simulation Program (WASP) (Ambrose et al., 1988; Di Toro et al., 1982). The chemical transformation part of WASP4 and TOXIWASP is based on Exposure Analysis Modeling System (EXAMS) (Burns et al., 1982). In brief, these models are derived from similar models and LM2 Report (Zhang, 2006) states that the same numerical approach of WASP4 framework is also used for LM2 model. Accordingly, the numerical solution of these models is explicit backward finite difference. There is no information about numerical solution or solution of mass balance equations of PMHR model (Farley et al., 1999). The mass balance equations of Recovery for surface sediment are solved by Adaptive-step-size Runge Kutta 4<sup>th</sup> (Crank Nicholson for deep sediment).

To sum up the evaluation of the models, some models developed for the fate of the pollutant in the bed sediment have the problem of not being applicable to each field due to no selection for dimension number during modeling, no flexibility of parameterization of input/output data, or use of probabilistic approach. Moreover, other models involve missing processes and/or lack of depth depending characteristics during the application of the fate of the pollutant in the bed sediment (Allan & Stegemann, 2007). Therefore, a model which has the ability to be applied to various field conditions and different HOCs (such as PCBs) is needed. Another task is that when individual PCB/PBDE congeners are degraded and dehalogenated in sediment, the mass balance equation should be performed for all degraded and accumulated congeners. This task is not dealt with in the literature.

### **2.3.2 Models for Degradation Pathway Identification of PCBs and PBDEs**

Apart from F&T models, approaches for quantification and identification of pathways of PCBs/PBDEs by statistical tools were also reviewed from the literature to use the sequential degradation of PCBs/PBDE congeners in biodegradation term of F&T models in detail.

The dehalogenation process has been investigated for a long time as a research topic. Degradation mechanisms of PCBs and PBDEs in the environment have been examined by biological and modeling studies. Biological data, although crucial to better understand the degradation mechanisms of the compounds in the environment (Wei et al., 2013), is limited since it requires a long time to test all microorganisms or different methods under laboratory conditions. However, modeling dehalogenation can help find new degradation pathways which may not have been identified previously in the laboratory. One advantage of such models is that they can aid in the investigation of effective remediation strategies and better management of the environment.

There are two types of dehalogenation model studies in the literature, (i) identification of pathways (Hughes et al., 2010, 2015; Karcher et al., 2004, 2007) and (ii) quantification of pathways with biologically confirmed data (Bzdusek et al., 2006a; Bzdusek et al., 2006b; Demirtepe et al., 2015; Imamoglu et al., 2002; Imamoglu et al., 2004; Wei et al., 2013; Zou et al., 2014).

### Identification of pathways

In the models for identification of pathways, numerical and statistical methods are used to identify the possible pathways. Studies (Hughes et al., 2010, 2015; Karcher et al., 2004, 2007) aimed to find dechlorination pathways of PCBs. Karcher et al (2004) developed a statistical model to determine the distribution of PCBs in Hudson River sediments by using comparison of relative abundance between original Aroclor mixtures and sediment data without knowledge of the source in the field. In the study, original Aroclor mixtures were used in Frame's (1996) Aroclor Congener Distribution Data (FACDD) consisting of percent weight relative abundances for 209 PCB congeners in multiple lots (totaling 17) of eight different Aroclor mixtures. By using these data, tracker congeners, which are called as correlated congeners, are defined. The correlated congeners have the benefit that these congeners, which have constant relative ratio, do not have pattern matching or bias problems in total PCB measurements (Karcher, 2005). Hence, PCB transformation was identified with shifts in tracker pairs from the relative abundance ratio of congeners in environmental samples to congeners in Aroclor mixtures.

After Karcher et al. (2004), a numerical method is developed to determine alternative dechlorination scenarios of sediment systems through congener pair relationship. The study performed statistical analysis using the natural dechlorination *in situ* (SANDI) method. An actual weathered sediment data collected from Hudson river was evaluated by this method. Two weathering methods were applied to understand the dechlorination pathways of PCB congeners in the environmental data by (i) applying Aroclors mixtures randomly until only monochlorinated congeners remain and (ii)

applying Aroclors mixtures based on the position of chlorine and the chlorine configuration; e.g. flanked and unflanked, *meta* or *para* removal. As a result of Karcher et al. (2007) study, the model indicated the removal of flanked chlorines with following *meta* chlorines is more preferential in the field of Hudson river sediment.

Another model for identification of pathways was by Hughes et al.(2010). In this study, possible dechlorination pathways of PCBs were identified by using the classification tree approach, which is a statistical method to predict pathway sets based on explanatory attributes. These attributes consist of physicochemical properties of the parent congener, target positions on parent congener considering configuration and homologue of the parent congener. The pathway selection was done considering the eight dechlorination processes given in the literature (Bedard, 2003). As a study by the same group (Hughes et al., 2015), a Monte Carlo analysis was applied to understand analytical uncertainties of individual congeners especially coeluting congeners. Hughes et al. (2015) pointed out that this work would help evaluate the extent of dechlorination.

#### Quantification of pathways

A model for quantification of pathways was developed by Imamoglu (2001) to identify the fate of PCBs in sediments by using biologically confirmed PCB data. The model is called as “anaerobic dechlorination model” and it is based on minimization of objective function by the sum of squares of differences between predicted and sample congener profiles and during simulation (Imamoglu, 2001). The model has two principles: (1) mass balance between dechlorinated (mother) and accumulated (daughter) congeners (2) pathways confirmed from laboratory and field studies are used. The mass balance is provided by subtraction of the abundance of mother to add to the abundance of daughter in a pathway. The pathways were identified according to different PCB dechlorination processes based on contaminated sites such as Activity H, H', Q, N, etc. taken from studies of Bedard & Quensen III (1995) Quensen III & Tiedje (1997), Bedard (2001). Sediment PCB profile, original source profile (either

Aroclor or t=0 day for microcosm PCB data) and possible reaction pathways are input data for the model. Model was applied to Ashtabula and Fox River sediments, USA (Imamoglu et al., 2002; Imamoglu et al., 2004). Results indicated that the dechlorination in the sediment was explained by the model successfully.

The model then was modified by Bzdusek (2005). While the model developed by Imamoglu considered all pathway possibilities described to model equally, Bzdusek (2005) added constraints to the model. A preferential reaction order is defined as arrangement of targeted chlorines from highest to lowest: doubly-flanked *meta* > doubly flanked *para* > singly-flanked *para* > singly-flanked *meta* > unflanked *meta* or *para* on di- or tri- substituted ring > isolated *meta* or *para* chlorine. The model was applied to the Lake Hartwell and Sheboygan River sediments (Bzdusek et al., 2006a; Bzdusek, 2006b) and the studies revealed the existence of anaerobic dechlorination and pathways in the sediment.

ADM approach under the name of stochastic least squares debromination pathway model was used by Wei et al. (2013) to identify the photolytic debromination pathways of PBDEs in hexane by sunlight. They revealed preferential pathways and debromination rate constant on the number of bromines in the PBDE molecule by the model.

An analogue Markov Chain Monte Carlo algorithm was developed by Zou et al. (2014) to identify the photolytic debromination pathways of PBDEs in hexane by sunlight. The model can be applied to biotic and abiotic debromination processes (i.e. microbial, photolytic, or both in natural environments).

Demirtepe (2012) also used anaerobic model by Bzdusek (2005) by addition of a goodness of fit parameter, cosine theta and by minimizing objective function for chlorinated congeners. In contrast to Bzdusek (2005), Demirtepe (2012) added another

dechlorination activity, namely T (Bedard et al., 2005). In the study of Demirtepe et al. (2015), dechlorination pathways were defined according to targeted chlorines including numbers and relative positions of chlorines. Accordingly, major pathways of PCBs in sediment microcosms of Baltimore Harbor were quantified successfully and dechlorination rate and toxicity change were evaluated.



## CHAPTER 3

### MATERIALS AND METHODS

Development of a model for the prediction of congener specific HOC concentrations in sediments that take into account anaerobic degradation is carried out as a two-tier task: (1) prediction of anaerobic dehalogenation rate constants, (2) prediction of congener specific HOC concentrations in sediments. The first task is handled through use of a modified version of a previously developed anaerobic dehalogenation model. This model uses laboratory microcosm HOC data (from the literature) as input to yield anaerobic dehalogenation pathway specific degradation rate constant data as output. The second task is handled through development of a new F&T model for sediment bound HOCs. Here, environmental HOC data (from the literature) is used as input to predict concentrations of sediment bound HOCs. The interrelations of the two tasks are shown in Figure 3.1. This chapter is divided into three parts where the first two subsections describe the anaerobic dehalogenation model and FTHP model, and the third subsection describe in detail the data sets and how they were handled before being used as input into the models.

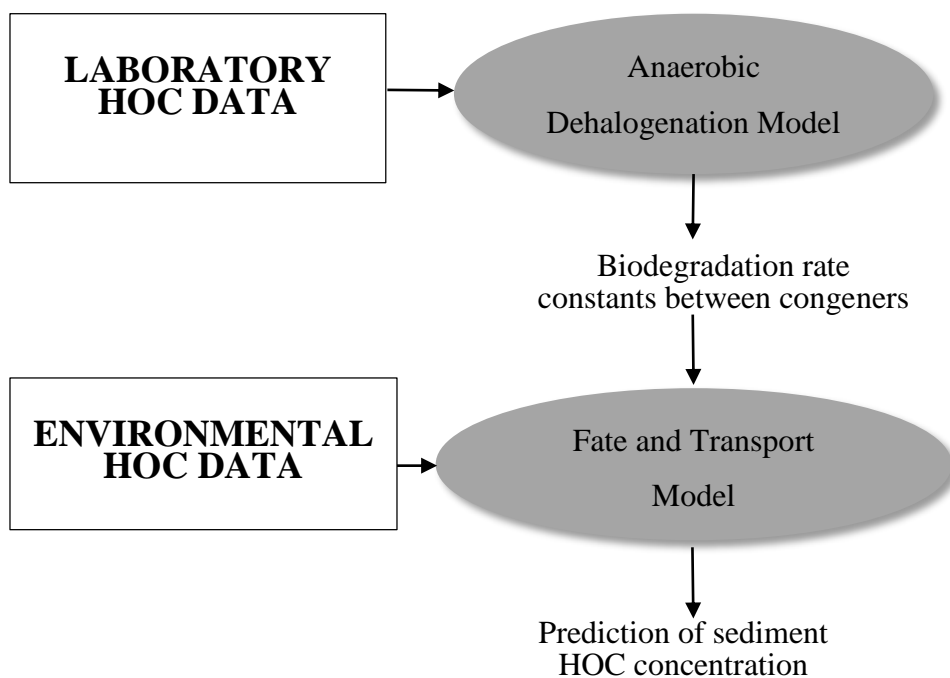


Figure 3.1 Interrelationship between ADM and FTMP models

### 3.1 Description of Terminology

*Coeluting congener:* During analytical determination of PCBs, some congeners can not be determined/quantified individually from the chromatogram. These are named coeluting congeners. IUPAC No of these congeners are used, separated by a slash, e.g. 28/31.

*DechlorInput:* It is the name of the input file of ADM prepared in Excel. File contains: degradation pathways, measured congener profiles and congener IUPAC No.

*Degraded:* Degraded is an array used in the program of FTMP model. It is sum of two arrays; Degradedm and Degradedd.

*Degradedd:* Degradedd is an array used in the program of FTMP model. Mass balance equation in FTMP model is run for each congener in input file. Biodegradation rate is calculated only for the congeners including pathways. Biodegradation rates of the congeners which are accumulated (increased) are filled in an array, Degradedd.

*Degradedm*: Degradedm is an array used in the program of FTHP model. Mass balance equation in FTHP model is run for each congener in input file. Biodegradation rate is calculated only for the congeners including pathways. Biodegradation rates of the congeners which are degraded (decreased) are filled in an array, Degradedm.

*Dehalogenation Activity*: A set of anaerobic dehalogenation pathways/reactions identified through laboratory studies in the literature, which describe halogen removal from specified positions on the structure of the compound. E.g. removal of doubly flanked *para* chlorines from chlorobiphenyl structure of PCB congeners. A dehalogenation activity may contain any number of dehalogenation pathways/reactions.

*Dehalogenation Pathway/Reaction*: The dehalogenation reaction where one congener is transformed into another, due to replacement of one of its chlorine with a hydrogen atom. E.g. 2345-2345 → 235-2345.

*Doubly flanked*: It is presence of chlorine in both adjacent positions. For example, in the structure 2345-CB, chlorine in position 4 (*para* position) is doubly flanked with chlorines in *meta* positions denoted by 3 and 5.

*FindPathway function*: It is a function in ADM to list all relevant anaerobic dehalogenation pathways of congeners according to a dechlorination activity. Input data to the function are: (1) list of congener IUPAC numbers, (2) description of dehalogenation activity.

*Mother-Daughter congener*: During anaerobic dehalogenation reactions, a chlorine from one congener is replaced by a hydrogen atom, resulting in another congener. The reactant of this reaction is called a mother congener (i.e. its concentration is reduced), while the congener that is the product of the reaction is called a daughter congener (it is accumulated as a result of the reaction).

*Patterns*: Patterns can be substitutions or congeners defined in a dehalogenation activity before simulating FindPathway function.

*Predicted congener profile*: Congener profile at initial time (i.e., an Aroclor mixture profile from Frame et. al (1996), or t=0 d of microcosm PCB data) is altered by the

anaerobic dehalogenation model according to identified dehalogenation pathways, and the predicted profile is generated.

*Reactive Congener:* Dehalogenation pathways are identified under dehalogenation activities, by considering the congeners present in the measured data set. Only a limited number of congeners take part in dehalogenation pathways. Those that take part in a dehalogenation pathway (i.e. as either the mother or the daughter in a pathway) are called reactive congeners.

*Substitution:* It indicates the position of the halogen atom in the HOC structure. E.g. 23456-chlorobiphenyl indicates five Cl atoms present in 2-*ortho*, 3-*meta*, 4-*para*, 5-*meta*, 6-*ortho* substitutions in a PCB congener.

*Shuffle:* The order by which microorganisms dechlorinate PCBs is not known. Therefore, the full list of pathways is shuffled a 100 times and subsequently a distribution of  $k_m$  values is obtained.

*Singly flanked:* presence of other chlorines in either of the adjacent positions. E.g. In the structure 2345-CB, chlorine in position 5 (*meta* position) is singly flanked with chlorine in *para* position denoted by 4.

*Unflanked:* absence of chlorine in any of the adjacent positions. E.g. In the structure 24-CB, chlorine in position 4 (*para* position) is unflanked, there are no chlorines in adjacent positions denoted by 3 and 5.

*Sumkvalm:* Sumkvalm is an array used in the program of FTHP model. It includes  $k_m$  values of mother congeners.

## **3.2 Anaerobic Dehalogenation Model**

### **3.2.1 Description of Model**

#### **3.2.1.1 Original: Anaerobic Dechlorination Model**

Anaerobic Dehalogenation Model (ADM) is based on a model originally, developed as the “Anaerobic Dechlorination Model” by Imamoglu (2001) and later modified by

Bzdusek (2005) and Demirtepe et al. (2015). It was not a generic model for all HOCs, but one developed specifically for sediment bound PCBs. It aimed to identify and quantify dechlorination pathways among congeners in PCB data sets measured at two different times.

The original model is based on minimization of objective function by the sum of squares of differences between predicted and sample congener (Imamoglu, 2001). The governing equation is given in Equation 3.1.

$$S = \sum_{j=1}^m (\hat{y}_j - x_j)^2 \quad 3.1$$

where  $\hat{y}_j$  is predicted congener profile (either from Frame et. al (1996) or microcosm PCB data at t=0 d) altered according to a dechlorination activity (mole ‰),  $x_j$  is congener profile of microorganism PCB data measured at day e.g. t=100 day(mole ‰), and m is number of the congeners.

The model is based on two principles: (i) a mass balance exists between dechlorinated (mother) and accumulated (daughter) congeners (ii) only dechlorination pathways confirmed from laboratory and field studies are considered. Details of original model can be found in Imamoglu (2001), while modifications are explained in Bzdusek (2005) and Demirtepe (2012).

### **3.2.1.2 Improved Version: Anaerobic Dehalogenation Model**

The first principle of the original model is kept in ADM, that is, a mass balance between dechlorinated and accumulated congeners. The second principle is also kept, however, pathways are now identified automatically according to observed

dehalogenation activity (DA) or group of activities. The same objective function is used to minimize as in the original model. An improved evaluation of model fit is brought about in the new model. The fit of all congeners as well as those that take part in a pathway (as mother or daughter) are separately investigated. This allows for a better evaluation of model results when congener profile changes in the overall are not significant. ADM indicates that correlation fit of these congeners are not satisfactory. If correlation fit of only overall congeners is evaluated, this result can not be understood. Using ADM, now a dehalogenation pathway is not only quantified but also the dehalogenation rate constant associated with it is estimated.

### **3.2.1.3 Modifications to original model**

Modifications to the original model as a part of this study are explained below:

1. *Pathway Estimation:* Each individual dechlorination pathway needs not to be entered as input to the model. Congener no or Cl substitution information can now be entered as input and all relevant dechlorination pathways are listed as output. Sometimes, when pathways are identified by this function, some pathways include congeners that are not measured. These pathways including unmeasured congeners are automatically removed from the pathway list.
2. *Handling of Coeluting Congeners in ADM:* The original model separates coeluting congeners, which creates a problem on how to share concentration values to coeluting congeners. However, this presents a problem and affect the results of the model since the amount of each congener is not known separately. In this version, coeluting congeners are not separated.
3. *Description of congeners to the model:* Another modification is done in an input for the number of congeners in original profile. The model enables the user to simulate for various number of congeners given at t=0, so it does not have to include all 209 congeners.

4. Simulation based on substitutions: Dechlorination pathways are identified based on various predetermined dechlorination activities (i.e., removal of doubly flanked *para* chlorines, etc.). Previously in the original model, pathways according to dechlorination activity (DA) definitions of Bedard (2003) were used as input to the model. However, in the modified versions of the model (i.e. Demirtepe et al., 2015) and in this study, DAs are defined by chlorine substitutions (as typically described in the literature by Fagervold et al. (2007), Wu et al. (2002), Fennell et al. (2004), Adrian et al. (2009)).
5. Description of constraints for each dehalogenation activity: The user can define constraints for each DA. The constraints can be defined for laboratory studies. For example, a DA based on a specific microorganism or microorganism group targets the removal of a substitution such as flanked chlorines in *ortho/para* positions, however, if this group can not degrade a certain substitution included in this target position, it can be defined as constraint of this activity and input to the model.
6. Simulation for more than one activity in a run: The original model worked on one activity at a time, however, in this study, the model is modified such that numerous activities can be handled at the same time in one run. By this way, various activities and their combinations can be tested in a short time.
7. Calculation of dechlorination pathway specific rate constant,  $k_m$ : Rate constant ( $k_m$ ) is calculated for each dechlorination pathway. For reactive congeners,  $k_m$  values are calculated for each activity.
8. Evaluation of model performance: New goodness of fit parameter is added to provide better observation of the performance of the model. The multiple correlation coefficient  $R^2$  is calculated for all measured congeners ( $R^2$ ) and reactive congeners ( $R^2_{\text{reac}}$ ).

9. *Flexibility*: The model was generalized because now the model enables the user add any kind of DAs so that it can now be applied to any halogenated HOC group (e.g. PBDEs).

### 3.2.1.4 Estimation of Biodegradation Rate Constants in ADM

In ADM, biodegradation rate constants for dehalogenation reactions are calculated. A first order decay is assumed for anaerobic dehalogenation (eqn 3.2).

$$\frac{dC}{dt} = -kC^i \quad 3.2$$

where  $C^i$  is concentration of compound degraded, k: degradation rate constant, t: time. When the equation is solved analytically, equation 3.3 is obtained.

$$k_{m \rightarrow d}^i = \ln \left( \frac{C_m^o}{C_m^f} \right) / \Delta t \quad 3.3$$

where  $C_m^o$  is concentration of mother congeners before subtracting amount reacted,  $C_m^f$  is concentration of mother congeners after reaction, and  $\Delta t$  is the time between initial and final concentrations of mother congeners. m, d and i are IUPAC No of mother and daughter congeners and pathway order, respectively.  $k_m$  calculation in ADM is explained with an example for congeners a, b, c. In ADM, firstly amount of reaction from mother to daughter is calculated (Table 3.1) considering the path order,  $a \rightarrow b$  and  $b \rightarrow c$ , respectively.

Table 3.1 Amount of reaction estimated by ADM

Pathway order	Pathway	Mother in the path	Daughter in the path	Amount reacted from ADM
1	$a \rightarrow b$	a	b	$R_1$
2	$b \rightarrow c$	b	c	$R_2$



Then, ADM calculates the concentration of the congeners at final days by adding or subtracting reaction amount and considering the same path order (Table 3.2). Third column in Table 3.2 is used to predict the  $k_{a \rightarrow b}^1$  in path=1 and fourth column is for estimating  $k_{b \rightarrow c}^2$  in path=2. These are;

$$k_{a \rightarrow b}^1 = \ln \left( \frac{C_a^0}{C_a^1} \right) / \Delta t$$

$$k_{b \rightarrow c}^2 = \ln \left( \frac{C_b^1}{C_b^2} \right) / \Delta t$$

Table 3.2 Concentration of congeners after reaction 1 and 2

Congeners	Initial concentration of the congeners	Concentration of congener after first reaction (path=1)	Concentration of congener after first reaction (path=2)
a	$C_a^0$	$C_a^1 = C_a^0 - R_1$	
b	$C_b^0$	$C_b^1 = C_b^0 + R_1$	$C_b^2 = C_b^1 - R_2$
c	$C_c^0$		$C_c^2 = C_c^0 + R_2$

During model simulation,  $k_m$  values are calculated for each shuffle considering path order. Therefore, 100  $k_m$  values are obtained for 100 shuffles. Then, average of  $k_m$  values is taken. Sometimes  $k_m$  can not be calculated since amount of mother congeners are lower than zero during simulation. The model will eliminate a shuffle if  $k$  value of it can not be calculated. In ADM, same values of biodegradation rate constants are estimated in same pathway order in shuffles.

In this study, first order kinetic model is assumed. Accordingly, number of microorganisms is not taken into consideration for the anaerobic dehalogenation. According to our literature review, first order kinetic model was commonly used to estimate dechlorination rates of PCB congeners (Cho et al., 2003; Siebielska & Sidelko, 2015). However, Lombard et al. (2014) consider number of microorganisms

to estimate dechlorination rate constants. They stated that dechlorination rate is dependent on number of microorganisms rather than concentration of congeners. That study also indicated the first order relationships between initial contaminant concentration and dechlorination rate as in Cho et al. (2003) and Siebielska and Sidelko (2015). Therefore, our assumption can be considered valid.

Although two types of studies observed the first order relationship between rate and contaminant concentration, their dechlorination rates differentiate from each other. Lombard et al. (2014) state the difference by number and types of microorganisms as well as concentration of congeners in pore water which is not reported or considered in Cho et al. (2003) and Siebielska and Sidelko (2015). However, the use of first order assumption during modeling is applicable to various sites and different halogenated HOCs since it is not always available to find number of microorganisms for a site. Therefore, number of microorganism is assumed constant in our model.

### **3.2.2 Computer Program**

The model is rewritten in MatLAB, version 7.10.0. The input and output of the model are depicted in Figure 3.2. The input of the model include: list of congeners, pathways and congener profiles at  $t_{\text{initial}}$  and  $t_{\text{final}}$  (% moles). The model gives biodegradation rate constant, predicted congener profile with quantification values and goodness of fit parameters as output. The input of the concentration profiles are from microcosm data measured at various time intervals. Goodness of fit parameters are objective functions the cosine theta ( $\cos\theta$ ) similarity, the multiple correlation coefficient for of all measured congeners the multiple correlation coefficient for all ( $R^2$ ) and reactive congeners  $R^2_{\text{reac}}$ .

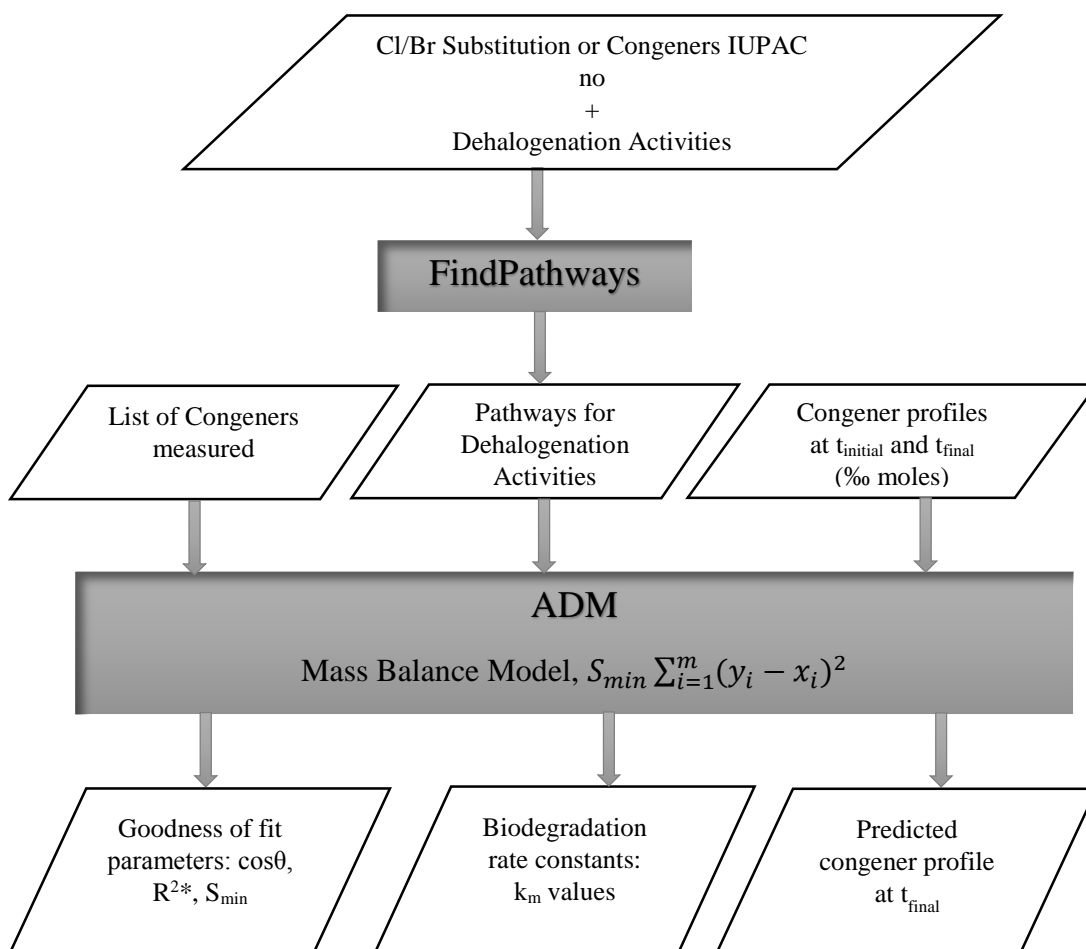


Figure 3.2 Description of ADM

Identifying the pathways, one of the input of ADM, is provided with a separate function, namely **FindPathways**. **FindPathways** was developed to evaluate each DA and find pathways of congeners for each DA. The function was written by using visual basic application of Excel 2010. This function works independently from ADM. The input to the function are substitutions or list of congeners and the DAs obtained from laboratory or field studies in the literature regarding *ortho*, *para* and/or *meta* halogen removal relative to configuration; flanked, doubly flanked and unflanked halogen substitutions. The output of the function is pathways for each DA. In a pathway, mother and daughter congeners are indicated. For example, one of the pathways in “double flanked *para*-any” in DA11 is expressed in Figure 3.3. As an example,

congener 114 is converted to congener 63. For this, Cl in the *para* position (2345-4) is removed to be converted to daughter product, congener 63 (235-4). One of the capability of the function is that the congeners in mother or daughter are removed from the pathway list of the DA by the algorithm if they are not present in the measured data set. If a congeners in either the mother or daughter of a pathway is not measured, this pathway is not evaluated in this DA.

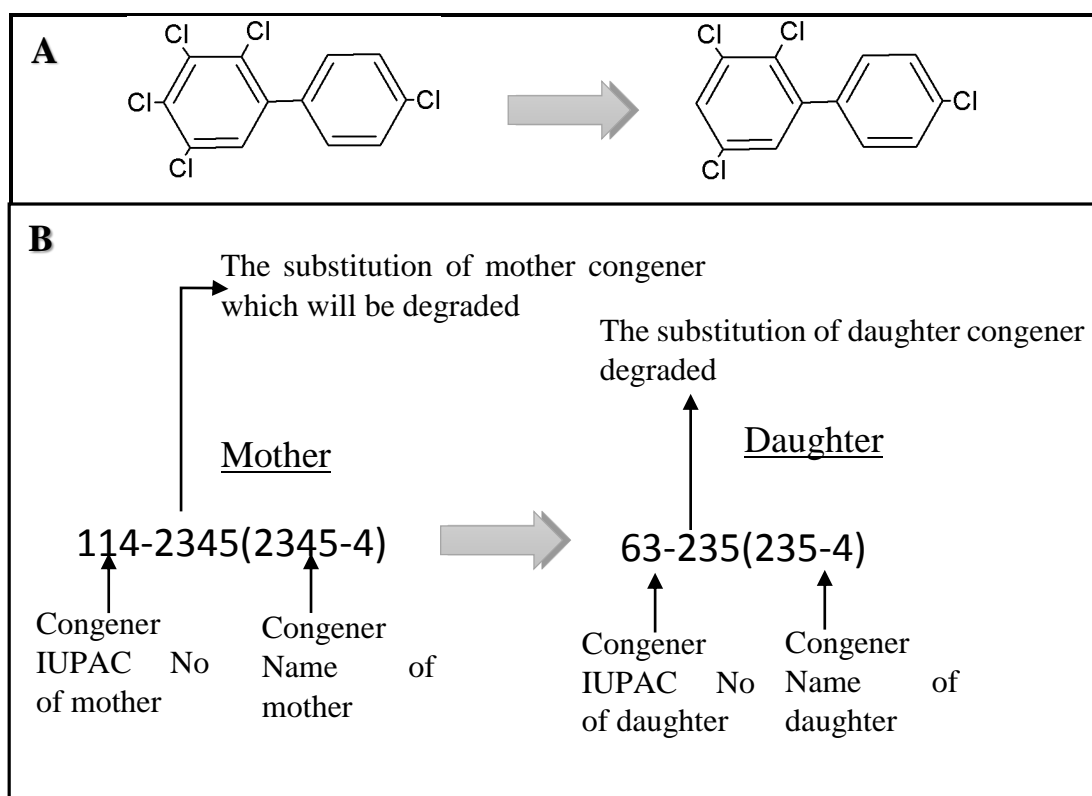


Figure 3.3 An example dechlorination pathway, output of the **FindPathways** function A. Structural depiction, B. Depiction in the model

ADM flowchart is given in Figure 3.4. In ADM, firstly, initial objective function ( $S_{\text{initial}}$ ) is calculated for a DA. The model arranges the congeners in the DA as coeluting congeners. Then, path is ordered randomly in the pathways of a DA since the path order is unknown in actual case. Therefore, the objective function is minimized to a randomly selected path order. This random ordering of pathways is

performed 100 times, each of which is called shuffle. Sometimes, the model may not give a result for a shuffle. Then, another run is conducted with a new random path order. Therefore, another number "it" is used to control whether the number of shuffles reach 100. This operation is conducted for each DA.

The cases where the model can not give a result for a shuffle are during calculation of  $k_m$  values. The calculation procedure of  $k_m$  in the model and these cases are explained below:

- In a path, if concentration of mother congener before reaction is equal to "0", then  $k$  value for that path is "0". Then, model moves on to the next congener.
- In a path, if concentration of mother congener before reaction,  $C_m(i)$  is not equal to "0" and concentration of mother congener after subtraction of reaction amount,  $C_m(f)$  is lower than "0", the model can not give result for this shuffle.
- In a path, if  $C_m(i)$  is not equal to "0" and  $C_m(f)$  is equal to "0", amount of detection limit (DL) is added to mother congener. Then,  $k_m$  value is calculated accordingly.
- In a path, if  $C_m(i)$  is not equal to "0" and  $C_m(f)$  is higher than "0", then  $k_m$  value is calculated.



Table 3.3 Descriptions of items used in ADM flow chart

Items	Unit	Descriptions
$t_i$	day	Initial time
$t_f$	day	Final time
DA	-	Dechlorination Activity Number
it	-	number to check the suffle number
$S_{initial}$	-	Objective function estimated initially before subtraction of degradation congeners
S	-	Objective function
$C_m(i)$	mole ‰	Concentration of mother congener at $t_i$
$C_m(f)$	mole ‰	Concentration of mother congener at $t_f$
$C_d(i)$	mole ‰	Concentration of daughter congener at $t_i$
$C_d(f)$	mole ‰	Concentration of daughter congener at $t_f$
$k_m$	$d^{-1}$	Biodegradation rate constant
DL	mole ‰	Detection limit
$m \rightarrow d$		A pathway findicating mother congener (m) and daughter congener (d)
$\Delta t$	day	Time step
$R^2$	-	The multiple correlation coefficient of all congeners modeled
$R^2_{reac}$	-	The multiple correlation coefficient of reactive congeners modeled
costheta	-	cosine theta ( $\cos \theta$ ) indicator between 0-1, the similarity between two data using angular profile of predicted and measured data.
SD	mole ‰	Standard deviation predicted profiles estimated for each shuffle
RSD	%	Relative standard deviation predicted profiles estimated for each shuffle
Avg	mole ‰	Average of predicted profiles estimated for each shuffle
Median	mole ‰	Median of predicted profiles estimated for each shuffle
pathorder	-	Order of each pathway in the shuffles

Program input and output files are depicted in Figure 3.5, Figure 3.6 and Figure 3.7. All files are Excel documents. The details about them are explained in the following paragraph considering cell names in Excel, such as, cell B1 is in row 1 and column 2.

The input file in Figure 3.5 depicts the information belonging to sample and predicted profiles. The cells of the input file used for ADM are explained individually below:

B1: The number of pathways. The model runs for all DAs and gives results based on them in different Excel sheets with one run. The pathways of each one is selected by the program automatically from DechlorInput sheet.

B2: Detection Limit of Input Data.

C1: Number of congeners in sample.

C2: Time difference ( $\Delta t$ ) between two sample data (initial and final days). It is used to calculate first order biodegradation rate constant.

D1: The number of congeners in predicted profile.

E1: Number of coeluting congeners. This is for old version of ADM including separation of coeluting congeners.

F1: The number of shuffles.

I2: Yes/No button to ask whether the number of congeners in predicted and sample profiles is the same or not. It includes the values in C1 and D1. In our study, they are always same. If it is “No”, it is run as in old version.

A3:G2I2: Congeners in sample profile. Up to seven are allowed.

H3:H2I2: Concentration of congeners in sample profile which is at initial day. Typically, data is in mole % and normalized to 1000 moles.

I3:I2I2: The concentration of congeners at time t which is at final day. The data in mole is normalized to 1000. If the value in I2 is yes, this will be considered.

J3:J2I2: Congeners in sample profile (This supports the old version when number of congener at final day is not the same as at initial day).

K3:K2I2: Concentration of congeners in predicted profile (mole %) (This supports the old version when number of congener at final day is not the same as at initial day)

M1:M1000: Mother congener IUPAC No in pathways of a DA. These values are automatically taken from DeChlorInput sheet.

N1:N1000: Daughter congener IUPAC No in pathways of a DA. These values are automatically taken from DeChlorInput sheet.

The input file in Figure 3.6 depicts the information belonging to DAs and their pathways. This input is the output of the **FindPathways** function. Therefore, this sheet is prepared by the function automatically. The names of all input in this sheet are expressed below:



A16:AX16: number of pathways in the corresponding DA.

A17:AX17: description of the DA.

A18:AX1000: pathways in the DA given as mother and daughter IUPAC No.

The output file in Figure 3.7 depicts the output of ADM. As can be seen in the figure, names of all output are expressed in three parts, A, B and C. In Part A, statistical analyses of goodness of fit parameter results such as  $R^2$ ,  $R^2_{\text{reac}}$  and  $Q$  are given. Average, standard deviation and relative standard deviation of first ten and all shuffles are calculated in Part A. It is between row cells 1 and 3. In Part B, the results of  $Q$  values,  $R^2$ ,  $\cos \theta$ ,  $R^2_{\text{reac}}$ , reactive congeners, path order, predicted congener profiles,  $k_m$  values, altered amount of reactive congeners are given in each shuffle and ranked according to  $Q$  values in ascending order. It is between cells 5 and 105 since it can include maximum 100 shuffles. In part C, statistical results of each parameter in Part B are given. Average, median, standard deviation, relative standard deviation of predicted profile and  $k_m$  values of first ten and all shuffles are calculated.

The ADM program also supports the old version. For example, the number of congeners are not always the same as that in sample profile at  $t_{\text{initial}}$ . However, in our study, same number of congeners exist in both profiles. If the user simulates the model as in old version, he/she can use a Yes/No in cell "I2" of input file in Figure 3.5.

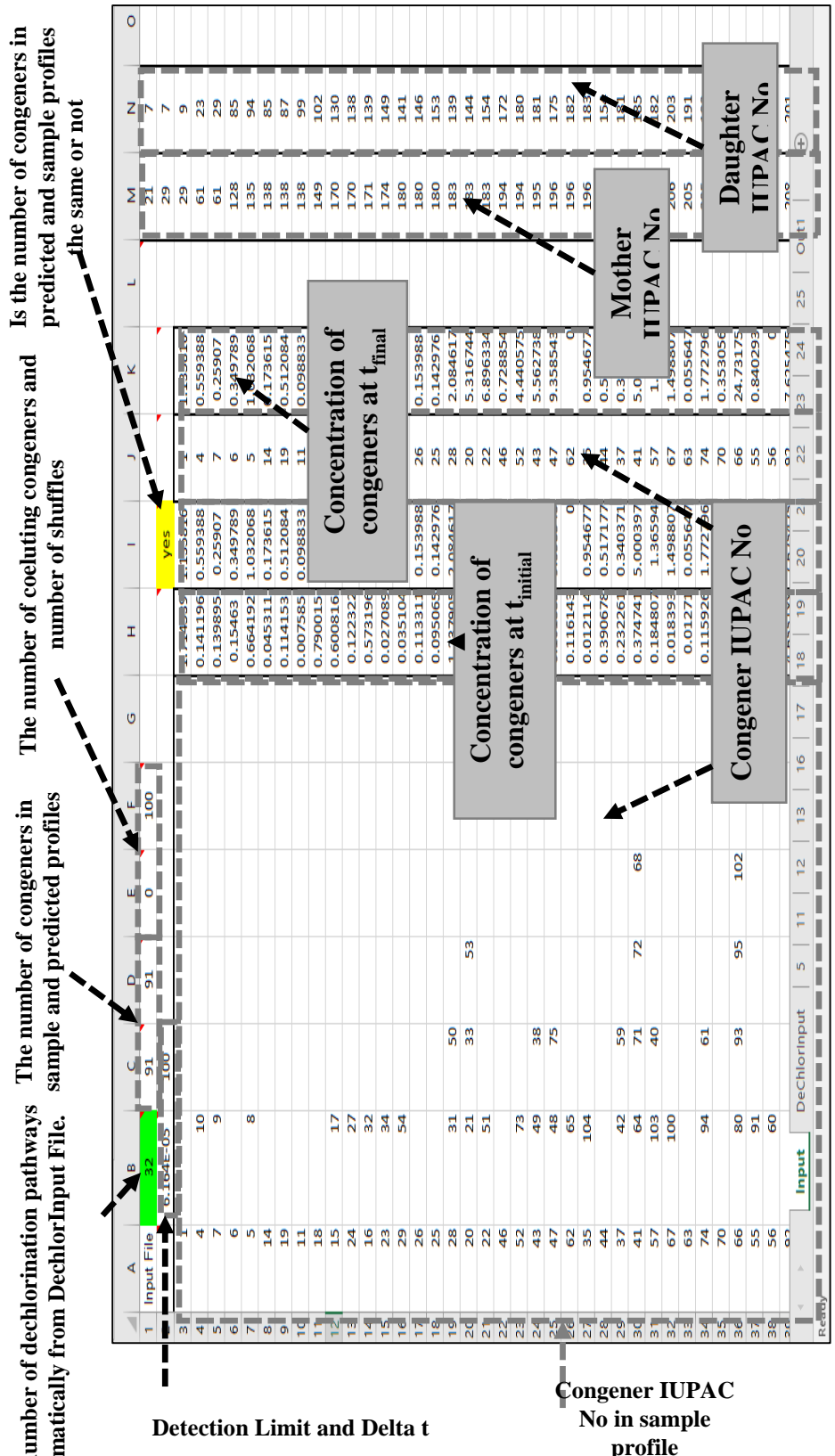


Figure 3.5 Input File: Sample and Predicted Profiles







### 3.2.3 Preparation of Dehalogenation Pathways as Input for ADM

#### 3.2.3.1 PCB Dechlorination Pathways

Each Dechlorination Activity is described by a set of pathways formed from information in Karcher (2005) and Demirtepe (2012), and microorganism based pathways defined in Fagervold et al. (2007), Wu et al. (2002), Fennell et al. (2004), Adrian et al. (2009). According to these data, 25 DAs are built as can be seen in Appendix D Table D.1. These patterns are used as input to **FindPathways** function to obtain a list of pathways that fit each DA description. The first fifteen DAs include theoretically possible Cl-substitutions amenable to dechlorination such as, doubly flanked *para*, etc. The others are based on dechlorination capabilities of microorganisms or microorganism groups. These DAs include some constraints. For instance, o-17 activity defined as DA 16 in Table D.1, target the removal of flanked chlorines in *ortho/para* positions (e.g. 2356→235), however, if 2356 substitution is in congener of 152 (2356-26), o-17 can not degrade congener 152. This congener is then defined as a constraint for **FindPathways** function. In DAs, the patterns are indicated by congeners (e.g. DAs 18, 19, 21, 22, 23) or both substitution and congeners (e.g. DAs 16, 17, 20, 24). After running the function, pathways of DAs to use for ADM is obtained and presented in Appendix D Table D.2. The number of pathways in a theoretical DA vary between 44 and 393, while those based on microorganism is much less, between 5 and 48.

#### 3.2.3.2 PBDE Dechlorination Pathways

Compared to the case of PCBs, there are considerably less number of studies on PBDE dehalogenation. Nevertheless, using all available literature information, 21 DAs are built (Appendix D Table D.3). Each Dechlorination Activity is described by a set of pathways formed from information in Karcher (2005), and microorganism based pathways defined in Tokarz et al. (2008), Robrock et al. (2008), Ding et al. (2013) and Huang et al. (2014). While DAs based on microorganisms are built, it is seen that they are not based on a targeting position such as removal of doubly flanked *meta* bromine.

Instead, they are based on pathways between congeners. This is perhaps, because PBDE debromination studies are relatively recent and not as extensive as those for PCBs. These patterns are used as input to **FindPathways** function to obtain a list of pathways that fit the DA description.

After running the function, pathways of DAs to use for ADM is obtained (Appendix D Table D.4). The results indicate that the number of pathways in all DAs are small (1 and 5) since the number of congeners in the microcosm data is only 8. Another result is that the function can not find pathways in some DAs such as 5, 11, 17 and 20. For these DAs, ADM is not run.

### **3.3 Fate and Transport (F&T) Model**

#### **3.3.1 Conceptual Model**

The system modeled, includes mixed sediment layer, interfaces of mixed sediment layer with water column and deep sediment layer. The model includes the effects of degradation and other fate mechanisms (settling, burial, resuspension and diffusion) affecting the HOC. Upper and lower boundaries of the model are set as the water-sediment interface and deeper sediment, respectively (Figure 3.8). This model can be used for the sediments of a lake, river, ocean or estuary.

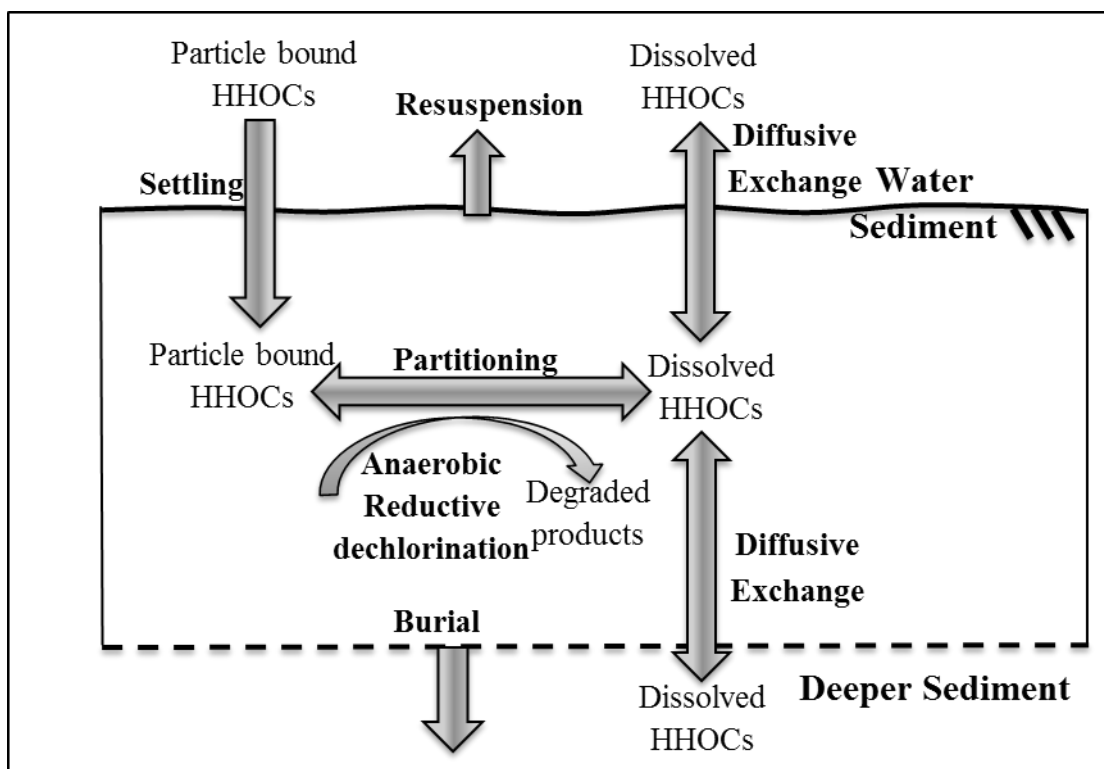


Figure 3.8 Conceptual Model (HHOCs: Halogenated HOCs)

There are two- and three-phase partitioning models widely used for diluted systems such as a lake or a river (Zhang, 2006). Two-phase partitioning model includes

- dissolved (freely dissolved and bound to DOC) and
- particulate bound phase (bound to POC)

In three-phase partitioning model, the compounds are in

- Dissolved,
- DOC particulate and
- POC particulate (POC-Particulate Organic Carbon composed of BIC-Biotic Carbon and PDC-Particulate Detrital Carbon) phases.

PCBs and PBDEs are used as model compounds for HOCs in this study. In the literature, two- or three- phase partitioning is applied to the models for such



compounds (Farley et al., 1999; Zhang, 2006). Zhang (2006) indicated that two-phase partitioning is satisfactory to apply the water and sediment systems for PCBs. In this study, two-phase partitioning is used for our system because

- data for dissolved, DOC and POC are not readily available or limited,
- DOC partitioning coefficient is not estimated for three-phase partitioning successfully.
- Three-phase partitioning is not appropriate to use in a natural water system due to heterogeneous organic carbon concentrations, PCB characteristics, and PCB concentrations (Zhang, 2006).

This approach can then be applied for other Halogenated HOCs. Overall, the model considers:

- Partitioning of contaminant between dissolved and particulate phases,
- Settling of contaminant in particulate phase and resuspension of contaminant in both particulate and dissolved phases at the interface between water column and sediment bed,
- Contaminant transport processes: molecular diffusion within sediment pore water and particle mixing,
- Biodegradation of contaminant.

### **3.3.2 Selection of A Model Equation**

A comprehensive evaluation of models with similar aim as the one in this study was performed as was presented in Chapter 2. Equations of the models are summarized in Table 3.4. The approach of the Recovery model was selected among the investigated models. The justification for the selection of Recovery model is presented below under the adopted selection criteria:

- Data requirement: Recovery model includes parameters which are available, easy to access, or frequently measured especially for biodegradation term. For

example, TOXIWASP and WASP4 require parameters such as bacterial population and yield coefficient, the calculation of rate constants depending on microbial population for biodegradation term. These parameters are readily available for any contaminated site. However, this not the case for Recovery model in which the concentration of toxic compounds measured for different time and rate constants are adequate to calculate biodegradation term. Another problem is about partitioning of contaminants. According to our literature review, there are two- and three phases partitioning. Three-phase partitioning causes the data problem since there is no available data for more than two phases or are not measured.

- Availability of equation for surface sediment: The equation for surface sediment is available only in Recovery Model. For all others, sediment is not considered in layers.
- Existence of a numerical solution: The numerical solution of WASP4, LM2, TOXIWASP and Recovery Models were readily presented in the relevant references, which is an advantage.
- Movement in 1D: we prefer a model which should have the movement only in vertical (depth) direction. Accordingly, concentration should only change in the direction of depth. As a result, it was seen that all models had this rule except for TOXIWASP, LM2 and WASP4.
- Complexity of the model: Some models such as LM2 include carbon and thermal mass balances. This increases the complexity of the model due to requirement of separate equations as well as the need for data.

Table 3.4 An overview of model equations in the literature

Models	Model Equations
<b>Recovery-mixed sed.</b> (Boyer et al., 1994)	$V_m \frac{dC_m}{dt} = -k_m V_m C_m + v_s A_w F_{pw} C_w - v_r A_m C_m - v_b A_m C_m - v_d A_m (F_{aw} C_w - F_{ap} C_m) + v_d A_m (F_{ap} C_s(0) - F_{ap} C_m)$
<b>Recovery-deep.</b> (Boyer et al., 1994)	$\frac{\partial C_s}{\partial t} = \varphi F_{ap} D_s \frac{\partial^2 C_s}{\partial Z^2} - v_b \frac{\partial C_s}{\partial Z} - k_s C_s = F_{aps} D_s \frac{\partial^2 C_s}{\partial Z^2} - v_b \frac{\partial C_s}{\partial Z} - k_s C_s$
<b>TOXIWASP</b> (Ambrose, 1983)	$V_4 \frac{dC_{1,4}}{dt} = \frac{W_{d,3} C_{2,3} C_{1,3} \alpha_{2,3}}{L_{w,3} C_{2,3}} - \frac{W_{s,4} C_{2,4} C_{1,4} \alpha_{2,4}}{L_{b,4} C_{2,4}} - D_{3-4}^b A_{3-4} \left( \frac{C_{1,4} \alpha_{1,4} - C_{1,3} \alpha_{1,3}}{L_{3-4}} \right) - D_{3-4}^b A_{3-4} f_{s,4} \frac{C_{2,4}}{\varphi_4} \left( \frac{C_{1,4} \alpha_{2,4}}{C_{2,4}} - \frac{C_{1,3} \alpha_{2,3} \pi_4}{C_{2,3} \pi_3} \right) - u_{p,4} \left( \frac{C_{1,4} \alpha_{1,4}}{\varphi_4} \text{ or } \frac{C_{1,4} \alpha_{1,4}}{\varphi_4} \right) - \left[ \sum_{k=1}^3 k_{bac,k} C_{bac} \alpha_{1,4} \right]$
<b>LM2</b> (Zhang, 2006)	$\frac{dC_j}{dt} = \sum_i^n R_{ij} (C_i - C_j) + S_{sw,j} + S_{b,j} + S_{k,j}$
<b>PMHR</b> (Farley et al., 1999)	$V \frac{dC_{sed_i}}{dt} = w_s A_s m_i \Gamma_i - w_{u_i} A_{s_i} m_{sed_i} \Gamma_{sed_i} - w_b A_{s_i} m_{sed_i} \Gamma_{sed_i} - k'_f A_{s_i} [C_{atis+DOC_{sed_i}} - C_{atis+DOC_i}] - k_{sed_i} V_{sed_i} C_{atis_{sed_i}}$
<b>WASP4</b> (Ambrose et al., 1988)	$\frac{\Delta(V_j C_j)}{\Delta t} = \sum_i (-Q_{ij} C_{ij}) + \sum_i (-Q_{pij} C_{ij} f_{Dj}) + \sum_i \sum_s (-w_{sij} A_{ij} C_j f_{sj}) + \sum_i (R_{ij} \Delta C_{ij}) + \sum_i \left( R_{pij} \frac{f_{Dj} C_j}{n_j} - \frac{f_{Dj} C_j}{n_j} \right) + \sum_L w_{Lj} + \sum_N w_{Nj} + \sum_B Q_{j0} C_{Bj} + \sum_k \sum_c (V_j S_{kcj})$
<b>Chapra (1997)</b>	$V_2 \frac{dC_2}{dt} = k_2 V_2 C_2 - v_s A F_{p1} C_1 - v_r A C_2 - v_b A C_2 - v_d A [F_{a1} C_1 - F_{a2} C_2]$
<b>Thomann and Di Toro (1984)</b>	$V_s \frac{dC_{Ts}}{dt} = w_a A f_p C_T - w_{r,s} A f_{ps} C_{Ts} + K_L A \left( \frac{f_p C_T}{\varphi} - \frac{f_{ds} C_{Ts}}{\varphi_s} \right) - w_s A C_{Ts} - K_s V_s C_{Ts}$
<b>MICHTOX</b> (Endicott et al., 2005)	$V_{s,H} \frac{dC_s}{dt} = v_{s,H} A f_{sH} C_H - v_{r,s} A f_{ss} C_s - v_b A f_{ss} C_s - K_f A_d \left[ (f_{ds} - f_{bs}) \frac{C_s}{n_s} - (f_{aH} - f_{bH}) C_H \right]$
<b>Qi (2003)</b>	$\frac{\partial C_s}{\partial t} = -v_z \frac{\partial C_s}{\partial Z} + D_s \frac{\partial^2 C_s}{\partial Z^2} + r_{sorp} + r_{reac} + S(C)_{source}$

Table 3.4 Continued

Models	Description of Terms
<p><b>Recovery-mixed sed.</b>(Boyer et al., 1994)</p>	<p><math>V_{mi}</math>: Volume of surface sediment, <math>m^3</math>, <math>A_{mi}</math>: Mixed layer surface area <math>m^2</math>, <math>A_w</math>: Water surface area <math>m^2</math>, <math>c_{ni}</math>: Contaminant concentration in the mixed layer, <math>\mu g/m^3</math>, <math>c_s(0)</math>: Initial contaminant concentration in the deep sediments, <math>\mu g/m^3</math>, <math>c_w</math>: Contaminant concentration in the water, <math>\mu g/m^3</math>, <math>v_i</math>: Resuspension velocity of the sediments into the water, <math>m/year</math>, <math>v_s</math>: Settling velocity of the particulate matter from the water to the sediments, <math>m/year</math>, <math>v_b</math>: Burial velocity, <math>m/year</math>, <math>v_d</math>: Diffusive mass transfer coefficient, <math>m/year</math>, <math>k_m</math>: Decay rate of the contaminant in the mixed layer, <math>1/year</math>, <math>F_{pw}</math>: Fraction of contaminant in particulate in water column, <math>F_{dw}</math>: Fraction of contaminant dissolved in water column, <math>F_{dp}</math>: Fraction of contaminant in pore water in surface sediment.</p>
<p><b>Recovery-deep.</b>(Boyer et al., 1994)</p>	<p><math>C_s</math>: Contaminant concentration in the deep sediments, <math>\mu g/m^3</math>, <math>D_s</math>: Molecular diffusivity, <math>m^2/s</math>, <math>k_s</math>: Decay rate of the contaminant in the mixed layer, <math>1/year</math>, <math>v_b</math>: Burial velocity, <math>m/year</math>, <math>\phi</math>: Porosity, <math>F_{dp}</math>: Fraction of contaminant in pore water in surface sediment, <math>F_{dps}</math>: Ratio of contaminant concentration in the deep sediment pore water to concentration in the total deep sediments.</p>
<p><b>TOXIWASP</b> (Ambrose, 1983)</p>	<p><math>V_4</math>: Volume of sediment layer, <math>A_{3-4}</math>: Area of surface sediment, <math>L_{w,3}</math>: Water column depth, <math>L_{b,4}</math>: Depth of sediment layer, <math>L_{3-4}</math>: Vertical distance, <math>w_{d,3}</math>: Deposition velocity of suspended sediment, <math>w_{s,4}</math>: Scour velocity in bed sediment, <math>c_{1,4}</math>: Contaminant concentration in sediment layer, <math>c_{1,3}</math>: Contaminant concentration in water column, <math>c_{2,4}</math>: Sediment concentration in sediment layer, <math>c_{2,3}</math>: Sediment concentration in water column, <math>\phi_3</math>: Porosity in water column, <math>\phi_4</math>: Porosity in sediment, <math>\alpha_{1,4}</math>: Dissolved fraction in sediment, <math>\alpha_{1,3}</math>: Dissolved fraction in water column, <math>\alpha_{2,3}</math>: Sorbed fraction in water column, <math>\pi_3</math>: Partitioning coefficient of contaminant in water column, <math>\pi_4</math>: Partitioning coefficient of contaminant in sediment, <math>D_{3,4}^b</math>: Vertical dispersion coefficient of dissolved contaminant.</p>
<p><b>LM2</b> (Zhang, 2006)</p>	<p><math>C_j</math>: Concentration of water quality constituent in segment <math>j</math> (<math>M/L^3</math>), <math>C_i</math>: Concentration of water quality constituent in segment <math>i</math>, <math>S_{sw,j}</math>: Mass change rate due to sediment-water exchange processes between segment <math>j</math> and adjacent sediment segments (<math>M/T</math>), <math>S_{b,j}</math>: Mass change rate due to burial process from surficial mixing layer <math>j</math> to deeper sediment layer (<math>M/T</math>), <math>S_{k,j}</math>: Mass change rate due to sum of kinetic transformation processes within segment <math>j</math> (<math>M/T</math>), positive is source, negative is sink, <math>R_{ij}</math>: <math>(E_{ij}A_{ij}/\Delta X_{ij})</math>, Bulk dispersion/diffusion coefficient (<math>L^2/T</math>), <math>E_{ij}</math>: Mixing (dispersion/diffusion) coefficient (<math>L^2/T</math>), <math>A_{ij}</math>: Interfacial area between segment <math>i</math> and <math>j</math> (<math>L^2</math>).</p>

<p><b>PMHR</b> (Farley et al., 1999)</p>	<p><math>V_{\text{sedi}}</math>: Volume of sediment (<math>\text{m}^3</math>), <math>A_{\text{si}}</math>: Surface area (<math>\text{m}^2</math>), <math>m_i</math>: Solids concentration in segment <math>i</math> (<math>\text{mg L}^{-1}</math>), <math>m_{\text{sedi}}</math>: Solids concentration in sediment (<math>\text{mg L}^{-1}</math>), <math>C_{\text{sedi}}</math>: Concentration of contaminant in sediment (<math>\text{mg/L}</math>), <math>\Gamma_i</math>: Solid phase chemical concentration in segment <math>i</math>, <math>I_{\text{sedi}}</math>: Solid phase chemical concentration in surface (active) sediment layer (<math>:\text{g g}^{-1}</math> (dry weight)); <math>w_{\text{ai}}</math>: Solids resuspension velocity in segment <math>i</math> (<math>\text{m day}^{-1}</math>); <math>w_s</math>: Solids settling velocity (<math>\text{m day}^{-1}</math>); <math>w_{\text{bi}}</math>: Burial rate for solids in segment <math>i</math> (<math>\text{cm yr}^{-1}</math>).</p>
<p><b>WASP4</b> (Ambrose et al., 1988)</p>	<p>Look at LM2 and TOXIWASP models for others. <math>Q_{ij}</math>: Advective flow between segments <math>i</math> and <math>j</math>, defined as positive when leaving segment <math>j</math>, and negative when entering, <math>\text{m}^3/\text{day}</math> <math>Q_{\text{po}}</math>: Boundary inflows segment <math>j</math>, <math>\text{m}^3/\text{day}</math>, <math>Q_{\text{pij}}</math>: Pore water flow between segments <math>i</math> and <math>j</math>, defined as positive when leaving segment <math>j</math>, and negative when entering <math>j</math>, <math>\text{m}^3/\text{day}</math>, <math>F_{\text{di}}</math> and <math>F_{\text{aj}}</math>: Dissolved fraction of chemical in segment <math>i</math> and <math>j</math>; <math>f_{\text{sj}}</math>: fraction of chemical sorbed to solid type "s" in segment <math>j</math>, <math>\text{CB}_j</math>: Boundary concentrations for segment <math>j</math>, <math>\text{g}/\text{m}^3</math>, <math>n_i</math>: Average porosity of segments <math>i</math> and <math>j</math>, <math>\text{m}^3\text{water}/\text{m}^3</math></p>
<p><b>Chapra (1997)</b></p>	<p>Look at Recovery model for units. <math>V_2</math>: Volume of surface sediment <math>A</math>: Surface area <math>C_2</math>: Contaminant concentration in surface sediment, <math>C_1</math>: Contaminant concentration in sediment, <math>v_s</math>: Settling velocity, <math>v_r</math>: Resuspension velocity, <math>v_b</math>: Burial velocity, <math>v_d</math>: Diffusion coefficient <math>F_{\text{di}}</math>: Fraction of contaminant dissolved in water column, <math>F_{\text{d2}}</math>: Fraction of contaminant in pore water in sediment</p>
<p><b>Thomann and Di Toro (1984)</b></p>	<p><math>V_s</math>: Sediment volume, <math>\text{km}^3</math>, <math>A</math>: Surface area, <math>\text{km}^2</math>, <math>C_{\text{TS}}</math>: Contaminant concentration in sediment, <math>\mu\text{g}/\text{L}</math>, <math>C_{\text{T}}</math>: Contaminant concentration in water column, <math>\mu\text{g}/\text{L}</math>, <math>w_a</math>: Settling velocity, <math>\text{m}/\text{year}</math>, <math>w_{\text{rs}}</math>: Resuspension velocity, <math>\text{m}/\text{year}</math>, <math>w_s</math>: Net effective sedimentation velocity, <math>\text{m}/\text{year}</math>, <math>f_p</math>: Fraction of contaminant particulate in water column, <math>f_{\text{ds}}</math>: Fraction of contaminant dissolved form in sediment, <math>K_L</math>: Sediment water diffusive transfer coefficient <math>\text{m}/\text{d}</math>, <math>\phi</math>: porosity <math>\phi_s</math>: porosity of sediment.</p>
<p><b>MICHTOX</b> (Endicott et al., 2005)</p>	<p><math>V_{\text{s,H}}</math>: Volume of hypolimnion, <math>A</math>: Surface area [<math>L^2</math>] <math>A_d</math>: Sediment deposition area [<math>L^2</math>], <math>v_{\text{s,H}}</math>: Settling velocity [<math>L/T</math>], <math>v_{\text{r,s}}</math>: Particle resuspension velocity from segment <math>S</math> [<math>L/T</math>], <math>v_b</math>: Sediment burial (or sedimentation) velocity [<math>L/T</math>], <math>C_{\text{H}}</math>: Chemical concentration in hypolimnion, <math>C_s</math>: Chemical concentration in surficial sediment, <math>f_{\text{sH}}</math>: <math>f_{\text{bH}}</math>: Dissolved, sorbed (to particles), and bound (to non-settling organic matter) chemical fractions in hypolimnion, respectively, <math>n_s</math>: Surficial sediment porosity, <math>K_d</math>: Diffusive exchange coefficient [<math>L/T</math>], <math>f_{\text{ss}}</math>, <math>f_{\text{ds}}</math> and <math>f_{\text{bs}}</math>: Dissolved, sorbed (to particles), and bound (to non-settling organic matter) chemical fractions in segment sediment, respectively.</p>
<p><b>Qi (2003)</b></p>	<p><math>C_s</math>: Concentration of PCBs in the water phase of the inter-particle pores in sediments, <math>C_s^*</math>: Solution phase concentration corresponding to the solid phase external concentration at radius <math>R_p</math>, The external-film mass transfer coefficient, <math>e</math>: Porosity of the sediments <math>v_z</math>: The fluid phase inter-particle pore velocity, <math>D_s</math>: The hydrodynamic dispersion coefficient, <math>k_f</math>: external-film mass transfer coefficient in the sediments, <math>\rho_s</math>: Density of the solid sediment phase <math>R_p</math>: Radius of sediment particle.</p>

### 3.3.3 Model Assumptions

Assumptions for Recovery (Ballschmiter & Zell, 1980) model is given below:

- The model is applicable for organic contaminants.
- Water is well mixed.
- Surface sediment layer is well mixed.
- The concentration of contaminant varies only in vertical direction in deep sediment.
- Initial concentration of contaminant in deep sediment is zero.
- Sediments are the only source of contamination.
- Initial concentrations of contaminant in water column and sediment are uniform throughout that region.
- Linear equilibrium sorption mechanism is valid.
- Degradation follows first-order kinetics.
- There is no compaction in sediment.

As different from these assumptions, in our study, two more assumptions were adopted:

- The concentration of contaminant in water column does not change with time.
- Degradation is due to only anaerobic biodegradation of contaminant in sediment. This is assumed for PCBs and PBDEs, however, it can be changed for other halogenated HOCs in the future.

### 3.3.4 Description of the FTHP model

The general mass balance equation used in this study is given in eqn. 3.4. The mass balance equation and numerical approach of Recovery model which was developed by Boyer et al. (1994) and Chapra and Reckhow (1983) were used.

$$\begin{aligned} \text{Accumulation} = & \text{-Decay + Settling - Resuspension - Burial} & - & \text{Diffusion between the} & + & \text{Diffusion between the surface} \\ & & & \text{sediment and water} & & \text{layer and the deep sediment} \\ \frac{dc_m^i}{dt} = & -k_m c_m^i + \frac{v_s A_w F_{pw} c_w^i(0)}{V_m} - \frac{v_r A_m c_m^i}{V_m} - \frac{v_b A_m c_m^i}{V_m} - \frac{v_d A_m (F_{dw} c_w^i(0) - F_{dp} c_m^i)}{V_m} + \frac{v_d A_m (F_{dp} c_s^i(0) - F_{dp} c_m^i)}{V_m} \end{aligned} \quad 3.4$$

$V_m$	volume of sediment, $m^3$
$A_w$ and $A_m$	surface areas of water and surface sediment, respectively, $m^2$
$k_m$	decay rate constant of the contaminant in the surface layer, $day^{-1}$
$v_b$	burial velocity, m/day
$v_s$	settling velocity of particulate matter, m/day
$v_r$	resuspension velocity of sediments, m/day
$v_d$	diffusion mass-transfer coefficient at the sediment, water and deep sediment interface, m/day
$c_s^i(0)$	$i^{th}$ contaminant concentration at the top of the deep contaminated layer, ng/L
$c_w^i$ and $c_m^i$	concentrations of contaminant $i$ in water and surface sediment, respectively, ng/L
$t$	Time, day
$F_{pw}, F_{dw}$	fraction of contaminant in particulate and dissolved forms in the water, respectively
$F_{dp}$	ratio of contaminant concentration in the sediment pore water to contaminant concentration in total sediment

As the major transport processes, settling, resuspension, burial and diffusion are considered. For transformation mechanisms, anaerobic dehalogenation (biodegradation) is considered as the only dominant process in sediment. In the mechanisms of burial, resuspension and biodegradation, the contaminant is considered in both dissolved and particulate phases while the mechanisms of settling and diffusion happen only in particulate and dissolved phases, respectively. As different from the Recovery model, in our model contaminant concentration in water column is accepted as constant.

### 3.3.5 FTHP Model Computer Program

The model is developed in MatLAB, version 7.10.0 and run for individual congeners. The flowchart of the model is given in Figure 3.9 and indicates the solution of Runge Kutta fourth order (RK4). As with the Recovery Model for mixed sediment, RK4 is derived. RK4 is used for numerical solution of ordinary differential equations. Firstly, the general model equation in Recovery model is divided by  $V_m$  on both sides to simplify the equation:

$$\frac{dc_m^i}{dt} = -k_m c_m^i + \frac{v_s A_w F_{pw} c_w^i(0)}{V_m} - \frac{v_r A_m c_m^i}{V_m} - \frac{v_b A_m c_m^i}{V_m} - \frac{v_d A_m (F_{dw} c_w^i(0)) - F_{dp} c_m^i}{V_m} + \frac{v_d A_m (F_{dp} c_s(0) - F_{dp} c_m^i)}{V_m} \quad 3.5$$

In RK4, the following equation is obtained by  $k_1$ ,  $k_2$ ,  $k_3$  and  $k_4$ :

$$c_m^{i,t+1} = c_m^{i,t} + \frac{\Delta t}{6} (k_1 + 2k_2 + 2k_3 + k_4) \quad 3.6$$

where;

$$k_1 = f(t^n, c_m^{i,t})$$

$$k_2 = f\left(t^n + \frac{\Delta t}{2}, c_m^{i,t} + \frac{\Delta t}{2} k_1\right)$$

$$k_3 = f\left(t^n + \frac{\Delta t}{2}, c_m^{i,t} + \frac{\Delta t}{2} k_2\right)$$

$$k_4 = f(t^n + \Delta t, c_m^{i,t} + \Delta t k_3)$$

By using expressions above, the  $k_1$ ,  $k_2$ ,  $k_3$  and  $k_4$  values are derived as below to use in the RK4 approach:



$$\begin{aligned}
k_1 = & -k_m c_m^{i,t} + \frac{v_s A_w F_{pw} c_w^i(0)}{V_m} - \frac{v_r A_m c_m^{i,t}}{V_m} - \frac{v_b A_m c_m^{i,t}}{V_m} \\
& - \frac{v_d A_m (F_{dw} c_w^i(0) - F_{dp} c_m^{i,t})}{V_m} + \frac{v_d A_m (F_{dp} c_s^i(0) - F_{dp} c_m^{i,t})}{V_m}
\end{aligned} \tag{3.7}$$

$$\begin{aligned}
k_2 = & -k_m (c_m^{i,t} + \frac{\Delta t}{2} k_1) + \frac{v_s A_w F_{pw} c_w^i(0)}{V_m} - \frac{v_r A_m (c_m^{i,t} + \frac{\Delta t}{2} k_1)}{V_m} \\
& - \frac{v_b A_m (c_m^{i,t} + \frac{\Delta t}{2} k_1)}{V_m} \\
& - \frac{v_d A_m (F_{dw} c_w^i(0) - F_{dp} (c_m^{i,t} + \frac{\Delta t}{2} k_1))}{V_m} \\
& + \frac{v_d A_m (F_{dp} c_s^i(0) - F_{dp} (c_m^{i,t} + \frac{\Delta t}{2} k_1))}{V_m}
\end{aligned} \tag{3.8}$$

$$\begin{aligned}
k_3 = & -k_m (c_m^{i,t} + \frac{\Delta t}{2} k_2) + \frac{v_s A_w F_{pw} c_w^i(0)}{V_m} - \frac{v_r A_m (c_m^{i,t} + \frac{\Delta t}{2} k_2)}{V_m} \\
& - \frac{v_b A_m (c_m^{i,t} + \frac{\Delta t}{2} k_2)}{V_m} \\
& - \frac{v_d A_m (F_{dw} c_w^i(0) - F_{dp} (c_m^{i,t} + \frac{\Delta t}{2} k_2))}{V_m} \\
& + \frac{v_d A_m (F_{dp} c_s^i(0) - F_{dp} (c_m^{i,t} + \frac{\Delta t}{2} k_2))}{V_m}
\end{aligned} \tag{3.9}$$

$$\begin{aligned}
k_4 = & -k_m(c_m^{i,t} + \Delta tk_3) + \frac{v_s A_w F_{pw} c_w^i(0)}{V_m} - \frac{v_r A_m (c_m^{i,t} + \Delta tk_3)}{V_m} \\
& - \frac{v_b A_m (c_m^{i,t} + \Delta tk_3)}{V_m} \\
& - \frac{v_d A_m (F_{dw} c_w^i(0) - F_{dp} (c_m^{i,t} + \Delta tk_3))}{V_m} \\
& + \frac{v_d A_m (F_{dp} c_s^i(0) - F_{dp} (c_m^{i,t} + \Delta tk_3))}{V_m}
\end{aligned} \tag{3.10}$$

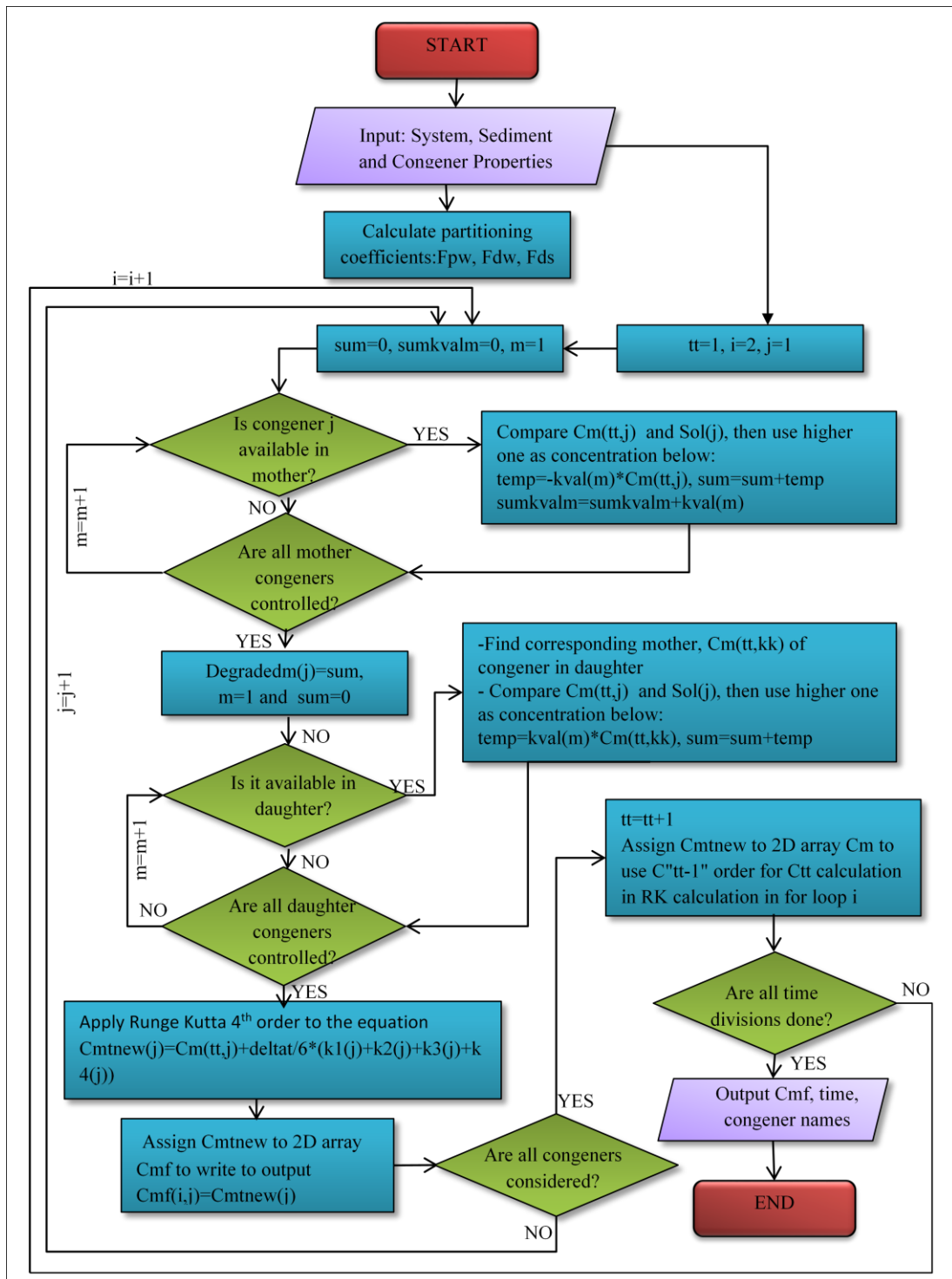


Figure 3.9 Flowchart of the FTHP Model

Table 3.5 Descriptions of items used in FTHP flow chart

Items	Unit	Descriptions
$c_m^i$ , $C_m$	ng/L	Concentration of contaminant i in surface sediment
Cmtnew	ng/L	Concentration of each congener calculated in each time step of FTHP model
Degraded	-	An array including sum of two arrays; Degradedm and Degradedd.
Degradedd	-	Array to which biodegradation rates of the congeners which are accumulated (increased) are filled.
Degradedm	-	Array to which biodegradation rates of the congeners which are degraded (decreased) are filled
$F_{dp}$	-	Ratio of contaminant concentration in the sediment pore water to contaminant concentration in total sediment
$F_{dw}$	-	Fraction of contaminant in dissolved forms in water
$F_{pw}$	-	Fraction of contaminant in particulate form in water
k1, k2, k3 and k4		Calculated terms in RK4.
$k_m$ , $k_{val}$	$d^{-1}$	Biodegradation rate constant of a dehalogenation pathway estimated for mixed surficial sediment
Sol	mg/L	Solubility of the congeners
sumkvalm	$d^{-1}$	An array including $k_m$ values of mother congeners
$t_i$	day	Initial time
$t_f$	day	Final time
$\Delta t$	day	Time step

In the program, firstly partitioning coefficients ( $F_{pw}$ ,  $F_{dw}$  and  $F_{ds}$ ) are estimated. The concentration of each congener in surface sediment is estimated for each time step defined in the model. **Degradedd** and **Degradedm** are the arrays considering biodegradation rate of each congener for daughter and mother congeners, respectively. In the calculation of **Degradedd** and **Degradedm**, concentration is compared with solubility limit of corresponding congener, then it is multiplied by the  $k_m$  value (Figure 3.9). The flowchart above indicates the code of RK4 solution of FT Model equations given by equations 3.5 to 3.10. This code is used during calibration, validation, sensitivity analysis and uncertainty analysis. The relationships between these analyses and use of the code of RK4 solution are demonstrated in Figure 3.10. In calibration procedure, the code of RK4 solution is called to test parameters by considering 50% and 150% of values and/or ranges given in the literature or data set. Calibration is conducted until no further improvement can be achieved in model predictions. Then, the code of RK4 solution is called again to test the calibrated model with a different data set ( $C_m$  values) for validation. Then, the most sensitive parameters and input that affect the predicted concentration the most are determined by considering 50% and

150% of values and/or ranges of parameters/input. Finally, uncertainty analysis is conducted. For this purpose, distributions of the most sensitive parameters/input are assumed and the code of RK4 solution is run for 1000 times using Monte Carlo Simulation. Hence, model is developed. These steps and all input are explained in detail in section 3.3.8. Lastly, the developed FTHP model is used to predict sediment PCB and PBDE concentrations according to selected scenarios for the next 20 years.

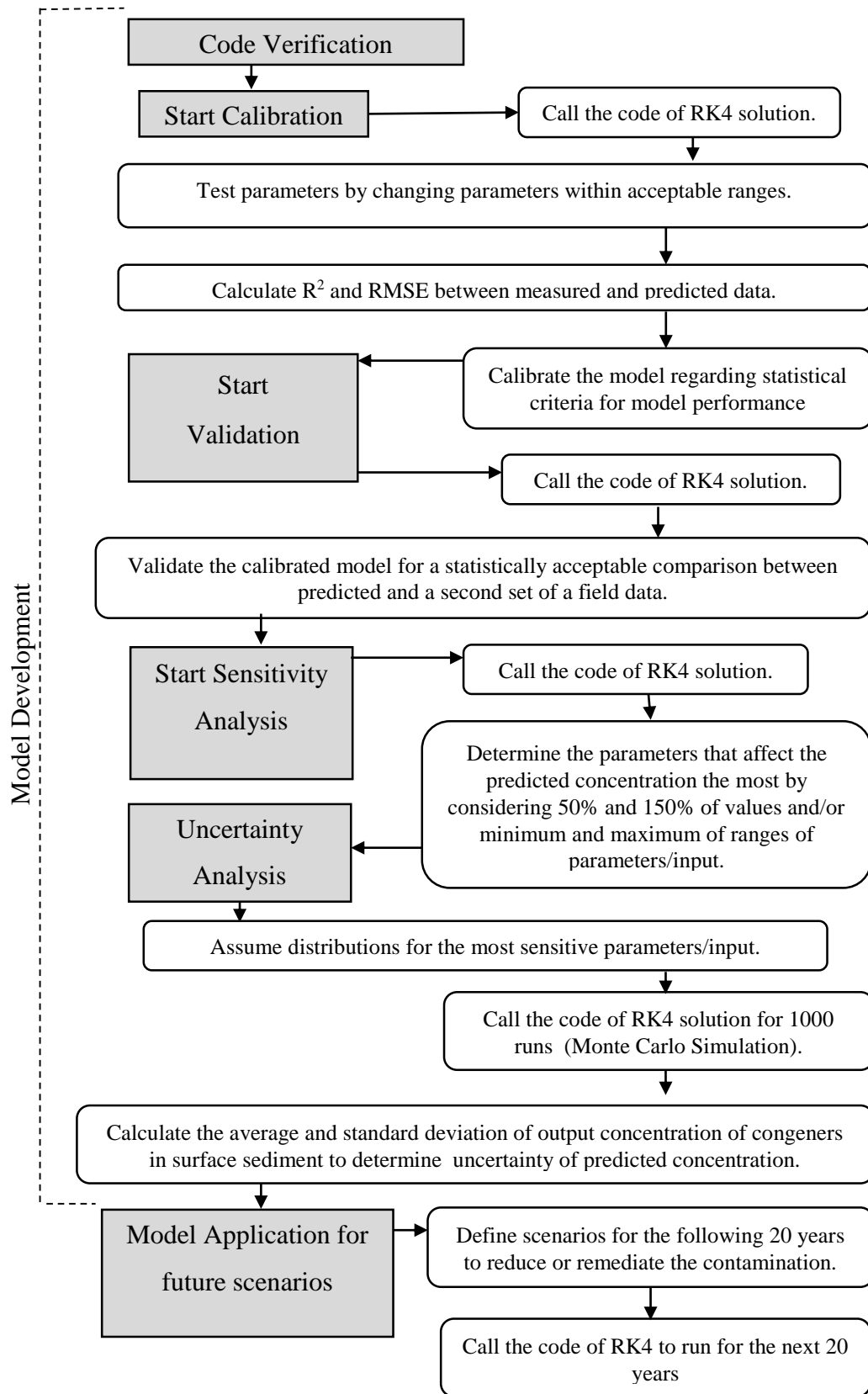


Figure 3.10 Steps of FTHP model development and application

Program input and output files are depicted in Figure 3.11-Figure 3.13, Figure 3.16 and Figure 3.17. Input and output files are in Excel documents. The details about them are explained in the following paragraph considering cell names in Excel.

In Figure 3.11, Figure 3.12 and Figure 3.13, input files of FTHP model are depicted. The names of all input in this sheet are expressed below:

A1: number of congeners

B1: number of pathways

C1: initial time modeling is started (day)

D1: final time modeling ends

E1:  $\Delta t$  selected for numeric solution (day)

F1: the number of data measured at different times. This value is important and used during calibration/validation process.

A4:G42: IUPAC no of congeners measured in sample. Up to seven congeners can be written.

H4:H42: Initial concentration of congeners in surficial sediment, ng/L

I4:I42: Initial concentration of congeners in water column, ng/L

J4:J42: Initial concentration of congeners in deep sediment, ng/L

K4:K42: molecular diffusion coefficients of congeners,  $\text{cm}^2/\text{s}$

L4:L42: Octanol water partitioning coefficients of congeners

M4:M42: Solubilities of congeners, mg/L

N2: Yes/No button to ask whether simulation is done for calibration/validation or not. If it is yes, goodness of fit parameters are performed between predicted and measured data.

O1:U43: Mother Congeners in pathways.

V1:AB43: Daughter Congeners in pathways.

AC1:AC43: Biodegradation rate constants,  $\text{day}^{-1}$ .

AI1: Depth of water column, m.

AI2: Area of water column,  $\text{m}^2$ .

AI3: Depth of surficial sediment, m.

AI4: Area of surficial sediment,  $\text{m}^2$ .

AI5: TSS concentration,  $\text{g}/\text{m}^3$ .

AI6: Sediment porosity.

AI7: Sediment density,  $\text{g}/\text{m}^3$ .

AI9: Organic carbon fraction in water column.

AI10: Organic carbon fraction in surficial sediment.

AI11: Characteristic length, m.

AI13-AI15: settling, resuspension and burial velocities,  $\text{m}/\text{day}$ .

AL2:AR29: IUPAC no of congeners measured in sample.

AS1:AX1: Day of sampling.

AS2:AX29: Concentration of congeners measured in surficial sediment,  $\text{ng}/\text{L}$ .

The uncertainty analyses of parameters in Inputfile-1 and Inputfile-2 are conducted by using files in Figure 3.14 and Figure 3.15, respectively. In these figures, the distributions of parameters assumed are written to shaded cells.

There are two output files, Out 1 and Out 2 which are demonstrated in Figure 3.16 and Figure 3.17, respectively. In Out 1 file, the predicted concentration of each congener



in surficial sediment is given for each delta t interval. In Out2 file, goodness of fit parameter, R2 and RMSE of each congener is calculated during calibration/validation process. Additionally, predicted concentration at times when measured concentration for each congener is given, is calculated by the model.

	A	B	C	D	E	F	G	H	I	J	K	L	M	N
2	Congener #		Path #	to	if	$\Delta t$	$t_{\text{findnum}}$							Calibration
3	Congeners													
4	16							Cm(O) in sediment, g/L	Cw(O), ng/L	Cs(O), ng/L	Molecular Diffusion, cm <sup>2</sup> /sec	log(Kow)	Solubility, mg/L at 25 °C	
5	26							61.20	0.000890316	0	5.714E-06	5.22	0.5050	
6	28	31						76.47	0.001665312	0	5.714E-06	5.68	0.2050	
7	33							1180.45	0.011863298	0	5.714E-06	5.73	0.1495	
8	44							233.50	0.006919283	0	5.714E-06	5.71	0.1610	
9	49							401.77	0.008688729	0	5.471E-06	5.79	0.0632	
10	52							241.1013734	0.003729885	0	5.471E-06	5.925	0.0202	
11	56	60						479.6981135	0.010903288	0	5.471E-06	5.95	0.035	
12	66	70	76					762.45108	0.004060772	0	5.471E-06	5.95	0.04155	
13	70							1523.727602	0.007834988	0	5.471E-06	6.105	0.02695	
14	74							756.5347582	0.006303562	0	5.471E-06	6.05	0.0432	
15	81							396.2153946	0.002210552	0	5.471E-06	6.16	0.0306	
16	84	92						31.30595776	0.000461789	0	5.471E-06	6.24	0.00313	
17	85							623.8959352	0.02377688	0	5.228E-06	6.11	0.03335	
18	87							284.8003662	0.00247805	0	5.228E-06	6.61	0.013	
19	99							266.4103106	0.003888919	0	5.228E-06	6.285	0.007415	
20	101							292.4862888	0.009342164	0	5.228E-06	6.41	0.0103	
21	118							547.1836036	0.006251191	0	5.228E-06	6.375	0.0155	
22	123	149						787.3734889	0.005000481	0	5.228E-06	6.615	0.0155	
23	105	132	153					277.1134904	0.003866119	0	5.107E-06	6.57	0.003275	
24	151							968.7220585	0.005869728	0	5.066E-06	6.8	0.00473433	
25	138	163						76.65291288	0.000810926	0	4.985E-06	6.49	0.00454	
26	170	190						1130.12231	0.011674153	0	4.985E-06	6.82	0.00392	
27	180							200.4332326	0.000957362	0	4.742E-06	7.08	0.0004315	
28	182	187						404.956881	0.00301889	0	4.742E-06	7.18	0.00065	
29	195	208						140.6072916	0.003922255	0	4.742E-06	7.0964	0.02107275	
30	146							54.24577096	0.000391825	0	4.378E-06	7.78	0.00013603	
31								132.3556621	0.001538809	0	4.985E-06	6.85	0.00228	
32														
33														
34														
35														
36														
37														
38														
39														
40														

Is the simulation for calibration/validation process?

$C_m(t)$ ,  $C_w(t)$ ,  $C_s(t)$ , molecular diffusion coefficients,  $\log(K_{ow})$  and solubility for each congener

Number of congeners in sample, number of pathways, initial time (day), final time (day),  $\Delta t$ (day) and number of measured data

Congeners modeled

Figure 3.11 Input File-1



	AL	AM	AN	AO	AP	AQ	AR	AS	AT	AU	AV	AW	AX	AY
	Congeners (ng/L) of Congeners/time (days)													
1								0	72	73	77	79	666	
2	16							61.20	46.13505	53.59389	12.0045	33.9322	5.85016	
3	26							76.47	65.94924	62.85597	60.06589	29.41343	13.86249	
4	28	31						1180.45	1033.988	865.9875	955.7587	444.316	214.2022	
5	33							235.50	194.8767	225.8739	144.2904	150.2468	42.03134	
6	44							401.77	302.6687	297.5742	276.5487	243.1411	117.4508	
7	49							241.1014	199.3782	161.3606	210.5413	111.1843	58.04484	
8	52							479.6981	390.1251	317.3957	437.201	339.2048	144.8052	
9	56	60						762.4511	548.8872	510.3243	618.4208	404.2403	170.4579	
10	66							1523.728	1198.449	978.8029	1453.517	840.7572	412.5075	
11	70	76						756.5348	566.4329	473.0536	707.8162	394.0846	206.7005	
12	74							336.2154	257.6993	213.6974	283.6863	129.3735	68.65357	
13	81							31.30596	22.42493	12.20942	36.05901	15.19859	8.188817	
14	84	92						623.8959	394.7237	295.1815	419.7457	303.7228	128.0034	
15	85							284.8004	202.823	147.1625	295.9383	193.9676	109.7596	
16	87							266.4103	185.4975	145.0467	234.8824	132.3894	79.75328	
17	99							292.4863	213.4549	149.4102	314.2432	190.5622	103.4177	
18	101							547.1836	386.137	292.4117	567.7935	337.8297	197.5241	
19	118							787.3723	529.6859	465.2516	867.3807	517.9317	300.8775	
20	123	149						277.1135	189.838	148.5392	305.6681	176.083	105.7174	
21	105	132	153					968.7221	610.5846	518.1956	1044.342	658.7179	360.0411	
22	151							76.65291	53.52159	43.91839	81.48072	49.46906	31.65617	
23	138	163						1130.122	698.3253	452.252	1321.249	654.0283	306.8924	
24	170	190						200.4332	117.0503	92.67421	223.3114	117.8076	65.30775	
25	180							404.9509	218.8636	171.088	430.8558	218.5348	136.046	
26	182	187						140.6073	90.46208	69.43114	155.4975	93.37208	57.28322	
27	195	208						54.24577	35.86773	28.42992	62.99231	36.46948	23.23067	
28	146							132.357	94.33922	68.07093	144.7447	84.01686	44.53529	
29								12271.78	8788.228	7259.792	11666.04	6799.995	3512.814	
30														
31														
32														
33														
34														
35														
36														
37														
38														
39														
40														
41														
42														

Day of sampling

Congeners modeled  
Concentration of congeners measured in surficial sediment (ng/L)

Figure 3.13 Input-3 for Calibration and Validation



	AB	AC	AD	AE	AAAI	AJ	AAAA	AQ	AR	AS	AT	AU	AV	AW	AX	AZ	BA	BB	BC	BD	BE	BF	BG
			km			Lognormal	min	max	avg	variance					Water column								
1																							
2		66				33	0	0.026593	0.005047	2.22E-05					Depth, m	m	48.1						
3		101				49	1E-04	0.053057	0.008988	0.00015					Surface Area, m2	m2	4425000000						
4		138	163			99	0.000607	0.021466	0.005307	1.91E-05					Depth, m	m	0.031						
5		105	132	153		99	0.001024	0.01106	0.003163	4.47E-06					Surface Area, m2	m2	4425000000						
6		146				101	0.001813	0.123422	0.018355	0.001251					Suspended solids concentration in water,SS	g/m3	2.41		0.2	2.41	0.942	0.162	Uniform
7		151				66	0	0.128956	0.006781	0.000273					Sediment porosity		0.953						
8															Sediment particle density,	g/m3	2540000						
9															Fraction organic carbon, g-orgC/gdry wt solids								
10															Water g-orgC/gdry wt solids		0.09						
11															Sediment g-orgC/gdry wt solids		0.05						
12															Characteristic Length	m	0.01						
13															Two of the following three velocities:								
14															Resuspension velocity, vr	m/day	Unknown						
15															Burial velocity, vb	m/day	Known	0.00000994					
16															Settling velocity, vs	m/day	Known	1.5	0.5	1.5	avg	variance	Uniform
17																		min	max				Distributions

Figure 3.15 Uncertainty File-2 for Values in Input file 2

	A	B	C	D	E	F	G	H	I	J	K	L	M	N	O	P	Q	R	S	T	U	V	W	X	Y	Z	AA	AB	
1																													
2																													
3																													
4																													
5																													
6																													
7																													
8																													
9																													
10																													
11																													
12																													
13																													
14																													
15																													
16																													
17																													
18																													
19																													
20																													
21																													
22																													
23																													
24																													
25																													
26																													
27																													
28																													
29																													
30																													
31																													
32																													
33																													
34																													
35																													
36																													
37																													
38																													
39																													
40																													

**Predicted concentration in surficial sediment by the model for each congener and each time step, ng/L**

**Congeners (first congeners of coeluting congeners)**

**Time steps, days**

Figure 3.16 Output File-Out I



Congeners	A	B	C	D	E	F	G	Predicted			J	K	L	Measured			N	O
								R2	RMSE	0				73	74	408		
1																		
2																		
3	16				34.30	17.30558	16.54043	16.5302	13.46014	11.51988	17.30558	90.35518	35.18394	20.23083	17.78276			
4	26				36.25	53.91463	51.63452	51.60404	42.45538	36.67353	53.91463	129.5073	53.08223	27.737	19.77304			
5	28	31			538.15	852.5267	814.6845	814.1785	662.341	566.3813	852.5267	1968.051	859.8123	465.5156	288.9548			
6	33				74.87	165.397	158.6979	158.6083	131.7288	114.7412	165.397	320.7583	152.6179	104.4827	83.37482			
7	44				114.18	269.1866	257.8435	257.6918	212.1788	183.4151	269.1866	504.1719	273.1087	272.3039	209.041			
8	49				114.76	166.36	159.4837	159.3917	131.8012	114.3643	166.36	409.2362	200.8726	115.5119	75.74162			
9	52				231.79	331.9271	318.8148	318.6394	266.0278	232.7778	331.9271	821.8611	427.0393	263.9211	170.9295			
10	56	60			245.45	504.8392	482.3739	482.0735	391.9343	334.9673	504.8392	1006.474	612.9463	456.4564	262.3764			
11	66				706.34	1032.3	1022.094	1021.933	945.6131	870.0055	1032.3	2514.4	1432.985	887.8898	561.283			
12	70	76			342.27	516.317	494.2047	493.909	405.1858	349.1136	516.317	1226.985	697.3024	453.0006	277.6252			
13	74				141.83	241.4166	231.0209	230.8819	189.1707	162.8096	241.4166	535.135	242.6517	139.3179	88.8424			
14	81				55.95	24.10007	56.18919	56.54362	106.9015	108.7133	24.10007	51.81855	38.25938	32.00147	10.27278			
15	84	92			170.37	296.4708	290.613	290.5347	267.031	252.177	296.4708	621.442	424.5818	391.3021	204.5706			
16	85				120.74	188.0232	222.0371	222.3998	262.1179	250.1751	188.0232	447.0083	327.8783	247.6559	145.5579			
17	87				107.51	192.0836	217.9913	218.2631	243.8187	229.9557	192.0836	399.9	233.9738	171.0673	91.53108			
18	99				145.58	188.9478	237.1655	237.6937	308.7758	306.8436	188.9478	483.5548	333.9801	239.617	130.2025			
19	101				283.91	365.67	352.1282	351.9471	297.6122	263.273	365.67	923.4435	592.9503	432.5766	245.6198			
20	118				450.21	411.8202	371.6113	371.0921	236.4315	171.9714	411.8202	1113.787	954.57	528.0926	364.566			
21	123	149			184.86	146.4172	133.3117	133.1425	89.25188	68.24209	146.4172	456.258	350.2629	204.1615	147.1612			
22	105	132	153		498.13	509.2828	491.8003	491.5665	421.4201	377.0882	509.2828	1300.147	1181.18	730.8751	503.1783			
23	151				48.18	45.20572	43.64933	43.62852	37.38371	33.43705	45.20572	137.7337	92.77077	53.60849	42.19744			
24	138	163			811.72	575.0352	408.4388	406.5652	108.3732	59.40762	575.0352	1601.452	1497.694	846.8974	427.0847			
25	170	190			126.67	100.2054	91.07731	90.95909	59.94083	44.74856	100.2054	307.724	240.0988	152.4597	94.5915			
26	180				236.04	196.6083	178.1982	177.9604	116.3044	86.79055	196.6083	572.154	452.5162	295.2612	213.1272			
27	182	187			91.21	75.30396	74.56948	74.55966	71.61265	69.75017	75.30396	236.7468	187.6995	118.0677	88.17962			
28	195	208			42.68	25.57248	25.18671	25.18156	23.63369	22.65546	25.57248	99.26309	75.23594	53.72529	37.20424			
29	146				71.60	66.54396	77.55945	77.69832	109.6835	120.4452	66.54396	197.1723	168.6628	102.7089	65.6275			
30			TOTAL		5515.81	7558.781	7278.92	7275.177	6152.189	5442.443	7558.781	18476.54	12139.92	7806.446	4866.397			
31																		

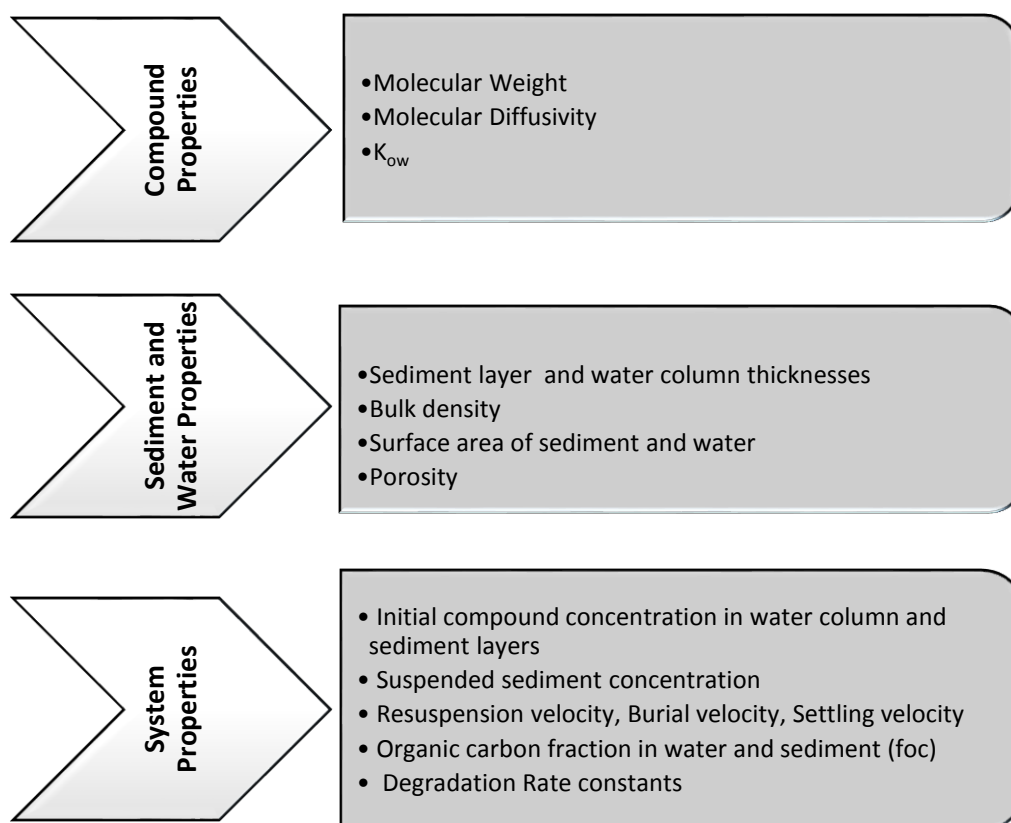
Figure 3.17 Outputfile-Out2 for Calibration and Validation



### 3.3.6 Estimation of Model Parameters

A general list of input parameters needed for the model is listed in Table 3.6. While some parameters (e.g., bulk density, porosity) are used in model equations directly, others (e.g.,  $K_{ow}$ , molecular diffusivity) are used to calculate certain parameters which are then used in the model equations. All equations used to estimate parameters are explained in this section, grouped according to the F&T processes in the general model equation.

Table 3.6 Input Parameters needed for the model



Biodegradation Term: The biodegradation rate constants are obtained as the output of ADM, and used as input in the FTHP model. Since the model is developed for

individual congeners,  $k_m$  values should be given in terms of the accumulated (daughter) and dehalogenated (mother) congeners.

$$\frac{dc_m}{dt} = -k_m c_m \quad 3.11$$

Settling/Resuspension/Burial Terms: The velocities of settling, resuspension and burial, and particulate fraction of the contaminant should be estimated. The velocities are predicted by conducting a solid mass balance.

$$\frac{dc_m}{dt} = \frac{v_s A_w F_{pw} c_w(0)}{V_m} - \frac{v_r A_m c_m}{V_m} - \frac{v_b A_m c_m}{V_m} \quad 3.12$$

As in Recovery model (Boyer et al., 1994; Ruiz et al., 2001), the equation below is used to predict one of the three velocities under steady state conditions (Figure 3.18). The same equation is also available in Chapra (1997). To use this equation, two of these velocities should be known.

$$0 = v_s A_w s_w - (v_r + v_b) A_m (1 - \varphi) \rho_p, \quad 3.13$$

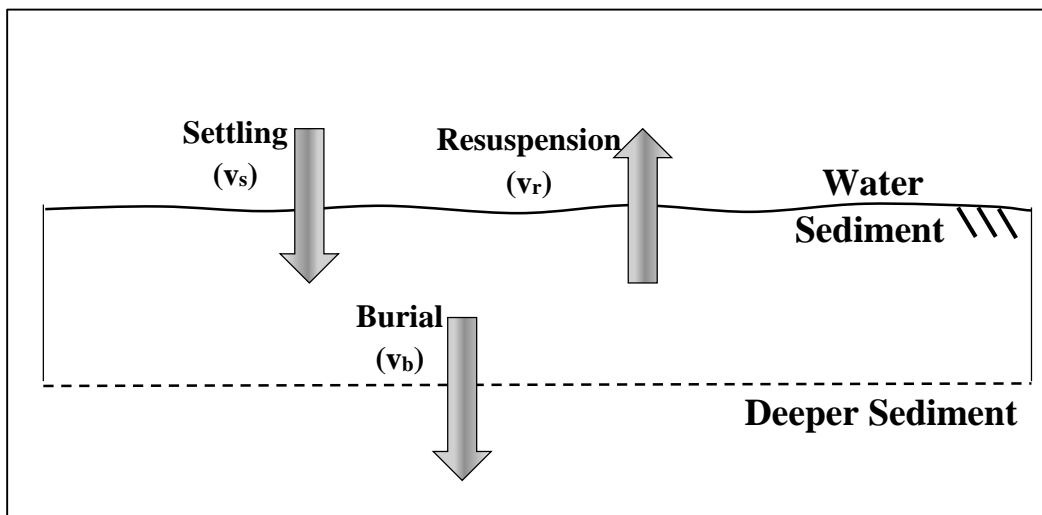


Figure 3.18 Solid Mass Balance in Sediment

Linear sorption is assumed for the contaminant in solid and dissolved phases. The settling of the contaminant in particulate phase occurs. Then, particulate fraction of contaminant in the water is calculated using the equation below (Boyer et al., 1994; Ruiz et al., 2001).

$$F_{pw} = \frac{K_{dw}S_w}{1 + K_{dw}S_w}$$

$$= \frac{\text{Mass of A (Particulate form)}}{\text{Mass of A (Dissolved form)} + \text{Mass of A (Particulate form)}} \quad 3.14$$

Where  $K_{dw}$  is equilibrium partitioning coefficient in water column (L/kg).  $S_w$  is suspended solid concentration in water column ( $\text{g/m}^3$ ). To estimate the equilibrium partitioning coefficient in both water and sediment, the equation selected by the Recovery model (Boyer et al., 1994; Ruiz et al., 2001) is used.

$$K_d = 0.617f_{oc}K_{ow} \quad 3.15$$

Where  $K_{ow}$  is octanol-water partitioning coefficient ( $\text{mg/m}^3$ - octanol/  $\text{mg/m}^3$ -water). The term  $f_{oc}$  is fraction of organic carbon in solid (g-orgC/g). By using different  $f_{oc}$  values for water and sediment, partitioning coefficients are obtained for the water column and sediment.

Diffusion Term: As can be seen in diffusion term, volume of surface sediment, mass transfer coefficient for diffusive sediment-water exchange and fractions ( $F_{dw}$  and  $F_{dp}$ ) should be calculated.

$$\frac{dc_m}{dt} = -\frac{v_d A_m (F_{dw} c_w(0) - F_{dp} c_m)}{V_m} + \frac{v_d A_m (F_{dp} c_s(0) - F_{dp} c_m)}{V_m} \quad 3.16$$

The mass transfer coefficient is calculated by the equation below (Boyer et al., 1994; Ruiz et al., 2001).

$$v_d = \frac{\varphi D_s}{z'} \quad 3.17$$

where  $D_s$  is molecular diffusivity ( $\text{cm}^2/\text{s}$ )

In the calculation of  $v_d$ , molecular diffusivity is unknown. It is calculated by the below equation (Boyer et al., 1994; Ruiz et al., 2001).

$$D_s = D_m \varphi^2 \quad 3.18$$

where  $D_m$  is the molecular diffusion ( $\text{cm}^2/\text{s}$ ) and  $\varphi$  is the porosity.

In the diffusion of the contaminant in water and pore water, dissolved fraction of contaminant is calculated by the equations below (Boyer et al., 1994; Ruiz et al., 2001).

$$\begin{aligned} F_{dw} = 1 - F_{pw} &= \frac{1}{1 + K_{dw}S_w} \\ &= \frac{\text{Mass of A (Dissolved form)}}{\text{Mass of A (Dissolved form)} + \text{Mass of A (Particulate form)}} \end{aligned} \quad 3.19$$

$$\begin{aligned} F_{dp} &= \frac{1}{\varphi + (1 - \varphi)\rho K_{ds}} \\ &= \frac{\text{Mass of A (Dissolved form)}}{\text{Mass of A (Dissolved form)} + \text{Mass of A (Particulate form)}} \end{aligned} \quad 3.20$$

### 3.3.7 Model Stability and Accuracy

The selected equation in Recovery Model is a first-order ordinary differential equation (ODE). When numerical solution is applied to ODEs, accuracy of results is dependent on magnitude of time intervals (Ramaswami et al., 2005). In other words, the numerical solution is computed by combining linear relationship between two points ( $t$  and  $\Delta t+t$ ). However, true solution has nonlinearity and derivatives. Therefore, selected time interval is important to estimate the true solution. Two types of errors occur while defining the accuracy of numerical integration (Ramaswami et al., 2005).

One of them is truncation error which means the difference between actual value and numerically estimated value in each time step. To decrease the truncation error,  $\Delta t$  is reduced (Ramaswami et al., 2005). This causes the second type of errors, round-off error. The round-off error occurs by the elimination of values during computing due to a limited number of significant digits in the computer. This is solved by increasing time step. There is an inverse relationship between two errors. To arrange the time step, Ramaswami et al. (2005) explain that the stability and accuracy of numerical integration can be checked by two ways; (i) analytical solution if it can be applied, and (ii) varying time steps by reducing it until no further change between model predictions is evident.

In this study, the second way is considered for the stability and accuracy of the model since solution of analytical solution is not available due to nonlinear ODE. Ramaswami et al. (2005) state that 4<sup>th</sup> order Runge Kutta method has more accuracy and stability than Euler, predictor-corrector methods as  $\Delta t$  is made smaller.

One of the operations in the FTHP model is to control  $C_{min}$  and  $C_{max}$  of individual congener in each time step.  $C_{max}$  is the stability criteria for the system i.e., maximum allowable segment concentration for each system for the first order assumption.  $C_{min}$  is the Accuracy Criteria.

Biodegradation is assumed to be first order in the FTHP model. This assumption is acceptable and true for most chemicals at environmental concentrations (Ambrose et al., 1983); however, it is not acceptable for concentrations near the solubility limit (Ambrose et al., 1983). EXAMs model is stopped if predicted concentration is higher than one half of the solubility limit, whereas in TOXIWASP, the model is stopped if the predicted concentration is equal or higher than one half of the solubility limit.  $C_{min}$  is not used by TOXIWASP due to numerical difficulties. Taking into account these issues, in our study,  $C_{max}$  is compared with the solubility limit of the contaminants as

was done in TOXIWASP in each time step. A control is performed on Cmin, such that Cmin concentrations are not allowed to have negative values.

### 3.3.8 Model Calibration, Validation, Sensitivity and Uncertainty Analyses

Model calibration is defined by Zheng and Bennett (2002) as “the process in which model input parameters are adjusted, either manually or through formal mathematical procedures, until the model output matches the field-observed conditions satisfactorily”. After model is calibrated, it should be validated with a different data set to confirm the model before using it for future prediction confidently (Chapra, 1997). The aim of the validation is expressed by Suk and Fikslin (2011) that calibrated model represents properly working of the model under all conditions. Schnoor (1996) states that while validation is conducted, coefficients and rate constants are the same as that in calibration. In this manner, it is proven that the model works properly.

The model calibration and validation are assessed by using statistical goodness of fit criteria between observed and predicted contaminant concentrations. Under the scope of this study, cosine theta ( $\cos\theta$ ), pearson correlation coefficient ( $r$ ), the root mean of squared errors (RMSE) (Zheng and Bennett 2002) and the multiple correlation coefficient ( $R^2$ ) are used for the evaluation of the model performance. The better the fit, the closer  $R^2$  approaches to “1”. In this study, when  $R^2$  is higher than 0.5, the fit is considered to be acceptable and satisfactory. The equations of the measures are listed below:

$$r = \frac{\sum_{i=1}^N (cal_i - \overline{cal})(obs_i - \overline{obs})}{\sqrt{\sum_{i=1}^N (cal_i - \overline{cal})^2 (obs_i - \overline{obs})^2}} \quad 3.21$$

$$RMSE = \left[ \frac{1}{N} \sum_{i=1}^N (cal_i - obs_i)^2 \right]^{1/2} \quad 3.22$$

$$R^2 = 1 - \frac{\sum_{i=1}^N (obs_i - cal_i)}{\sum_{i=1}^N (obs_i - \overline{obs})} \quad 3.23$$

where N is the total number of observations, cal and obs are the calculated and observed values in the model, respectively, and  $\overline{cal}$  and  $\overline{obs}$  are the means of the calculated and observed values, respectively. A perfect fit is indicated by a zero for RMSE, and 1 for  $R^2$  (changes between 0 and 1). Schnoor (1996) states that “model results should be within one order of magnitude of the field concentrations at all times” or “RMSE should be a minimum prescribed or optimal value”. r changes between -1 and 1. For +1, the correlation is a perfect increasing linear relationship while the correlation is a poor linear relation for -1.  $\cos \theta$  indicator is the similarity between two data using angular profile of predicted and measured data.

Sensitivity analysis is carried out to identify parameter(s) in the model that affect the predicted concentration the most (Allan and Stegemann 2007). Sensitivity analysis is performed considering the following steps: (i) reasonable changes are conducted on parameters and input of e.g. Lake Michigan considering 20-year model simulation based on calibrated data and (ii) each simulation reviews the change of each parameter or input (Weston solutions, 2004). After these steps, predicted concentration is drawn for all changes in a graph together with the calibration result for comparison. Finally, the most sensitive parameters or input which create the most significant effect on model results are determined. They are then ranked.

The reasons of uncertainties in parameters and input are explained by Ramaswami et al. (2005). These are measurement errors, errors in estimated parameters which are not measured and approximation errors straying the model from reality. The uncertainty

analysis is evaluated considering following steps: (i) determining the most sensitive parameters and input from sensitivity analysis, (ii) running the model with the proper and adjusted distributions for parameters and input, (iii) analyzing the model output to define the confidence intervals on the output (Weston solutions, 2004). In uncertainty analysis, the distribution of parameters is assumed uniform, lognormal and/or normal distributions. In uncertainty analysis, the model is analyzed for each congener concentration at the end of 20-year and runs for 1000 times by using Monte Carlo (MC) simulations to develop confidence intervals on the model output produced by the changes in the input and parameters.

For the most sensitive parameters, the distributions given in Table 3.7 are assumed such as lognormal, normal, uniform. Assumptions were made with two considerations; (i) statistical analysis of measured values and (ii) if not available, literature review for distribution use. Changes in the parameters are made according to assumption on their distribution.

Table 3.7 Equation of Distribution Used for MC in uncertainty analysis

Distribution	Equation
Uniform <sup>a</sup>	$X=(b-a)*U+a$
Normal <sup>b</sup>	$X=Z*\sigma+\mu$
Lognormal <sup>b,c</sup>	$\mu = \log\left(\frac{m^2}{\sqrt{v + m^2}}\right)$ $\sigma = \log\left(\frac{v}{m^2} + 1\right)$
Description of Terms	X: Parameter values produced by MC, a and b: lower and upper limits of parameters, respectively, U: Uniform random number, Z: Normal distributed random number, $\sigma$ : standard deviation, $\mu$ : Mean, m and v: The mean m and variance v of a lognormal random variable, respectively.

<sup>a</sup>: Ramaswami et al. (2005) <sup>b</sup>: Martinez et al. (2002) <sup>c</sup>: MC is applied by lognrnd function in MatLAB.



### 3.4 PCB Data

Two different data sets were needed to be used by the ADM and FTHP model. Their use is explained in Figure 3.19. The first, microcosm PCB data set from Baltimore Harbor (Fagervold et al., 2007, 2011), USA was used for ADM in order to estimate biodegradation rate constants of congeners (Figure 3.19). These constants are then used in the FTHP model as input. The second, field data taken from Lake Michigan sediment layer and water column, is used to run the FTHP model. The data were obtained from the U.S. EPA Office of Research and Development; Mid-Continent Ecology Division; Large Lakes and Rivers Forecasting Research Branch by personal communication (USEPA, 2015). Handling of both data sets are explained in the following sections.

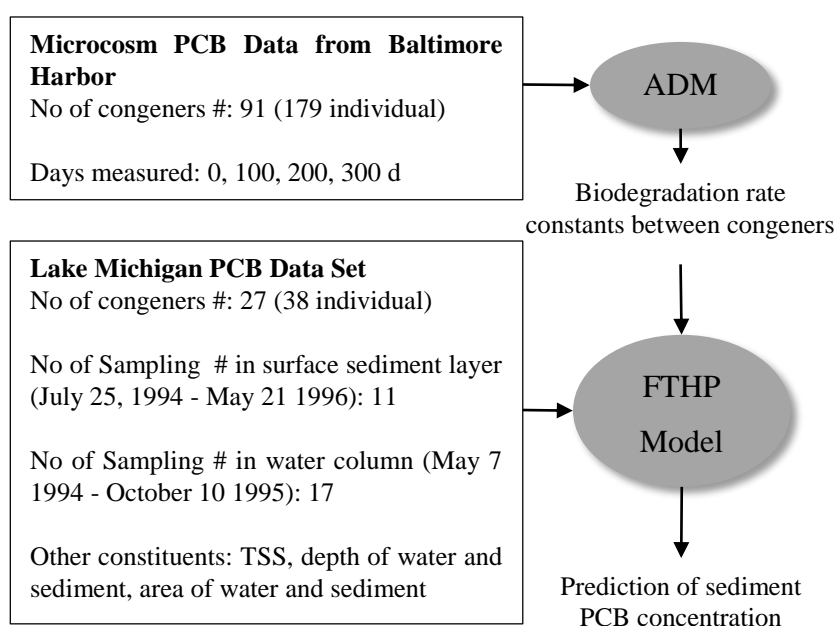


Figure 3.19 Uses of PCB Data Sets

### **3.4.1 Microcosm PCB Data: Baltimore Harbor Sediments, USA**

Laboratory PCB sediment data used in this study was obtained from microcosm experiments using Baltimore Harbor (BH) sediments (Fagervold et al., 2007, 2011), courtesy of Dr. Kevin Sowers from Department of Marine Biotechnology, University of Maryland Baltimore County. These data sets were specifically set up to observe microbial reductive dechlorination of PCBs, without major effect of physicochemical and other biotic/abiotic transformations. Four data sets from BH were prepared by addition of (i) no microorganism (no bioaugmentation), (ii) SF-1 and DEH-10, (iii) o-17 and DF-1 and (iv) SF-1, DF-1, DEH-10 and o-17 microorganisms.

The microcosm studies were prepared by Baltimore Harbor sediments spiked with Aroclor 1260 and incubated for 300 days with samples taken at day 0, 100, 200 and 300. 91 group of congeners (177 individual congeners with coelution) were analyzed (Table 3.8). Details about the preparation of microcosms and analysis are given elsewhere by Fagervold et al. (2007, 2011).

Changes in the concentration of PCBs (as average of triplicate microcosms) in mole percent with respect to time are depicted in Figure 3.20, Figure 3.21, Figure 3.22 and Figure 3.23. As can be seen from these figures, the greatest shift in PCB congener patterns occur between 100 and 200 days. Dramatical changes are observed in higher chlorinated homolog groups, such that, especially hexa and hepta including congeners 153/127, 141, 138/163/164, 187/159/182, 174/181, 177, 180, 170/190 and 196/203 are reduced after 100 days. There are other congeners belonging to lower homolog groups such as, congeners 20/21/33/53, 22/51, 52/73, 43/49/38 and 47/48/75 which are observed to be accumulated.



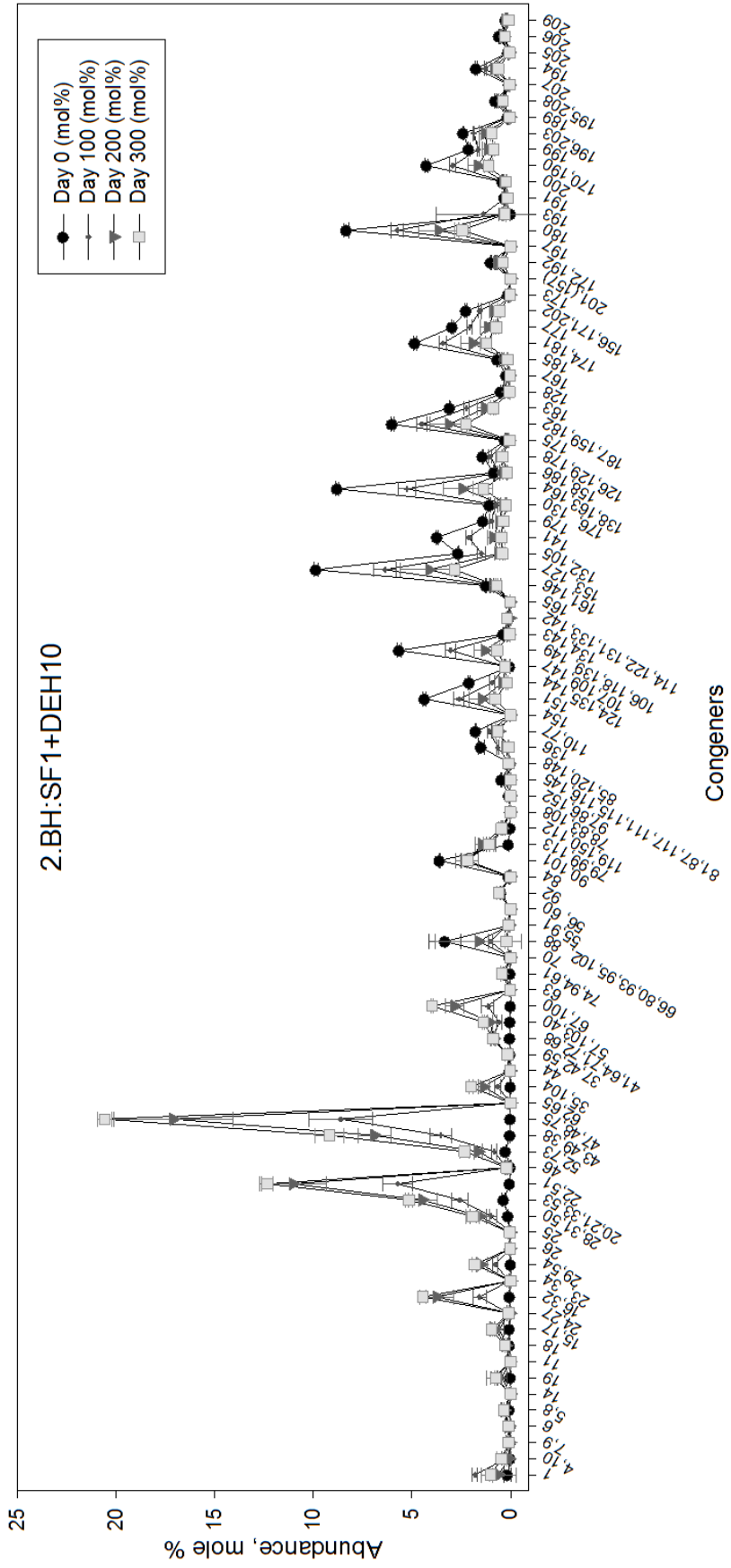


Figure 3.21 BH (SF1+DEH10) Microcosm Data (Fagervold et al., 2007, 2011)

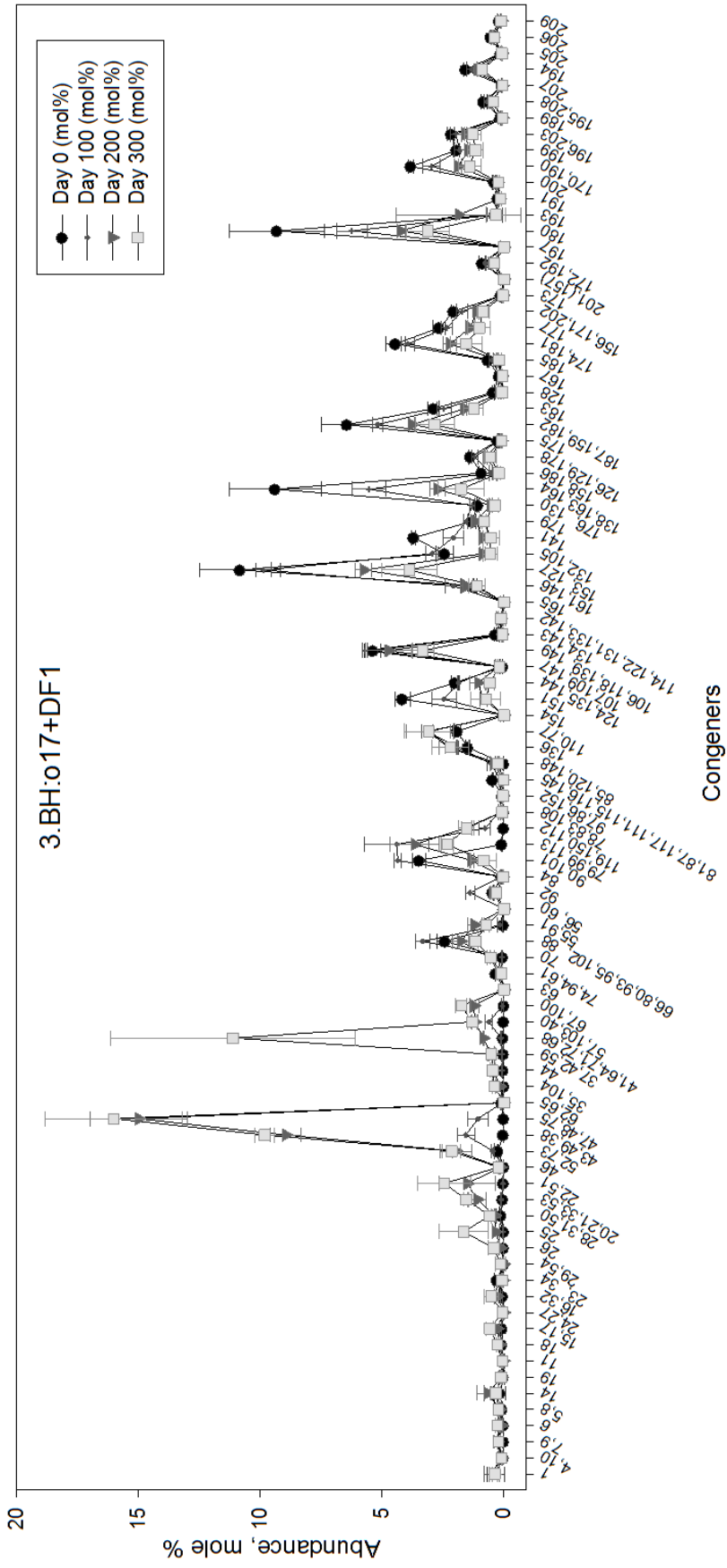


Figure 3.22 BH (o17+DF1) Microcosm Data (Fagerbold et al., 2007, 2011)



Table 3.8 IUPAC numbers of PCB congeners analyzed in microcosm sediments  
(Fagervold et al., 2007, 2011)

1	35/104	81/87/117/111/115/116/145	151	187/159/182
4/10	37/42/59	84	153/127	189
5/8	41/64/71/72/68	85/120/148	154	191
6	43/49/38	90/101	156/171/202	193
7/9	44	92	158/186	194
11	46	97/86/152	161/146	195/208
14	47/48/75	106/118/139/149	167	196/203
15/17	52/73	107/109/147	165	197
16/32	55/91	110/77	170/190	199
18	56/60	114/122/131/133/142	172/192	200
19	57/103/40	119/150/112	173	201/157
20/21/33/53	62/65	124/135/144	174/181	205
22/51	63	126/129/178	175	206
23/34	66/80/93/95/102/88	128	176/13	207
24/27	67/100	132/105	177	209
25	70	134/143	179	
26	74/94/61	136	180	
28/31/50	78/83/108	138/163/164	183	
29/54	79/99/113	141	185	

### 3.4.2 FTHP model PCB Data: Lake Michigan Sediments, USA

#### 3.4.2.1 Lake Michigan Mass Balance Project

The Lake Michigan Mass Balance Project (LMMBP) was conducted to develop an integrated mass balance model for the simulation of the transport, fate, and bioaccumulation of toxic chemicals in Lake Michigan. LMMBP was started and managed by USEPA Great Lakes National Program Office in 1994 for the toxic chemicals; PCBs, atrazine, transnonachlor, and mercury (Rossmann, 2006). The sampling for PCBs and other water and sediment constituents was conducted between 1994 and 1995 in various media such as air, water, sediment and biota. In our study,

PCB and property data concerning the Lake Michigan system were taken from LMMBP.

History of PCB contamination in Lake Michigan is given in Table 3.9 (Rossmann, 2006). Accordingly, despite the end of the production, toxic effects of PCBs on Lake Michigan ecosystem have still continued. Therefore, this contaminant is registered under the bioaccumulative chemicals of concern (BCCs) in the Great Lakes listed in the Water Quality Guidance for the Great Lakes System in 40 CFR 132 (Zhang et al., 2009). The first remediation process was started in 1980s for Sheboygan Harbor and finished in 1991. Now, remediation is going on for other rivers and harbors around lake.



Table 3.9 History of PCB contamination in Lake Michigan Basin (Rossmann, 2006)

Date	Event
1865	First PCB-like chemical discovered
1881	First PCBs synthesized
1914	Measurable amounts of PCBs found in bird feathers
1927	PCBs first manufactured at Anniston, Alabama
1935	PCBs manufactured at Anniston, Alabama and Sauget, Illinois
1948-1971	Outboard Marine Corporation at Waukegan, Illinois purchased eight million gallons of hydraulic fluid with PCBs
Mid-1950s to Mid-1960s	PCBs loaded to Kalamazoo River from deinking
1950s to 1980s	PCBs discharged to Manistique River and Harbor
1954	Appleton Paper Company began using PCBs as PCB-coated carbonless copy paper
1959-1971	PCBs used by Tecumseh Products Company as a hydraulic fluid was loaded to Sheboygan River
1959-1972	Outboard Marine Corporation at Waukegan, Illinois used hydraulic fluid with PCBs for die-casting
1969-1970	Paper company discharges of PCBs to Fox River peaked
1970	PCB production peaked at 85 million pounds and huge contamination noted at Sauget, Illinois plant
1971-1972	Appleton Paper Company and NCR Corporation phased out PCB use. Recycling of carbonless paper had occurred for several decades
1973	U.S. Food and Drug Administration (USFDA) establish 5 ppm PCB tolerance level in fish
1975	124,000 cans of salmon from Lake Michigan seized because of PCBs
1977	PCB production ends
1984	USFDA lowered PCB tolerance level in fish to 2 ppm
1985	Commercial fishing for carp and other valuable species outlawed on Green Bay
1991	End Sheboygan River PCB remediation of upper river
1991	U.S. Department of Health and Human Services label PCBs as possible carcinogen
1992	End Waukegan Harbor PCB remediation
1998	The eight Great Lakes states agreed on a "Great Lakes Protocol for Fish Consumption Advisories" that lowered the regional standard from the USFDA commercial standard of 2 ppm down to 0.05 ppm
1997-1998	Milwaukee River PCB remediation
2001	Manistique Harbor PCB remediation completed
2002	Possibly begin Grand Calumet River PCB remediation

As part of the LMMBP, the mass balance of PCBs was conducted by a contaminant and transport model called LM2-Toxic. The model includes contaminant transport, partitioning, and biogeochemical transformations in both the water column and sediments. Furthermore, MICHTOX model is used to compare the results of contaminant transport and transformation to LM2 results. LM2-Toxic was calibrated and validated for selected individual congeners and the sum of PCBs. However, total PCBs are considered to predict and identify transport, sources of contamination, and loss pathways (Rossmann, 2006). Various model resolutions for water column and sediment are defined for state variables and scale of predictions (Figure 3.24). The lake

is divided into 10 spatial segments. Five layers in depth are for water column, hence the segments between numbers 1 and 41 are for water column. One layer is for surficial sediment. The segments between numbers 42 and 94 are divided into 5x5 km<sup>2</sup> grid cells for surficial sediment considering non-depositional areas, transitional areas, and depositional areas (Figure 3.24). Within the scope of LMMBP, PCB concentration was measured for 42 and 40 groups of congeners in sediment and water column, respectively.

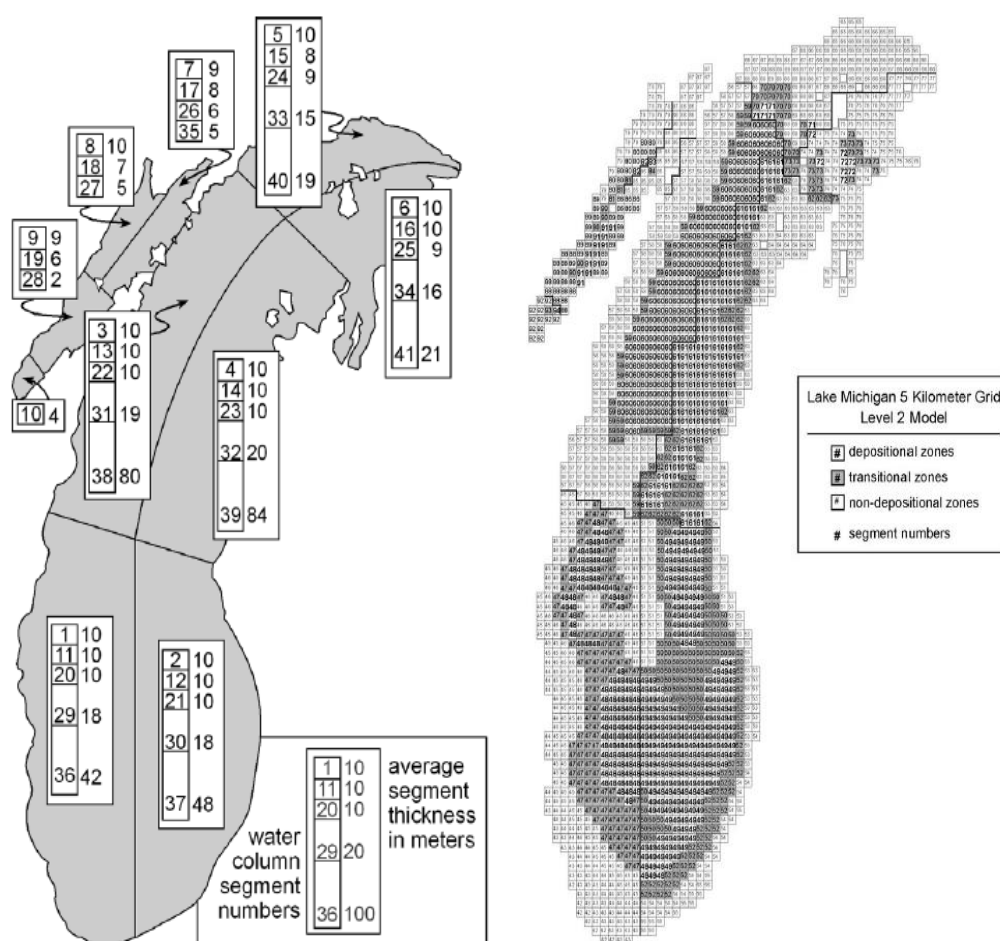


Figure 3.24 Segmentation of the water column (Left) and surficial sediments (Right) used in LM2-Toxic Model (Rossmann, 2006)

### 3.4.2.2 Description of LMMBP data

All lake is not considered in the FTHP model developed in this study. A limited region of the lake is used. This region is selected considering high PCB distribution in surficial segment between numbers 42 and 94. According to distribution of total PCB concentration in Lake Michigan surface sediment, the data set for the southeastern part of the lake is selected since sediments contain the highest concentration of PCBs. Furthermore, the highest PCB concentration in water column is also in the southeastern part of the lake. Accordingly, segment number 49 is selected for sediment, which is a transitional zone (Figure 3.25). Segment 37 is selected for water column, because it is located above segment 49.

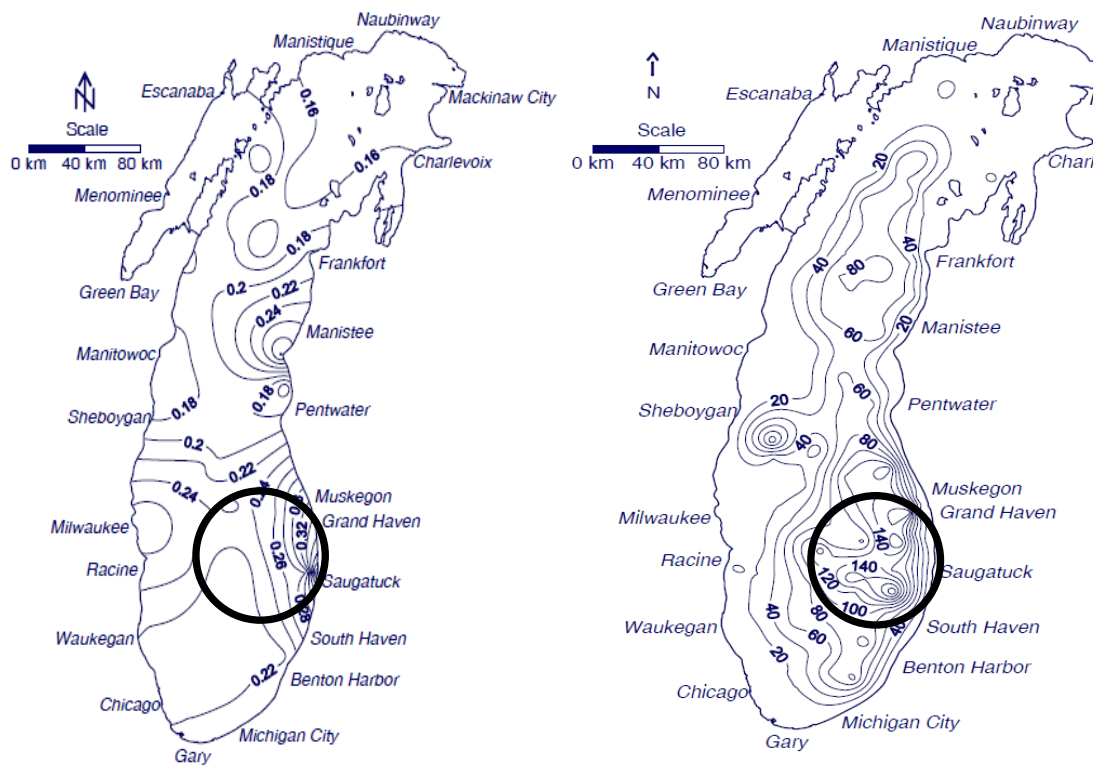


Figure 3.25 Distribution of total PCBs (ng/L) in 1994-1995 Lake Michigan water column (Left) and surficial sediments (Right) (Zhang, 2006, part1ch5)

133 sediment samples were collected from all around the lake between May 1994 and May 1996. In Segment 49, 21 sediment samples were collected between July 25, 1994 and May 21 1996 (Figure 3.26). Some of these samples are taken on the same day, but from different locations (Table 3.10). These sediment samples were used in our study.



Figure 3.26 Surface sediment samples collected in Segment 49

Table 3.10 Sediment samples collected from Segment 49

<b>Sample No</b>	<b>Latitude</b>	<b>Longitude</b>	<b>Station Name</b>	<b>Station depth, m</b>	<b>Sampling Date</b>
1	42.818	-86.486	LM94-36	80	7/25/1994
2	43.016	-86.328	LM94-47	47	7/25/1994
3	42.293	-86.652	LM94-16	60	7/26/1994
4	41.984	-87.014	LM94-8	65	7/26/1994
5	42.175	-86.734	LM94-13	79	7/26/1994
6	42.142	-86.662	LM94-H22	52	7/26/1994
7	42.175	-86.733	LM94-13S		10/5/1994
8	42.385	-86.592	LM94-22		10/6/1994
9	42.285	-86.633	LM94-15		10/6/1994
10	42.496	-86.829	LM94-25		10/8/1994
11	42.587	-86.856	LM94-27		10/8/1994
12	42.819	-86.474	LM94-36S	78	10/10/1994
13	42.643	-86.532	LM94-29		10/10/1994
14	42.834	-86.999	LM94-39		10/10/1994
15	42.733	-86.999	LM94-33		10/10/1994
16	42.834	-86.999	LM94-39		10/12/1994
17	43.016	-86.407	LM94-46	73	10/12/1994
18	42.122	-87.053	LM94-11	87	9/6/1995
19	42.773	-87.081	LM94-34	157	9/6/1995
20	42.354	-86.957	LM94-18		5/20/1996
21	42.122	-87.053	LM94-11		5/21/1996

PCB concentrations in the water column were measured as particulate and dissolved phases. Water samples were collected from three locations in Segment 37, these are shown in Figure 3.27. From these three locations, a total of 17 water samples were collected between May 7 1994 and October 10 1995.





Figure 3.27 Water column sampling locations in Segment 37

In LMMBP (USEPA, 2015), PCBs were measured as 40 groups of congeners for water samples and 42 groups of congeners for sediments. However, 10 groups of congeners (namely, 5/8, 12, 13, 15/17, 18, 77, 89, 197, 196/203, 201) could not be detected in the sediments. When both PCB data sets were compared, 27 groups of congeners were

found to be present in both. These are: 16, 26, 28/31, 33, 44, 49, 52, 56/60, 66, 70/76, 74, 81, 84/92, 85, 87, 99, 101, 118, 123/149, 105/132/153, 151, 138/163, 170/190, 180, 182/187, 195/208 and 146. Hence, these congener groups could be used as input in the FTHP model.

### 3.4.2.3 Data Handling

The 21 sediment samples were taken on 10 different dates, as can be seen from Table 3.10. The arithmetic average of concentrations in the same dates are taken. Accordingly, a total of 10 measurements in different dates are used for the model and data is given in **Hata! Başvuru kaynağı bulunamadı.** in ng/L. To convert ng/g dry weight to ng/L, the equation below (Rossmann, 2006) is used. In the FTHP model, unit ng/L is used for the concentration of PCBs in the sediments as in LM2 model.

$$C_s^a = C_s^b * \rho * (1 - \varphi) * 10^3 \quad 3.24$$

where  $C_s^a$ : PCB concentrations in surface sediment per sediment volume a, ng/L,  $C_s^b$ : PCB concentration in surface sediment per sediment mass b, ng/g dry weight,  $\rho$ : bulk density of surficial sediments, (gdw/cm<sup>3</sup>),  $\varphi$ : porosity (dimensionless). PCB congener concentrations in the sediments range from 5.64 to 1444.63 ng/L.

Table 3.11 Concentration of individual PCB congeners in 10 sediment samples (ng/L) (USEPA, 2015)

Sample No	1	2	3	4	5	6	7	8	9	10	Min	Max	Med.	Avg	SD	RSD
	0 <sup>a</sup>	1	72	73	75	77	79	408	665	666						
South/North <sup>b</sup>	N	S	S	S	N	N	N	N	S	S	S	S	S	S	S	S
16	31.4	15.9	44.5	37.0	33.9	18.7	47.0	32.8	17.2	5.6	47.0	32.1	28.4	13.5	47.4	
26	42.1	52.2	63.6	59.1	51.2	52.7	69.9	43.1	19.1	13.4	69.9	51.7	46.6	18.2	39.0	
28/31	645.1	817.5	997.4	839.8	829.4	810.5	1007.2	685.0	278.7	206.6	1007.2	814.0	711.7	272.4	38.3	
33	126.1	155.8	188.0	187.5	147.2	147.1	210.0	173.4	80.4	40.5	210.0	151.5	145.6	51.9	35.6	
44	216.8	241.0	291.9	248.9	263.4	291.8	333.9	449.3	201.6	113.3	449.3	256.1	265.2	88.4	33.3	
49	131.6	154.4	192.3	152.7	193.8	181.0	213.9	177.5	73.1	56.0	213.9	165.9	152.6	52.2	34.2	
52	262.0	293.1	376.3	294.8	411.9	379.1	424.8	412.1	164.9	139.7	424.8	335.5	315.9	103.1	32.6	
56/60	408.2	462.6	529.4	442.4	591.2	564.2	636.6	666.1	253.1	164.4	666.1	496.0	471.8	162.8	34.5	
66	818.2	931.2	1156.0	926.3	1382.2	1259.6	1363.8	1305.9	541.4	397.9	1382.2	1043.6	1008.2	346.3	34.3	
70/76	403.7	463.4	546.4	455.7	672.6	619.6	655.3	683.6	267.8	199.4	683.6	504.9	496.7	170.2	34.3	
74	182.7	223.9	248.6	206.2	234.1	246.1	271.8	209.2	85.7	66.2	271.8	216.6	197.4	68.9	34.9	
81	17.4	20.0	21.6	14.3	36.9	29.0	25.9	51.8	9.9	7.9	51.8	20.8	23.5	13.3	56.5	
84/92	326.9	250.6	322.9	234.1	409.5	380.2	405.5	601.0	197.3	123.5	601.0	324.9	325.1	134.8	41.5	
85	151.3	160.2	195.6	130.5	316.3	264.1	262.0	371.2	140.4	105.9	371.2	177.9	209.7	88.8	42.4	
87	144.4	167.4	178.9	134.4	225.7	205.1	225.4	259.2	88.3	76.9	259.2	173.1	170.6	60.3	35.3	
99	157.0	159.0	205.9	139.2	322.2	273.1	276.3	375.9	125.6	99.8	375.9	182.4	213.4	93.2	43.7	
101	295.7	308.8	372.5	268.7	571.9	494.3	496.8	685.3	236.9	190.5	685.3	340.6	392.1	162.0	41.3	
118	415.7	359.4	510.9	394.9	920.8	746.3	718.4	773.2	351.7	290.2	920.8	463.3	548.2	221.3	40.4	
123/149	147.8	124.3	183.1	124.5	337.9	266.4	253.1	320.7	142.0	102.0	337.9	165.5	200.2	87.1	43.5	
105/132/153	512.0	433.1	589.0	435.4	1139.3	924.8	840.0	1117.1	485.4	347.3	1139.3	550.5	682.3	296.9	43.5	
151	41.4	38.2	51.6	35.6	89.5	72.5	70.4	81.0	40.7	30.5	89.5	46.5	55.1	21.2	38.5	
138/163	600.0	484.0	673.6	420.3	1444.6	1064.3	952.6	1281.6	412.0	296.0	1444.6	636.8	762.9	398.8	52.3	
170/190	105.3	84.8	112.9	80.8	231.6	194.7	168.3	231.1	91.2	63.0	231.6	109.1	136.4	64.3	47.1	
180	212.3	168.6	211.1	157.3	436.5	378.9	309.4	456.3	205.6	131.2	456.3	211.7	266.7	119.7	44.9	
182/187	74.1	63.1	87.3	59.1	181.1	140.4	123.9	188.4	85.1	55.3	188.4	86.2	105.8	49.8	47.1	
195/208	28.4	21.3	34.6	22.7	72.6	58.5	45.7	87.6	35.9	22.4	87.6	35.2	43.0	23.0	53.5	
146	70.0	56.7	91.0	56.9	162.7	126.7	118.9	161.6	63.3	43.0	162.7	80.5	95.1	44.5	46.9	

<sup>a</sup>: Day 0 is 7/25/1994, <sup>b</sup>: Segment 49 (120 km from north to south), is divided as South and North (60 km – 60 km)



Part of the sediment data is used for calibration and the other is used for model validation. Segment 49 is a wide region (120 km from north to south), so the region is divided as South and North (60 km – 60 km) and the samples belonging to the south are used for calibration, while the ones belonging to the north are used for validation (Figure 3.28 and Table 3.12). Such a split allows for both spatial and temporal variation of the sediment data to be used in calibration and validation.

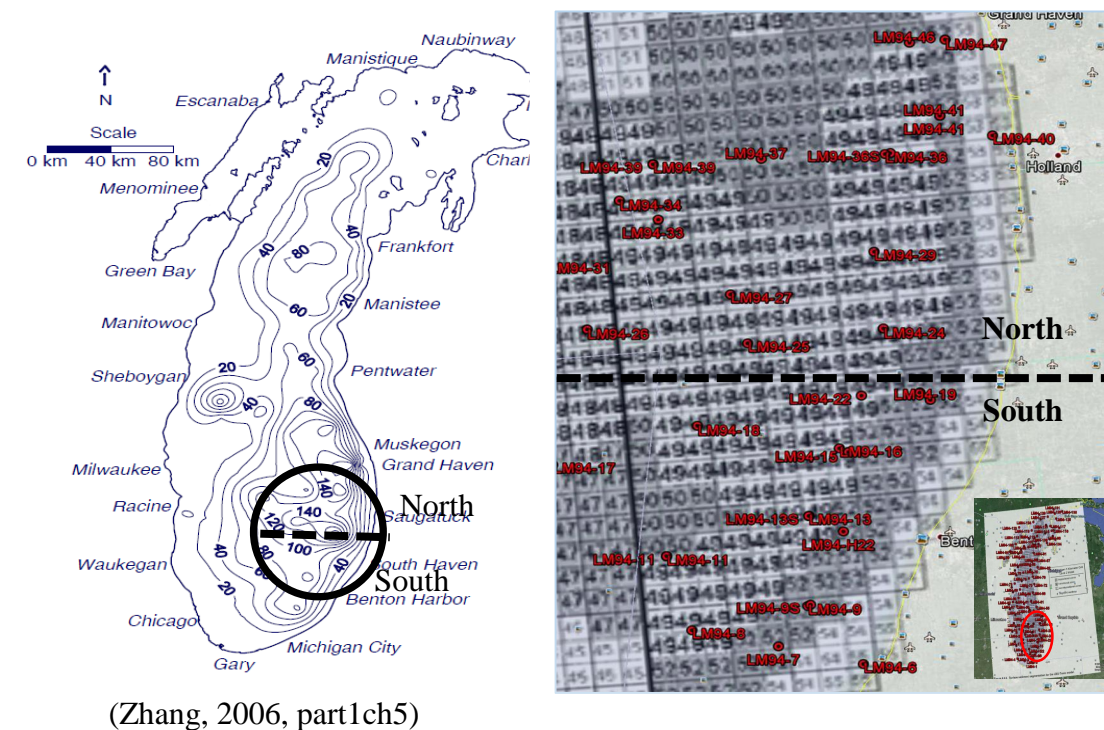
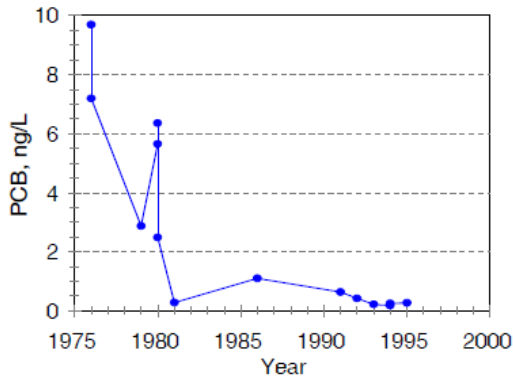


Figure 3.28 Samples at South and North used for calibration and validation in segment 49, respectively

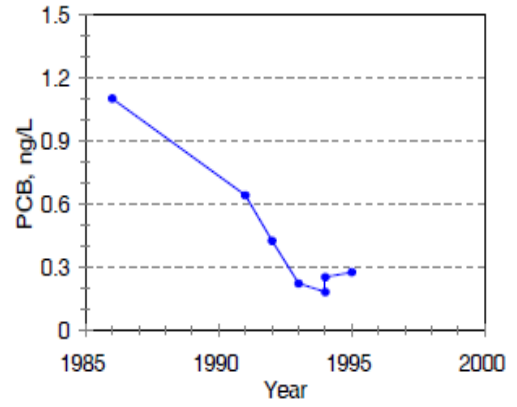
Before being used in the FTHP model, water column PCB concentrations, which are measured in both particulate and dissolved phase, are added to give one total concentration for each congener in the water phase. A total of 17 water column samples were taken on 12 different dates. The arithmetic average of sediment concentrations

in the same dates are taken as was done for sediment samples. Accordingly, a total of 12 measurements in different dates are evaluated here.

In the FTHP model, we assume that water column PCB congener concentrations do not change with time. To test the validity of this assumption, Figure 3.29 and Figure 3.30 are prepared. Accordingly, water column total PCBs show a decreasing trend from 1977 to the 1990s, however, seems constant after 1993 (Figure 3.29). Figure 3.30 depict changes in the individual congener concentrations within the time frame of the LMMBP sampling. Although some fluctuations exist, no major increasing or decreasing trend is evident for PCB congener concentrations in the water column. Lastly, descriptive statistics of the data presented in Figure 3.30 is given separately in Table 3.12 and Table 3.13 for north and south parts, respectively. This also shows that concentration distributions in water column do not show a major fluctuation. When the sediment and water phase PCB concentrations are compared, it can be stated that sediment concentrations are four to six orders of magnitude higher. The average and median of water column PCB concentrations are very close and mostly identical to each other (Table 3.12 and Table 3.13). In the FTHP model, average water column congener concentrations for the samples collected in the south region (from stations 18M and 380) (Table 3.13) are used during model calibration and the average water column congener concentrations for the samples collected in the north region (from station 6) (Table 3.12) are used during model validation.



(a)



(b)

Figure 3.29 Time Variation of Total PCBs PCBs in Lake Michigan water column (ng/L) (a) between 1975 and 1995 (b) between 1986 and 1995 (Rossmann, 2006)

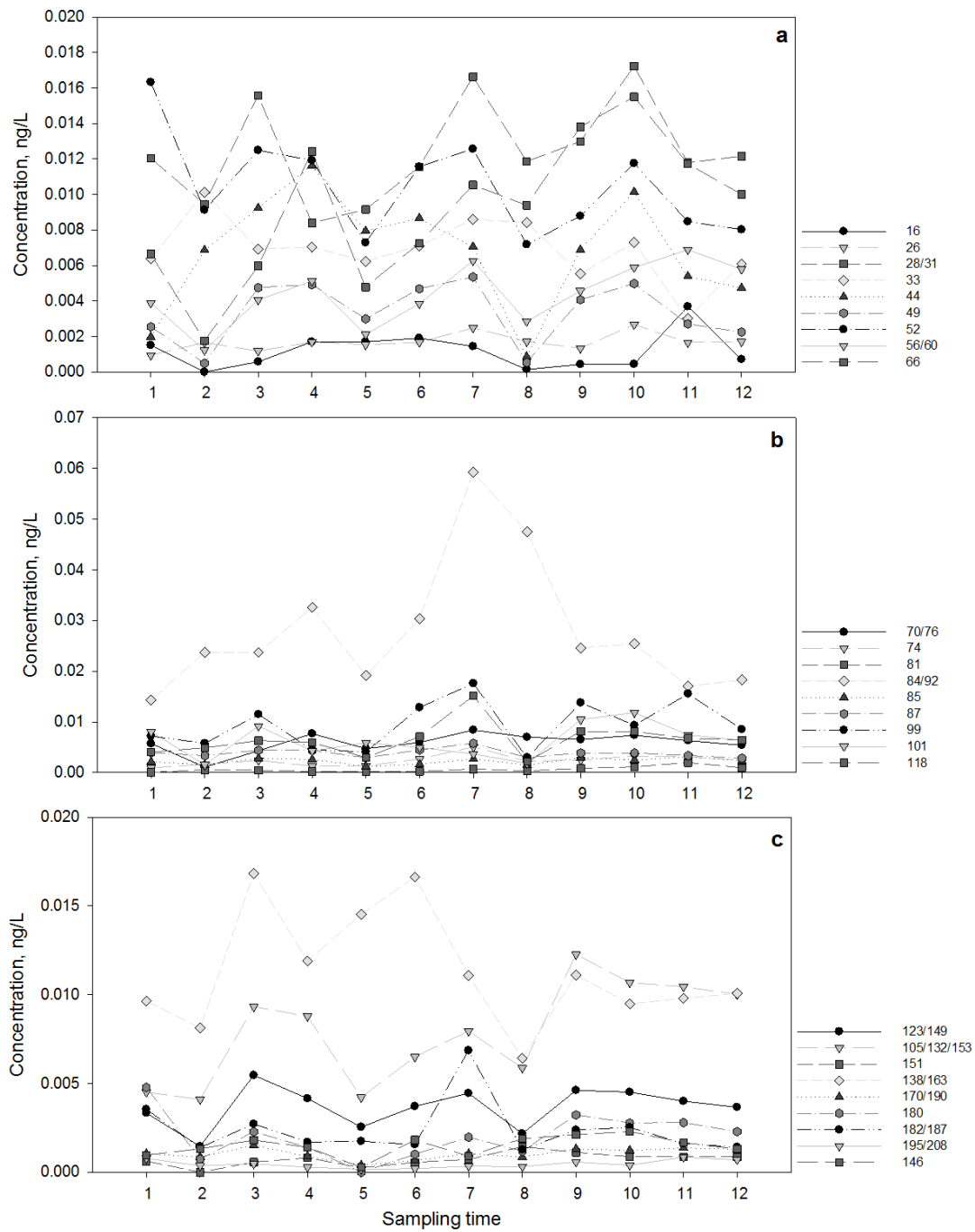


Figure 3.30 Distribution of Total Concentration of Congeners Through Time

(Water column concentrations of congeners a. from IUPAC no 16 to 66, b. from IUPAC No 70/76 to 118, c. from IUPAC No 123/149 to 146 with respect to each sample)

Table 3.12 Descriptive statistics of PCB congener concentrations (ng/L) in the water column at the north region

Statistics/Congeners	16	26	28/31	33	44	49	52	56/60	66	70/76	74	81	84/92	85
Average (ng/L)	0.001	0.002	0.013	0.007	0.006	0.003	0.011	0.005	0.010	0.006	0.002	0.001	0.028	0.002
Standard Deviation	0.001	0.001	0.004	0.002	0.004	0.002	0.004	0.002	0.005	0.002	0.001	0.001	0.016	0.001
Relative Standard Deviation (%)	92.01	42.94	31.23	31.87	59.85	53.82	33.24	49.88	53.29	40.94	59.20	85.90	56.67	44.98
Median	0.001	0.002	0.012	0.007	0.007	0.003	0.011	0.004	0.008	0.006	0.002	0.001	0.024	0.002

Statistics/Congeners	87	99	101	118	123_149	105/132 /153	151	138/163	170/190	180	182/187	195/208	146
Average (ng/L)	0.004	0.010	0.007	0.007	0.004	0.008	0.001	0.011	0.001	0.002	0.003	0.001	0.001
Standard Deviation	0.001	0.006	0.004	0.005	0.002	0.005	0.001	0.004	0.001	0.002	0.002	0.0003	0.001
Relative Standard Deviation (%)	29.38	56.47	55.06	70.57	44.26	62.43	73.95	40.28	58.70	76.06	73.72	63.86	50.94
Median	0.004	0.009	0.007	0.006	0.004	0.006	0.001	0.010	0.001	0.002	0.002	0.0004	0.002

Table 3.13 Descriptive statistics of PCB congener concentrations (ng/L) in the water column at the south region

Statistics/Congeners	16	26	28/31	33	44	49	52	56/60	66	70/76	74	81	84/92	85
Average (ng/L)	0.002	0.002	0.012	0.007	0.009	0.005	0.012	0.004	0.007	0.006	0.003	0.0002	0.030	0.002
Standard Deviation	0.000	0.000	0.005	0.002	0.003	0.001	0.002	0.003	0.010	0.003	0.001	0.0001	0.017	0.001
Relative Standard Deviation (%)	8.90	26.35	44.90	23.59	39.19	25.48	21.39	66.30	141.42	53.86	42.49	51.90	56.62	79.89
Median	0.002	0.002	0.012	0.007	0.009	0.005	0.012	0.004	0.007	0.006	0.003	0.0002	0.030	0.002

Statistics/Congeners	87	99	101	118	123_149	105/132 /153	151	138/163	170/190	180	182/187	195/208	146
Average (ng/L)	0.004	0.013	0.005	0.007	0.004	0.007	0.001	0.017	0.001	0.001	0.002	0.0002	0.002
Standard Deviation	0.001	0.007	0.000	0.005	0.002	0.006	0.001	0.001	0.001	0.001	0.001	0.0003	0.001
Relative Standard Deviation (%)	14.71	57.53	6.33	70.44	53.97	97.72	141.42	3.85	123.94	141.42	33.19	141.42	75.79
Median	0.004	0.013	0.005	0.007	0.004	0.007	0.001	0.017	0.001	0.001	0.002	0.0002	0.002

### 3.4.2.4 Other Constituents used in the FTHP model

**TSS Concentration:** In the segment 37 modeled, 48 samples are taken for TSS between May 6 1994 and October 12 1995 (USEPA, 2015). In the FTHP model, TSS concentration is assumed to be independent of time. Therefore, TSS data is evaluated to establish one TSS concentration that can be used as input to the model. Accordingly, TSS data is presented in Figure 3.31 while the descriptive statistics of TSS data is given in Table 3.14. The median of TSS (0.9 mg/L) is used as input in the model.

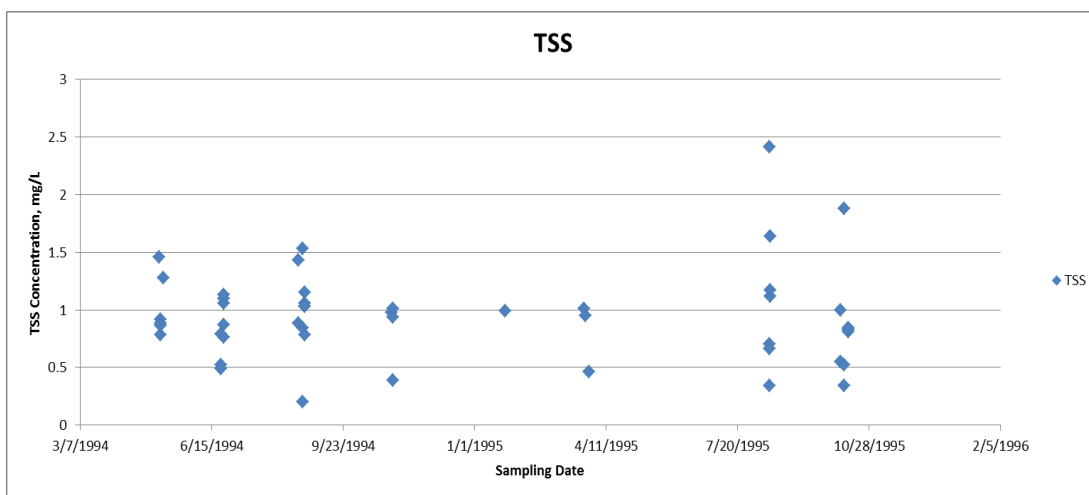


Figure 3.31 TSS Concentration

Table 3.14 Descriptive statistics of TSS Data

Constituent	Sample no	Average	SD	RSD(%)	Median	Min	Max
TSS, mg/L	48	0.942	0.402	42.68	0.900	0.20	2.41

**Sediment and Water Properties:** The properties of sediment and water column are given in Table 3.15 and Table 3.16 (Rossmann, 2006). The average values are selected from the

ranges given in Table 3.16 for organic carbon fraction ( $f_{oc}$ ) in water column and sediment layer. For water column and sediment layer,  $f_{oc}$  values are taken as 0.0645 and 0.0375, respectively.

Table 3.15 Volume and Area of Sediment Layer and Water Column (Rossmann, 2006)

<b>Sediment Layer</b>	
#of grids Pertained by segment 49	177
1 of grid Area, km <sup>2</sup>	25
Area Segment 49, km (A <sub>m</sub> )	4425
Sediment depth, m (d <sub>m</sub> )=Mixing Layer	0.013
Sed. Volume, m <sup>3</sup> (V <sub>m</sub> )	57525000
<b>Water Column</b>	
Average Segment Thickness (of segment 37), m	48.1
Area Segment 37, km (A <sub>w</sub> )	4425
Water Volume, m <sup>3</sup> (V <sub>w</sub> )	2.13 10 <sup>11</sup>

Table 3.16 Water and sediment properties measured in LMMBP (Rossmann, 2006)

<b>Constituent</b>	<b>Unit</b>	<b>LM2 Model</b>	<b>MichTOX Model</b>
Porosity	-	0.953	0.943-0.966
Monthly water temperatures	°C		1.7-19.2
Pore water diffusion coefficient	m <sup>2</sup> /day	1.80x10 <sup>-5</sup>	
Diffusion Coefficient	m <sup>2</sup> /day	1.73x10 <sup>-4</sup>	
Bulk density of surficial sediments	gdw/cm <sup>3</sup>	2.45	
<b>Monthly fraction organic carbon (f<sub>oc</sub>):</b>			
for stratified water surface segments 1-7	-		0.127-0.290
for completely mixed water segments 8-10	-		0.039-0.090
for sediment segments 11-17	-		0.023-0.052



**Contaminant Properties:** The properties for congeners are given in Table 3.17. These are taken from Mackay et al. (2006). When there is more than one value for  $K_{ow}$  and solubility, the median value is taken to be used as input in the FTHP model.

Table 3.17 Molecular weight, solubility and  $K_{ow}$  of congeners (Mackay et al., 2006)

Congener IUPAC No	Median $\log K_{ow}$	Min $\log K_{ow}$	Max $\log K_{ow}$	Median solubility, mg/L at 25 °C
16	5.215	4.15	5.36	0.505
26	5.68	5.52	5.76	0.205
28/31	5.725	4.38	6.33	0.1495
33	5.71	5.48	5.98	0.161
44	5.79	4.79	6.67	0.06315
49	5.925	5.73	6.38	0.0202
52	5.89	3.91	6.26	0.035
56/60	5.95	5.33	7.8733	0.04155
66	6.105	5.8	6.31	0.02695
70/76	6.05	5.72	6.39	0.0432
74	6.16	6.1	6.67	0.0306
81	6.24	5.96	6.64	0.00313
84/92	6.11	5.6	6.97	0.03335
85	6.61	6.18	6.63	0.013
87	6.285	5.45	6.85	0.007415
99	6.41	6.26	7.21	0.0103
101	6.375	4.12	7.64	0.0103
118	6.615	6.24	7.42	0.0153
123/149	6.57	6.14	7.28	0.003275
105/132/153	6.8	4.97	8.35	0.004734
151	6.49	6.32	7.35	0.00454
138/163	6.82	6.39	7.9	0.00392
170/190	7.08	6.83	7.46	0.000432
180	7.18	6.56	7.4	0.00063
182/187	7.0964	6.76	7.4	0.021073
195/208	7.78	7.35	9.05	0.000136
146	6.85	6.57	7.12	0.00228

**Deep Sediment Contaminant Concentration:** In our model, deep sediment concentration is assumed to stay constant with time. No measurement or data is presented in the LMMBP regarding this concentration. Therefore, studies for Lake Michigan in the literature are investigated. In our model, surface sediment depth is given as 3.1 cm for sediment layer

49 which is our modelling region (Rossmann, 2006). Li et al. (2006) studied in Lake Michigan and took core samples in May 2002. Their sampling point LM18 is close to our study region (Figure 3.32). Therefore, concentration of total PCBs through the core is investigated. As can be seen from Figure 3.32, concentration of total PCBs approaches to zero after 4 cm depth. Therefore, in our model, deep sediment PCB concentration is initially assumed as zero for all congeners.

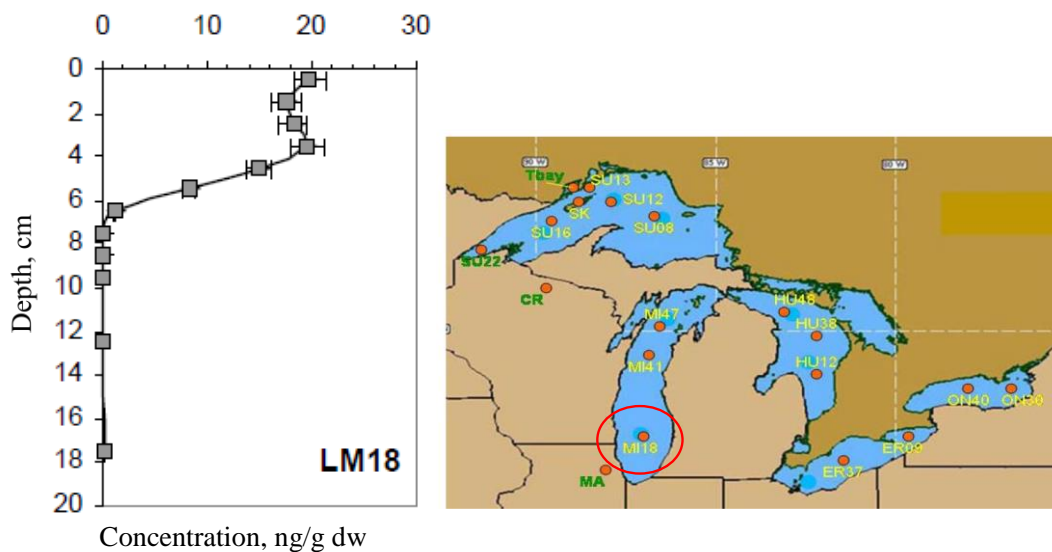


Figure 3.32 Total PCB concentration versus depth in Lake Michigan -  $\Sigma_{39}$  PCBs (USEPA, 2006)

**Settling, Resuspension and Burial Velocities:** Settling velocity is the value used in MichTOX model (Endicott et al., 2006) and burial velocity is taken from LM2-Toxic model. The values are given in Table 3.18. Resuspension velocity is calculated by using solid mass balance equation which is explained in section 3.2.6.

Table 3.18 Settling, Resuspension and Burial Velocities (Rossmann, 2006)

Segment	BIC Settling Velocity	PDC Settling Velocity
37	0.06	0.75
Parameter	Value	Unit
Particle settling velocity	1.5	m/day
Segment	Burial velocity (m/d)	depth (m)
49	9.94E-06	0.031

***Diffusion Coefficient:*** Molecular diffusion of congeners is given in Table 3.19. As can be seen, molecular diffusion of congeners changes according to number of chlorine. Therefore, in our model, molecular diffusion of some of congeners not listed in Table 3.19 is estimated and used according to this rule. The equation for Cl # higher than 5 in Figure 3.33 will be used by using molecular diffusion of number of chlorines 2, 3, 4 and 5 in Schneider (2005). Accordingly, molecular diffusion of the PCB congeners is tabulated in Table 3.20.

Table 3.19 Molecular Diffusion Coefficient of Congeners (Schneider, 2005)

Congener IUPAC No	Cl#	D <sub>m</sub> (cm <sup>2</sup> /s)	log(K <sub>ow</sub> )	log(K <sub>p</sub> )	D <sub>m</sub> (m <sup>2</sup> /day)
<b>PCB 4, 10</b>	2	5.97E-06	4.65	3.52	5.16E-05
<b>PCB 8, 5</b>	2	5.97E-06	5.07	4.36	5.16E-05
<b>PCB 19</b>	3	5.70E-06	5.02	4.31	4.92E-05
<b>PCB 17</b>	3	5.70E-06	5.24	4.53	4.92E-05
<b>PCB 18</b>	3	5.70E-06	5.25	4.54	4.92E-05
<b>PCB 33, 21, 53</b>	3	5.70E-06	5.6	4.89	4.92E-05
<b>PCB 52</b>	4	5.46E-06	5.84	5.13	4.72E-05
<b>PCB 49</b>	4	5.46E-06	4.85	5.14	4.72E-05
<b>PCB 66, 95</b>	4	5.46E-06	6.2	5.49	4.72E-05
<b>PCB 110</b>	5	5.24E-06	6.48	5.77	4.53E-05

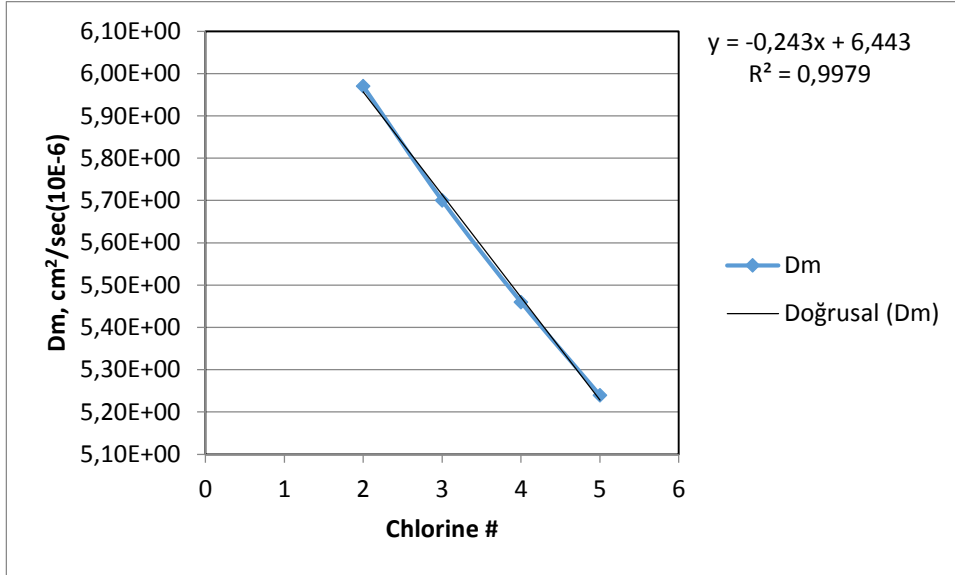


Figure 3.33 Molecular Diffusion vs. No of Cl on biphenyl structure

Table 3.20 Molecular Diffusion used in the FTHP model

<b>IUPAC Congener No</b>	<b>Molecular Diffusion, cm<sup>2</sup>/sec</b>	<b>IUPAC Congener No</b>	<b>Molecular Diffusion, cm<sup>2</sup>/sec</b>
<b>16</b>	0.00000571	<b>87</b>	0.00000523
<b>26</b>	0.00000571	<b>99</b>	0.00000523
<b>28/31</b>	0.00000571	<b>101</b>	0.00000523
<b>33</b>	0.00000571	<b>118</b>	0.00000523
<b>44</b>	0.00000547	<b>123/149</b>	0.00000511
<b>49</b>	0.00000547	<b>105/132/153</b>	0.00000507
<b>52</b>	0.00000547	<b>151</b>	0.00000499
<b>56/60</b>	0.00000547	<b>138/163</b>	0.00000499
<b>66</b>	0.00000547	<b>170/190</b>	0.00000474
<b>70/76</b>	0.00000547	<b>180</b>	0.00000474
<b>74</b>	0.00000547	<b>182/187</b>	0.00000474
<b>81</b>	0.00000547	<b>195/208</b>	0.00000438
<b>84/92</b>	0.00000523	<b>146</b>	0.00000499
<b>85</b>	0.00000523		

### 3.5 PBDE Data

Two different PBDE data sets were used in this study (Figure 3.34). Microcosm PBDE data was used for ADM in order to obtain biodegradation rate constants of congeners undergoing debromination pathways (Figure 3.34). These constants, are then used in the FTHP model as input. Environmental PBDE data were obtained from the Regional Monitoring Program for Water Quality in the San Francisco Bay (RMP) (SFEI, 2015). The details about them are explained in the following sections.

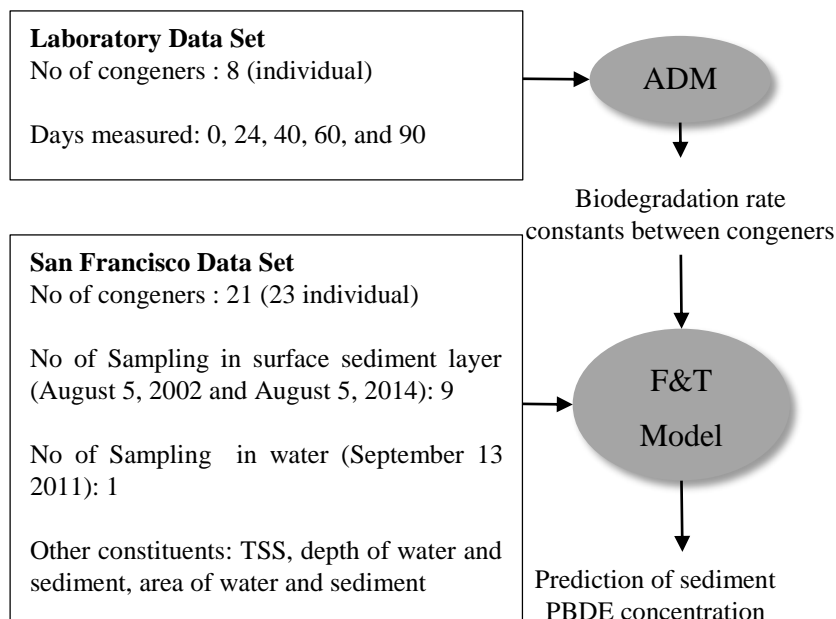


Figure 3.34 Uses of PBDE Data Sets

#### 3.5.1 Laboratory PBDE Data: Contaminated Soil, China

The data set used in the study was obtained from soils in the e-waste recycling town of Qingyuan, Guangdong province, South China (23.57° N, 113.0° E) (Song et al., 2015). The samples were taken between 0 and 15 cm depth. The microcosm samples were

prepared in 15 ml glass and triplicates. Eight PBDE congeners (28, 47, 99, 100, 153, 154, 183 and 209) were analyzed at 0, 24, 40, 60, and 90 days. These sets contain microbial reductive debromination of PBDEs, without major effect of physicochemical and other biotic/abiotic transformations. Lactate is added as electron donor. Details about the preparation of microcosms and analysis are given in Song et al. (2015). Changes in the concentration of PBDEs in ng/g dry weight (dw) with respect to time are depicted in Figure 3.35. As can be seen from the figure, while amount of BDE 209 decreases in 90 days, amount of BDEs 99, 100, 153, 154 and 183 increase. Especially the changes in these six congeners are observed sharply between 0 and 24 days. Song et al. (2015) discuss that while BDE 47 and BDE 209 are gradually degraded, significant degradation is not observed in other congeners. They state that increase in 99, 100, 153, 154 and 183 is explained by degradation of higher brominated congeners. In the literature, increase of these *ortho* substituted congeners in time due to octa-BDE mixture (Robrock et al., 2008) and BDE 209 (He et al., 2006; Tokarz et al., 2008) are observed.

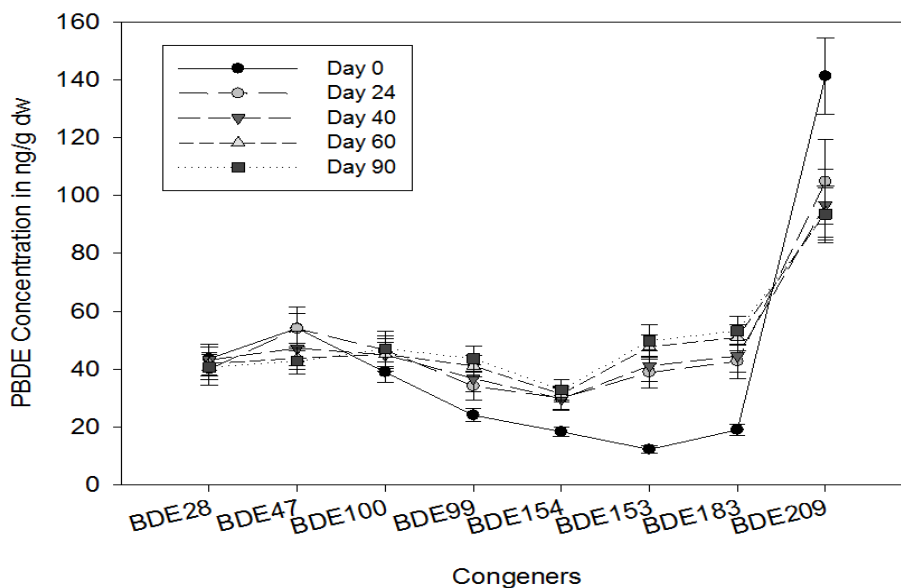


Figure 3.35 Microcosm PBDE data (Song et al., 2015)

### **3.5.2 Environmental PBDE Data: San Francisco Bay, USA**

#### **3.5.2.1 San Francisco Regional Monitoring Program (RMP) and Box Model**

The Regional Monitoring Program (RMP) for Water Quality in the San Francisco Bay, referred to as shortly, RMP was founded by the San Francisco Estuary Institute (SFEI) in 1993. The duty of RMP is to investigate and monitor the impacts of the chemicals such as dioxins, PCBs, emerging pollutants (e.i., PBDEs) (SFEI, 2015; Sutton et al., 2014) on the San Francisco environment. Sampling for PBDEs in the water column, sediment layer and TSS was conducted yearly between 2002-2013, 2002-2014 and 1993-2001, respectively. In our study, the use of the newly developed FTHP model was applied on PBDEs using this RMP data (SFEI, 2015).

According to USEPA's Toxic Release Inventory, two facilities which manufacture PBDE containing product in the Peninsula region were sources of PBDE contamination (Sutton et al, 2014). Volatilization from these manufactured products are also sources. The less probable source of entering the bay is predicted to be from e-waste recycling facilities, autos shredders, carpet and foam recycling facilities, sewage sludge application to rural lands, and sewage sludge incinerators. According to a study of the California EPA, the PBDE contamination was found in highest level in biota in 2002 around USA so the region is called as a hot spot region. Therefore, in the federal level, penta- and octa- BDE mixtures were prohibited in 2006 in the USA. Deca-PBDE for which the phased-out started in 2013, is available in the region and it is still produced (Sutton et al., 2014).

RMP also used mass budget models in addition to monitoring study. These models are to predict the fate and transport of contaminants in San Francisco Bay and output concentration, and to develop remediation plan in the region (Davis, 2004). The model is for investigation of PCB fate in Lake Ontario, Canada. The model assumes that the whole bay is completely mixed volume with two compartments; sediment and water. Therefore,

it is called as one-box model. This model was then used for the fate and transport of PBDEs in the bay (Oram et al., 2008b) after development and use of PCBs by Davis (2004). For the resolution of the salinity study in the model, the bay is divided into 50 segments for either water column and sediment layer (Figure 3.36). Hence, a total of 100 boxes is obtained. Considering the resolution in Figure 3.36, the boundary of the region is selected to use in our FTHP model. Figure 3.36 also indicates the depth of the segments. Accordingly, Lower South Bay which is considered in our study includes depth between 2 m and 7 m.

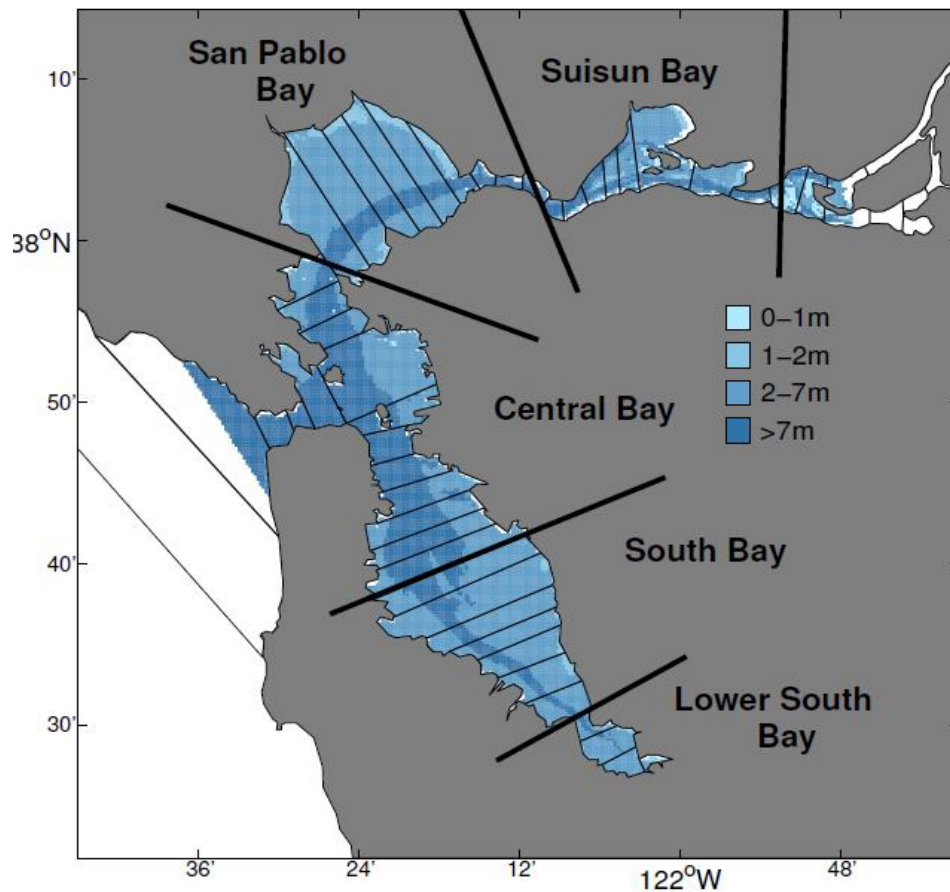


Figure 3.36 Segmentation (Oram et al., 2008a)



### 3.5.2.2 Description of RMP data to be used in the FTHP model

Distribution of total PBDEs between 2002-2014 in San Francisco Bay surficial sediment is shown by Sutton et. al (2015) and given in Figure 3.37. The highest concentration of BDE 47 and 209 is observed in the Lower South Bay region and can be seen in 2012 data, presented in Figure 3.38 (Sutton et. al, 2015). These congeners are the major components of mixture penta-BDE and deca-BDE, and also contribute most to the total PBDE concentration in San Francisco Bay surficial sediment. All bay is not considered in the FTHP model. A limited region is selected considering high PBDE concentration in surface sediment. Accordingly, station BA10 from the Lower South Bay is selected since the highest concentration of BDE 47 and 209 is observed in that region. Furthermore, BA10 has the higher number of samples to use for calibration and validation than others. Location of station BA10 is shown in Figure 3.39. At this station, nine samples are collected at 9 different times between 2002-2014 (**Hata! Başvuru kaynağı bulunamadı.**) from a depth of 5 cm at latitude 37.469 and longitude -122.063. PBDE data was taken yearly between 2002 and 2014. In water column, the station LSB054W which is above the station BA10 is considered for the FTHP model (Figure 3.39). One sample is taken from the station LSB054W in 09/13/2011.

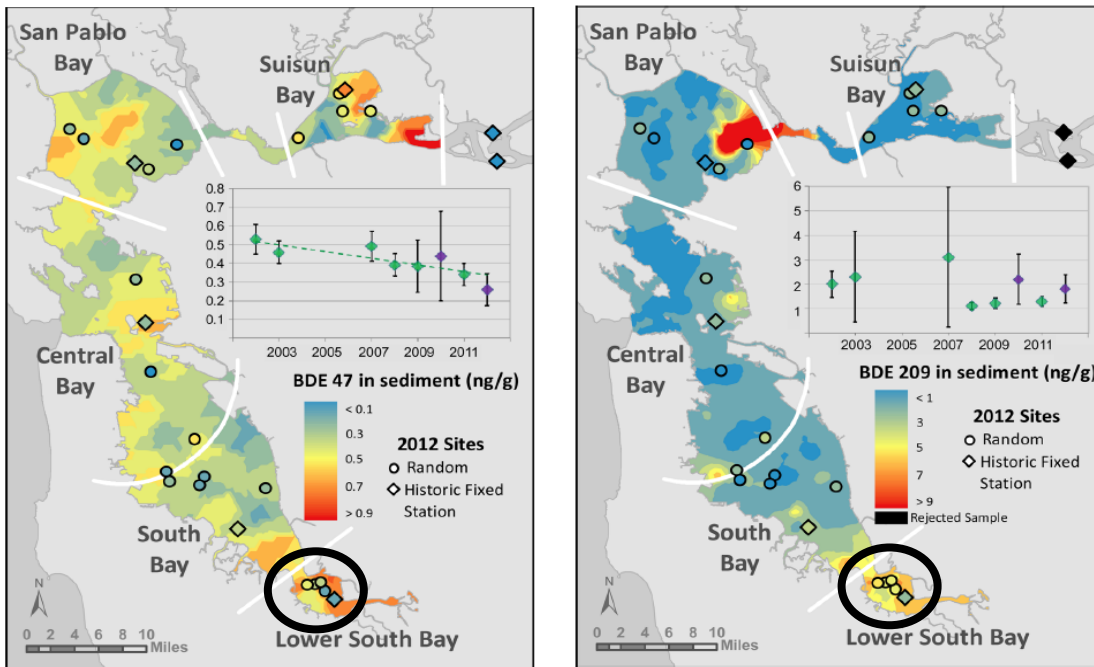


Figure 3.37 Distribution of BDE 47 (Left) and BDE209 (Right) (ng/g) in 2012 in San Francisco Bay Surficial Sediment (Sutton et. al, 2015)

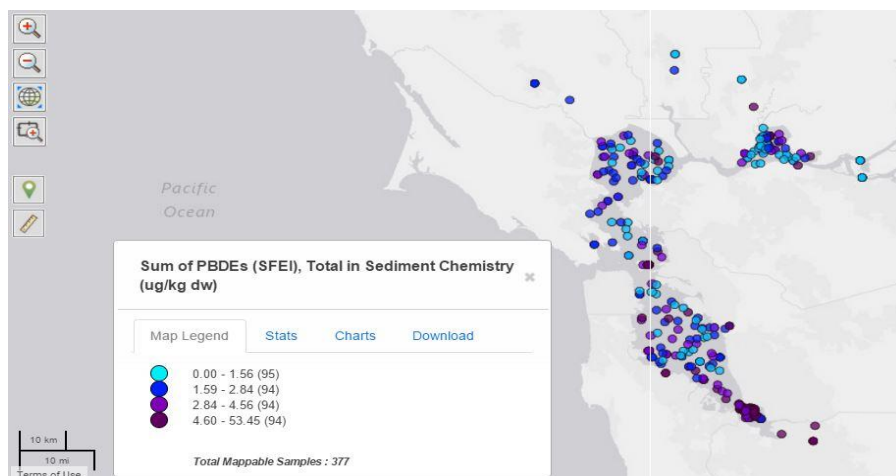


Figure 3.38 Distribution of Total PBDEs (ng/g) between 2002-2014 in San Francisco Bay Surficial Sediment (Sutton et. al, 2015)



Figure 3.39 Sampling Points of PBDEs in Surface Sediment and water column

While selecting the congeners for our FTHP model,

- (i) the same congeners measured in both compartments (sediment and water) and same dates in the study of RPM (SFEI, 2015),
- (ii) the most commonly studied congeners in the environment (USEPA, 2010), and
- (iii) the congeners discussed in a one-box mass budget model for PBDE by Oram et al. (2008b) were taken into consideration.

A total of 52 and 50 groups of congeners were measured by RPM in the water column and surficial sediment, respectively. According to the selection criteria, 21 groups of

congeners were selected to be used in the FTHP model (7, 8, 15, 17/25, 28/33, 32, 35, 47, 49, 66, 85, 99, 100, 153, 154, 183, 197, 206, 207, 208 and 209).

In our model, 9 samples from the same location collected periodically (approximately each year) are used in the FTHP model. The data set is given in **Hata! Başvuru kaynağı bulunamadı.** in ng/L. To convert ng/g dry weight to ng/L, the equation (Rossmann, 2006) given in section 3.4.2.3 is used. In the FTHP model, unit ng/L is used for the concentration of PBDEs in sediment layer. Individual PBDE concentrations range from 0 to 6858 ng/L in the sediment.

Table 3.21 Concentration of individual PBDE congeners in 9 sediment samples (ng/L) (SFEL, 2015)

Sample no	Days	Date of Collection	Congener IUPAC.No														
			7	8	15	17/25	28/33	32	35	47	49	66					
1	0	8/5/2002	39.74	30.56	30.62	189.54	68.04	5.67	7.40	685.80	228.42	39.31					
2	385	8/25/2003	17.87	11.77	9.13	67.50	29.70	3.42	3.35	167.94	64.26	8.80					
3	1842	8/21/2007	23.65	21.44	14.82	133.92	35.07	1.15	0.11	426.06	94.50	13.85					
4	2180	7/24/2008	16.42	12.74	10.15	56.16	15.39	1.30	2.19	131.76	51.35	6.75					
5	2598	9/15/2009	41.26	36.61	24.95	164.70	45.47	3.45	5.13	246.24	145.26	14.90					
6	2738	2/2/2010	6.64	4.87	3.97	16.52	4.98	1.83	0.95	41.63	14.69	2.19					
7	3304	8/22/2011	24.25	20.52	22.95	82.62	25.38	0.00	8.91	282.96	114.48	17.71					
8	3544	4/18/2012	6.05	0.00	0.00	21.71	0.00	0.00	0.00	60.48	20.95	2.85					
9	4383	8/5/2014	34.61	31.48	35.48	69.66	26.41	0.00	0.00	197.10	85.86	14.53					
		Min	6.05	0.00	0.00	16.52	0.00	0.00	0.00	41.63	14.69	2.19					
		Max	41.26	36.61	35.48	189.54	68.04	5.67	8.91	685.80	228.42	39.31					
		Median	23.65	20.52	14.82	69.66	26.41	1.30	2.19	197.10	85.86	13.85					
		Average	23.39	18.89	16.90	89.15	27.83	1.87	3.11	248.89	91.09	13.43					
		SD <sup>a</sup>	13.10	12.55	12.24	60.82	20.75	1.96	3.35	201.51	66.55	11.16					
		RSD <sup>b</sup>	56.03	66.44	72.41	68.22	74.55	104.78	107.70	80.97	73.07	83.07					

<sup>a</sup>Standard deviation, <sup>b</sup>Relative standard deviation

**Hata! Başvuru kaynağı bulunamadı. Continued**

Sample no	Days	Date of Collection	Congener IUPAC No														
			99	100	153	154	206	207	208	209	183	197	85				
1	0	8/5/2002	476.82	118.26	54.54	63.72	239.22	184.68	124.74	6858.00	22.41	35.15	25.06				
2	385	8/25/2003	93.42	24.14	21.82	11.88	41.74	37.48	39.15	993.60	7.18	30.67	12.91				
3	1842	8/21/2007	225.18	49.38	24.06	20.63	74.25	58.59	38.42	2940.30	0.00	0.00	0.00				
4	2180	7/24/2008	70.74	18.52	8.37	8.96	31.43	20.52	14.47	1015.20	4.57	4.28	5.40				
5	2598	9/15/2009	100.44	27.70	14.15	15.93	81.54	53.95	31.21	2305.80	0.00	0.00	4.77				
6	2738	2/2/2010	31.10	6.26	2.82	3.07	17.98	21.87	12.91	702.00	4.27	2.61	1.38				
7	3304	8/22/2011	194.94	57.24	47.63	30.94	95.04	88.56	48.38	3153.60	107.46	44.82	0.00				
8	3544	4/18/2012	34.40	10.37	0.00	4.47	20.63	0.00	0.00	556.20	0.00	0.00	0.00				
9	4383	8/5/2014	86.94	22.46	13.99	11.29	165.24	165.24	112.86	4914.00	8.10	43.25	0.00				
		Min	31.10	0.00	6.26	0.00	3.07	0.00	0.00	17.98	0.00	0.00	556.20				
		Max	476.82	25.06	118.26	54.54	63.72	107.46	44.82	239.22	184.68	124.74	6858.00				
		Median	93.42	1.38	24.14	14.15	11.88	4.57	4.28	74.25	53.95	38.42	2305.80				
		Average	146.00	5.50	37.15	20.82	18.99	17.11	17.87	85.23	70.10	46.91	2604.30				
		SD <sup>a</sup>	140.43	8.48	34.69	18.94	18.81	34.59	20.03	74.02	64.88	43.58	2146.67				
		RSD <sup>b</sup>	96.18	154.21	93.37	90.99	99.07	202.16	112.10	86.84	92.56	92.92	82.43				

<sup>a</sup>Standard deviation, <sup>b</sup>Relative standard deviation

In the FTHP model, a constant BDE concentration in the water column is assumed. In RMP monitoring study, the samples are measured only for a sample collected from one date (9/13/2011). It is given in Table 3.22. The concentration values of congeners in this date is used as initial and constant concentration in the water column. When water and sediment PBDE concentrations are compared, sediment concentrations are five to seven orders of magnitude higher.

Table 3.22 Concentration of congeners in water column and in 9/13/2011

Congeners	Concentration, ng/L	Congeners	Concentration, ng/L
7	0.00601	100	0.00941
8	0.00371	153	0.00404
15	0.00294	154	0.00401
17/25	0.0187	206	0.0157
28/33	0.00499	207	0.0246
32	0	208	0
35	0	209	0.302
47	0.0561	183	0.00153
49	0.0136	197	0.00243
66	0.00242	85	0.00128
99	0.0367		

### 3.5.2.3 Other Constituents used in the FTHP model

**TSS Concentration:** In station BA10, 9 samples are taken between dates June 19 1997 and May 11 2001 (SFEI, 2015). In the FTHP model, TSS concentration is assumed to be independent of time. Therefore, TSS data is evaluated to establish one TSS concentration that can be used as input to the model. Accordingly, TSS data is presented in Figure 3.40 while the descriptive statistics of TSS data is given in Table 3.23. The median of TSS (35.07 mg/L) is used as input in the model.

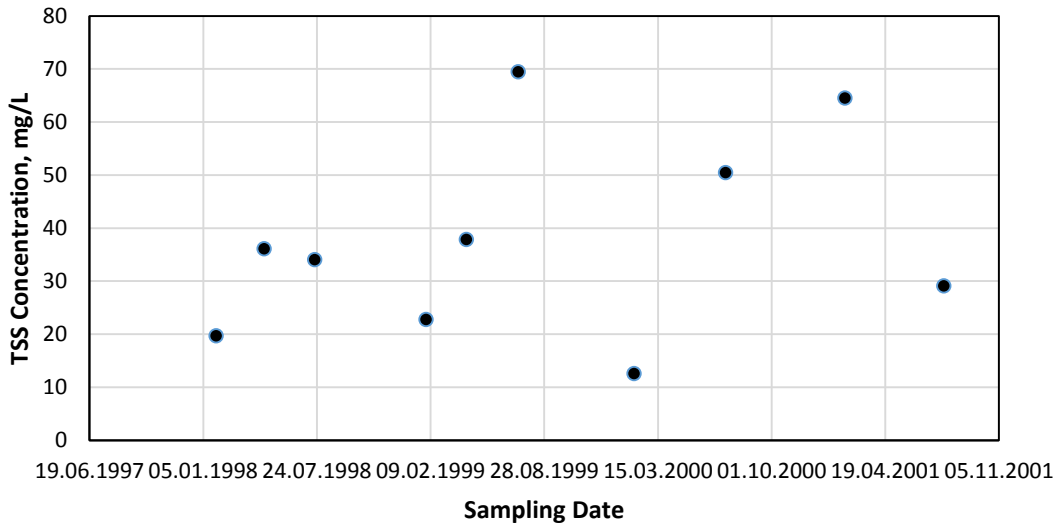


Figure 3.40 TSS Concentration

Table 3.23 Descriptive statistics of TSS Data

Constituent	Sample Station	Average	SD	RSD(%)	Median	Min	Max
TSS, mg/L	BA10	37.67	18.73	49.74	35.07	12.60	69.46

**Sediment and Water Properties:** The properties of sediment and water column are given in Table 3.24 and Table 3.25. In Choe et. al (2004), average depth of bay is given as 6 m. It is accepted as the water depth in our model. Sutton et. al (2015) state that the samples are collected with a surface area of 0.1 m<sup>2</sup> for RMP. Thus, the region can be accepted as homogeneous in this area. The maximum values are selected from the ranges given in Table 3.25 for sediment porosity. For this value, it is taken as 0.082.



Table 3.24 Depth and Area of Sediment Layer and Water Column

<b>Sediment Layer</b>	<b>Value</b>	<b>Reference</b>
Depth (m)	6	SFEI, (2015)
Surface Area(m <sup>2</sup> )	0.1	Sutton et al. (2015)
<b>Water Column</b>		<b>Reference</b>
Depth(m)	0.05	Choe et al. (2004)
Surface Area (m <sup>2</sup> )	0.1	Sutton et al. (2015)

Table 3.25 Water and Sediment Properties

<b>Reference</b>	<b>Constituent</b>	<b>Unit</b>	<b>Range/Value</b>
Caffrey (1995)	Sediment porosity	-	0.72-0.82
Davis (2004)	Sediment particle density,	g/m <sup>3</sup>	2700000
	Monthly fraction organic carbon (f <sub>oc</sub> ):		
	For water column	-	0.01
	For sediment layer	-	0.03

**Contaminant Properties:** The properties for congeners are given in Table 3.26. Contaminant properties were taken from Mackay et al. (2006) and calculated by EPA SUITE version 4.1.1. In Mackay et al. (2006),  $K_{ow}$  and solubility of some congeners are not available. Therefore, these values are taken from another study, Eva et al. (2005) estimating their homolog groups. When combination of these two studies is listed (Table 3.26), the values differentiate each other. Therefore, for our FTHP model,  $K_{ow}$  and solubility values calculated by EPI SUITE were used since the values vary significantly through congeners.

Table 3.26 Solubility and  $K_{ow}$  of PBDE congeners (Mackay, 2006)

Congener	MW	Median			Max	EPI SUITE		Median
		logKow	Avg	Min		logKow	Solubility, mg/L at 25 °C	
IUPAC No	(g/mole)	logKow	logKow	logKow	logKow	logKow	Solubility, mg/L at 25 °C	Solubility, mg/L at 25 °C
<b>7</b>	327.999	5.03	5.03	5.03	5.03	4.99	0.46	0.654 <sup>a</sup>
<b>8</b>	327.999	5.03	5.03	5.03	5.03	4.99	0.46	0.654 <sup>a</sup>
<b>15</b>	327.999	5.03	5.224	5.03	5.55	5.83	0.08826	0.654 <sup>a</sup>
<b>17/25</b>	406.895	<sup>c</sup>	5.525	5.47	5.58	5.88	0.02642	0.00038
<b>28/33</b>	406.895	5.58	5.672	5.47	5.98	5.88	0.02642	0.03519
<b>32</b>	406.895	<sup>c</sup>	5.53	5.47	5.59	5.88	0.02642	0.00038
<b>35</b>	406.895	<sup>c</sup>	5.525	5.47	5.58	6.72	0.00507	0.00038
<b>47</b>	485.791	6.14	6.135	6.135	6.135	6.77	0.001461	0.007535
<b>49</b>	485.791	6.2 <sup>b</sup>	6.2 <sup>b</sup>	6.2 <sup>b</sup>	6.2 <sup>b</sup>	6.77	0.001461	0.096928 <sup>a</sup>
<b>66</b>	485.791	6.16	6.158	5.87	6.73	6.77	0.001461	0.009035
<b>99</b>	564.687	6.81	6.805	6.805	6.805	7.66	0.000394	0.0094
<b>100</b>	564.687	6.64	6.64	6.64	6.64	7.66	7.861 E-05	0.04705
<b>153</b>	643.583	7.39	7.39	7.39	7.39	8.55	4.148E-06	2.48E-06
<b>154</b>	643.583	7.39	7.39	7.39	7.39	8.55	4.148E-06	2.48E-06
<b>206</b>	880.2717	8.50 <sup>b</sup>	8.50 <sup>b</sup>	8.50 <sup>b</sup>	8.50 <sup>b</sup>	11.22	5.63E-10	0.000555 <sup>a</sup>
<b>207</b>	880.2717	8.50 <sup>b</sup>	8.50 <sup>b</sup>	8.50 <sup>b</sup>	8.50 <sup>b</sup>	11.22	5.63E-10	0.000555 <sup>a</sup>
<b>208</b>	880.2717	8.50 <sup>b</sup>	8.50 <sup>b</sup>	8.50 <sup>b</sup>	8.50 <sup>b</sup>	11.22	5.63E-10	0.000555 <sup>a</sup>
<b>209</b>	959.167	9.97	9.97	9.97	9.97	12.11	2.841E-11	4.17 × 10 <sup>-9</sup>

<sup>a</sup>: From solubility of homolog groups in Eva et. al. <sup>b</sup>: From log $K_{ow}$  of homolog groups in Eva et al. (2005). <sup>c</sup>: No value since only range defined for logKow.

**Deep Sediment PBDE Concentration:** In our model, deep sediment concentration does not change with time as is also the case in Recovery model. Any measurement is not provided in deep sediment PBDE data set of RPM. Therefore, the studies for San Francisco Bay in the literature are investigated. In our model, surface sediment depth is given as 5 cm for station BA10 which is our modelling region (SFEI, 2015). Yee et. al (2011) studied San Francisco Bay deep sediment. They took a core sample in 2006 from Alviso Slough wetland site in Lower South Bay (Figure 3.41). Alviso Slough wetland site is near our study region. Additionally, a mining site, called as the New Almaden Quicksilver Mine (Yee et al., 2011), is located close to our study region. Therefore, concentration of total PBDEs through core is investigated in this station. However, Yee et. al (2011) state that the wetland is likely to include less sediment of the bay. Therefore, this data (Figure 3.41) could not represent the deep sediment samples perfectly. In view of this discussion and as seen in Figure 3.41, concentration of total PBDEs decreases with depth. Therefore, in our model, initial deep sediment PCB concentration is taken as zero for all congeners.

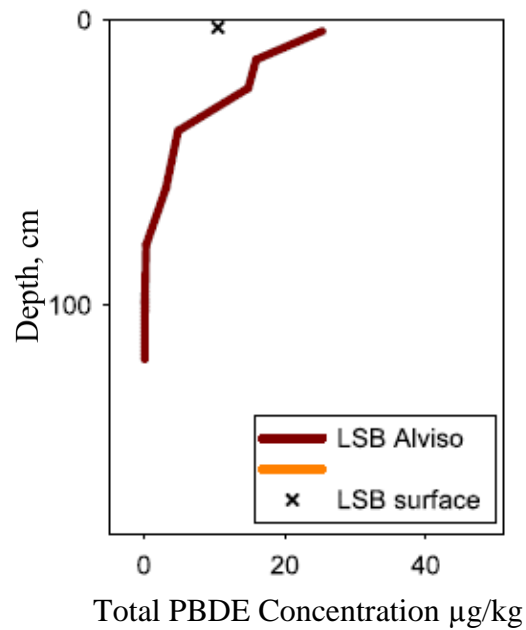


Figure 3.41 Total PBDE Concentration in sediment from Adviso Wetland Core (Grenier and Davis, 2011) (Yee et al., 2011)

***Settling, Resuspension and Burial Velocities:*** Settling and burial velocities (1 and 0 m/day, respectively) are taken from the box model (Davis, 2004) prepared for the study of PCBs. These values are used for the box model assuming homogeneous over all San Francisco Bay sediment. Resuspension velocity is calculated as 0.00011 m/day by using solid mass balance equation which is explained in section 3.4.2.4.

**Diffusion Coefficient:** Molecular diffusion of some congeners in our model is given in Table 3.27, which were studied by Blauenstein (2007). Diffusion velocity of congeners is estimated by the diffusion equations in the FTHP model (equations 3.17 and 3.18). As can be seen from Table 3.27, molecular diffusion of congeners changes according to number of bromine. Therefore, in our model, molecular diffusion of some of congeners not listed in Table 3.27 is estimated and used according to this rule (Figure 3.42). Accordingly, molecular diffusion of the BDE congeners is tabulated in Table 3.28.

Table 3.27 Molecular diffusion coefficient of PBDE congeners (Blauenstein, 2007)

<b>Congener IUPAC No</b>	<b>Cl -</b>	<b>Diffusion velocity sediment-water (<math>v_d</math>) (m/hr)</b>	<b>Molecular Diffusion* <math>D_m</math> (cm<sup>2</sup> 10<sup>-4</sup>/s)</b>
<b>15</b>	2	0.00458	1.745
<b>28</b>	3	0.00433	1.650
<b>47</b>	4	0.00411	1.566
<b>99</b>	5	0.00392	1.494
<b>100</b>	5	0.00392	1.494
<b>153</b>	6	0.00375	1.429
<b>183</b>	7	0.0036	1.372
<b>209</b>	10	0.00323	1.231

\*: Estimated by using equations:  $v_d = \frac{\varphi D_s}{z'}$  and  $D_s = D_m \varphi^2$

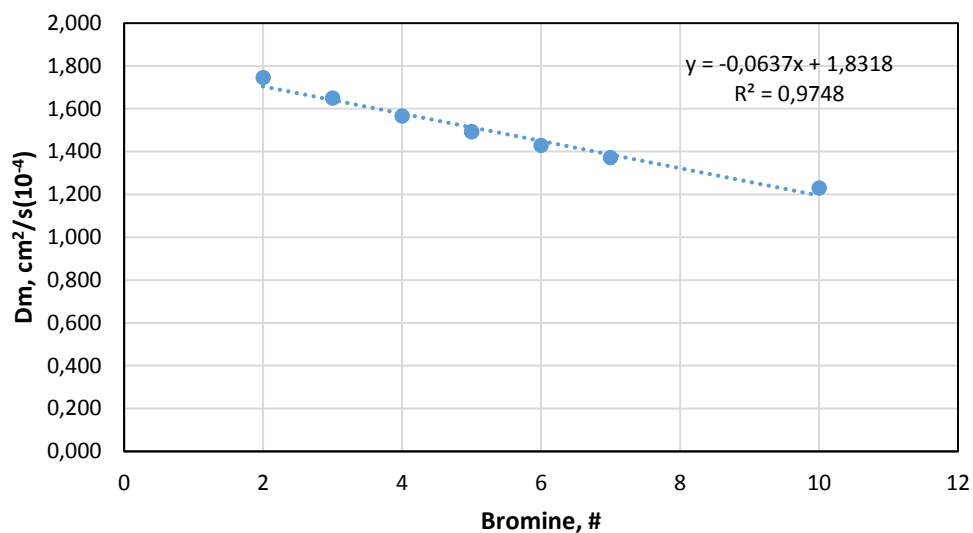


Figure 3.42 Molecular Diffusion vs. No of Br in diphenyl ether structure

Table 3.28 Molecular Diffusion used in the FTHP model

Congener IUPAC No	Molecular Diffusion, cm <sup>2</sup> /sec	Congener IUPAC No	Molecular Diffusion, cm <sup>2</sup> /sec
<b>7</b>	0.00017	<b>100</b>	0.000151
<b>8</b>	0.00017	<b>153</b>	0.000145
<b>15</b>	0.00017	<b>154</b>	0.000145
<b>17/25</b>	0.000167	<b>206</b>	0.000126
<b>28/33</b>	0.000164	<b>207</b>	0.000126
<b>32</b>	0.000164	<b>208</b>	0.000126
<b>35</b>	0.000164	<b>209</b>	0.000119
<b>47</b>	0.000158	<b>183</b>	0.000139
<b>49</b>	0.000158	<b>197</b>	0.000132
<b>66</b>	0.000158	<b>85</b>	0.000151
<b>99</b>	0.000151		

## CHAPTER 4

### VERIFICATION OF MODELS

In the scope of this study, FTHP model was developed for the prediction of congener specific HOC concentrations in sediments. This model predicts congener specific HOC concentrations taking into account biodegradation rate constants estimated by ADM. For this purpose, previously developed anaerobic dechlorination models were improved and modified as a part of this study. Hence, the codes of two models were verified. This chapter is divided into three parts where a small artificial data set is generated for the verification of ADM. FTHP model is then verified with a small data set a part of Lake Michigan data.

#### 4.1 Artificial Data Set

A small artificial data set is created to be used for testing the ADM. Congeners are selected by considering abundance of the congeners in original mixtures, pathways in accordance with relevant dechlorination activity and presence of coelution. Concentrations of congeners are taken from Frame et al. (1996). Seven congeners are assumed as measured congeners for model input. Aroclor 1260 in weight percentage is firstly converted to mole %. Of these 7 congeners, congener 132 is present in high amount, congeners 84, 105, 131 and 133 are in low amounts and congener amounts of 55 and 56 are zero in Aroclor 1260. Table 4.1 shows the abundance of seven congeners to be used as input for the ADM.

The congeners assumed are seven congeners as 55, 56, 84, 105, 131, 132 and 133 as considering relation between dechlorination activity and congeners which is discussed

following sentences. The doubly flanked *para* removal is chosen as dechlorination activity. The positions of chlorine substitutions removed are displayed in Table 4.2. When reactive congeners are investigated for doubly flanked *para* removal, mother and daughter congeners given in Table 4.2 and Figure 4.1 are obtained. In this scenario, congeners 55 and 56 can not be degraded since they do not have chlorine in a doubly flanked position. For path order, ascending order for mother congener is selected as 132→84, 131→84, 105→55 and 105→56 (Figure 4.1).

Table 4.1 Abundance of seven congeners in the original Aroclor 1260 and after dechlorination

Selected Congener IUPAC No	Original Profile (mole % <sup>a</sup> )	Normalized to 1000 <sup>b</sup> mole ‰	Artificially Dechlorinated Profile (mole ‰)
55	0.00	0.00	30.00
56	0.00	0.00	1.50
84	0.11	32.66	242.66
105	0.26	75.12	43.62
131	0.05	14.77	4.77
132	3.02	859.72	659.72
133	0.06	17.73	17.73
Sum	3.51	1000	1000

<sup>a</sup>: Frame et al. (1996) reports concentrations as weight percentage. Here, these are converted into **mole ‰**. <sup>b</sup>: Abundance of congeners are normalized to 1000 and prepared as input to ADM as mole ‰.

Table 4.2 Doubly Flanked *para* Removal

Chlorine substitution in mother	Chlorine substitution in daughter
345	35
2345	235
23456	2356



Figure 4.1 describe how anaerobic dechlorination is applied on the artificial data set. The reaction amounts are selected randomly. Table 4.1 shows the initial and dechlorinated PCB congener concentration (in mole ‰). The  $\Delta t$  which will be needed for  $k_m$  calculation is assumed as 100 days. For example, as can be seen in Figure 4.1, in the first pathway, 200 ‰ is subtracted from mother congener (132) to add 200 ‰ to daughter congener (84). Then, new values of congeners 132 and 84 are calculated as 659.72 ‰ and 232.66 ‰, respectively. In the second pathway, 10 ‰ is subtracted from mother congener (131) to add 10 ‰ to daughter congener (84) new value (232.66 ‰) of which is used for this calculation. Then, new values of congeners 131 and 84 are calculated as 4.77 ‰ and 242.66 ‰, respectively. The preparation of the dechlorinated profile goes on in this fashion. Eventually, the final abundance of the congeners in mole ‰ are shown in the last column of Table 4.1. As can be seen, abundance of 133 does not change since it does not take part in a reaction.

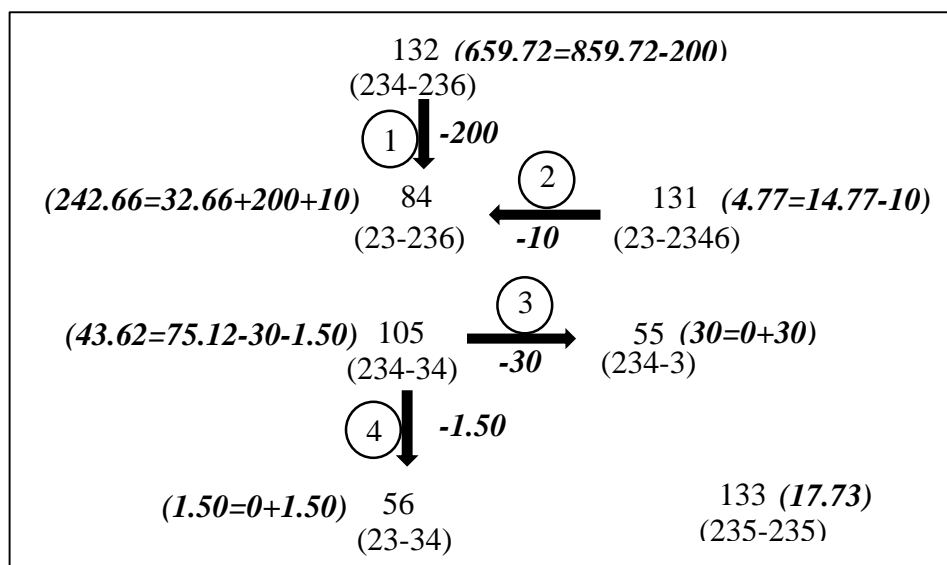


Figure 4.1 Application of artificial anaerobic dechlorination on data set

(Arrows indicate dechlorination pathway, **bold** numbers on arrows indicate reaction amounts (in mole ‰), **bold italic** numbers indicate mole ‰ after reaction and the numbers in circle display the reaction orders)

Since PCB congeners can coelute during analytical determination, the congeners selected for verification of ADM were also rearranged in accordance with literature. Congeners 131 and 132 typically coelute with congeners 133 and 105, respectively, so, abundance of these congeners are summed. Then, they are normalized to 1000 mole % (Table 4.3). The calculation for coeluting congeners can also be seen in Figure 4.2. During model verifications, Table 4.1 and Table 4.3 will be used.

Table 4.3 Abundance of All Coeluting Congeners After Dechlorination

Congener IUPAC No	Abundance, mole ‰
55	30.00
56	1.50
84	242.66
131/133	22.50
132/105	703.34
Sum:	1000

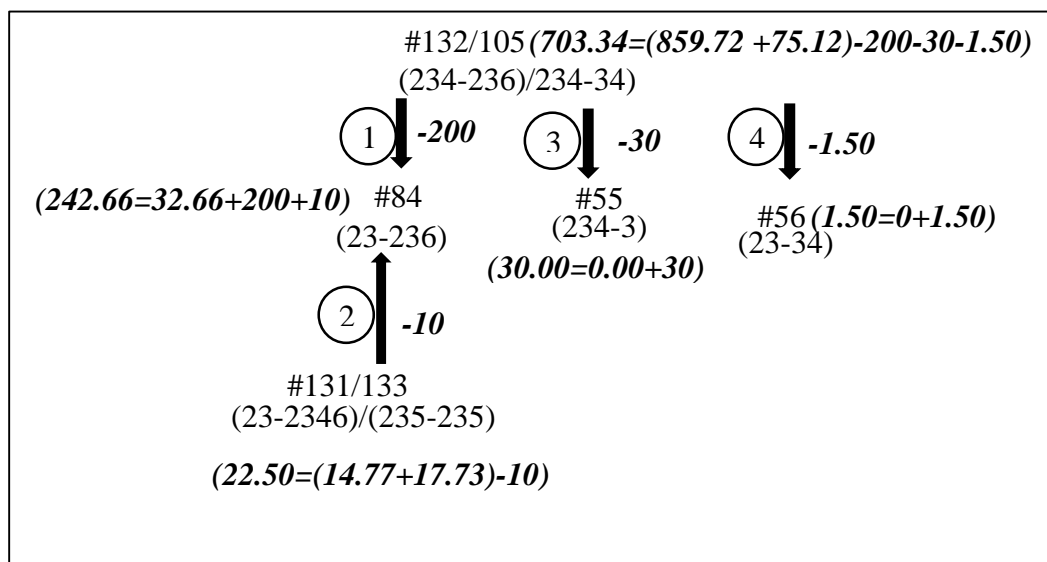


Figure 4.2 Anaerobic dechlorination pathways depicted with coeluting congeners

## 4.2 ADM Verification

### 4.2.1 Example Run

The model is verified with a small data set artificially created as explained in the previous section. The verification is done in MS excel to compare with the model results in MatLAB. Only one shuffle is performed since in each shuffle, same operations are done. In each shuffle, reaction amount subtracting from mother congener to add daughter congener,  $k_m$  values in each pathway and amount of congeners in mother and daughter arrays are calculated. After the end of all shuffles which is not performed here, average and median of these values in all shuffles is taken. Input file is shown in Table 4.4.

Table 4.4 Model Input

DL	Pathways #	Total congeners # at to	markers #	$\Delta t$	iteration no	lambda									mother	daughter
0.065609521	4	5	5	100	100	no	6	10							132	84
Congeners										Conc t0	Conc tf	mark	Conc mark		131	84
55							0	30	55	30				105	55	
56							0	1.5	56	1.5				105	56	
84							32.66	242.7	84	242.7						
131	133						32.5	22.5	131	22.5						
132	105						934.8	703.3	105	703.3						

In Table 4.5 and Figure 4.3, final concentration of coeluting congeners are indicated and abundances calculated in the excel and by the model are compared. As can be seen from the figure, the model predicts the data satisfactorily.

Table 4.5 Initial and final concentration of coeluting congeners by the model and in the data set

aroreacong	Measured t=0 day (mole ‰)	Measured t=100 day (mole ‰)	ADM output t=100 day , (mole ‰)
55	0	30.00	21.31
56	0	1.50	0.00
84	32.66	242.66	257.02
105/132	934.84	703.34	689.16
131/133	32.50	22.50	32.50

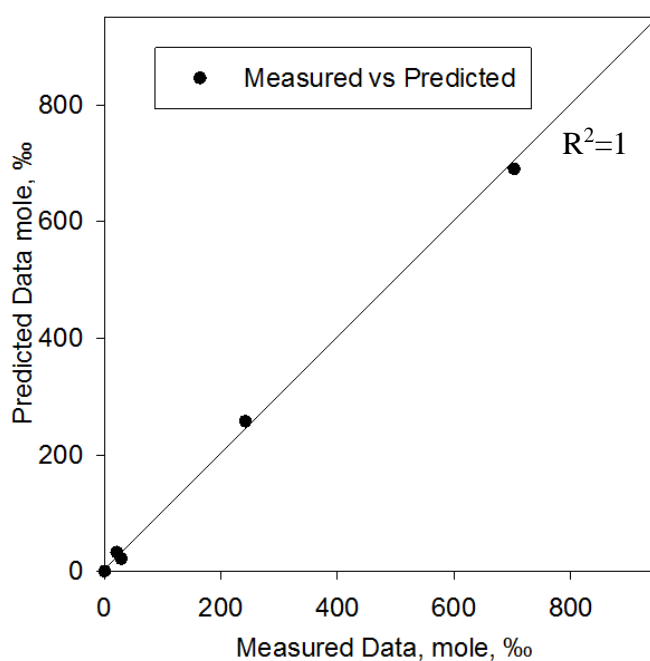


Figure 4.3 Measured vs. ADM predicted data plot

*Distribution of Biodegradation Rate Constants:*

In this part, biodegradation rate constants are calculated for artificial data set exposed to dechlorination activity “doubly flanked *para*” in Section 4.1. Artificial data includes two files including all seven congeners. First one is aro array obtained from original A1260 mixture. It is assumed that this is at initial time. Second one is sam array obtained after applying dechlorination activity “doubly flanked *para*”. To generate sam array, path order is in order of 1, 2, 3 and 4. Accordingly,  $k_m$  values in each path are compared with model results including same path order with in generated data (Table 4.6). In Table 4.7, biodegradation rate constants are calculated by excel and estimated by the model. Accordingly, the table indicates that the model works correctly.

Table 4.6 Calculation of  $k_m$  values for Artificial data by excel

Path orders	Mother congeners	Daughter congeners	Concentration of Mother Congeners, Cm,i		Reaction	Concentration of Daughter Congeners, Cd,i		Concentration of Mother Congeners, Cm,f (=Cm,i-Reaction)		Concentration of Daughter Congeners, Cd,f (=Cd,i+Reaction)		Biodegradation Rate constants, $k_{m,d}^{***}$
			32.84	1.15		20	12.84	21.15	21.15	21.45		
1	105*	84	32.84	1.15	20	12.84	21.15	12.84	21.15	21.15	0.00274	
2	131**	84	1.14	21.15	0.30	0.84	21.45	0.84	21.45	21.45	0	
3	105	55	12.84	0	0.20	12.64	0.20	12.64	0.20	0.20	0.00030	
4	105	56	12.64	0	1.50	11.14	1.50	11.14	1.50	1.50	0	

\*means amounts of 105+132 due to coelution, \*\*means amounts of 131+133 due to coelution, \*\*\*:  $k_{m,d} = \ln(C_{m,i}/C_{m,f})/\Delta t$

Table 4.7 Model  $k_m$  results

Path orders	Mother congeners	Daughter congeners	Reaction Amount	$k_m$ values
1	105/132	84	224.36	0.00274
2	131/133	84	0	0
3	105	55	2.31	0.00030
4	105	56	0	0

### 4.3 FTHP Model Code Verification

#### 4.3.1 Example Run

The code of the model is verified with a part of Lake Michigan data set given in Zhang (2006), Mackay (2006) and Schneider (2005). In this part, calculations conducted for FTHP model are expressed only for one time step.

Input files are shown in Table 4.8 to Table 4.11 which are in format of Input files in the program. In Table 4.8, number of congeners, paths, and final, initial time and time steps are entered by the user. Biodegradation rate constants are entered by the user for corresponding congeners in Table 4.9. Table 4.10 presents initial concentration in surface and deep sediment, and water column, molecular diffusivity, octanol-water partitioning constant and solubility of congeners. The properties belonging to water column, sediment layer and system are given in Table 4.11.

Table 4.8 Model Input Information for numbers of congeners, paths and time

Congener, #	Path, #	$t_0$	$t_f$	$\Delta t$
5	3	0	100	5

Table 4.9 Model Input Information for biodegradation rate constants

Mother	Daughter	$k_m$ (day <sup>-1</sup> )
101	49	0.0001
138/163	99	0.000607
105/132/153	99	0.001024

Table 4.10 Model Input Information

Congeners	$C_m(o)$ , ng/L	$C_w(o)$ , ng/L	$C_s(o)$ , ng/L	Molecular Diffusivity, cm <sup>2</sup> /sec	log( $K_{ow}$ )	Solubility, mg/L at 25 °C
49	241.10	0.00373	0.00	0.000173	5.93	0.0202
99	292.49	0.00934	0.00	0.000173	6.41	0.0103
101	547.18	0.00625	0.00	0.000173	6.38	0.0103
138/163	1130.12	0.01167	0.00	0.000173	6.82	0.0039
105/132/153	968.72	0.00587	0.00	0.000173	6.72	0.0047

Table 4.11 Model Input Information belonging to water column, sediment layer and system properties

Water column	Depth (Depthw)	m	48.1	
	Surface Area ( $A_w$ )	m <sup>2</sup>	4425	
Sediment Layer	Depth (Depths)	m	0.031	
	Surface Area ( $A_m$ )	m <sup>2</sup>	4425	
System Properties	Suspended solids concentration in water ( $S_w$ )	g/m <sup>3</sup>	0.941666667	
	Sediment porosity ( $Pos$ )	-	0.953	
	Sediment particle density ( $Rou$ )	g/m <sup>3</sup>	2540000	
	Fraction organic carbon, g-orgC/g dw solids			
	Water	g-orgC/g dw solids	0.09	
	Sediment	g-orgC/g dw solids	0.05	
	Characteristic Length	m	0.01	
	Two of the following three velocities:			
	Resuspension velocity, $v_r$	m/day	Unknown	-
	Burial velocity, $v_b$	m/day	Known	0.00001
Settling velocity, $v_s$	m/day	Known	1.5	

The calculations conducted in MS Excel are given in the following paragraphs and tables. Firstly, contaminant partitioning coefficients in the sediment ( $K_{ds}$ ) and in water column ( $K_{dw}$ ) are calculated (Table 4.12 and Table 4.13). As can be seen in the last columns of Table 4.12 and Table 4.13, unit conversion is done for  $K_d$  values.



Table 4.12 Calculation of contaminant partitioning coefficients in the sediment (K<sub>ds</sub>)

Congeners	$K_{ow}=10^{\log K_{ow}}$ unitless	$K_{ds}=0.617*f_{ocs}*K_{ow}$ L/kg	$K_{ds}=K_{ds}*0.000001$ m <sup>3</sup> /g
49	841395.14	25957.04	0.03
99	2570395.78	79296.71	0.08
101	2371373.71	73156.88	0.07
138/163	6569011.16	202653.99	0.20
105/132/153	5268253.53	162525.62	0.16

Table 4.13 Calculation of contaminant partitioning coefficients in the water (K<sub>dw</sub>)

Congeners	$K_{ow}=10^{\log K_{ow}}$ unitless	$K_{dw}=0.617*f_{ocw}*K_{ow}$ L/kg	$K_{dw}=K_{dw}*0.000001$ m <sup>3</sup> /g
49	841395.14	46722.67	0.05
99	2570395.78	142734.08	0.14
101	2371373.71	131682.38	0.13
138/163	6569011.16	364777.19	0.36
105/132/153	5268253.53	292546.12	0.29

The partitioning coefficients are calculated to find the fractions of contaminant mass in dissolved form in pore water of sediment (F<sub>dp</sub>), in particulate form in the water column (F<sub>pw</sub>) and in dissolved form in water column (F<sub>dw</sub>). Their calculations are depicted in Table 4.14.

Table 4.14 Calculation of fractions of contaminant (unitless)

Congeners	$F_{dp}(i)=1/(1+K_{ds}(i)*R_{ou})$ *(1-Pos)*R <sub>ou</sub>	$F_{pw}(i)=(K_{dw}(i)*S_w)/(1+K_{dw}(i)*S_w)$	$F_{dw}(i)=1/(1+K_{dw}(i)*S_w)$
49	0.00032	0.04214	0.95786
99	0.00011	0.11848	0.88152
101	0.00011	0.11032	0.88968
138/163	0.00004	0.25567	0.74433
105/132/153	0.00005	0.21598	0.78402

Diffusion mass-transfer coefficient at the sediment-water interface (v<sub>d</sub>) is calculated to use in diffusion term of mass balance equation. In the model, v<sub>d</sub> is converted from cm<sup>2</sup>/(m.sec) to m/day (Table 4.15).

Table 4.15 Estimation of diffusion mass-transfer coefficient at the sediment-water interface

Congeners	$v_d = \text{Pos} * D_s / Z$ cm <sup>2</sup> /(m.sec)	$v_d = v_d * 0.0001 * 3600 * 24$ m/day
49	0.0165	0.1424
99	0.0165	0.1424
101	0.0165	0.1424
138/163	0.0165	0.1424
105/132/153	0.0165	0.1424

In the model, the resuspension velocity ( $v_r$ ) among three velocities is unknown. Therefore,  $v_r$  is calculated from solid mass balance equation (Table 4.16).

Table 4.16 Estimation of resuspension velocity ( $v_r$ )

Item	$v_r = v_s * S_w / ((1 - \text{Pos}) * \text{Rou}) - v_b$ m/day
$v_r$	0.000002

Volume of surface sediment needed in the numerical solution of the model is calculated as

$$\text{Volume} = A_m * \text{Depths} = 4425 \times 0.031 = 137.18 \text{ m}^3$$

and  $k_1$ ,  $k_2$ ,  $k_3$  and  $k_4$  values are calculated as discussed in RK4 numerical solution. “Degraded”, “Degradedm” and “Degradedd” arrays are used in biodegradation term to make easy calculations of  $k_1$ ,  $k_2$ ,  $k_3$  and  $k_4$  (Table 4.17). In Table 4.17, concentration and  $k_1$ ,  $k_2$ ,  $k_3$  and  $k_4$  are calculated for only one step  $\Delta t$ . Concentration of five congeners in surface sediment is calculated by MS Excel and estimated by the model for 50 days with 5 day  $\Delta t$  intervals. They are compared in Figure 4.4. Accordingly, the figure indicates that the model works correctly, hence model verification is successful.

Table 4.17 Calculations in biodegradation term

Congener IUPAC No	Biodegradation Rate Eqn	ng/L		ng/(day L)		ng/(day L)		day <sup>-1</sup>
		C <sub>m</sub> =C <sub>m</sub> (0)	Degradedm=-k <sub>m</sub> *C <sub>m</sub> (0);	Degradedd=k <sub>m</sub> *C <sub>m</sub> (0)	Degraded=Degradedd+ Degradedm	sumkvalm		
<b>49</b>	=k <sub>(101→49)</sub> *C <sub>m</sub> (0) <sub>101</sub>	241.101		0.055	0.055	0		0
<b>99</b>	=k <sub>(138/163→99)</sub> *C <sub>m</sub> (0) <sub>138/163</sub> +k <sub>(105/132/153→99)</sub> * C <sub>m</sub> (0) <sub>105/132/153</sub>	292.486		1.678	1.678	0		0
<b>101</b>	=-k <sub>(101→49)</sub> * C <sub>m</sub> (0) <sub>101</sub>	547.184	-0.055		-0.055	0.0001		0.0001
<b>138/163</b>	=-k <sub>(138/163→99)</sub> * C <sub>m</sub> (0) <sub>138/163</sub>	1130.122	-0.686		-0.686	0.001		0.001
<b>105/132/153</b>	=-k <sub>(105/132/153→99)</sub> * C <sub>m</sub> (0) <sub>105/132/153</sub>	968.722	-0.992		-0.992	0.001		0.001

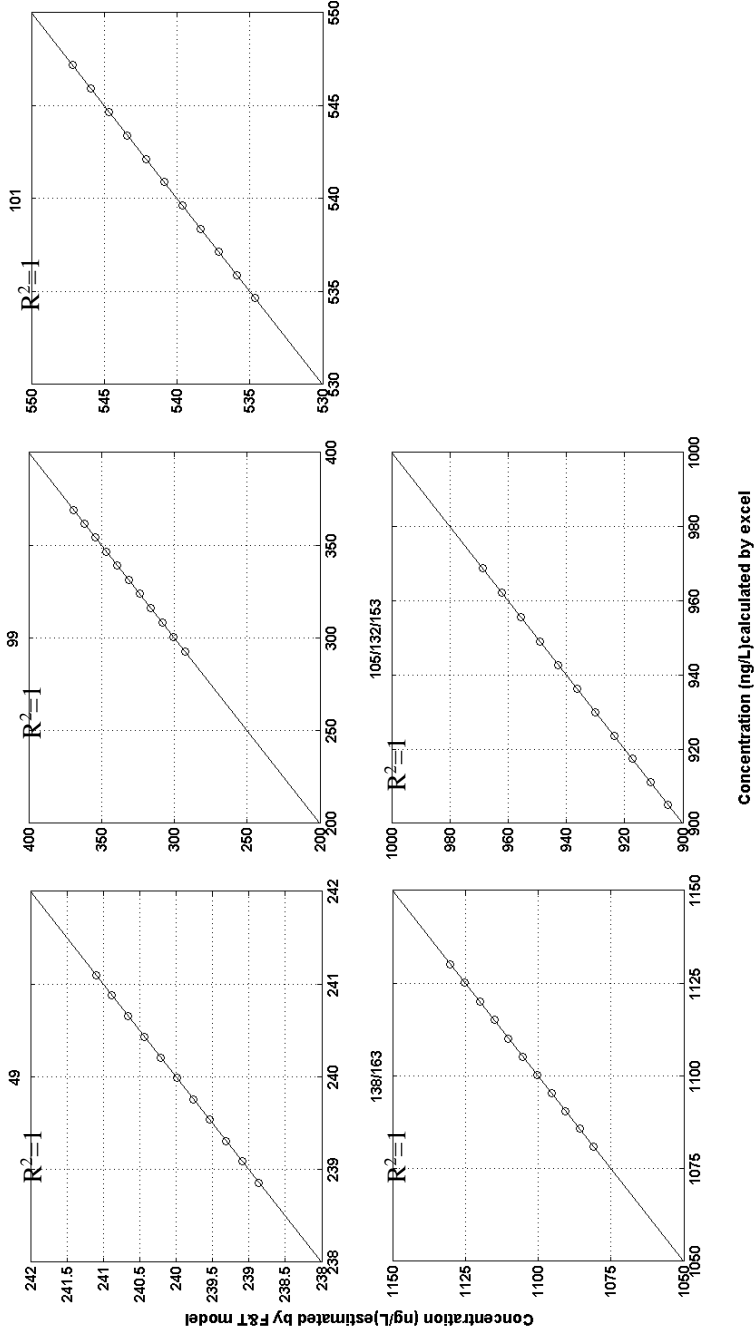


Figure 4.4 Comparison of concentrations estimated by F&T model in MatLAB and MS Excel

## CHAPTER 5

### ESTIMATION OF BIODEGRADATION RATE CONSTANTS OF PCB DECHLORINATION REACTIONS USING AN ANAEROBIC DEHALOGENATION MODEL

#### 5.1 Introduction

Polychlorinated biphenyls (PCBs) are a class of persistent organic pollutants (POPs). They were specifically produced for their chemical and thermal stability. Therefore, these chemicals had a widespread use in many industries such as heat exchange fluids, dielectric fluids in electric transformers and capacitors, and as additives in paint, carbonless copy paper, and plastics (POPs, 2008). Historically, about 1.7 million tons of PCBs was globally produced between 1930 and 1993 (Breivik et al., 2007). Despite prohibition of commercial production of PCBs firstly in 1977 in USA, and lastly in 1993 in Russia (Breivik et al., 2002), PCBs are still widely available in many equipments. Upon entry into the environment, PCBs cause adverse effects on human and animals due to their persistence, bioaccumulative and toxic properties. PCBs are internationally regulated as part of the original twelve POPs under the Stockholm Convention, which necessitates elimination of the use of equipment containing PCBs by 2025 and management of wastes containing PCBs by 2028.

PCBs are chemically persistent in the environment, however they can undergo transport and transformation mechanisms such as physicochemical weathering (volatilization, atmospheric transport, and wet/dry deposition, sorption/desorption) (Gouin & Harner, 2003) and biodegradation (anaerobic and aerobic) (Bedard, 2003). PCB dechlorination is attributed to various dehalorespiring bacteria (Zanaroli et al., 2010) in the sediment. Dehalogenation takes place by replacing one or more chlorines with a hydrogen in the PCB structure and production of less chlorinated congeners

(Abramowicz, 1995). Over the years, many studies identified pathways a number of dechlorination pathways (Adrian et al., 2009; Cutter et al., 2001; Fennell et al., 2004; May et al., 2006; Wu et al., 2002) according to congener selectivity of microorganisms, targeted Cl positions and dechlorination products (Bedard, 2003; Sowers & May, 2013). The targeted positions for dechlorination are defined as *para*, *meta* or *ortho* positions in terms of configuration; flanked, doubly flanked and unflanked in terms of the presence/absence of chlorines in adjacent position(s). The *ortho* site Cl removal was confirmed only in laboratory studies (May et al., 2006).

Dechlorination of PCBs has been a research topic of interest for a long time. In addition to the many laboratory studies, it has also been the topic of modelling studies. In the literature, a number of studies identified pathways (Hughes et al., 2010, 2015; Karcher et al., 2004, 2007) while others evaluated quantification of pathways with biologically confirmed data (Bzdusek et al., 2006a; Bzdusek et al., 2006b; Demirtepe et al., 2015; Imamoglu et al., 2002; Imamoglu et al., 2004). Imamoglu et al. (2002) developed an anaerobic dechlorination model concerned with quantification of pathways, which provides abundance of dechlorination reactions (mole %) as an output. This model was later modified by Bzdusek et al. (Bzdusek, Lu, et al., 2006) and Demirtepe et al. (2015). These studies can help develop an approach for effective remediation strategies to contaminated sites with PCBs by enabling monitoring and predicting change in concentration and toxicity. Furthermore, a more detailed systematic evaluation of congener pattern changes may also lead to identification of new degradation pathways in addition to those identified in laboratory studies.

Congener specific degradation information can be very useful, such that they can now be incorporated into numeric fate and transport (F&T) models for modeling contaminant concentration in sediments. Biodegradation term is typically handled simply as first order and one rate constant is assumed to apply for all PCB congeners (Connolly et al., 2000; Russell et al., 2006). However, if pathway specific degradation

rate constants can be obtained, then congener specific modeling of PCBs in aquatic sediments can also be accomplished.

In this respect, this study aims to estimate biodegradation rate constants of dechlorination reactions of individual PCB congeners using the ADM. Baltimore Harbor sediment microcosm data is used for this purpose. As different from previous versions, ADM is modified in this study by adding new features such as calculation of biodegradation rate constants and can now be applied to sediments contaminated with any halogenated hydrophobic organic compound (HOC). By this way, biodegradation rate constants obtained from ADM can be used as input to FTHP models for a better and more detailed investigation of the fate of individual HOCs in contaminated sediments. Various remediation scenarios such as monitored natural attenuation or bioremediation with bioaugmentation can be handled in a more quantitative manner with the help of the rate constants estimated in this study.

## **5.2 Methodology**

### **5.2.1 Baltimore Harbor (BH) Microcosm Data Set**

Microcosms enable microbial reductive dechlorination of PCBs, without a major effect of physicochemical or other biotic/abiotic transformations. Details about the preparation of microcosms and analysis for the BH data set are given in Fagervold et al. (2007, 2011). Four microcosm data sets from BH were spiked with Aroclor 1260 and prepared by addition of (i) no microorganism (no bioaugmentation) (denoted “BH”), (ii) SF-1 and DEH-10 (denoted “SF-1+DEH-1”), (iii) o-17 and DF-1 (denoted “o-17+DF-1”) and (iv) SF-1, DF-1, DEH-10 and o-17 microorganisms (denoted “SF-1+DF-1+DEH-10+o-17”) (Fagervold et al., 2007, 2011). Microcosms were sampled at 0, 100, 200 and 300 days. 91 congener groups (177 individual congeners due to coelution) were analyzed. Average PCB profiles of three microcosm replicas for four data sets were presented in Figure 3.20-Figure 3.23, section 3.4.1.

### 5.2.2 Anaerobic Dehalogenation Model (ADM)

ADM was developed by Imamoglu et. al (2004) and modified by Bzdusek et. al (2006) and Demirtepe et al. (2015). It aims to identify and quantify dechlorination pathways among congeners in PCB data sets measured at two different times. Two modifications are present in this study when compared to the most recent published version of the model: (1) model can now be used for any hydrophobic organic compound (not only PCBs), hence the name is now Anaerobic Dehalogenation Model (2) model now additionally gives dechlorination rate constants as output.

The model is rewritten in MatLAB, version 7.10.0. ADM is based on mass balance between dechlorinated and accumulated congeners. The model works according to two principles: (i) mass balance between mother and daughter congeners is maintained (ii) only pathways confirmed with laboratory or field studies are used. The same objective function in original model (Bzdusek, Lu, et al., 2006; Demirtepe et al., 2015; Imamoglu et al., 2002) is aimed to be minimized. The governing equation is given below:

$$S = \sum_{j=1}^m (\hat{y}_j - x_j)^2 \quad 5.1$$

where  $\hat{y}_j$  is predicted congener profile (either from Frame et. al (1996) or microcosm PCB data at  $t=0$  d) altered according to a dechlorination activity (mole ‰),  $x_j$  is congener profile of microorganism PCB data measured at day e.g.  $t=100$  day (mole ‰), and  $m$  is number of the congeners. As different from old version, the groups of congeners in coelution are not separated. The model input are the list of congeners analyzed in all samples, ‰ moles of original profile at  $t_{\text{initial}}$ , ‰ moles of predicted profile at  $t_{\text{final}}$  and a list of anaerobic dechlorination pathways.



Pathways are now identified automatically according to a specified dechlorination activity (DA) or group of activities. The DAs can contain pathways that are theoretically possible and/or confirmed by biological studies. Besides, congeners or substitutions can be defined to the activities as the constraint such as that a specific congener including Cl in a *para* position can be defined as a constraint such that it will not undergo dechlorination in an activity including removal of *para* chlorines.

An improved evaluation of model fit is brought about in the new model. The fit of all congeners as well as those that take part in a pathway (as mother or daughter) are separately investigated by the multiple correlation coefficient  $R^2$ . It is calculated for of all measured congeners ( $R^2$ ) and reactive congeners ( $R^2_{\text{reac}}$ ) which participate in dechlorination as either mother or daughter congener.  $R^2$  is deemed satisfactory if it is above 0.70.

Using ADM, a dechlorination pathway is now not only quantified but also the dechlorination rate constant ( $k_m$ ) associated with it is calculated. The order by which microorganisms dechlorinate PCBs is not known. Therefore, the full list of pathways are shuffled a 100 times and subsequently a distribution of  $k_m$  values are obtained. Sometimes a  $k_m$  value can not be computed for a pathway (e.g. if concentration of mother congener before reaction is equal to "0") in which case no  $k_m$  estimation is presented for that shuffle. Please see Section 3.2 for details of the application of ADM.

## **5.3 Results and Discussion**

### **5.3.1 Analysis of ADM Results for All Dechlorination Activities**

ADM was run for BH microcosm sediment data with input as concentration of 91 congeners/coeluting groups and pathways of 25 DAs. They are given in Table 5.1. Biological studies include microorganism based pathways defined in Fagervold et al. (2007), Wu et al. (2002), Fennell et al. (2004) and Adrian et al. (2009). As can be seen

from the last four columns of Table 5.1, ADM provided an estimation of biodegradation rate constants for fourteen of these activities. Ten of these activities, namely DA-16 to 25, are microorganism based ones (Fagervold et al., 2007, 2011). A distribution of  $k_m$  values is obtained for each dechlorination pathway in a DA. In Table 5.1, the maximum, median and minimum  $k_m$  values calculated by the ADM are shown. When we compare the median of the maximum  $k_m$  values (last column of Table 5.1) of each activity, a range of almost three orders of magnitude can be seen.

The goodness of fit results for DAs that  $k_m$  values could be estimated are presented in Table 5.2. It can be seen that even when degradation rate constants are estimated by the ADM, a DA may not satisfactorily explain the degradation of congeners as indicated by the  $R^2$  and  $R^2_{\text{reac}}$  (Table 5.2). Accordingly, goodness of fit parameters,  $R^2$  and  $R^2_{\text{reac}}$  are evaluated considering two criteria; (i) Finding the DA explaining degradation of congeners for all samples and in their all or most of their time intervals satisfactorily. (ii) Checking the correlation of each sample with their corresponding DA which includes the same microorganism or microorganism groups (i.e. 2.BH with DA23, 3.BH with DA24 and 4.BH with DA25).

When the performance of all DAs are investigated, DA18 was identified as the one to most successfully explain pattern changes with satisfactory fit results (i.e.  $R^2 > 0.74$  and  $R^2_{\text{reac}} > 0.86$  for all four BH data sets). Moreover, as can be seen from the figures of four data sets in Section 3.4.1, the greatest shift in PCB congener patterns occur between 100 and 200 days in BH data sets. Accordingly, there was no significant correlation between measured and modeled t100- t200 day data profiles in DAs except for DA18 (Table 5.2). In four data set graphs between 100 and 200 days, dramatical changes are observed in higher chlorinated homolog groups, especially penta, hexa and hepta including congeners 92, 110/77, 124/135/144, 165, 179, 161/146, 172/192, 153/127, 126/129/178, 167 and 191 after 100 days. There is corresponding accumulation in lower chlorinated homolog groups such as, congeners 20/21/33/53, 23/34, 24/27, 28/31/50, 52/73, 43/49/38, 57/103/40, 62/65 and 70. Four groups of

congeners among these (20/21/33/53, 43/49/38, 153/127 and 161/146) take part in pathways of DA18 (Table 5.3). These congeners have better correlation in the time interval of 100 and 200 days of 1BH, 3BH and 4BH (Figure E.4, Figure E.5 and Figure E.6) since congeners 20/21/33/53 and 43/49/38 are accumulated congeners, and 161/146 and 153/127 are dechlorinated. Therefore, dechlorination, as seen in Figure E.1, E.3 and E.4, is predicted relatively more successfully by DA18.

As the second criterion, it is expected that three activities successfully should explain the dechlorination in the corresponding data sets. when  $R^2$  values for measured data are compared with those of predicted data of corresponding activities, contrary to expectations, these activities did not predict dechlorination pathways as successfully as DA18. However, it is seen that the greatest shift in PCB congener patterns occur between 100 and 200 days is not predicted well with DA23, DA24 or DA25 (Table 5.2). The main reason for low  $R^2$  is that the congeners having shifted patterns between day 100 and 200, and day 0 and 100 are not predicted well by DA23, DA24 or DA25 (Figure E.2, E.3 and E.4). In prediction of data 2.BH with DA23 (Figure E.7 and Figure E.8), for example the model can not explain the dechlorination since the shifted congeners except 161/146 and 153/127 are not available in the pathway list. On the other hand, while these congeners in DA23 should accumulate according to the DA (Table 5.3), their abundance decrease by time. There may be a number of reasons why the expected DAs did not yield the best fit to measured data:

- Pathways identified for specific microorganism in the literature may not be an exhaustive list. That is, perhaps microorganisms are capable of conducting the pathways of DA18, but could not be noticed in microcosm studies in the previous studies. ADM can systematically check presence of many dechlorination pathways which can be much more advantageous when compared to a manual evaluation of dechlorinated profiles.
- Microorganisms, when brought together on a consortium, such as the case for 2.BH, 3.BH and 4.BH, may be capable of dechlorinating PCBs in pathways that are different from the case when they are individually present in sediments.

Such a phenomenon was discussed by Sowers and May (Sowers & May, 2013) Therefore, for example, when o17 and DF1 are introduced in the sediment together, uncharacteristically they may start dechlorinating *para* flanked *meta* chlorines and no longer dechlorinate flanked chlorines in *ortho* positions.

Table 5.1 Dechlorination activities and  $k_m$  values estimated by ADM.

DA No	Description of DA	Number of Pathways	$k_m$ ( $d^{-1}$ )		Median <sup>b</sup> of $k_m$ ( $d^{-1}$ )	
			Min <sup>a</sup>	Max	Min <sup>a</sup>	Max
DA1	Flanked any (DA3+DA4+DA5)	371				
DA2	Flanked <i>meta</i> any or flanked <i>para</i> any (DA3+DA5)	281				
DA3	Flanked <i>meta</i> any	170				
DA4	Flanked <i>ortho</i> any	90				
DA5	Flanked <i>para</i> any	111	0.0001	0.1190	0.0001	0.0439
DA6	<i>Meta</i> any	229				
DA7	<i>Ortho</i> any	193				
DA8	<i>Para</i> any	150				
DA9	Flanked or <i>meta</i> (DA1+DA6)	413				
DA10	Flanked or <i>para</i> (DA1+DA8)	393				
DA11	Doubly flanked <i>para</i> -any	44	0.0001	0.3662	0.0001	0.1106
DA12	Doubly flanked <i>meta</i> -any	60	0.0001	0.3672	0.0003	0.1181
DA13	Doubly flanked <i>para</i> any or doubly flanked <i>meta</i> any	104	0.0001	0.3619	0.0001	0.1007
DA14	Singly flanked <i>para</i> any or singly flanked <i>meta</i> any	179				
DA15	Doubly flanked <i>meta</i> and <i>para</i> +singly flanked <i>meta</i> + <i>para</i>	283				
DA16	Microorganism o-17 (Flanked chlorines in <i>ortho</i> and <i>para</i> positions)	48	0.0001	0.1027	0.0001	0.0094
DA17	Microorganism DF-1 (Doubly flanked chlorines in <i>meta</i> and <i>para</i> positions with some congener constraints)	23	0.0001	0.3652	0.0002	0.0926
DA18	Microorganism DEH10 (Doubly flanked chlorines in <i>meta</i> and <i>para</i> positions, <i>para</i> flanked chlorines in <i>meta</i> position)	9	0.0001	0.1330	0.0015	0.0112
DA19	Microorganism SF1 (Doubly flanked chlorines in the <i>meta</i> position, <i>ortho</i> flanked chlorines in the <i>meta</i> position)	10	0.0001	0.3657	0.0002	0.0824
DA20	Microorganism cdbb1 (Singly and doubly flanked chlorines in <i>para</i> position, doubly flanked chlorines in <i>meta</i> position)	120	0.0001	0.3622	0.0000	0.2176
DA21	Microorganism deh. m. 195 (Flanked chlorines in <i>meta</i> and <i>para</i> positions)	42	0.0001	0.3672	0.0002	0.1067
DA22	Microorganism SF-2 (Doubly flanked <i>meta</i> position)	2	0.0001	0.0039	0.0016	0.0021
DA23	DEH10+SF1	5	0.0001	0.0095	0.0003	0.0030
DA24	o17+DF1	29	0.0001	0.1027	0.0002	0.0103
DA25	Deh10+SF1+o17+DF1	32	0.0001	0.0901	0.0001	0.0106

<sup>a</sup> Minimum values disregarding "0" values, <sup>b</sup> The median of min and max of  $k_m$  values are shown.

Table 5.2 Goodness of fit results ( $R^2$  and  $R^2_{\text{reac}}$ ) for each sample run for each time interval

DA	1.BH		2.BH-SF1+DEH10		3.BH-017+DF1		4.BH-SF1+DEH10+o17+DF1	
	t0-t100 $R^2$ $R^{2*}$	t100-t200 $R^2$ $R^{2*}$	t0-t100 $R^2$ $R^{2*}$	t100-t200 $R^2$ $R^{2*}$	t0-t100 $R^2$ $R^{2*}$	t100-t200 $R^2$ $R^{2*}$	t0-t100 $R^2$ $R^{2*}$	t100-t200 $R^2$ $R^{2*}$
None	0.97	0.21	0.46	0.68	0.85	0.25	0.60	0.52
DA5	0.99	0.99	0.43	0.77	0.96	0.96	0.99	0.99
DA11	0.98	0.99	0.43	0.84	0.95	0.97	0.63	0.71
DA12	0.99	0.99	0.59	0.70	0.97	0.98	0.99	0.99
DA13	0.98	0.99	0.42	0.86	0.97	0.98	0.57	0.70
DA16	0.97	0.99	0.45	0.77	0.94	0.95	0.60	0.81
DA17	0.98	0.99	0.83	0.93	0.92	0.95	0.84	0.94
DA18	0.97	0.99	0.49	0.48	0.99	0.96	0.87	0.97
DA19	0.97	0.99	0.49	0.71	0.86	0.90	0.63	0.52
DA20	0.99	0.99	0.51	0.48	0.98	0.99	0.64	0.62
DA21	0.97	0.97	0.46	0.97	0.85	0.99	0.60	1.00
DA22	0.97	0.99	0.45	0.92	0.86	0.97	0.59	0.96
DA23	0.97	0.99	0.43	0.86	0.92	0.95	0.58	0.89
DA24	0.97	0.99	0.43	0.85	0.93	0.95	0.58	0.89
DA25	0.97	0.99	0.43	0.74	0.93	0.93	0.57	0.67

\*: $R^2_{\text{reac}}$ . Blanks in  $R^2$  and  $R^2_{\text{reac}}$  cells indicate no simulation by ADM. Bold numbers indicate the samples having the best fit DA. Italic and underlined numbers indicate that microorganisms added to the sample and considered for relevant DA are the same.

Table 5.3 List of all dechlorination pathways for the best performing dechlorination activities, DA18, DA23, DA24 and DA25

Pathways	DA18	DA23	DA24	DA25
20/21/33/53→7/9			√	√
29/54→7/9			√	√
66/80/93/95/102/88→20/21/33/53	√			
66/80/93/95/102/88→22/51	√			
74/94/61→23/34			√	√
74/94/61→29/54			√	√
79/99/113→47/48/75	√			
90/101→43/49/38	√			
128→85/120/148			√	√
124/135/144→74/94/61		√		√
132/105→55/91	√			
138/163/164→85/120/148			√	√
138/163/164→81/87/117/111/115/116/145			√	√
138/163/164→79/99/113	√		√	√
106/118/139/149→66/80/93/95/102/88		√		√
151→66/80/93/95/102/88	√			
153/127→79/99/113	√			
161/146→90/101				
170/190→176/130			√	√
170/190→138/163/164			√	√
156/171/202→106/118/139/149			√	√
174/181→106/118/139/149		√		√
180→141			√	√
180→161/146		√	√	√
180→153/127		√	√	√
183→106/118/139/149			√	√
183→124/135/144			√	√
183→154			√	√
194→172/192			√	√
194→180			√	√
195/208→174/181			√	√
196/203→175			√	√
196/203→183			√	√
196/203→154			√	√
196/203→174/181			√	√
196/203→185			√	√
206→187/159/182			√	√
206→196/203			√	√

### 5.3.2 Evaluation of $k_m$ values in DA 18

ADM simulates maximum 100 times  $k_m$  values for a data of two time intervals using a DA. Therefore, a distribution is obtained for  $k_m$ . The box plot of  $k_m$  distributions of each pathway in DA 18 is given in Figure 5.1.  $k_m$  values show one or two order of

magnitude with their median values. As seen in Figure 5.1, the median  $k_m$  values of all pathways are below  $0.02 \text{ d}^{-1}$ . The distribution of  $k_m$  values depending on time was compared with each other in different data sets. Generally,  $k_m$  values of all congeners are the highest at t100-t200. However, considering all pathways and all data sets, there is no pattern between them. When the toxicity-related pathways are examined in DA18, only 132/105 $\rightarrow$ 55/91 is available and it is seen that toxicity of congener 105 decreases with time.

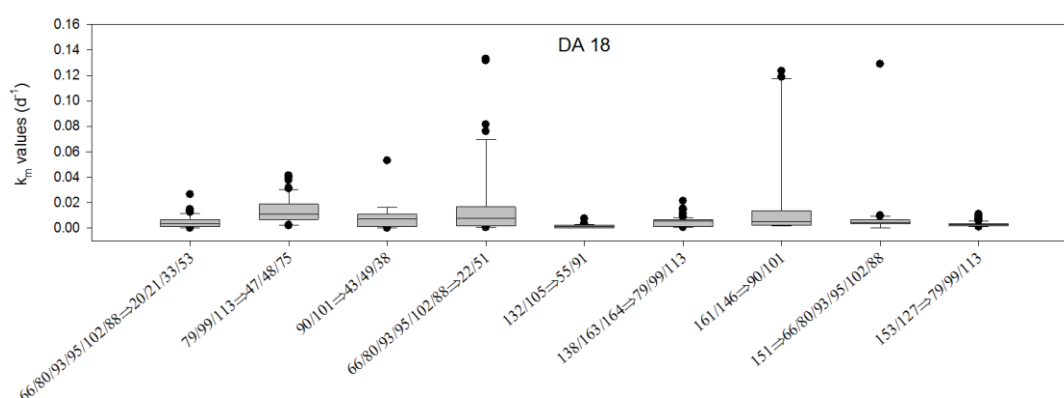


Figure 5.1 Distribution of  $k_m$  values modeled by ADM for DA 18

The  $k_m$  values were compared with relevant environmental and laboratory studies in the literature (Table 5.4). Median and maximum  $k_m$  results in this study were found comparable with those in laboratory and environmental studies, respectively. As can be seen in Table 5.4,  $k_m$  values for nine pathways are in the range of 0 and  $0.129 \text{ d}^{-1}$  (Table 5.4). Cho et al. (2003) estimated  $k_m$  values for 23 coeluting PCB congeners using sediment microorganisms from the St. Lawrence River (NY). As different from our study, products of dechlorination were not considered in these studies. There are eight common congeners (66, 95, 99, 92/84/90, 101, 66, 95, 105) between dechlorinated congeners in Cho et al. (2003) and our study. These congeners have the same order of magnitude of  $k_m$  values (as average and median) with those run by ADM, that is around  $10^{-3} \text{ day}^{-1}$ . Siebielska and Sidelko (2015) studied degree of PCB degradation in composting and anaerobic digestion processes without considering



products of dechlorination. Common congeners are 101, 138 and 153. Similarly,  $k_m$  values associated with these congeners are at the same order of magnitude as maximum  $k_m$  values run by ADM. Differences between rate constants can be attributed to sediment PCB concentration, numbers of PCB dechlorinators and desorption rates from sediment into the aqueous phase. As a result, the ranges of our results are consistent with those in the literature, especially with that of the microcosm study (Cho et al., 2003). As distinct from these studies,  $k_m$  values in this study are also compared with the values of Lombard et al. (2014) which considers the number of microorganisms in estimation of  $k_m$  values. The study investigated rates of congener 61 to congener 23 by DF1 in the pore water considering environmentally relevant concentrations (1 to 500 ng/L) of contaminant and concentration of cells ( $>10^6$  cells/mL) in sediment free medium. Since dechlorination of congener 61 to congener 23 is not available in DA 18, the values in the study are compared with the values in all pathways. Accordingly, the maximum values of most of the pathways estimated in this study have the same order of magnitude with the findings (0.339-0.541  $d^{-1}$ ) of Lombard et al. (2014) for aqueous phase dechlorination. This discussion indicates that if sufficient number of microorganisms is provided during remediation e.g. via bioaugmentation, maximum  $k_m$  values in our study can be used for systematic identification and quantification of anaerobic dechlorination pathways coupled with congener specific modeling.

Table 5.4 Comparison of  $k_m$  values with the values in the literature

Dechlorination pathway (Mother-->Daughter)	ADM $k_m$ (day <sup>-1</sup> )* Results in DA 18						Cho et al. (2003)		Siebielska and Sidelko (2015)		
	Avg	Median	SD	RSD	Min	Max	#	k (d <sup>-1</sup> )*	#	k1 (d <sup>-1</sup> )*	k2(d <sup>-1</sup> )*
66/80/93/95/102/88 →20/21/33/53	0.005	0.003	0.005	93.295	0	0.027	66	0.006			
							95	0.009			
79/99/113→47/48/75	0.013	0.011	0.009	70.238	0.002	0.041	99	0.009			
90/101 →43/49/38	0.009	0.007	0.012	136.159	0.0001	0.053	92/84/90	0.006			
							101	0.008	101	0.012	0.085
66/80/93/95/102/88 →22/51	0.020	0.008	0.035	171.138	0.0005	0.133	66	0.006			
							95	0.009			
132/105 →55/91	0.002	0.002	0.002	122.745	0	0.008	105	0.008			
138/163/164 →79/99/113	0.005	0.006	0.004	82.317	0.001	0.021			138	0.015	0.059
161/146→90/101	0.018	0.005	0.035	192.695	0.002	0.123					
151→66/80/93/95/102/88	0.007	0.005	0.017	243.867	0.000	0.129					
153/127→79/99/113	0.003	0.003	0.002	66.857	0.001	0.011			153	0.014	0.12

\*: First order model, #: Congener no, k1: for Composting, k2: for anaerobic digestion

## 5.4 Conclusions

This study set out to estimate biodegradation rate constants of PCB congeners undergoing anaerobic dehalogenation using a model, ADM. Overall:

- Microcosm data provides a valuable source for eliminating any major effect of physicochemical or other biotic/abiotic transformations. In that respect, for BH sediments, possible dechlorination pathways are identified and tested by the ADM. Accordingly, dechlorination rates are estimated for the activity that enabled the best fit to dechlorinated microcosm PCB profiles. Also, coeluting congeners could be handled by ADM without the need to separate congeners. This enables a simpler evaluation of anaerobic dechlorination in sediments.
- $k_m$  values estimated in this study are comparable to values in the literature. As Cho et al (2003) points out, the estimated dechlorination rates may not be

applicable for all contaminated sites because of the possible dependency on physical, chemical and/or biological factors. In that respect, sediment composition, age of contamination as well as the type and cell mass of microbial consortia is expected to have an effect on biodegradation rates. Nevertheless, a  $k_m$  estimate that is based on actual dechlorination data via a detailed systematic evaluation of congener pattern changes and individual degradation pathways would be useful for fate studies.

- Systematic and relatively simple estimation of  $k_m$  leads the way to better understanding fate and transport of individual congeners in the environment. For example, toxic congeners being the mother or daughter of dechlorination reactions can be predicted, toxicity reduction could be made possible by this way.
- Numeric fate and transport models can incorporate real  $k_m$  values rather than simplistic first-order degradation rates for total-PCBs. Systematic identification and quantification of anaerobic dechlorination pathways coupled with congener specific modeling can aid remediation efforts such that congener specific monitoring/enhancement of bioremediation could be possible for sediment-bound PCBs.



## CHAPTER 6

### PREDICTION OF BIODEGRADATION RATE CONSTANTS OF PBDE CONGENERS USING AN ANAEROBIC DEHALOGENATION MODEL

#### 6.1 Introduction

Polybrominated diphenyl ethers (PBDEs) are a group of flame retardants. These chemicals have been widely used in building materials, electronics, furnishings, motor vehicles, airplanes, plastics, polyurethane foams and textiles (ATSDR, 2004). Their first commercial productions began in the 1970s in Germany (ATSDR, 2004). The production of tetra-, penta-, hexa- and hepta- PBDE congeners are banned by the Stockholm Convention due to their bioaccumulative property and persistence (POPs, 2008). PBDEs are released into the environment during their manufacture, incineration of municipal waste, deposition to landfills, discharge to municipal sewage-treatment plants, or emission directly to the atmosphere as particulate matter (ATSDR, 2004).

Fate of PBDEs is affected by physicochemical weathering processes such as sorption, volatilization, atmospheric transport, and wet/dry deposition, etc. (ATSDR, 2004). One of the most important processes for the breakdown of PBDEs is biodegradation (USEPA, 2010). Anaerobic debromination of PBDEs is the replacement of bromine atoms with hydrogen by the action of anaerobic microorganisms. Products of debromination reactions result in the accumulation of less brominated PBDEs, which can bioaccumulate on humans or biota (Tokarz et al., 2008). Anaerobic debromination of PBDEs were investigated and evaluated in the last decade (Ding et al., 2013; Huang et al., 2014; Robrock et al., 2008; Tokarz et al., 2008). These recent studies examined debromination pathways of PBDEs by a number of microorganisms and/or microbial groups. Additionally, some of these studies observed debromination pathways in terms of bromine configuration with various products. For example, Tokarz et al. (2008) and

Huang et al. (2014) noted that removal of *ortho* bromine is also possible along with removal of *para* and *meta* bromines, while Ding et al. (2013) and Robrock et al. (2008) indicated preferential removal of *para* and *meta* bromines from the diphenyl ether structure. Further studies are needed to understand the pathways of the congeners in the environment.

Environmental degradation mechanisms of halogenated compounds, especially for family of compounds such as PCBs, PBDEs can be examined by modeling studies with ease. Biologically confirmed data can be limited to further understand degradation mechanisms of such compounds in the environment (Wei et al., 2013). Therefore, modeling dehalogenation can help identify new degradation pathways which were not previously identified in laboratory studies. For PBDEs, two studies (Wei et al., 2013; Zou et al., 2014) are available to investigate the dehalogenation mechanisms in the literature, but these are on photolytic debromination pathways.

In this respect, this study aims to estimate rate constants of these reactions for individual PBDE congeners using the ADM. The data set used for this purpose was obtained from a contaminated soil in South China (Song et al., 2015). As different from previous versions, ADM is modified in this study by adding new features such as calculation of biodegradation rate constants and can now be applied to sediments contaminated with any halogenated hydrophobic organic compound (HOC). By this way, biodegradation rate constants obtained from ADM can be used as input to fate and transport models for a better and more detailed investigation of the fate of individual HOCs in a contaminated sediment. Various remediation scenarios such as monitored natural attenuation or bioremediation with bioaugmentation can be tested in a more quantitative manner with the help of this study.

## **6.2 Methods and Materials**

### **6.2.1 Soil Data Set**

The data set used in the study is from soils in the e-waste recycling town of Qingyuan, Guangdong province, South China (23.57° N, 113.0° E) (Song et al., 2015). The samples were taken between 0 and 15 cm depth. The microcosm samples were prepared in 15 ml glass and triplicates. Eight PBDE congeners (28, 47, 99, 100, 153, 154, 183 and 209) were analyzed after 0, 24, 40, 60, and 90 d. These sets contain microbial reductive debromination of PBDEs, without major effect of physicochemical and other biotic/abiotic transformations. Lactate added to the sample is used as electron donor. Details about the preparation of microcosms and analysis are given in Song et. al (2015). Three parallel microcosms were analyzed. The average concentration of PBDEs in ng/g dry weight (dw) with respect to time are depicted in Figure 3.35. One of three parallel data is used in the model.

### **6.2.2 Anaerobic Dehalogenation Model (ADM)**

ADM was developed by Imamoglu et. al (2004) and modified by Bzdusek et. al (2006) and Demirtepe et al. (2015). It aims to identify and quantify dechlorination pathways among congeners in PCB data sets measured at two different times. Two modifications are present in this study when compared to the most recent published version of the model: (1) model can now be used for any hydrophobic organic compound (not only PCBs), hence the name is now Anaerobic Dehalogenation Model (2) model now additionally gives debromination rate constants as output.

The model is rewritten in MatLAB, version 7.10.0. ADM is based on mass balance between dechlorinated and accumulated congeners. The model works according to two principles: (i) mass balance between mother and daughter congeners is maintained (ii) only pathways confirmed with laboratory or field studies are used. The same objective function in original model (Bzdusek, Lu, et al., 2006; Demirtepe et al., 2015;

Imamoglu et al., 2002) is aimed to be minimized. The governing equation is given below:

$$S = \sum_{j=1}^m (\hat{y}_j - x_j)^2 \quad 6.1$$

where  $\hat{y}_j$  is predicted congener profile (either from Frame et. al (1996) or microcosm PCB data at t=0 d) altered according to a debromination activity (mole %),  $x_j$  is congener profile of microorganism PBDE data measured at day e.g. t=100 day(mole %), and m is number of the congeners. As different from old version, the groups of congeners in coelution are not separated. The model input are the list of congeners analyzed in all samples, ‰ moles of original profile at  $t_{\text{initial}}$ , ‰ moles of predicted profile at  $t_{\text{final}}$  and a list of anaerobic debromination pathways.

Pathways are now identified automatically according to a specified debromination activity (DA) or group of activities. The DAs can contain pathways that are theoretically possible and/or confirmed by biological studies. Besides, congeners or substitutions can be defined to the activities as the constraint such as that a specific congener including Cl in a *para* position can be defined as a constraint such that it will not undergo debromination in an activity including removal of *para* chlorines.

An improved evaluation of model fit is brought about in the new model. The fit of all congeners as well as those that take part in a pathway (as mother or daughter) are separately investigated by the multiple correlation coefficient  $R^2$ . It is calculated for of all measured congeners ( $R^2$ ) and reactive congeners ( $R^2_{\text{reac}}$ ) which participate in debromination as either mother or daughter congener.  $R^2$  is deemed satisfactory if it is above 0.70.



Using ADM, a debromination pathway is now not only quantified but also the debromination rate constant ( $k_m$ ) associated with it is calculated. The order by which microorganisms dechlorinate PCBs is not known. Therefore, the full list of pathways are shuffled a 100 times and subsequently a distribution of  $k_m$  values are obtained. Sometimes a  $k_m$  value can not be computed for a pathway (e.g. if concentration of mother congener before reaction is equal to “0”) in which case no  $k_m$  estimation is presented for that shuffle. Please see Section 3.2 for details of the application of ADM.

### 6.3 Results and Discussion

DAs contain pathways that are theoretically possible and/or confirmed by biological studies (Table 6.1). ADM was run for microcosm soil data with input as concentration of 8 congeners and pathways of 21 DAs. Biological studies include microorganism based pathways defined in Ding et al. (Ding et al., 2013), Huang et al. (2014), Robrock et al. (2008), Tokarz et al. (2008). As can be seen in Table 6.1, there are no pathways for five of these activities with the PBDE congener data used in this study. Therefore, ADM provided an estimation of biodegradation rate constants for sixteen of the activities.

A distribution of  $k_m$  values is obtained for each pathway of each DA by ADM. In Table 6.1, the maximum, median and minimum  $k_m$  values calculated for all pathways in an activity are shown. The  $k_m$  values vary in a range of 0.0003 to 0.02 d<sup>-1</sup>. The difference is due to comparison of min and max values, existence of various pathways and different DAs.

The goodness of fit results are presented in Table 6.2. While  $R^2$  values vary between 0.57 and 1.00,  $R^2_{\text{reac}}$  values change between 0.03 and 1.00. When no major congener shift is observable in a time interval, then application of a DA may not result in any improvement, as is the case for DA7 and DA21 for the first and last time intervals.

There is no correlation of reactive congeners for a few of the cases as shown in bold in Table 6.2.

Table 6.1 DAs and  $k_m$  values estimated by ADM.

DA No	Description of DA	Number of Pathways	$k_m$ ( $d^{-1}$ )		Median <sup>b</sup> of $k_m$ (-1)	
			Min <sup>a</sup>	Max	Min <sup>a</sup>	Max
1	Flanked any(3+4+5)	5	0.0003	0.0241	0.0002	0.0031
2	Flanked meta any or flanked para any(3+5)	1	0.0031	0.0173	0.0015	0.0015
3	Flanked meta any	4	0.0003	0.0241	0.0002	0.0031
4	Flanked ortho any	1	0.0026	0.0026		
5	Flanked para any <sup>c</sup>	0				
6	Meta any	1	0.0031	0.0173	0.0015	0.0015
7	Ortho any	3	0.0010	0.0180	0.0021	0.0021
8	Para any <sup>c</sup>	0				
9	Flanked or meta(1+6)	1	0.0031	0.0173	0.0015	0.0015
10	Flanked or para(1+8)	1	0.0031	0.0173	0.0015	0.0015
11	Doubly flanked para-any <sup>c</sup>	0				
12	Doubly flanked meta-any	1	0.0031	0.0173	0.0015	0.0015
13	Doubly flanked para any or doubly flanked meta any	1	0.0031	0.0173	0.0015	0.0015
14	Singly flanked para any or singly flanked meta any	3	0.0003	0.0241	0.0002	0.0029
15	Doubly flanked meta and para+singly flanked meta+para	4	0.0003	0.0241	0.0002	0.0031
16	The study of Tokarz et. al (2008)	4	0.0003	0.0241	0.0002	0.0024
17	The study of Tokarz et. al (2008) without biometrics <sup>c</sup>	0				
18	The study of Huang et. al (2014)	5	0.0006	0.0180	0.0021	0.0022
19	The study of Robrock et. al (2008)	5	0.0003	0.0241	0.0002	0.0021
20	The study of Ding et. al (2013) for penta mixture <sup>c</sup>	0				
21	The study of Ding et. al (2013) for octa mixture	2	0.0015	0.0173	0.0010	0.0010

<sup>a</sup>: Minimum values disregarding “0” values, <sup>b</sup>: The median of min and max of  $k_m$  values are shown. <sup>c</sup>:

A pathway could not be identified for this description of DA because relevant congeners are not measured in the data set.

Table 6.2 Goodness of fit results ( $R^2$  and  $R^2_{\text{reac}}$ ) for each sample run and each time interval

Soil Data Parallel 1								
DA no	t0-t24		t24-t40		t40-t60		t60-t90	
	R2	$R^2_{\text{reac}}$	R2	$R^2_{\text{reac}}$	R2	$R^2_{\text{reac}}$	R2	$R^2_{\text{reac}}$
DA1	0.75	0.93	0.81	0.89	0.86	0.87	0.70	0.79
DA2	0.72	1.00	0.61	1.00	0.88	1.00	0.57	1.00
DA3	0.75	0.93	0.81	0.89	0.88	0.89	0.70	0.79
DA4	0.70	1.00	0.61	1.00	0.86	1.00	0.57	1.00
DA6	0.72	1.00	0.61	1.00	0.88	1.00	0.57	1.00
DA7	0.70	<b>0.44</b>	0.75	0.99	0.92	0.85	0.57	<b>0.33</b>
DA9	0.72	1.00	0.61	1.00	0.88	1.00	0.57	1.00
DA10	0.72	1.00	0.61	1.00	0.88	1.00	0.57	1.00
DA12	0.72	1.00	0.61	1.00	0.88	1.00	0.57	1.00
DA13	0.72	1.00	0.61	1.00	0.88	1.00	0.57	1.00
DA14	0.73	0.88	0.81	0.97	0.88	0.89	0.69	0.80
DA15	0.75	0.93	0.81	0.89	0.88	0.89	0.70	0.79
DA16	0.73	0.56	0.84	0.99	0.90	0.98	0.60	0.98
DA18	0.72	0.57	0.75	0.92	0.92	0.85	0.66	0.61
DA19	0.75	0.65	0.79	0.87	0.89	0.97	0.60	0.93
DA21	0.72	<b>0.28</b>	0.61	<b>0.03</b>	0.86	1.00	0.57	0.99

**Bold:** lower than average values in the table. Standard deviation of each  $R^2$  and  $R^2_{\text{reac}}$  in the table was examined, they are lower than  $10^{-16}$ .

In this study,  $k_m$  value for BDE 209 can not be estimated by ADM. The reason for this is that octa and nona homolog groups are not analyzed in the data set of Song et. al (2015). As can be seen from the figure of data set in Section 3.5.1, while amount of BDE 209 decreases in 90 days, amount of BDEs 99, 100, 153, 154 and 183 increase. Song et al. (2015) state that increase in 99, 100, 153, 154 and 183 is explained by degradation of higher brominated congeners.

The median and maximum  $k_m$  values are presented in Table 6.3. When  $k_m$  values of 8 pathways are compared, the median  $k_m$  values take 0, 0.001, 0.002 or 0.003  $d^{-1}$ . The maximum values are close to 0.001 to 0.0024  $d^{-1}$ . There are very limited number of environmental and laboratory studies in the literature investigating biodegradation rate

constants of individual PBDE congeners. Gerecke et al. (2005) investigating anaerobic debromination of BDE 209 to BDE 208 in sewage sludge in a mesophilic digester. They found a pseudo-first-order degradation rate constant as  $0.001 \text{ d}^{-1}$ . Our median and maximum  $k_m$  results are comparable with this value (Table 6.3).

Table 6.3 Degradation rate constants of eight debromination pathways according to the DAs

DA no	Debromination pathways							
	47→28	99→47	100→47	153→99	154→99	154→100	183→153	183→154
1		0.003/0.001		0.024/0		0.008/0.003	0.003/0	0.017/0.002
2								0.017/0.002
3		0.003/0.001		0.024/0		0.008/0.003		0.017/0.002
4							0.003/0	
6								0.017/0.002
7	0.007/0.002		0.001/0		0.018/0			
9								0.017/0.002
10								0.017/0.002
12								0.017/0.002
13								0.017/0.002
14		0.003/0.001		0.024/0		0.008/0.003		
15		0.003/0.001		0.024/0		0.008/0.003		0.017/0.002
16	0.007/0.002	0.003/0.002		0.024/0	0.018/0			
18	0.007/0.002		0.001/0		0.018/0	0.008/0		0.017/0.002
19	0.007/0.002	0.003/0.001		0.024/0			0.003/0	0.017/0.001
21							0.003/0	0.017/0.001

The number before slash is the maximum  $k_m$  value, The number after slash is the median  $k_m$  value.

Overall, for favorable debromination pathways, such as that of  $183 \rightarrow 154$ , a min  $k_m$  of  $0.001 \text{ day}^{-1}$  and a max of  $0.017 \text{ day}^{-1}$  could be used. In general, a min of  $0.001 \text{ day}^{-1}$  and a max of  $0.024 \text{ day}^{-1}$  could be advisable.

## 6.4 Conclusions

In this study,  $k_m$  values and possible pathways of debromination that can take place in contaminated soil were investigated by ADM. The model evaluated only limited number of pathways since only 8 congeners were measured. However, these congeners

tend to bioaccumulate (Hale et al., 2003) and their abundance, and fate would be of concern. The estimated  $k_m$  values in this study are comparable to those from the literature. This result indicates that such models can help a more detailed systematic evaluation of congener pattern changes by the identification of new degradation pathways in addition to those identified in laboratory studies. Furthermore,  $k_m$  values considering debrominated products can help understand the fate and transport of individual congeners, especially bioaccumulative congeners in the environment by numerical models. By this way, this kind of studies can enhance the bioremediation in contaminated sites with PBDEs.



## CHAPTER 7

### MODELING BIODEGRADATION OF PCBS IN SEDIMENT CONSIDERING FATE AND TRANSPORT MECHANISMS

#### 7.1 Introduction

Polychlorinated biphenyls (PCBs) are among the persistent organic pollutants regulated by the Stockholm Convention. Although they are chemically persistent in the environment, they are still affected by various transport and transformation mechanisms such as physicochemical weathering (sorption, volatilization, atmospheric transport, and wet/dry deposition) (Gouin & Harner, 2003) and biodegradation (anaerobic and aerobic) (Bedard, 2003). Stockholm Convention aims to eliminate the use of equipment containing PCBs by 2025 as well as management of wastes containing PCBs by 2028. The convention is implemented in more than 152 countries that are signatories (POPs, 2008).

There are several sites that has received attention due to PCB contamination. One of them is Lake Michigan. Lake Michigan was polluted by widespread use and consequent loading of synthetic organic chemicals into the lake since 1940s. As a result of pollution, Enhanced Monitoring Plan (EMP) was founded by federal, state, tribal, and local entities to eliminate or reduce the risks to human health and aquatic organisms in the ecosystem of the lake (Zhang et al., 2008). Under the scope of EMP, the lake was monitored between 1994 and 1995. Then, the Lake Michigan Mass Balance Project (LMMBP) was conducted. One of the scopes of the project was simulation of the transport, fate, and bioaccumulation of toxic chemicals in the lake. Remediation affords firstly started in Sheboygan Harbor in 1980s and completed in 1991. Since 1991, remediation efforts have continued at other locations through the rivers discharging to the lake (Rossmann, 2006).

Fate and transport (F&T) models are valuable in predicting the remediation outcome and better management of sites contaminated with chemicals. In the literature, numerous studies exist for modeling of PCBs in terms of total-PCBs, PCBs as homologs or individual congeners (Connolly et al., 2000; Davis, 2004; Farley et al., 1999; Shen et al., 2012; Zhang et al., 2008, 2009). For example, LM2 and MichTOX models were used in the LMMBP to develop an integrated mass balance model for the simulation of transport, fate, and bioaccumulation of toxic chemicals, including PCBs, in Lake Michigan. Individual PCB congeners were modeled, however, after simulation, all results were evaluated in terms of total PCBs (Zhang et al., 2008, 2009). In LM2, biodegradation was ignored. There is one study in the literature, by Davis (2004) which models the general degradation term of each individual congener, however, without separating biological/chemical degradation or taking into account any products. Consideration of the products in biodegradation is important to evaluate the change in toxicity as well as persistence and total concentration of PCBs. According to our literature review, the common fate mechanism of the studies for sediment is microbial degradation for PCBs. Yet, there is no model that considers anaerobic degradation among individual congeners where reactants and products of the reactions are both taken into account.

Our literature review indicates that there is no model that runs on an individual congener basis, considering biodegradation of these compounds with their relevant products, and other F&T processes together. As distinct from the literature, this study aims to develop a model that evaluates biodegradation pathways of individual congeners together with F&T processes in the sediment. The developed model is versatile in terms of applicability to various chemicals (such as halogenated hydrophobic organic compounds) and different sites. For this purpose, biodegradation of individual PCB congeners in bed sediments of Lake Michigan is selected as the study site for model development. Biodegradation rate constants for congener specific degradation pathways are estimated by a separate model and fed as input to the F&T



model. Overall, this study investigates the biodegradation of PCBs in sediment comprehensively and evaluates a number of remedial strategies for better management of the site such as natural attenuation or bioaugmentation.

## **7.2 Methodology**

In this study, development and application of fate and transport of hydrophobic pollutant (FTHP) model to Lake Michigan sediments for PCBs are explained. A flowchart of the full process of model development and application is presented in Figure 7.1. The main stages of model development are shown in shaded boxes as code verification, calibration, validation, sensitivity and uncertainty analyses. The FTHP was then applied on LM PCB data set. The model code and flowchart of Runge Kutta 4<sup>th</sup> order (RK4) solution, as referred to in Figure 7.1 are explained in section 3.3.

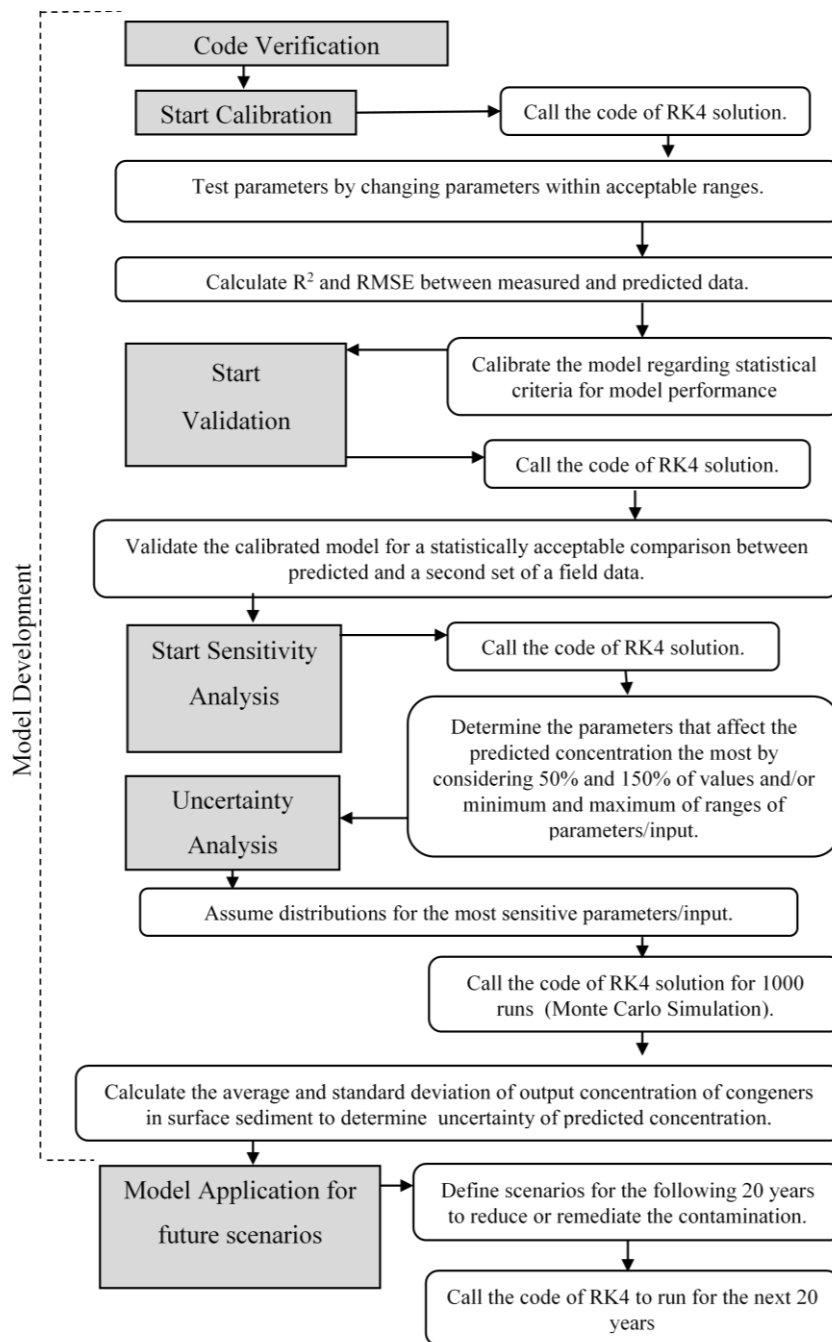


Figure 7.1 FTHP model development for and application to Lake Michigan Sediments

### 7.2.1 Fate and Transport of Hydrophobic Pollutant (FTHP) model

The general mass balance equation used in this study is given in Eqn. 7.1. The mass balance equation and numerical approach of Recovery model which was developed by Boyer et al. (1994) and Chapra and Reckhow (1983) were adopted. The model was written in MatLAB and individual PCB congeners were run as state variables.

$$\begin{aligned} \text{Accumulation} = & \text{Decay} + \text{Settling} - \text{Resuspension} - \text{Burial} - \text{Diffusion between the surface layer and the water column} + \text{Diffusion between the surface layer and the deep sediment} \\ \frac{dc_m^i}{dt} = & -k_m c_m^i + \frac{v_s A_w F_{pw} c_w^i(0)}{V_m} - \frac{v_r A_m c_m^i}{V_m} - \frac{v_b A_m c_m^i}{V_m} - \frac{v_d A_m (F_{dw} c_w^i(0) - F_{dp} c_m^i)}{V_m} + \frac{v_d A_m (F_{dp} c_s^i(0) - F_{dp} c_m^i)}{V_m} \end{aligned} \quad 7.1$$

$V_m$	volume of sediment, $m^3$
$A_w$ and $A_m$	surface areas of water and surface sediment, respectively, $m^2$
$k_m$	decay rate constant of the contaminant in the surface layer, $day^{-1}$
$v_b$	burial velocity, m/day
$v_s$	settling velocity of particulate matter, m/day
$v_r$	resuspension velocity of sediments, m/day
$v_d$	diffusion mass-transfer coefficient at the sediment, water and deep sediment interface, m/day
$c_s^i(0)$	$i^{th}$ contaminant concentration at the top of the deep contaminated layer, ng/L
$c_w^i$ and $c_m^i$	concentrations of contaminant $i$ in water and surface sediment, respectively, ng/L
$t$	time, day
$F_{pw}$ , $F_{dw}$	fraction of contaminant in particulate and dissolved forms in the water, respectively
$F_{dp}$	ratio of contaminant concentration in the sediment pore water to contaminant concentration in total sediment

Upper and lower boundaries of the model are set as the water-sediment interface and deeper sediment, respectively (Figure 7.2). As the major transport processes, settling, resuspension, burial and diffusion are considered in simulating the temporal change in the concentration of an individual congener. For transformation mechanisms, anaerobic dehalogenation (biodegradation) is considered as the only dominant process in sediment. PCBs are assumed to partition into particulate and dissolved phases in the system. In the mechanisms of burial, resuspension and biodegradation, the contaminant is considered in both dissolved and particulate phases while the mechanisms of settling and diffusion are carried out in particulate and dissolved phases, respectively. Biodegradation rate constants change from one congener to the other as individual dechlorination pathways between congeners are taken into account. Solubility limit of congeners are also considered during incorporation of biodegradation into the model. The assumptions conducted in this study as in Boyer et al. (1994) are well-mixed water and sediment layer, variability in  $C_m$  in depth direction, linear equilibrium sorption mechanisms, first order kinetic, no compaction in sediment. As different from Recovery model, in this model it is assumed that contaminant concentration in water column is accepted as constant.

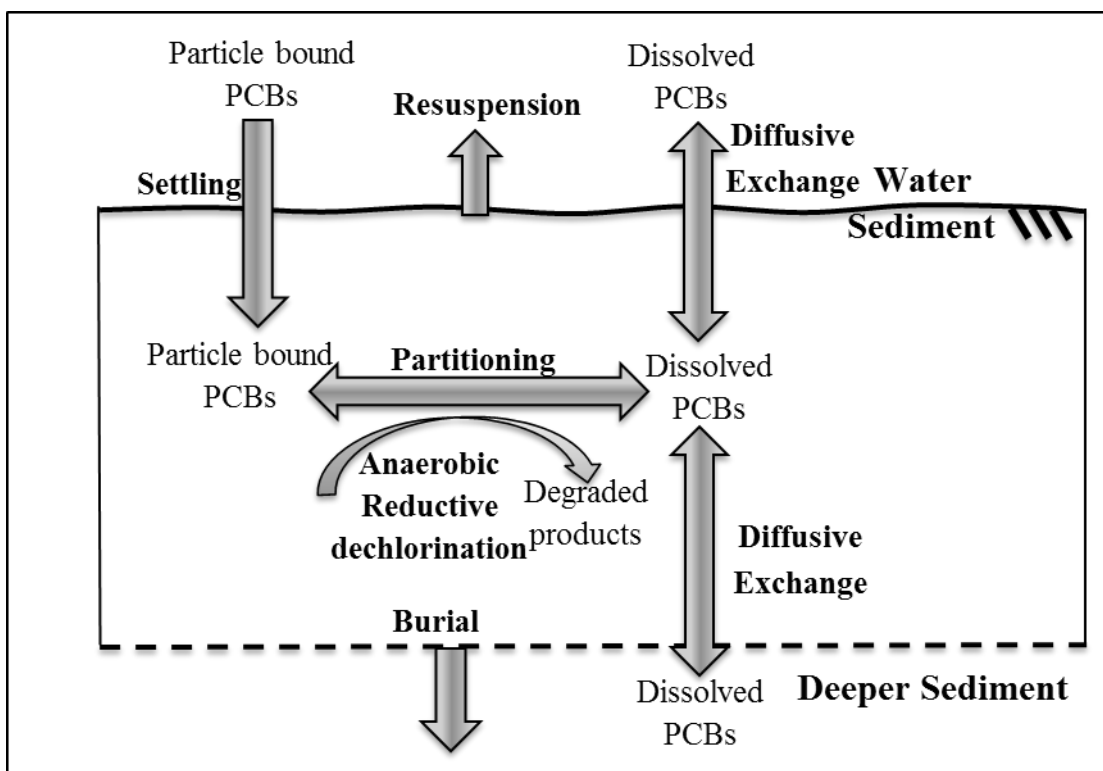
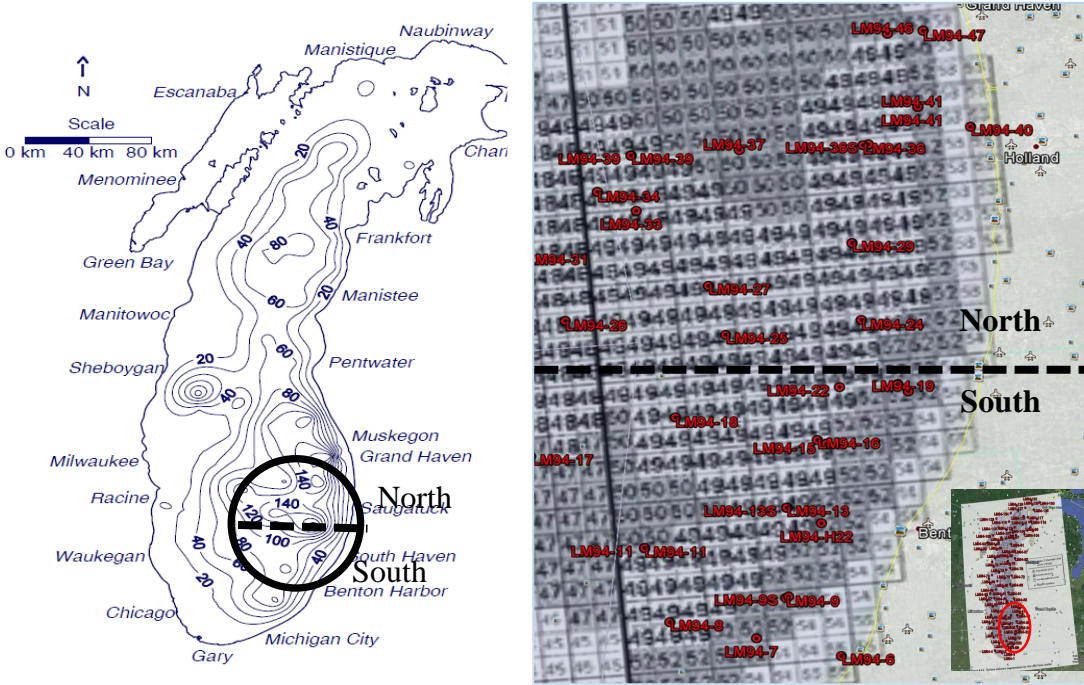


Figure 7.2 PCB Conceptual Model

### 7.2.2 Lake Michigan (LM) Sediment Data Set

For the application of the FTHP model, LM data set consisting of 38 congeners (16, 26, 28/31, 33, 44, 49, 52, 56/60, 66, 70/76, 74, 81, 84/92, 85, 87, 99, 101, 118, 123/149, 105/132/153, 151, 138/163, 170/190, 180, 182/187, 195/208 and 146) provided by the USEPA (USEPA, 2015) was used after eliminating non-detected congeners. The data set for the southeastern part of the lake was selected because sediments in this region contains the highest PCB concentration. Congener specific PCB concentrations in surficial sediments were measured at 10 different days between 7/25/1994-5/21/1996 (on days 0, 1, 72, 73, 75, 77, 79, 409, 665 and 666) (Table 7.1). Measured sediment concentrations ranged from 5.85 to 2514.40 ng/L while those in water column ranged from 0.0004 to 0.0237 ng/L. Segment number 49 is selected for simulating the distribution of congeners in surficial sediment. Segment 37 which is above segment 49 is used for water column. The details about segments are indicated in the study of Zhang (2006). Physicochemical parameters used in the model are taken from Zhang et

al. (2006), Mackay (2006) and Schneider (2005). Part of the sediment data is used for calibration and the other is used for model validation. Segment 49 is a wide region (120 km from north to south), so the region is divided as South and North (60km - 60km) and the samples belonging to the south are used for calibration, while the ones belonging to the north are used for model validation (Figure 7.3 and Table 7.1). Such a split allows for both spatial and temporal variation of the sediment data to be used during calibration and validation. Other parameter and inputs are given in section 3.4.2.



(Zhang, 2006, part1ch5)

Figure 7.3 Samples at South and North used for calibration and validation in segment 49, respectively

Table 7.1 Concentration of individual PCB congeners in 10 sediment samples (ng/L) (USEPA, 2015)

Sample No	1	2	3	4	5		6		7		8		9		10		RSD
					75	77	79	408	665	666	666	666	666	666	666	666	
Time (day)	0 <sup>a</sup>	1	72	73	75	77	79	408	665	666	666	666	666	666	666	666	
South/North <sup>b</sup>	N	S	S	S	N	N	N	N	S	S	S	N	N	S	S	S	
16	31.4	15.9	44.5	37.0	33.9	18.7	47.0	32.8	17.2	5.6	5.6	47.0	32.1	28.4	13.5	47.4	
26	42.1	52.2	63.6	59.1	51.2	52.7	69.9	43.1	19.1	13.4	13.4	69.9	51.7	46.6	18.2	39.0	
28/31	645.1	817.5	997.4	839.8	829.4	810.5	1007.2	685.0	278.7	206.6	206.6	1007.2	814.0	711.7	272.4	38.3	
33	126.1	155.8	188.0	187.5	147.2	147.1	210.0	173.4	80.4	40.5	40.5	210.0	151.5	145.6	51.9	35.6	
44	216.8	241.0	291.9	248.9	263.4	291.8	333.9	449.3	201.6	113.3	113.3	449.3	256.1	265.2	88.4	33.3	
49	131.6	154.4	192.3	152.7	193.8	181.0	213.9	177.5	73.1	56.0	56.0	177.5	165.9	152.6	52.2	34.2	
52	262.0	293.1	376.3	294.8	411.9	379.1	424.8	412.1	164.9	139.7	139.7	424.8	335.5	315.9	103.1	32.6	
56/60	408.2	462.6	529.4	442.4	591.2	564.2	636.6	666.1	253.1	164.4	164.4	666.1	496.0	471.8	162.8	34.5	
66	818.2	931.2	1156.0	926.3	1382.2	1259.6	1363.8	1305.9	541.4	397.9	397.9	1382.2	1043.6	1008.2	346.3	34.3	
70/76	403.7	463.4	546.4	455.7	672.6	619.6	655.3	683.6	267.8	199.4	199.4	683.6	504.9	496.7	170.2	34.3	
74	182.7	223.9	248.6	206.2	234.1	246.1	271.8	209.2	85.7	66.2	66.2	271.8	216.6	197.4	68.9	34.9	
81	17.4	20.0	21.6	14.3	36.9	29.0	25.9	51.8	9.9	7.9	7.9	51.8	20.8	23.5	13.3	56.5	
84/92	326.9	250.6	322.9	234.1	409.5	380.2	405.5	601.0	197.3	123.5	123.5	601.0	324.9	325.1	134.8	41.5	
85	151.3	160.2	195.6	130.5	316.3	264.1	262.0	371.2	140.4	105.9	105.9	371.2	177.9	209.7	88.8	42.4	
87	144.4	167.4	178.9	134.4	225.7	205.1	225.4	259.2	88.3	76.9	76.9	259.2	173.1	170.6	60.3	35.3	
99	157.0	159.0	205.9	139.2	322.2	273.1	276.3	375.9	125.6	99.8	99.8	375.9	182.4	213.4	93.2	43.7	
101	295.7	308.8	372.5	268.7	571.9	494.3	496.8	685.3	236.9	190.5	190.5	685.3	340.6	392.1	162.0	41.3	
118	415.7	359.4	510.9	394.9	920.8	746.3	718.4	773.2	351.7	290.2	290.2	773.2	463.3	548.2	221.3	40.4	
123/149	147.8	124.3	183.1	124.5	337.9	266.4	253.1	320.7	142.0	102.0	102.0	320.7	165.5	200.2	87.1	43.5	
105/132/153	512.0	433.1	589.0	435.4	1139.3	924.8	840.0	1117.1	485.4	347.3	347.3	1139.3	550.5	682.3	296.9	43.5	
151	41.4	38.2	51.6	35.6	89.5	72.5	70.4	81.0	40.7	30.5	30.5	89.5	46.5	55.1	21.2	38.5	
138/163	600.0	484.0	673.6	420.3	1444.6	1064.3	952.6	1281.6	412.0	296.0	296.0	1444.6	636.8	762.9	398.8	52.3	
170/190	105.3	84.8	112.9	80.8	231.6	194.7	168.3	231.1	91.2	63.0	63.0	231.1	109.1	136.4	64.3	47.1	
180	212.3	168.6	211.1	157.3	436.5	378.9	309.4	456.3	205.6	131.2	131.2	456.3	211.7	266.7	119.7	44.9	
182/187	74.1	63.1	87.3	59.1	181.1	140.4	123.9	188.4	85.1	55.3	55.3	188.4	86.2	105.8	49.8	47.1	
195/208	28.4	21.3	34.6	22.7	72.6	58.5	45.7	87.6	35.9	22.4	21.3	87.6	35.2	43.0	23.0	53.5	
146	70.0	56.7	91.0	56.9	162.7	126.7	118.9	161.6	63.3	43.0	43.0	162.7	80.5	95.1	44.5	46.9	

<sup>a</sup>: Day 0 is 7/25/1994, <sup>b</sup>: Segment 49 (120 km from north to south), is divided as South and North (60 km – 60 km)

## 7.3 Results and Discussions

### 7.3.1 Testing of the FTHP Model

In this study, site-specific parameters regarding Lake Michigan were taken directly from the reports of LM2 and MichTOX models (Rossmann, 2006). Aqueous solubility, octanol water partitioning coefficient, molecular diffusion coefficient values were taken from Mackay (2006) and Schneider (2005). All input data to the model were given in section 3.4.2. FTHP model code verification (written in MatLAB version 7.10.0) was performed in Microsoft Excel (version 2016).

During model calibration,  $v_s$ ,  $v_b$ ,  $K_d$  for both water and sediment are tested by varying their values from 50% to 150% and/or according to ranges given in the literature/data set. Biodegradation rate constants ( $k_m$ ) for congener specific anaerobic dechlorination pathways were obtained from the anaerobic dehalogenation model (ADM). Minimum, median and maximum  $k_m$  values depending on dechlorination activity (DA18) of DEH10 microorganism are tested in the model, according to the results presented in Chapter 5 (Appendix F Table F.1). ADM uses laboratory microcosm PCB data for determination of biodegradation rate constants. Hence, the rate constants indicate potentially the optimum conditions for anaerobic dehalogenation. During calibration, 10% of  $k_m$  values was also tested, considering less than optimum conditions (limited concentration of electron acceptors, unsuitable redox conditions, low concentration of contaminants or dehalogenators, reduced bioavailability, etc.) can prevail in the environment. DA18 dechlorination pathways involve removal of doubly flanked chlorines (Cl) in *meta* and *para* positions, *para* flanked Cl in *meta* position. Six pathways and congeners involved in pathways were presented in Section 3.4.2. Biodegradation affects only the congeners (33, 49, 66, 99, 101, 138/163, 105/132/153, 146, 151) that take part in these pathways.

Results of all trials ( $R^2$  and RMSE values for individual congeners and  $\sum$ PCBs) conducted during calibration are presented in Appendix F Table F.2. Results were



compared with the “no dechlorination” case which is the case in LM2 model. Accordingly, values of relevant parameters are then adjusted. The  $R^2$  results of most of the congeners are improved when  $v_s=0.75$  m/d (reduced to 50%) (Table F.2). Other parameters did not indicate improvement in  $R^2$  except for  $k_m$ . When 10% of minimum  $k_m$  was tested, it is observed that RMSE values of 105/132/153, 138/163 and 146 decrease ( $R^2$  values remain the same) when compared to the case of  $v_s=0.75$ m/d. As a result, the model is calibrated by adjusting  $v_s$  to 0.75 m/d and using 10% of  $k_m$ . The calibration results of 27 congeners and  $\sum$ PCBs is shown in Figure 7.4. As can be seen from the figure, for a majority of the congeners, and total-PCBs, the model can follow the trend of congener concentration changes. The only case where FTHP model can not predict well is for congener no 99. The congener concentration shows a decreasing trend while the model predicts an increasing concentration with time. This is because congener 99 is accumulated congener and its amount increases due to the degradation of 105/132/153 and 138/163. The calibration result also indicated that most of higher chlorinated congeners such as 146, 195/208, 182/187 are not correlated satisfactorily (Table 7.2). Accordingly, output concentrations of congeners other than these listed ones are likely to be more reliable during the selection/evaluation of the future scenarios.

In the study by Zhang et al. (2008), fate and transport of PCBs in Lake Michigan is simulated with the LM2 model by using 54 PCB congeners in both water and sediment. Only the results for water simulation for 105/132/153, 138/16 and  $\sum$ PCBs are given in Zhang et. al (2008). Even though concentrations in water column are modeled in our study, the calibration results are compared. In our study,  $R^2$  values obtained for these congeners (0.81, 0.51 and 0.73, for 105/132/153, 138/16 and  $\sum$ PCBs, respectively) are comparable to the values (0.76, 0.58 and 0.73, for 105/132/153, 138/16 and  $\sum$ PCBs, respectively) from the study of Zhang et al. (2008).  $R^2$  values of other congeners for the LM2 model obtained by the same group are given in Rossmann (2006). Those are different from the values in Zhang et al. (2008) and are lower. The min, max and average  $R^2$  values of all congeners in LM2 model are 0.0004, 0.62 and 0.36,

respectively. While the same values for our study, as can be seen in Table 7.2, are more satisfactory when compared to those of Rossmann (2006).

After calibration, validation was conducted by using concentration in sediment and water column of north part of the selected region without changing other parameters used during calibration. The validation results of 27 congeners and  $\Sigma$ PCBs is shown in Figure 7.5.  $R^2$  and RMSE results for validation are given in Table 7.2. In overall, while min and max  $R^2$  values are improved according to the values in calibration, average  $R^2$  value and RMSE value for individual congener such as 16, 26, 28/31, 118 and  $\Sigma$ PCBs are lower when compared to the those of calibration (Table 7.2). This outcome is expected, as during calibration, all model parameters are adjusted for the best fit possible to the data set. In this case, however, even though from the same region, a different PCB data set is used. One other reason for a relatively less satisfactory fit in validation is the nature of the data set. As can be seen from Figure 7.5, three data points out of the five used for validation are sampled very close in time, that is validation data was sampled at 0, 75, 77, 79 and 408 days. This uneven distribution of samples over time is expected to have an impact on the prediction success. Especially when anaerobic dechlorination is concerned, time is required for major congener changes to be observed in sediments. Overall, model validation is deemed successful.

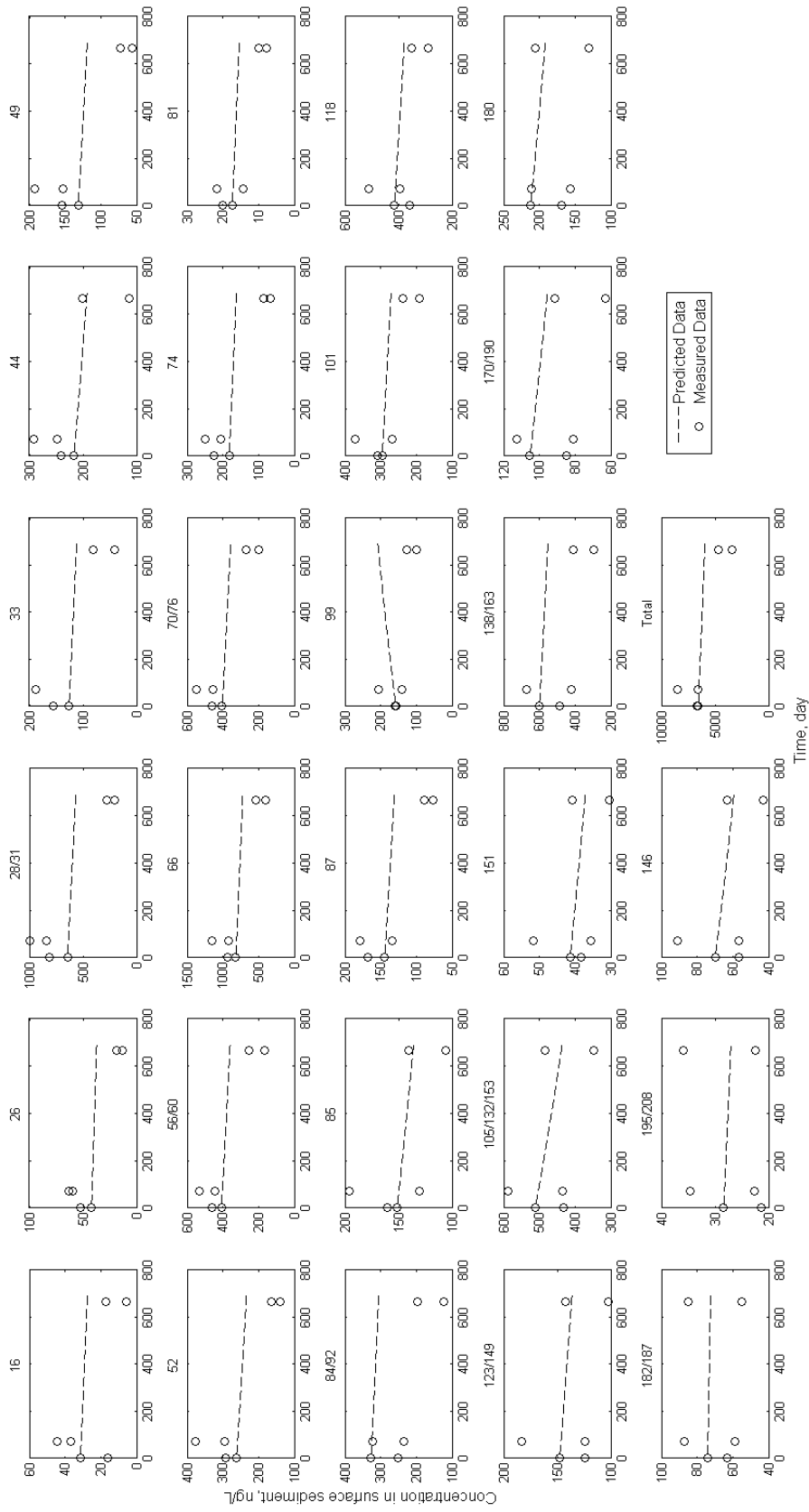


Figure 7.4 FTHP model calibration plots (time vs. sediment PCB concentration)

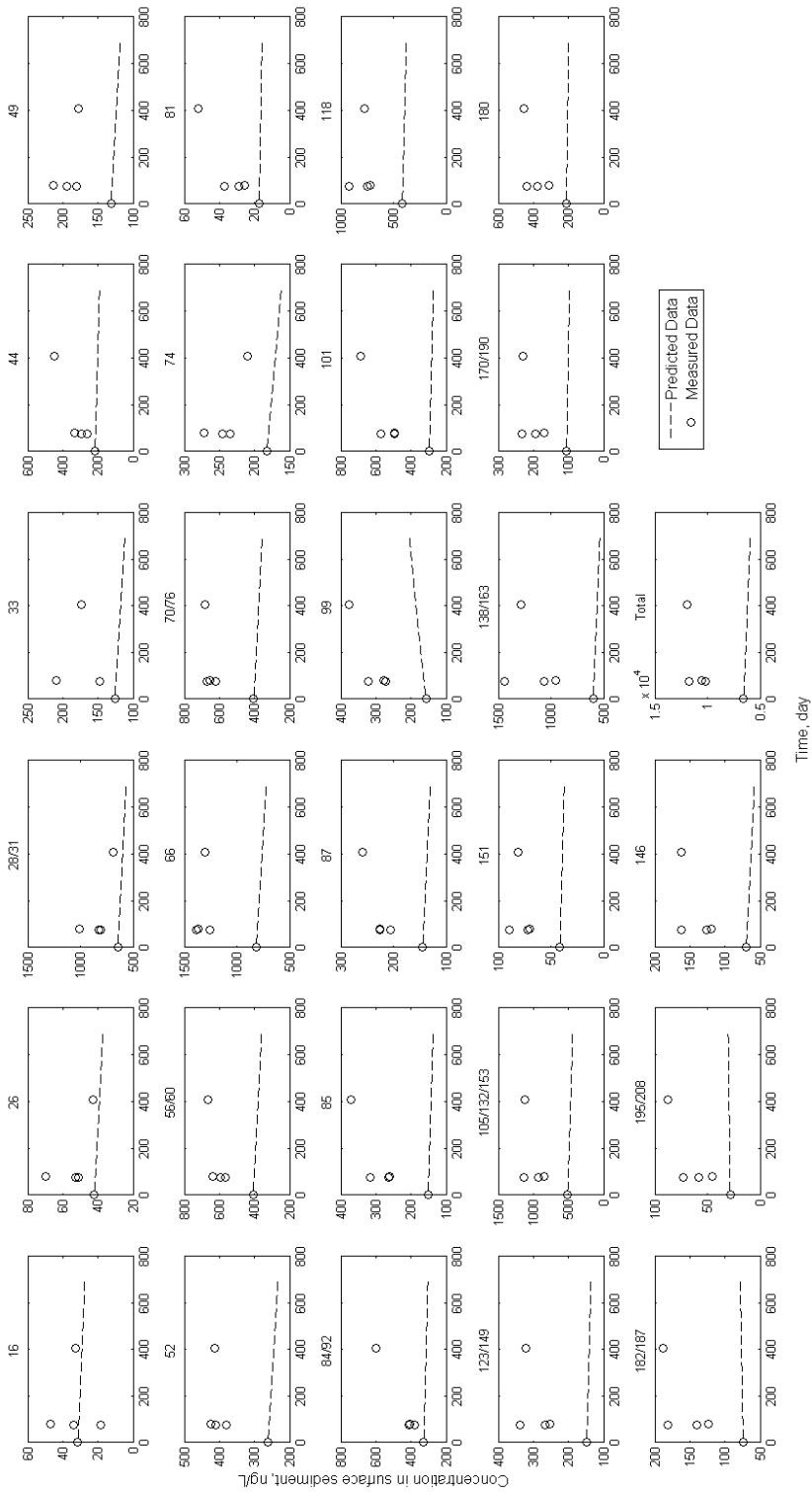


Figure 7.5 PCB concentration in Lake Michigan surface sediment from PCB validation of the FTHP model

Table 7.2 Results of the goodness of fit parameters for calibration and validation

Congener IUPAC No	Calibration				Validation			
	cos $\theta$	r	R <sup>2</sup>	RMSE	cos $\theta$	r	R <sup>2</sup>	RMSE
16	0.90	0.67	0.45	13.28	0.96	-0.02	0.001	9.28
26	0.93	0.90	0.81	17.38	0.98	0.29	0.08	14.41
28/31	0.93	0.90	0.81	264.43	0.99	0.26	0.07	206.44
33	0.94	0.86	0.73	50.14	0.98	-0.34	0.12	47.9
44	0.98	0.75	0.57	48.87	0.96	-0.94	0.89	129.88
49	0.95	0.89	0.79	42.96	0.99	-0.16	0.03	57.58
52	0.96	0.86	0.75	70.7	0.99	-0.48	0.23	136.83
56/60	0.96	0.92	0.84	108.87	0.98	-0.68	0.47	199.53
66	0.97	0.87	0.76	219.72	0.98	-0.39	0.16	478.02
70/76	0.97	0.89	0.8	102.02	0.98	-0.56	0.31	238.83
74	0.94	0.93	0.87	60.98	0.99	0.12	0.02	58.55
81	0.96	0.88	0.78	4.55	0.93	-0.92	0.84	19.25
84/92	0.97	0.83	0.68	99.41	0.97	-0.99	0.98	141.31
85	0.99	0.61	0.37	24.2	0.96	-0.80	0.65	145.35
87	0.97	0.91	0.84	33.45	0.98	-0.77	0.59	80.97
99	0.95	-0.73	0.53	58.01	0.98	0.80	0.64	131.43
101	0.98	0.79	0.62	49.83	0.97	-0.82	0.68	253.93
118	0.99	0.65	0.42	60.74	0.97	-0.36	0.13	349.45
123/149	0.99	0.40	0.16	24.52	0.97	-0.57	0.33	137.64
105/132/153	0.99	0.45	0.21	69.14	0.96	-0.62	0.38	472.5
151	0.99	0.42	0.18	5.92	0.97	-0.48	0.23	34.57
138/163	0.97	0.71	0.51	151.16	0.96	-0.52	0.27	565.42
170/190	0.99	0.54	0.29	18.89	0.97	-0.63	0.40	95.38
180	0.99	0.30	0.09	37.87	0.97	-0.68	0.46	174.6
182/187	0.98	0.01	0.0002	12.74	0.96	0.70	0.48	78.23
195/208	0.98	-0.22	0.05	6.06	0.95	0.81	0.66	36.02
146	0.98	0.46	0.21	13.58	0.96	-0.65	0.42	70.08
$\Sigma$ PCBs	0.97	0.86	0.73	1426.54	0.98	-0.62	0.38	4229.98
Min	0.90	-0.73	0.0002		0.93	-0.99	0.001	
Max	0.99	0.93	0.87		0.99	0.81	0.98	
Average	0.97	0.62	0.53		0.97	-0.36	0.39	
Std	0.02	0.39	0.28		0.01	0.52	0.27	

Sensitivity of 10 parameters is investigated during sensitivity analysis in order to understand which parameters affect output congener concentrations the most. 50% and 150% of values and/or minimum and maximum of ranges in calibration input were tested for 20 years, separately. The sensitivity analysis results are presented in Appendix F Figure F.1 through Figure F.10. The sensitivity analysis revealed that most of the congeners are sensitive to changes in seven parameters;  $C_w$ ,  $k_m$ ,  $K_{ow}$ , TSS,  $v_s$ ,  $f_{ocw}$  and  $D_m$ . The quality of these input parameters has a great impact on the model outcome. Therefore, low quality of these parameters (i.e. data required for measurements frequently) can create errors on output concentrations. The figures indicated that increase in  $C_w$ ,  $f_{ocw}$  and  $K_{ow}$ , and decrease in TSS,  $D_m$  and  $v_s$  cause decrease of output concentration of most of the congeners in sediment with time. Review of change of each parameter in mass balance equation indicated that while increases of  $C_w$ ,  $f_{ocw}$  and  $K_{ow}$  cause increase of the settling term, decreases of TSS and  $v_s$ , and  $D_m$  result in reduction of the resuspension and diffusion terms, respectively. Addition to these discussion, trend of 182/187 changes when its  $C_w$  increases as different from other congeners. This is because of accumulation of this congener due to settling is the dominant process. Similarly, when  $K_{ow}$  values increases, trend of 84/92, 87, 99, 101, 123/149, 151, 138/163, 182/187 and 195/208 changes due to same reason. On the other hand, the distribution for  $k_m$  is different for nine congeners which take part in anaerobic dechlorination pathways. While  $k_m$  values increase, concentrations of congeners 33, 49 and 99 initially increase, then decrease, while concentrations of congeners 66, 101, 105/132/153, 151, 138/163 and 146 shows a much sharper decreasing trend with time. The reason for this that congeners 33, 49 and 99 accumulate in the sediment since they are daughter congeners in DA18 and are produced. They are then affected by other F&T processes and start to slowly decrease. Other six congeners degrade since they are mother congeners except for congener 66. Then, their concentration in sediment decrease. The sensitivity analysis also indicated that settling, resuspension and anaerobic degradation are the processes that control PCBs in LM sediments. The settling and resuspension processes are found as main processes for Lake Michigan by Zhang et. al (2009).

As a result of sensitivity analysis, seven parameters which are the most sensitive ones are considered for uncertainty analysis in order to evaluate their change, distribution (Table 7.3) and potential effect on the model output (Appendix F Table F3). For uncertainty analysis, the model was run for 1000 times using Monte Carlo simulation. As can be seen from probability distribution of each congener (Figures F.11 and F.12), lognormal distribution is appropriate for output concentration of all congeners in surface sediment. For other parameters, on the other hand, Table 7.3 shows the distributions assumed. The congener concentration changes as a result of the uncertainty analysis can be seen in Figure F.13. The RSD of results range from 0 to 139.87 (Table 7.4). As was also indicated by the results of the sensitivity analysis, a number of congeners have greater uncertainty when compared to others. For example, congeners 99, 101, 123/149, 182/187 can be counted among these. Since these congeners have higher uncertainty, their output concentrations can be considered to have higher unreliability. When  $R^2$  values of these congeners in calibration are reviewed, congeners 123/149 and 182/187 have a lower fit among other congeners during calibration ( $R^2$ : 0.16 and 0.0002, respectively). However, congeners 99 and 101 have a better fit ( $R^2 > 0.50$ ). In validation, although  $R^2$  values associated with these congeners increase, their  $r$  values indicate an inverse relationship ( $r$  values between -0.80 and 0.80). One of the parameters that has a great impact on output is  $\log K_{ow}$ , because this physicochemical parameter is used in the estimation of  $K_d$ , and fractions in water column and sediment which in turn affect F&T processes settling and diffusion. Hence it is an important source of uncertainty, while degradation rate constants have some impact on the relevant congeners and TSS also contributes to the uncertainty. Overall, uncertainty analysis allows for an evaluation of which congeners contribute most to the overall uncertainty and the parameters affecting their simulation. Also, confidence intervals could also be formed to represent uncertainty during final assessment of results, but it was out of scope of this study.

Table 7.3 Distribution of parameters assumed for uncertainty analysis

Parameters	Distribution	References
$v_s$	Uniform	Oram et al. (2008a)
TSS	Lognormal	From distribution of LM data
LogK <sub>ow</sub>	Lognormal	Oram et al. (2008a)
C <sub>w</sub>	Lognormal	From distribution of LM data
D <sub>m</sub>	Lognormal	Oram et al. (2008a)
f <sub>ocw</sub>	Uniform	Oram et al. (2008a)
k <sub>m</sub>	Lognormal	From distribution of LM data

Table 7.4 RSD of Future Prediction Calculated for 1000 times in Uncertainty Analysis

Congener IUPAC No	min	max	Congener IUPAC No	min	max
16	0	109.69	87	0	64.66
26	0	79.03	99	0	72.95
28	0	95.78	101	0	88.06
33	0	63.06	118	0	86.75
44	0	101.07	123	0	69.10
49	0	72.15	105	0	139.87
52	0	119.42	151	0	97.67
56	0	95.60	138	0	60.31
66	0	96.50	170	0	97.17
70	0	82.42	180	0	98.34
74	0	71.19	182	0	47.36
81	0	72.96	195	0	137.98
84	0	112.90	146	0	91.51
85	0	76.38			

As a result of testing the model, it is seen that the risk of obtaining unreliable output concentration can be due to low quality of the most sensitive seven input parameters (C<sub>w</sub>, k<sub>m</sub>, K<sub>ow</sub>, TSS, v<sub>s</sub>, f<sub>ocw</sub> and D<sub>m</sub>) or the congeners (16, 85, 118, 123/149, 105/132/153, 151, 170/190, 180, 182/187, 195/208 and 146) including low fit (R<sup>2</sup><0.50) during calibration. The reliable inputs of these parameters decrease the



uncertainty in the output and improve the fits in calibration and validation. Furthermore, another result is that the congeners (out of congeners 99, 101, 123/149, 182/187) including low uncertainty should be evaluated for future scenarios.

### **7.3.2 FTHP Model Future Prediction Results**

The calibrated model was used to predict future conditions for the next 20 years after 2016 under 8 alternative management scenarios. These are described in Table 7.5, while their input are given in Table F.2. Accordingly, calibration scenario is to see the effects of current modeling conditions without any change. Scenario of Dredging is to understand effects of removal of sediments on future sediment PCB concentration. Scenario of “No degradation” was prepared to show the effect and extent of biodegradation on modeling results. Other scenarios concern with bioaugmentation and biostimulation. The future concentrations for individual congeners and  $\Sigma$ PCBs are depicted in Figure 7.6. It is expected that concentration of  $\Sigma$ PCBs does not vary with time except for dredging. This is because anaerobic dechlorination can not result in a change in the total mass of PCBs in sediments, although major changes can occur in the congener patterns. On the other hand, dredging does not result in a noticeable change in the concentration of  $\Sigma$ PCBs in 20 years when compared to the calibrated model (Figure 7.6). However, it is seen that trend of increase is observed in some of congeners (84/92, 87, 123/149, 105/132/153, 138/163 and 146).

Table 7.5 Future scenarios

Scenario	Explanation
Calibration	Same input in calibration
Dredging	150% value of Cw and max of TSS
No Degradation	Same input in calibration except $k_m=0$ for all congeners
Biostimulation	Median $k_m$ of DA18 (Table F.1) Activity of Microorganism DEH10 (Doubly flanked chlorines in <i>meta</i> and <i>para</i> positions, <i>para</i> flanked chlorines in <i>meta</i> position)
Bioaugmentation with DA13	Addition of median $k_m$ of DA13 to median $k_m$ of DA18 (Table F.1) Possible removal for targeted positions (Doubly flanked <i>para</i> any or doubly flanked <i>meta</i> any)
Bioaugmentation with SF1 (DA18+DA19)	Addition of median $k_m$ of DA19 to median $k_m$ of DA18 (Table F.1) Activity of Microorganism SF1 (Doubly flanked chlorines in the <i>meta</i> position, <i>ortho</i> flanked chlorines in the <i>meta</i> position)
Bioaugmentation with CBDB1 (DA18+DA20)	Addition of median $k_m$ of DA20 to median $k_m$ of DA18 (Table F.1) Activity of Microorganism cdbb1 (Singly and doubly flanked chlorines in <i>para</i> position, doubly flanked chlorines in <i>meta</i> position)
Bioaugmentation with Deh10+SF1+o17+DF1 (DA18+DA25)	Addition of median $k_m$ of DA25 to median $k_m$ of DA18 (Table F.1) Activity of Deh10, SF1, o17 (17 (Flanked chlorines in <i>ortho</i> and <i>para</i> positions)) and DF1 (Doubly flanked chlorines in <i>meta</i> and <i>para</i> positions with some congener constraints)

As seen in Figure 7.6, when no change is conducted as in calibration condition, it was seen that concentration of all congeners and  $\sum$ PCBs decrease with time except congener 99 which decelerates with time. Major changes in individual congeners are observed depending on the dechlorination activities considered. When the effect of different bioaugmentation/biostimulation scenarios are evaluated, it is seen that typically lower chlorinated congeners increase - sometimes ten fold (e.g.26, 52, 49, 81) whereas higher chlorinated congeners decrease in concentration – sometimes approaching zero (e.g. 101, 182/187, 170/190).

An evaluation of future prediction results can be made on the basis of PCB homologs. With forecasts of dredging and no degradation, hexa- and penta-homologs increase. The forecasts of Biostimulation, DA13, and DA25 increase tri, tetra- and penta-homologs. However, tetra homologs increase with DA19 and tri and tetra homologs

increase with DA20. In other words, DA19 and DA20 decrease concentration of higher homologs and increase lower homologs which are less bioaccumulative on humans and aquatic biota. Furthermore, these congeners are more soluble than higher chlorinated congeners and are susceptible to complete aerobic degradation (Sowers & May, 2013).

Change of PCB toxicity in LM sediments was evaluated considering 8 scenarios in concentration of toxic dioxin-like coplanar congeners through the next 20 years. The toxic dioxin-like congeners analyzed are 81, 118, 123/149 and 105/132/153. It is seen that congeners 81 and 105/132/153 have lower uncertainty than congeners 118 and 123/149. However, their  $R^2$  values in validation and calibration change between 0.13 and 0.82. Therefore, congeners 81 and 105/132/153 are considered to find the best scenarios for toxicity reduction. TEQ change with respect to these congeners for the 8 scenarios are plotted in Figure 7.7. From the toxicity perspective, DA25 is the one affecting the congeners the most, by causing significant increase in TEQ of  $\sum$ PCBs due to a major increase in congener 81, even though TEQ of 118, 123/149 and 105/132/153 are decreased. Overall, final total toxicity is reduced by bioaugmentation with CBDB1 (DA18+DA20) and DA 18+ DA13. This result demonstrated that bioremediation strategies of DA20 and DA13 are effective to potentially reduce PCB-related toxicity of sediments. As a result, considering the change of concentration and toxicity, bioaugmentation with CBDB1 would be a more advantageous bioremediation strategy for reduction in concentration of all congeners and  $\sum$ PCBs.

Sowers and May (2013) state the importance of coupling anaerobic PCB dechlorination with aerobic degradation if *in situ* treatment is to be a viable option for PCB contaminated sediments. They emphasize the importance of dechlorination from the *ortho* position as tri-*ortho* and tetra-*ortho* chlorobiphenyls are recalcitrant to aerobic degradation. In this case, DA25 would be a more advantageous activity for bioaugmentation because it includes o-17, an *ortho*-Cl dechlorinator in the consortia of microorganisms. Predicting the course of such a scenario with the FTHP model, which provides predictions on a congener specific level, enables the user to see that

there is a potential for an increase in toxicity – either the final toxicity of the sediment or an increase somewhere in time during bioremediation, before aerobic degradation starts. This shows the usefulness and power of the FTHP model. Sowers and May (2013) argue that “many of the critical components are in place” for optimizing and testing this technology in field. Incorporation of aerobic degradation was beyond the scope of this modeling study. However, if required data could be measured in sediments (esp. concentration of potential products of aerobic PCB degradation) during such field trials, then incorporation of aerobic degradation into FTHP, coupled with anaerobic dechlorination, would provide a promising tool for monitoring and optimizing this challenging *in situ* treatment technology for PCB contaminated sediments.

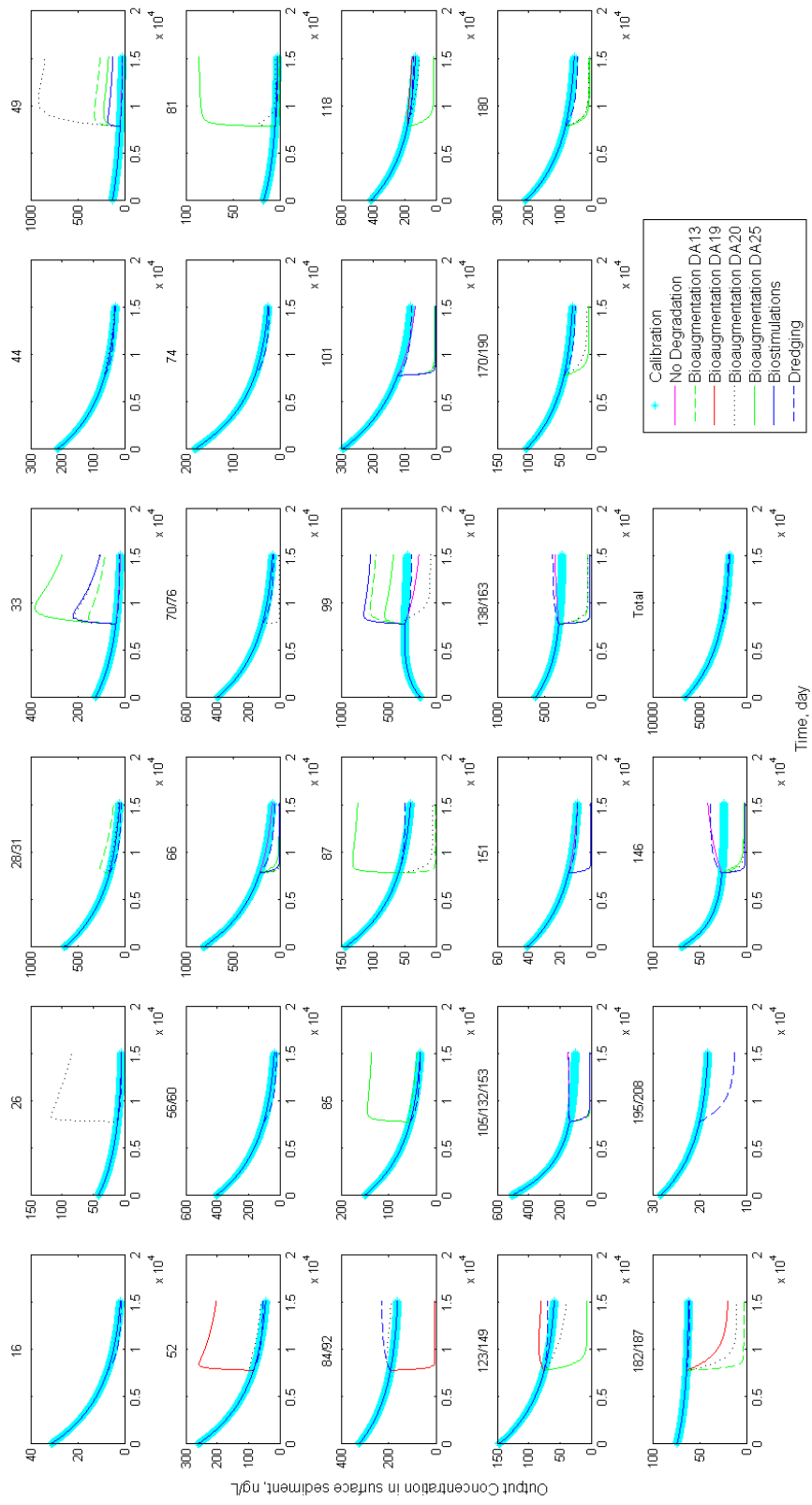


Figure 7.6 Future prediction concentrations in surface sediment

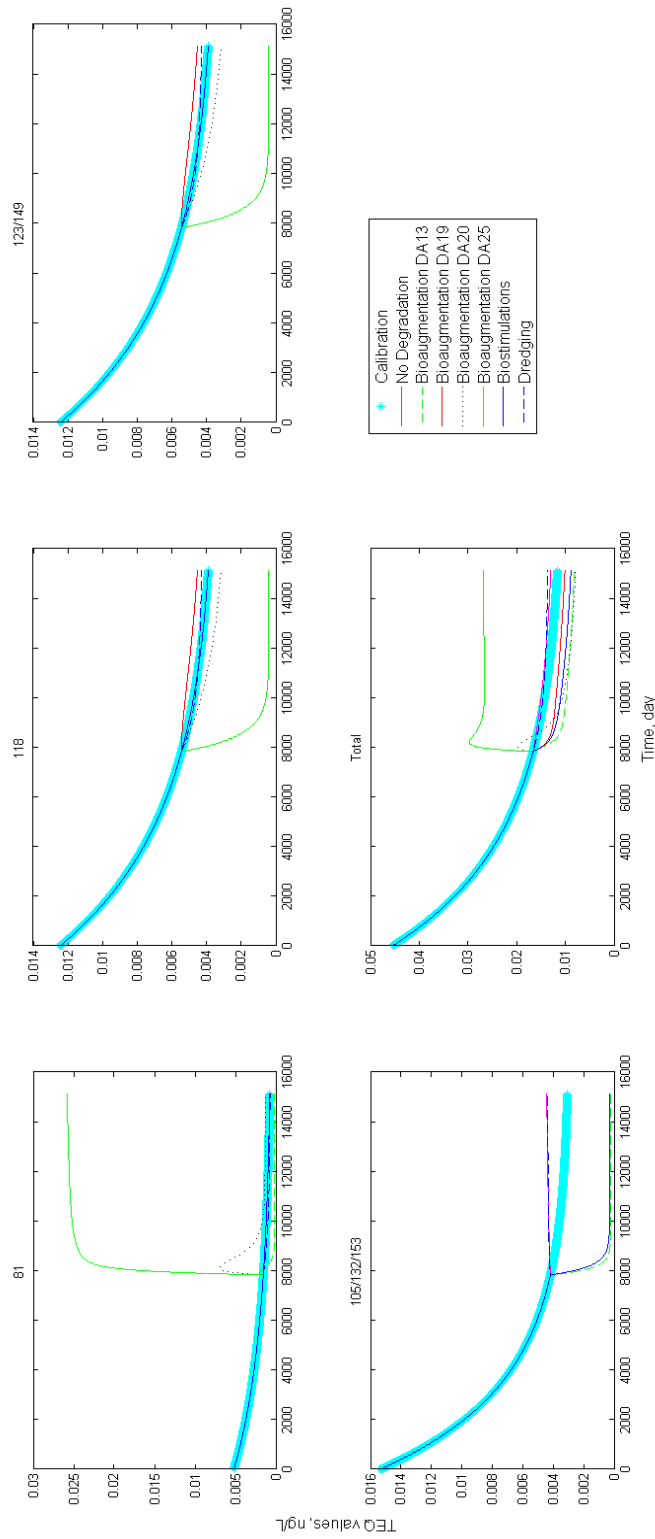


Figure 7.7 TEQ temporal changes in surface sediment

## 7.4 Conclusions

In this study, FTHP model was applied to Lake Michigan sediment data to investigate anaerobic dechlorination of PCBs in sediments by considering fate and transport processes. The calibration of the newly developed model yield satisfactory results, which were comparable or better than the water column calibration results of LM2 model for developed as part of the LMMBP. FTHP model results indicated that reliable inputs of the most sensitive parameters can decrease the uncertainty in the output and improve the goodness of fit in calibration and validation. By this way, the risk of obtaining unreliable output concentration can be decreased. FTHP model results also demonstrated that settling, resuspension, and biodegradation are important processes controlling PCB fate and transport in Lake Michigan sediments. Comparative evaluation of model forecasts indicated that toxicity reduction and decrease of amount of higher homolog groups can be realized by the scenario of DA20+DA18 – bioaugmentation of LM sediments with *dehalococcoides sp.* CBDB1 and phylotype DEH10. This study also emphasizes the importance of congener specific modeling of PCBs as well as incorporation of anaerobic dechlorination into modeling contaminated sediments.





## CHAPTER 8

### MODELING BIODEGRADATION OF PBDES IN SEDIMENTS USING A FATE AND TRANSPORT MODEL

#### 8.1 Introduction

Polybrominated diphenyl ethers (PBDEs) are a group of flame retardants. These chemicals have been widely used in building materials, electronics, furnishings, motor vehicles, airplanes, plastics, polyurethane foams and textiles (ATSDR, 2004). Their first commercial production began in the 1970s in Germany (ATSDR, 2004). The production of tetra-, penta-, hexa- and hepta- PBDE congeners are banned by the Stockholm Convention due to their bioaccumulative and persistent nature (POPs, 2008). PBDEs are released into the environment during their manufacture, incineration of municipal waste, deposition to landfills, discharge to municipal sewage-treatment plants, or emission directly to the atmosphere as particulate matter (ATSDR, 2004).

San Francisco Bay is known to be contaminated by PBDEs (Oram et al., 2008b). According to USEPA's Toxic Release Inventory, two facilities which manufacture PBDE containing product in the Peninsula region were sources of PBDE contamination (Sutton et al., 2014). Volatilization from these manufactured products are also sources. Another, though less probable source of PBDE entering the bay is predicted to be from e-waste recycling facilities, autos shredders, carpet and foam recycling facilities, sewage sludge application to rural lands, and sewage sludge incinerators. According to a study of the California EPA, the PBDE contamination in biota measured in 2002 was found to be the highest in USA, so the region is called as a hot spot region. At the federal level, penta- and octa- BDE mixtures were prohibited in 2006 in the USA. Deca-PBDE for which the phased-out started in 2013, is still produced and available in the region (Sutton et al., 2014).

Fate and transport (F&T) models are valuable in predicting the outcome of remediation and typically used for better management of sites contaminated with these chemicals. In the literature, there are much less number of studies about modeling the fate and transport of PBDEs (Oram et al., 2008b; Rowe, 2009) when compared to other hydrophobic organics such as PCBs. Numerous studies exist in the literature that aims to model PCBs as total-PCBs, homologs or individual congeners (Connolly et al., 2000; Davis, 2004; Farley et al., 1999; Shen et al., 2012; Zhang et al., 2008, 2009) and total maximum daily load (TMDL) of PCBs (LimnoTech, 2007; Shen, 2011; Shen et al., 2012). There are F&T models working on individual PCB and PBDE congeners (Davis, 2004; Oram et al., 2008b; Rowe, 2009; Shen, 2011; Shen et al., 2012; Zhang et al., 2008). However, after simulation, the output of the model is evaluated for total PCBs or PBDEs. There is one study in the literature, by Davis (2004) which models the general degradation term of each individual PCB congener, however, considering all possible degradation pathways (i.e., photolytic, biological, and chemical) but not taking into account any products. Consideration of the products in biodegradation is important to evaluate the change in toxicity as well as persistence and total concentration of PCBs.

According to our literature review, there is no model considering both biodegradation of these compounds with their products and F&T processes together. It is seen that not all congeners in a PBDE are bioaccumulative to human health and aquatic organisms. Therefore, investigation of bioaccumulative congeners are important to reduce adverse effects of them to human health and aquatic organisms. Accordingly, this study aims to develop a model that evaluates biodegradation pathways of individual congeners considering F&T processes in the sediment. Biodegradation rate constants for congener specific degradation pathways are estimated by a separate model and fed as input to the F&T model. Overall, this study investigates the biodegradation of PBDEs in sediment comprehensively and evaluates a number of remedial strategies for better

management of the contaminated site such as natural attenuation, bioaugmentation and/or biostimulation.

## **8.2 Methodology**

In this study, development and application of fate and transport for hydrophobic pollutant (FTHP) model to San Francisco Bay sediments for PBDEs are explained. A flowchart of the full process of model development and application is presented in Figure 8.1. The main stages of model development are shown in shaded boxes as code verification, calibration, validation, sensitivity and uncertainty analyses. Accordingly, the code of the model is verified firstly. Then, the code of Runge Kutta 4<sup>th</sup> order (RK4) solution of FTHP model applied to Equation 8.1 is called to test the model (Figure 8.1). The model code and flowchart of RK4 solution are explained in Section 3.3.

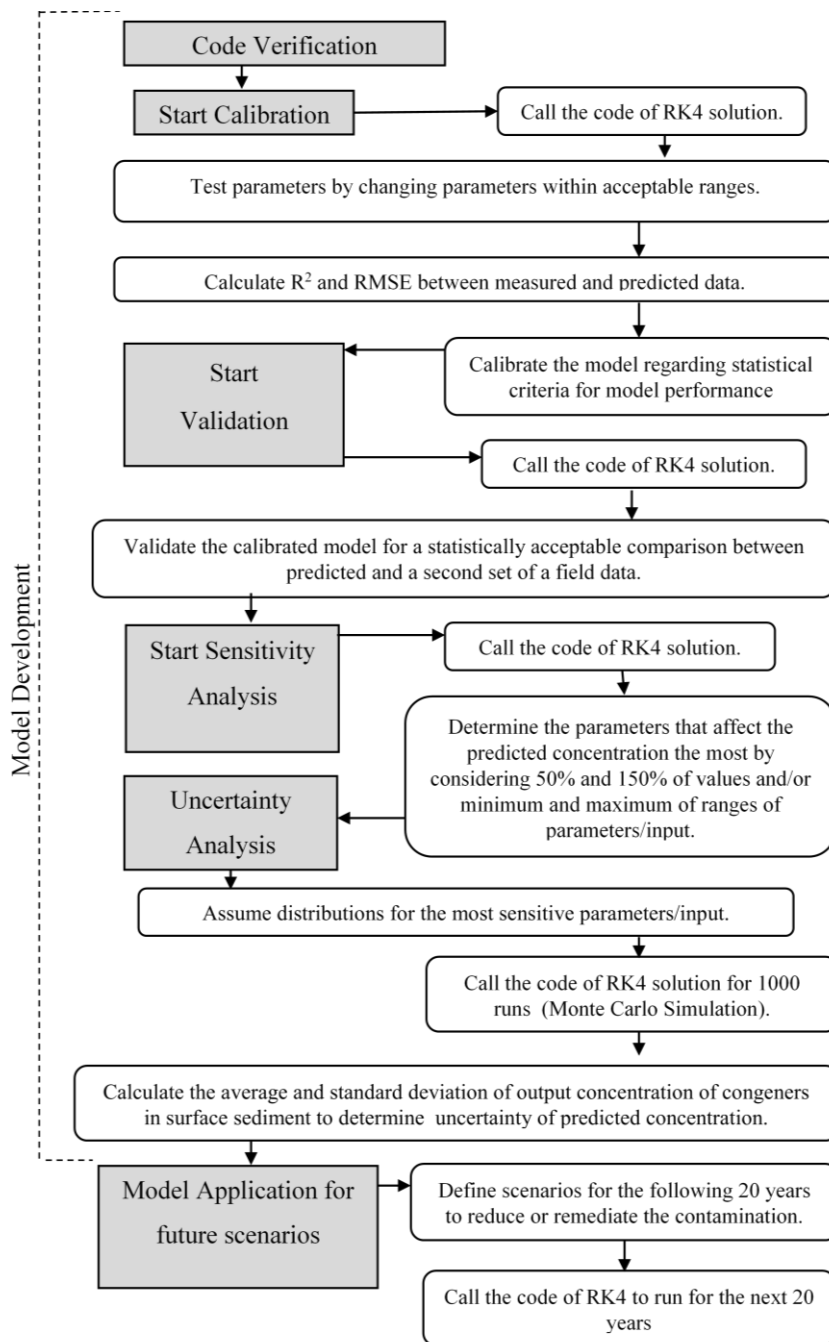


Figure 8.1 FTHP model development for and application to Lake Michigan Sediments

### 8.2.1 Fate and Transport of Hydrophobic Pollutant (FTHP) model

The contaminant mass balance equation used in the FTHP model is given in Equation 8.1. The mass balance equation and numerical approach of Recovery model (Boyer et al. 1994; Chapra and Reckhow, 1983) is adopted in this study. The model was written in MatLAB and individual PCB congeners were run as state variables.

$$\text{Accumulation} = -\text{Decay} + \text{Settling} - \text{Resuspension} - \text{Burial} - \frac{\text{Diffusion between the surface layer and the water column}}{V_m} + \frac{\text{Diffusion between the surface layer and the deep sediment}}{V_m}$$

$$\frac{dc_m^i}{dt} = -k_m c_m^i + \frac{v_s A_w F_{pw} c_w^i(0)}{V_m} - \frac{v_r A_m c_m^i}{V_m} - \frac{v_b A_m c_m^i}{V_m} - \frac{v_d A_m (F_{dw} c_w^i(0) - F_{dp} c_m^i)}{V_m} + \frac{v_d A_m (F_{dp} c_s^i(0) - F_{dp} c_m^i)}{V_m} \quad 8.1$$

$V_m$	volume of sediment, $m^3$
$A_w$ and $A_m$	surface areas of water and surface sediment, respectively, $m^2$
$k_m$	decay rate constant of the contaminant in the surface layer, $day^{-1}$
$v_b$	burial velocity, m/day
$v_s$	settling velocity of particulate matter, m/day
$v_r$	resuspension velocity of sediments, m/day
$v_d$	diffusion mass-transfer coefficient at the sediment, water and deep sediment interface, m/day
$c_s^i(0)$	$i^{th}$ contaminant concentration at the top of the deep contaminated layer, ng/L
$c_w^i$ and $c_m^i$	concentrations of contaminant $i$ in water and surface sediment, respectively, ng/L
$t$	time, day
$F_{pw}, F_{dw}$	fraction of contaminant in particulate and dissolved forms in the water, respectively
$F_{dp}$	ratio of contaminant concentration in the sediment pore water to contaminant concentration in total sediment

Upper and lower boundaries of the model are set as the water-sediment interface and deeper sediment, respectively (Figure 7.2). As the major transport processes, settling,

resuspension, burial and diffusion are considered in simulating the temporal change in the concentration of an individual congener. For transformation mechanisms, anaerobic dehalogenation (biodegradation) is considered as the only dominant process in sediment. PBDEs are assumed to partition into particulate and dissolved phases in the system. In the mechanisms of burial, resuspension and biodegradation, the contaminant is considered in both dissolved and particulate phases while the mechanisms of settling and diffusion are carried out in particulate and dissolved phases, respectively. Biodegradation rate constants change from one congener to the other as individual debromination pathways between congeners are taken into account. Solubility limit of congeners are also considered during incorporation of biodegradation into the model. The assumptions conducted in this study as in Boyer et al. (1994) are well-mixed water and sediment layer, variability in  $C_m$  in depth direction, linear equilibrium sorption mechanisms, first order kinetic, no compaction in sediment. As different from Recovery model, in this model it is assumed that contaminant concentration in water column is accepted as constant.

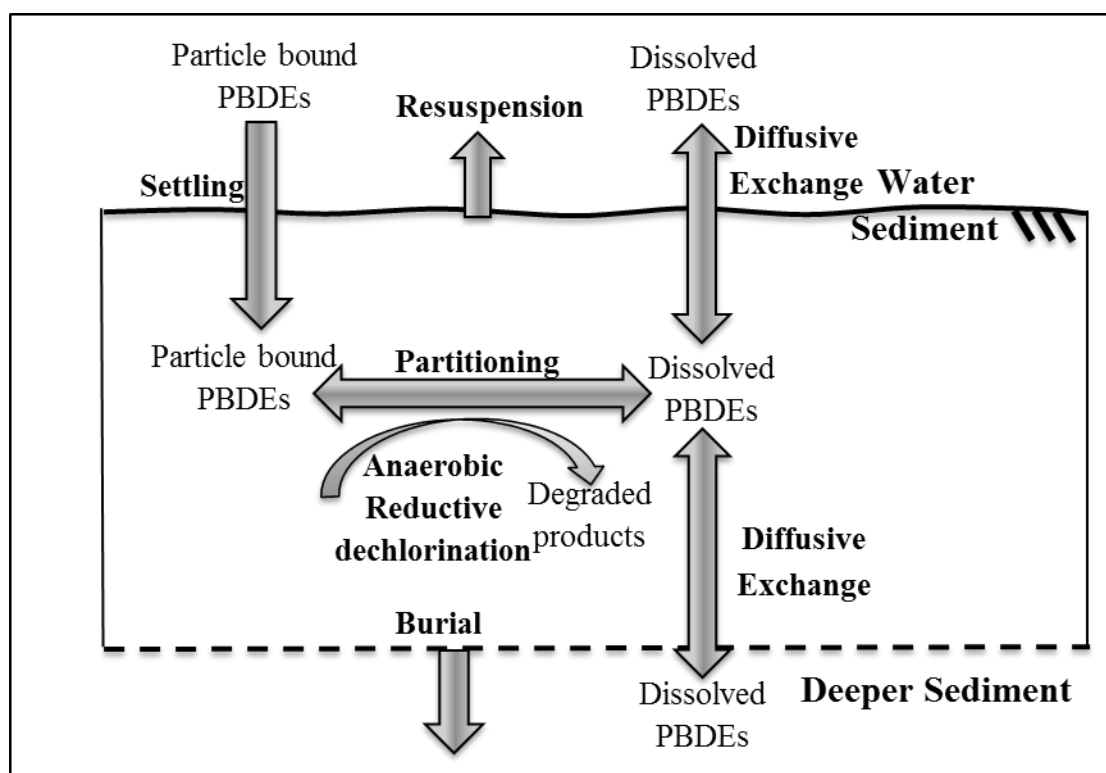


Figure 8.2 PBDE Conceptual Model

### **8.2.2 Environmental PBDE Data: San Francisco Bay, USA**

For the application of the FTHP model, SF Bay data set consisting of 21 groups of congeners (7, 8, 15, 17/25, 28/33, 32, 35, 47, 49, 66, 85, 99, 100, 153, 154, 183, 197, 206, 207, 208 and 209) provided by the San Francisco Estuary Institute (SFEI) (SFEI, 2015) was used after eliminating non-detected congeners. The data set for a limited region in the Lower South Bay was selected because sediments in that region contain the highest concentration of BDE 47 and 209 (Figure 8.3). 9 samples from the same location (station BA10) were collected between 2002-2014 approximately each year, from a depth of 5 cm at latitude 37.469 and longitude -122.063 (Table 8.1). The concentration values in sediment layer range from 0 to 6858 ng/L. When water and sediment PBDE concentrations are compared, sediment concentrations are five to seven orders of magnitude higher. The parameters and inputs are tabulated in Section 3.5.2. Site-specific properties on San Francisco Bay was taken from SFEI (2015), Davis (2004), Caffrey (1995), Choe et al (2004) and Sutton et al. (2015). Physicochemical properties are obtained from Mackay (2006) and Blauenstein (2007) and EPI SUITE. FTHP model code verification (written in MatLAB version 7.10.0) was performed in MS Excel (version 2016). First four sediment data is used for calibration except for initial one, and the rest is used for model validation.

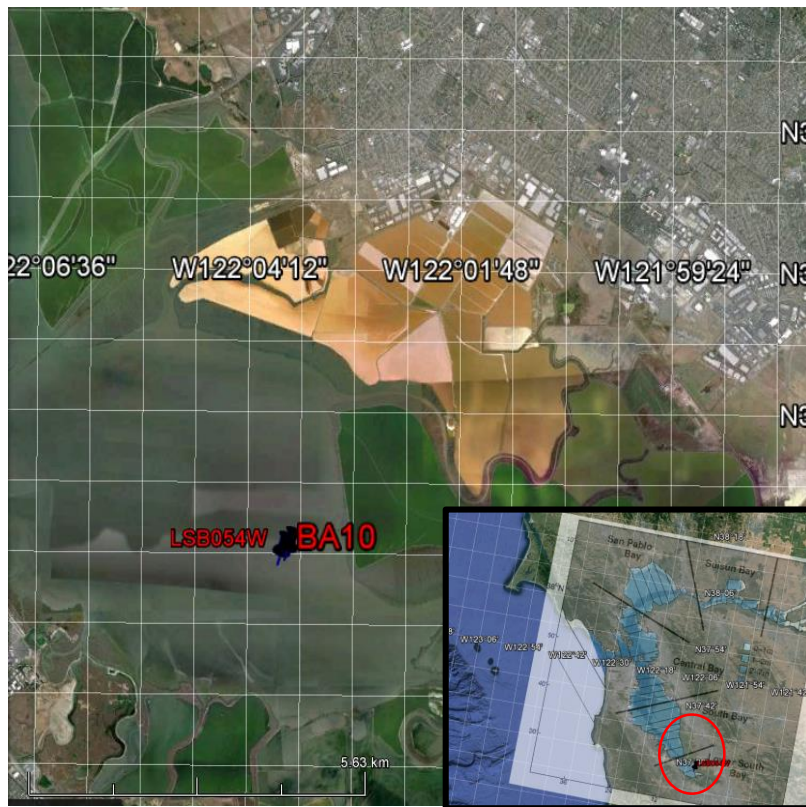


Figure 8.3 Surface sediment and water column sampling points for PBDE data used



Table 8.1 Concentration of individual PBDE congeners in 9 sediment samples (ng/L) (SFEI, 2015)

Sample no	Days	Date of Collection	Congener IUPAC No												
			7	8	15	17/25	28/33	32	35	47	49	66			
1	0	8/5/2002	39.74	30.56	30.62	189.54	68.04	5.67	7.40	685.80	228.42	39.31			
2	385	8/25/2003	17.87	11.77	9.13	67.50	29.70	3.42	3.35	167.94	64.26	8.80			
3	1842	8/21/2007	23.65	21.44	14.82	133.92	35.07	1.15	0.11	426.06	94.50	13.85			
4	2180	7/24/2008	16.42	12.74	10.15	56.16	15.39	1.30	2.19	131.76	51.35	6.75			
5	2598	9/15/2009	41.26	36.61	24.95	164.70	45.47	3.45	5.13	246.24	145.26	14.90			
6	2738	2/2/2010	6.64	4.87	3.97	16.52	4.98	1.83	0.95	41.63	14.69	2.19			
7	3304	8/22/2011	24.25	20.52	22.95	82.62	25.38	0.00	8.91	282.96	114.48	17.71			
8	3544	4/18/2012	6.05	0.00	0.00	21.71	0.00	0.00	0.00	60.48	20.95	2.85			
9	4383	8/5/2014	34.61	31.48	35.48	69.66	26.41	0.00	0.00	197.10	85.86	14.53			
		Min	6.05	0.00	0.00	16.52	0.00	0.00	0.00	41.63	14.69	2.19			
		Max	41.26	36.61	35.48	189.54	68.04	5.67	8.91	685.80	228.42	39.31			
		Median	23.65	20.52	14.82	69.66	26.41	1.30	2.19	197.10	85.86	13.85			
		Average	23.39	18.89	16.90	89.15	27.83	1.87	3.11	248.89	91.09	13.43			
		SD <sup>a</sup>	13.10	12.55	12.24	60.82	20.75	1.96	3.35	201.51	66.55	11.16			
		RSD <sup>b</sup>	56.03	66.44	72.41	68.22	74.55	104.78	107.70	80.97	73.07	83.07			

<sup>a</sup>Standard deviation, <sup>b</sup>Relative standard deviation

Table 8.1 Continued

Sample no	Days	Date of Collection	Congener IUPAC No												
			99	100	153	154	206	207	208	209	183	197	85		
1	0	8/5/2002	476.82	118.26	54.54	63.72	239.22	184.68	124.74	6858.00	22.41	35.15	25.06		
2	385	8/25/2003	93.42	24.14	21.82	11.88	41.74	37.48	39.15	993.60	7.18	30.67	12.91		
3	1842	8/21/2007	225.18	49.38	24.06	20.63	74.25	58.59	38.42	2940.30	0.00	0.00	0.00		
4	2180	7/24/2008	70.74	18.52	8.37	8.96	31.43	20.52	14.47	1015.20	4.57	4.28	5.40		
5	2598	9/15/2009	100.44	27.70	14.15	15.93	81.54	53.95	31.21	2305.80	0.00	0.00	4.77		
6	2738	2/2/2010	31.10	6.26	2.82	3.07	17.98	21.87	12.91	702.00	4.27	2.61	1.38		
7	3304	8/22/2011	194.94	57.24	47.63	30.94	95.04	88.56	48.38	3153.60	107.46	44.82	0.00		
8	3544	4/18/2012	34.40	10.37	0.00	4.47	20.63	0.00	0.00	556.20	0.00	0.00	0.00		
9	4383	8/5/2014	86.94	22.46	13.99	11.29	165.24	165.24	112.86	4914.00	8.10	43.25	0.00		
		Min	31.10	0.00	6.26	0.00	3.07	0.00	0.00	17.98	0.00	0.00	556.20		
		Max	476.82	25.06	118.26	54.54	63.72	107.46	44.82	239.22	184.68	124.74	6858.00		
		Median	93.42	1.38	24.14	14.15	11.88	4.57	4.28	74.25	53.95	38.42	2305.80		
		Average	146.00	5.50	37.15	20.82	18.99	17.11	17.87	85.23	70.10	46.91	2604.30		
		SD <sup>a</sup>	140.43	8.48	34.69	18.94	18.81	34.59	20.03	74.02	64.88	43.58	2146.67		
		RSD <sup>b</sup>	96.18	154.21	93.37	90.99	99.07	202.16	112.10	86.84	92.56	92.92	82.43		

<sup>a</sup>Standard deviation, <sup>b</sup>Relative standard deviation

## 8.3 Results and Discussions

### 8.3.1 Testing of the FTHP Model

The parameters and their input values were given in section 3.5.2. Excluding the initial day, samples no 2, 3, 4 and 5 are used for calibration, while the following four samples (no 6, 7, 8 and 9) were used for model validation (Table 8.1). FTHP model code verification (written in MatLAB version 7.10.0) was performed in MS Excel (version 2006).

During model calibration,  $v_s$ ,  $v_b$ ,  $K_d$  for both water and sediment are tested by varying their values from 50% to 150% of their values, and/or according to ranges given in the literature/data set. Biodegradation rate constants ( $k_m$ ) for congener specific anaerobic debromination pathways were obtained from the anaerobic dehalogenation model (ADM). These  $k_m$  values are used in the FTHP model during calibration. Median and maximum  $k_m$  values (min values are 0) of 8 pathways generated for all dehalogenation activities (DAs) are tested (Table 8.2). Each DA includes pathways based on microbial activity in laboratory microcosms and theoretically possible removal of targeted positions and debromination products. The details are given in Tables D.3 and D.4. Biodegradation affects only 7 BDE congeners (28/33, 47, 99, 100, 153, 154 and 183) that take part in debromination pathways. When  $k_m$  is changed during calibration, only the concentrations of these 7 BDE congeners are affected. Preference over selection of one particular debromination activity could not be done for the case of PBDEs. The main reason is the limited number of pathways available in each DA and the limited number of PBDEs in the measured data set. Therefore, each pathway is considered regardless of the DA, by taking into account numeric value of their degradation rate constants. Table 8.2 lists the median and maximum  $k_m$  values for all pathways in each DA. These  $k_m$  values are sorted for each pathway and collected in an ascending order to yield five cases with increasing debromination rate (Table 8.3). Here, five cases are generated; three median and two max  $k_m$  pathway cases.

Various cases are tested out by adjusting three parameters ( $v_s$ ,  $v_b$ ,  $K_d$ ) and  $k_m$  (Table 8.3) while monitoring for any improvement in  $R^2$  and RMSE values for both individual congeners and  $\Sigma$ PBDEs.  $R^2$  and RMSE results of all calibration trials are given in Appendix G Table G.1. All cases were compared with no debromination case to see the effect of anaerobic debromination on the model fit. Accordingly, values of relevant parameters are then adjusted. The model  $R^2$  results of most of the congeners are improved when  $v_s$  is increased to 150% (Table G.1). Other parameters did not yield any improvement in  $R^2$  except for  $k_m$ . When the case of  $k_{max\_II}$  is applied,  $R^2$  of 7 congeners is improved especially BDE 47 and 99 ( $R^2$  change from 0.38 to 0.70 and 0.52 to 0.81, for 47 and 99, respectively). Therefore, the case of combination of 150% of  $v_s$  and  $k_{max\_II}$  is examined. When this case is compared with “No degradation” case, it is seen that correlation of all congeners are improved ( $R^2$  between 0.43 and 0.96). For di and tri homologs, even though there is improvement in the fit, their correlation is still not satisfactory (where the  $R^2$  change from a range of 0.00 – 0.68 to 0.02 – 0.73). The goodness of fit results of model calibration of 21 congeners and  $\Sigma$ PBDEs is shown in Figure 8.4. As can be seen from the figure and tabulated values in Table 8.4, BDE 28/33 and 207 are overestimated and BDE 7 and BDE 8 are consumed after about 1500 days. However, degradation of higher brominated congeners can result in accumulation of these di homolog groups through time. The model could not account for the accumulation of congeners 7, 8 and decrease of congeners such as 206 and 207. This is because the laboratory data set that could be found in the literature had a very limited data set of PBDE congeners and hence  $k_m$  values could only be calculated for the pathways including the measured congeners. If a larger laboratory debromination data set was available, then a much larger number of debromination pathways could have been used as input in the ADM, resulting the calculation of  $k_m$  values that would enable us to account for the changes in higher brominated and lower brominated congeners. The calibration result also indicated that five congeners (7, 8, 15, 17/25 and 49) have lower  $R^2$  than 0.50 (Table 8.4). Accordingly, output concentrations of other congeners are likely to be more reliable in the selection of the best future scenario.

Oram et al. (2008a) simulated a box model for the fate and transport of BDE 47 and 209 across the bay. They found that  $R^2$  of these two congeners vary between 0.6 and 1.0. As seen in Table 8.4, the  $R^2$  of BDE 47 is in this range (0.72) and that of BDE 209 is close to the range (0.52).

After calibration, validation was conducted using sediment PBDE concentrations from a different region of the bay, without changing any parameters or rate constants used during calibration. The validation of 21 congeners and  $\Sigma$ PBDEs is shown in Figure 8.5.  $R^2$  and RMSE results for validation are given in Table 8.4. In validation, it was observed that while correlation of mono, di, tri homolog groups is improved, correlation of higher homolog groups such as hexa, hepta and octa reduces.

Table 8.2 Maximum and median  $k_m$  values of 8 pathways in corresponding Das by ADM

DA no	Mother → daughter for 8 pathways							
	47 28	99 47	100 47	153 99	154 99	154 100	183 153	183 154
1		0.003/0.001		0.024/0		0.008/0.003	0.003/0	0.017/0.002
2								0.017/0.002
3		0.003/0.001		0.024/0		0.008/0.003		0.017/0.002
4							0.003/0	
6								0.017/0.002
7	0.007/0.002		0.001/0		0.018/0			
9								0.017/0.002
10								0.017/0.002
12								0.017/0.002
13								0.017/0.002
14		0.003/0.001		0.024/0		0.008/0.003		
15		0.003/0.001		0.024/0		0.008/0.003		0.017/0.002
16	0.007/0.002	0.003/0.002		0.024/0	0.018/0			
18	0.007/0.002		0.001/0		0.018/0	0.008/0		0.017/0.002
19	0.007/0.002	0.003/0.001		0.024/0			0.003/0	0.017/0.001
21							0.003/0	0.017/0.001

The number before slash is the maximum  $k_m$  value, The number after slash is the median  $k_m$  value.

Table 8.3 Cases for use of km values during calibration of FTHP model

congener IUPAC No		Max $k_m$		Median $k_m$		
mother	daughter	$k_{m\_I}$	$k_{m\_II}$	$k_{m\_I}$	$k_{m\_II}$	$k_{m\_III}$
47	28	0.007	0.007	0.002	0.002	0.002
99	47	0.004	0.004	0.001	0.002	0.002
100	47	0.001	0.001	0	0.001	0.001
153	99	0.024	0.024	0.000	0.000	0.000
154	99	0.018	0.018	0	0	0
154	100	0.008	0.008	0	0.003	0.003
183	153	0.003	0.003	0	0	0
183	154	0.017	0.017	0.001	0.002	0.002

Table 8.4 Results of the goodness of fit parameters for calibration and validation

Congener IUPAC No	Calibration				Validation			
	cos $\theta$	r	R <sup>2</sup>	RMSE	cos $\theta$	r	R <sup>2</sup>	RMSE
7	0.65	0.33	0.11	22.51	0.68	0.63	0.39	19.32
8	0.59	0.13	0.02	19.87	0.63	0.50	0.25	16.95
15	0.84	0.47	0.23	10.85	0.73	0.42	0.18	16.17
17/25	0.83	0.37	0.14	74.52	0.96	0.91	0.82	28.55
28/33	0.69	-0.83	0.69	639.21	0.41	-0.90	0.81	655.06
32	0.88	0.86	0.73	1.66	0.95	0.95	0.9	0.79
35	0.83	0.71	0.5	2.44	0.64	0.51	0.26	3.99
47	0.95	0.85	0.72	121.66	0.96	0.92	0.86	92.24
49	0.92	0.65	0.43	66.66	0.88	0.87	0.76	74.79
66	0.90	0.79	0.63	13.99	0.87	0.89	0.79	13.95
85	0.79	0.97	0.94	14.2	0.73	-0.39	0.15	83.84
99	0.96	0.91	0.83	74.13	0.83	1.00	1	141.09
100	0.78	-0.80	0.64	83.53	0.71	-0.90	0.81	90.6
153	0.97	0.90	0.8	7.51	0.85	0.67	0.45	17.34
154	0.93	0.83	0.68	12.55	0.95	0.90	0.81	10.28
183	0.61	-0.94	0.9	19.27	0.58	0.08	0.01	40.4
197	0.61	-0.95	0.9	32.3	0.77	-0.25	0.06	26.38
206	0.75	-0.79	0.63	192.97	0.76	-0.77	0.59	189.57
207	0.61	-0.83	0.68	321.17	0.66	-0.62	0.39	331.97
208	0.93	0.90	0.82	23.5	0.71	0.64	0.4	55.05
209	0.84	0.72	0.52	3492.68	0.84	0.74	0.55	3153.51
$\Sigma$ PBDEs	0.85	0.73	0.54	4783.76	0.84	0.78	0.61	4542.16
Min	0.59	-0.95	0.02		0.41	-0.90	0.01	
Max	0.97	0.97	0.94		0.96	1.00	1.00	
Average	0.81	0.27	0.59		0.77	0.34	0.54	
Std	0.13	0.74	0.26		0.14	0.66	0.30	

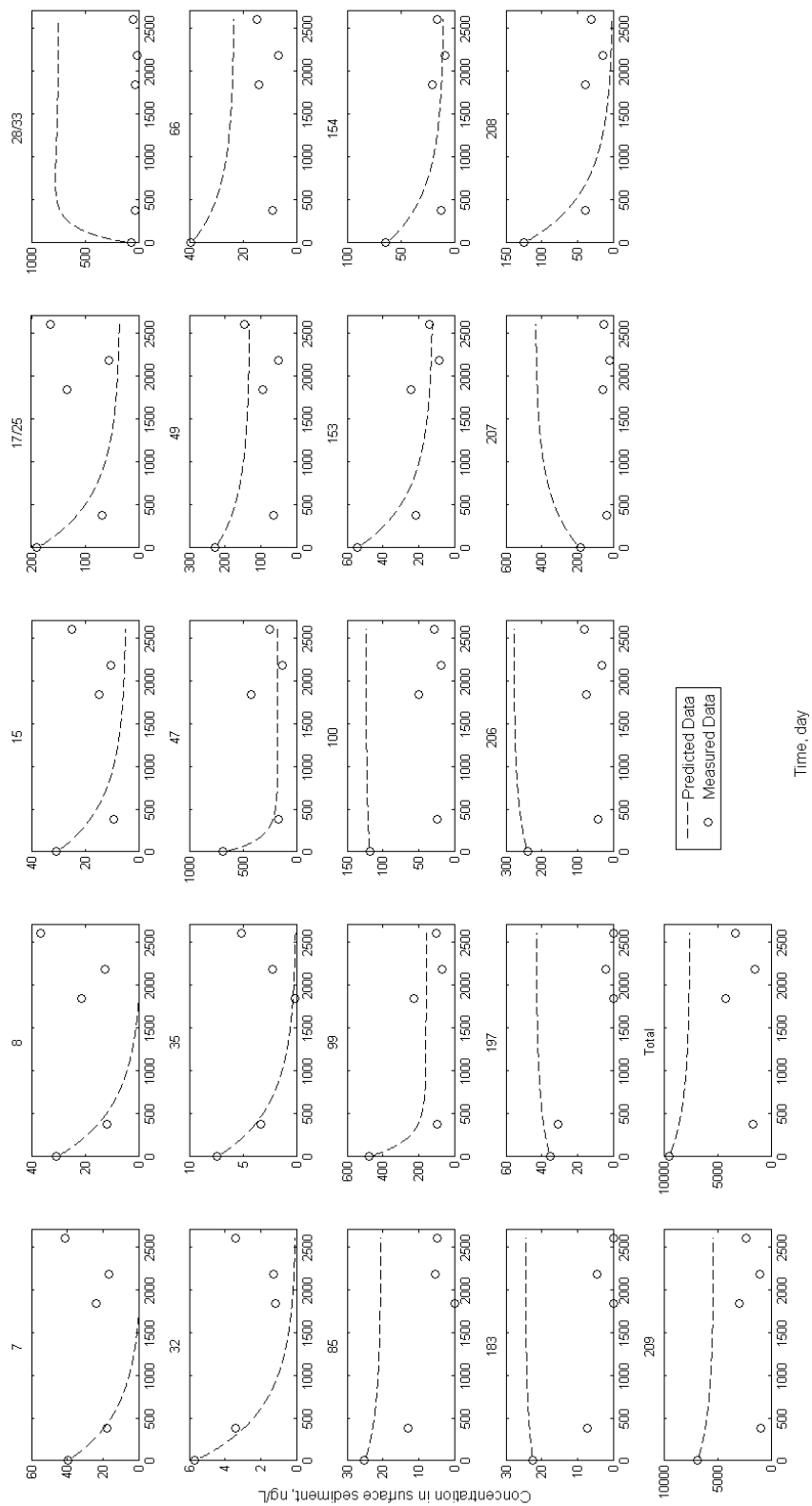


Figure 8.4 PBDE concentration in San Francisco sediment from PBDE calibration of the FTTHP model



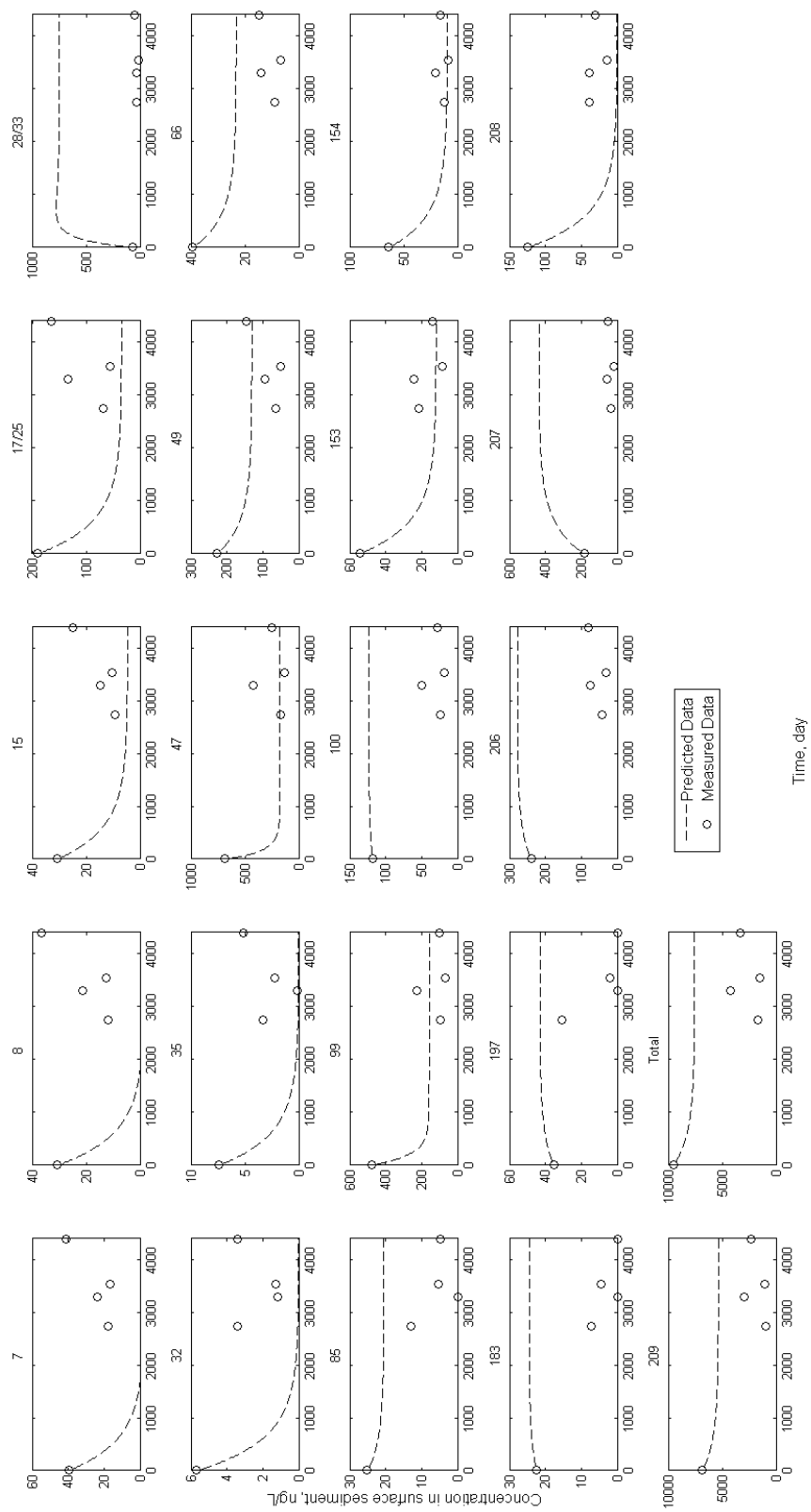


Figure 8.5 PBDE concentration in San Francisco sediment from PBDE validation of the FTHP model

Sensitivity of 10 parameters is investigated during sensitivity analysis in order to understand which parameters affect output congener concentrations the most. 50% and 150% of values and/or minimum and maximum of ranges in calibration input were tested for 20 years, separately. The sensitivity analysis results are presented in Appendix G Figure G.1 through Figure G.10. The sensitivity analysis revealed that most of the congeners are sensitive to changes in five parameters;  $C_w$ ,  $k_m$ ,  $K_{ow}$ , TSS and  $f_{ocw}$ . The quality of these input parameters has a great impact on the model outcome. Therefore, low quality of these parameters (i.e. data required for measurements frequently) can create errors on output concentrations. The figures indicated that increase in  $C_w$ ,  $f_{ocw}$  and  $K_{ow}$ , and decrease in TSS cause decrease of output concentration of most of the congeners in sediment with time. Review of change of each parameter in mass balance equation indicated that while increases of  $C_w$ ,  $f_{ocw}$  and  $K_{ow}$  cause rising of settling term, decrease of TSS results in reduction of resuspension. For  $k_m$ , decrease of  $k_m$  is investigated for 7 congeners. When it's equal to 0, output congeners concentrations of these decreases with time except for BDE 28/33 which is accumulated since it is taken into consideration only as daughter congener. Overall, the sensitivity analysis indicated that settling, resuspension and anaerobic degradation are the processes controlling PBDEs in San Francisco Bay.

As a result of sensitivity analysis, five parameters which are the most sensitive parameters ( $C_w$ , TSS,  $k_m$ ,  $K_{ow}$  and  $f_{ocw}$ ) are considered for uncertainty analysis to evaluate changes and distribution of these parameters on effect of output concentration (Appendix G Table G.3). For uncertainty analysis, the model was run for 1000 times using Monte Carlo Simulation. As can be seen from probability distribution of each congener (Figure G.11 and G.12), lognormal distribution is appropriate for output concentration of all congeners in surface sediment. The congener concentration changes as a result of the uncertainty analysis can be seen in Figure G.13. As seen from the figure, uncertainties of BDE 100, 153, 154, 183, 206 and 209 are the highest among the congeners. When  $R^2$  values of these congeners in calibration and validation are reviewed, congener 183 has the lowest fit among other congeners during validation ( $R^2 < 0.50$ ). However, its correlation is better for calibration ( $R^2 = 0.90$ ) with a  $r$  value of

-0.94. This inverse relationship in validation and or calibration is also available in congeners 100 and 206 which include higher uncertainty (r values between -0.77 and -0.90). Overall, uncertainty analysis allows for an evaluation of which congeners contribute most to the overall uncertainty and the parameters affecting their simulation. Also, confidence intervals could also be formed to represent uncertainty during final assessment of results, but it was out of scope of this study.

As a result of testing the model, it is seen that the risk of obtaining unreliable output concentration can be due to low quality of the most sensitive five input parameters ( $C_w$ ,  $k_m$ ,  $K_{ow}$ , TSS and  $f_{ocw}$ ) or the congeners (7, 8, 15, 17/25 and 49) including low fit ( $R^2 < 0.50$ ) during calibration. The reliable inputs of these parameters decrease the uncertainty in the output and improve the fits in calibration and validation. Furthermore, another result is that the congeners (out of congeners 100, 153, 154, 183, 206 and 209) including low uncertainty should be evaluated for future scenarios.

### **8.3.2 FTHP Model Future Prediction Results**

The calibrated model was used to predict future conditions for the next 20 years after 2016 under four scenarios as alternative management options for San Francisco Bay sediments. Scenarios are explained in Table 8.5. Accordingly, calibration is set as the “no change” scenario by which the rest of the alternatives are compared. It aims to show the effects of current conditions without any change of the current situation. Scenario of Dredging is added in order to understand effects of removal of sediments on total concentration because dredging is the typical remediation action for hot spot contaminated regions. The scenario of “No degradation” was prepared as an indicator for the effect of biodegradation on sediment concentrations. The last one includes bioaugmentation with possible extra debromination pathways that can take place in the environment. To develop last scenario, all relevant debromination pathways in the literature (regarding PBDE congeners measured in San Francisco Bay) are taken from the studies of Tokarz et al. (2008), Robrock et al. (2008), Ding et al. (2013) and Huang et al. (2014), and depicted in Figure 8.6. Congeners measured/modeled for San

Francisco Bay are only considered in these pathways. Since laboratory data (BDE congener concentrations at a number of time intervals) is not present, ADM can not be used to predict biodegradation rate constants as before. Therefore, here, estimation of rate constants are done based on previously estimated  $k_m$  values of pathways involving similar PBDE homologs (Table 8.6). As shown in Table 8.6, unknown  $k_m$  values in a homolog are specified according to three tiers: (i) same value in this homolog if no range is specified, (ii) average of the values if a range is specified, and (iii) same value in one higher homolog if no value is available for this homolog. The  $k_m$  values of all pathways (extra ones in addition to the already existing ones) used in the model for the last scenario are given in Appendix G Table G.2.

Table 8.5 Future scenarios

<b>Scenario</b>	<b>Explanation</b>
Calibration	Same input in calibration
Dredging	150% value of $C_w$ and max of TSS
No Degradation	Same input in calibration except $k_m$ 's (0 values for all $k_m$ 's)
Bioaugmentation with possible extra pathways	Addition of possible pathways defined in Tokarz et al. (2008), Robrock et al. (2008), Ding et al. (2013) and Huang et al. (2014) (Figure 8.6)

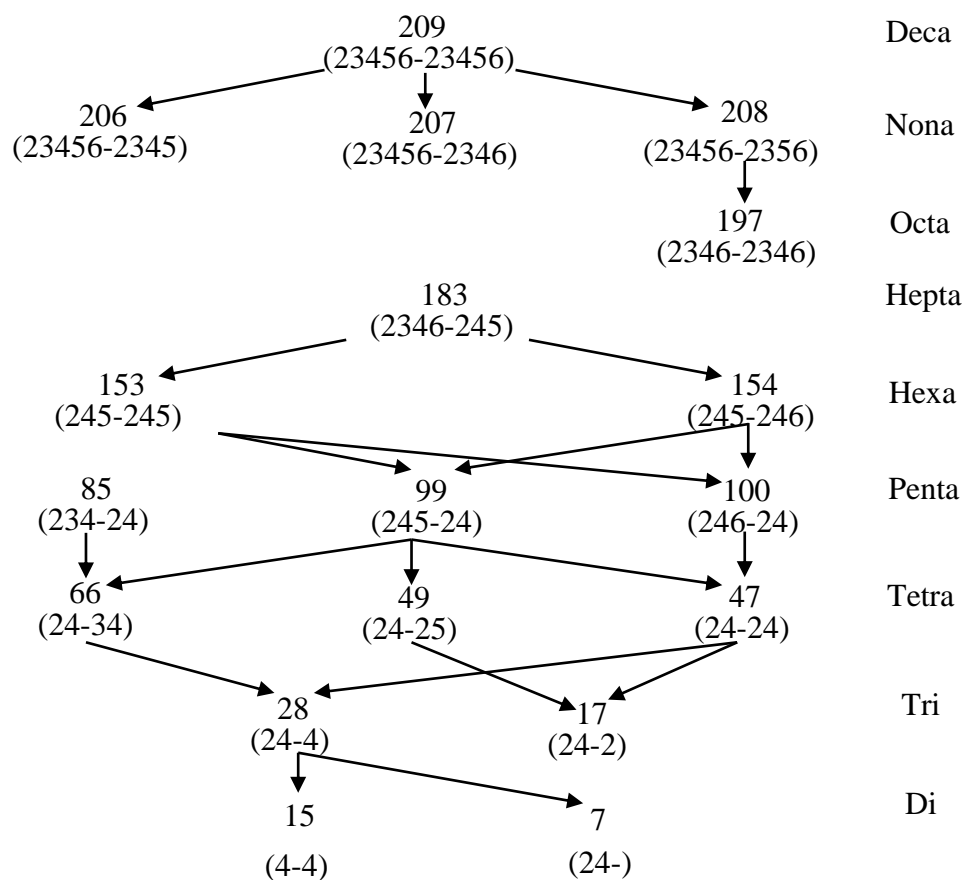


Figure 8.6 Possible pathways of debromination in the literature considering congeners measured in San Francisco Bay sediments

Table 8.6  $k_m$  values used for the other pathways which are not available ( $d^{-1}$ )

Pathways between homologs	Range ( $d^{-1}$ )	Reference	$k_m$ values used for the extra pathways ( $d^{-1}$ )	Assumption*
Deca→Nona	0.001	(Gerecke et al., 2005)	0.001	Same as the homolog
Nona→Octa	-	-	0.001	Same as Deca→Nona
Hepta→Hexa	0.003-0.017	ADM	0.01	Average of min and max $k_m$ 's
Hexa→Penta	0.008-0.024	ADM	0.016	Average of min and max $k_m$ 's
Penta→Tetra	0.001-0.004	ADM	0.003	Average of min and max $k_m$ 's
Tetra→Tri	0.007	ADM	0.007	Same as the homolog
Tri→Di	-	-	0.007	Same as Tetra→Tri

\*A  $k_m$  value is assumed to be used in the FTHP since laboratory data was not available to predict a rate by ADM.

The change in individual congener and  $\Sigma$ PBDE concentrations with changing future scenarios are depicted in Figure 8.7. Hale et. al (2003) stated that penta-mixtures, major components of which are BDE 47, 99, 100, 153, 154 and 85, are especially problematic because they are bioaccumulative. It is seen that congeners 47 and 99, have lower uncertainty than congeners other bioaccumulative congeners. Moreover, these congeners with congeners 153 and 154 are considered to find the best scenario for reduction of bioaccumulative congeners since  $R^2$  values of them in both validation and calibration include better fit ( $R^2 > 0.50$ ). As seen in Figure 8.7, all congeners specified in penta-mixture decrease with the bioaugmentation scenario except for BDE 100. This congener is one of the congeners where predictions are done with the highest uncertainty (as can be seen from Figure G.13). There is actually a debromination pathway with 100 as the mother, which means its concentration can reduce with biodegradation. However, model can not satisfactorily predict this congener, as can be seen from Figure 8.4. This also comes up in model predictions. More in-depth laboratory as well as environmental studies on PBDE debromination pathways would enable a better estimation for these pathways in the FTHP model as well. Nevertheless, Figure 8.7 shows that bioaugmentation can be a significant way for reducing or eliminating bioaccumulative congeners. On the other hand,  $\Sigma$ PBDEs can only be reduced by dredging as anaerobic biodegradation only has the potential to reduce bromines from PBDEs. Another finding is that removal of degradation in case of “No degradation” result in an increase in concentration of bioaccumulative congeners (BDE47, 99, 100, 153, 154 and 183). This shows that biodegradation can reduce the risk of bioaccumulative congeners in a contaminated site. As a result, the reduction of bioaccumulative congeners 47, 99, 153 and 154 can be carried out by bioaugmentation scenario.

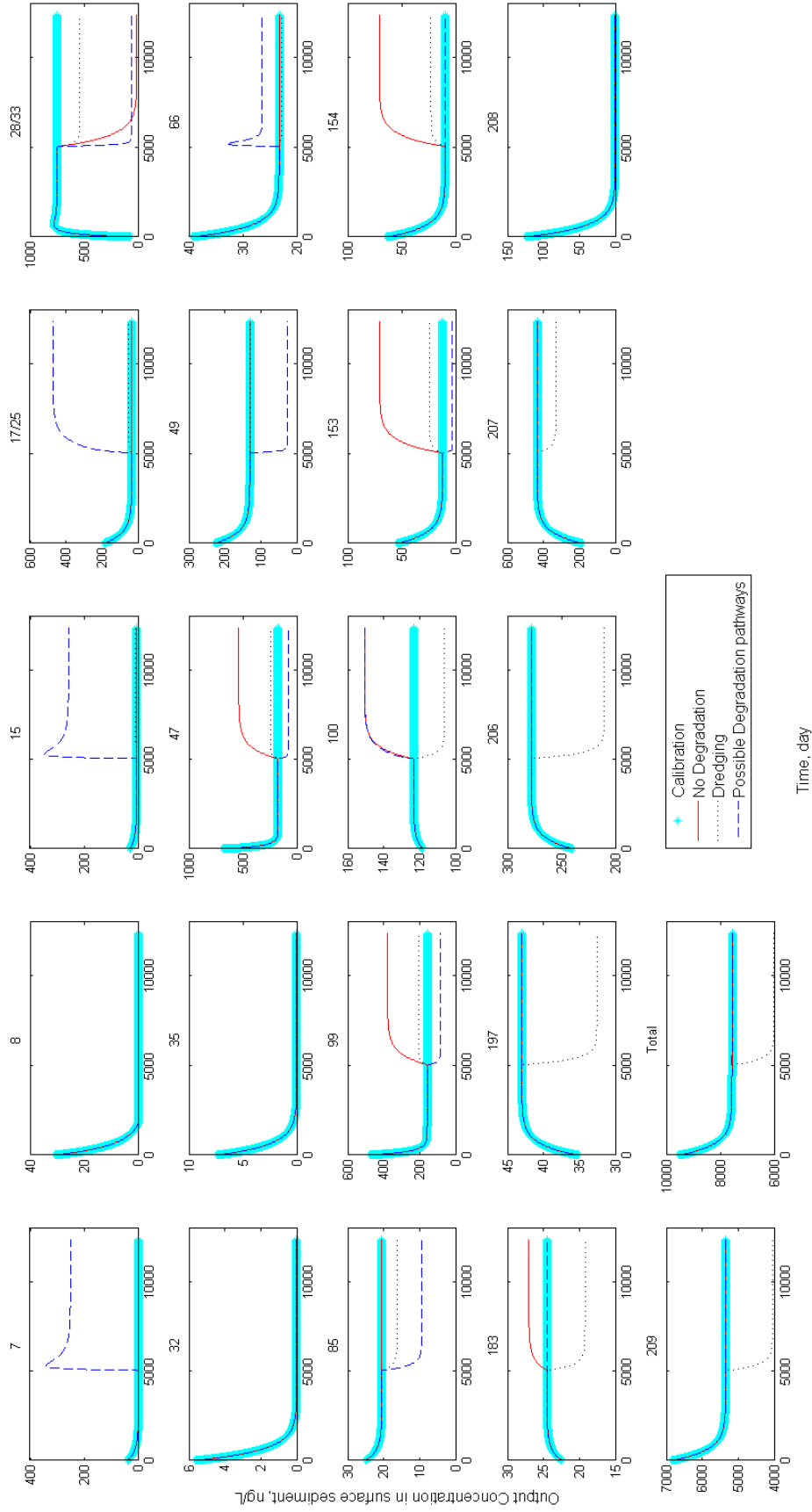


Figure 8.7 Future prediction concentrations in surface sediment

## 8.4 Conclusions

In this study, FTHP model was applied to San Francisco bay sediments for modeling biodegradation of PBDEs in sediment comprehensively considering fate and transport processes. Although studies on PBDE debromination is relatively few and recent, a number of debromination reactions could be incorporated into the calibrated model with biodegradation rate constants obtained from the anaerobic dehalogenation model. Model calibration of PBDE congeners resulted in satisfactory fit between predicted and measured sediment concentrations. FTHP model results demonstrated that settling, resuspension, and biodegradation are the important processes controlling PBDE fate and transport in San Francisco bay sediments. During trial of various scenarios, extra debromination pathways for which microcosm data could not be obtained were also incorporated into the model with assumed biodegradation rate constants. This bioaugmentation scenario using extra debromination pathways yield the best outcome in terms of reducing most of the bioaccumulative PBDE congeners from the sediments. A change in toxicity evaluation unfortunately could not be performed as TEF values for PBDE congeners are not yet present in the literature. This study shows the importance of biodegradation in a fate and transport model for family of hydrophobic compounds such as PBDEs when many reactions can take place, changing the congener profiles and persistence. Use of such models can help monitor and plan remediation efforts focused on decreasing the concentration as well as risk associated with toxic compounds from contaminated sediments.



## CHAPTER 9

### OVERVIEW

The present study aimed to investigate biodegradation of hydrophobic organic pollutants with the products in the sediment considering fate and transport mechanisms. For this purpose, FTHP model was developed. In the model, future concentration of individual congeners and total of them were determined by using dehalogenation pathways of individual congeners as well as transport and other fate mechanisms. The anaerobic dehalogenation rate constants of dehalogenation pathways were estimated by ADM to use as input to FTHP model.

This model can be applied to any halogenated HOCs. By this way, concentration of individual compounds and their total in surface sediment can be estimated in the future via scenarios. The literature review indicated that not all congeners (e.g. congeners of PCBs or PBDEs) are bioaccumulative or toxic. Therefore, future estimation enables to monitor distribution, degradation and accumulation of these toxic/bioaccumulative congeners in the sediment. Hence, strategies can be developed and applied during bioremediation accordingly.

FTHP model user should take into account the congeners which include lower uncertainty while future scenarios are discussed. Another finding is that the risk of obtaining unreliable output concentration can be decreased by using higher quality input (i.e. frequently measured data) of the most sensitive parameters (i.e. during FTHP calibration for PCBs, the most sensitive parameters were  $C_w$ ,  $k_m$ ,  $K_{ow}$ , TSS,  $v_s$ ,  $f_{ocw}$  and  $D_m$ ) which can decrease uncertainty in the output and improve the goodness of fit during calibration and validation.

FTHP model was developed such that it can be applied for different sediments such as lake, river or bay sediments contaminated with various other halogenated hydrophobic organic compounds. In that respect, the developed FTHP model was applied to two different sediments (Lake Michigan and San Francisco Bay) contaminated with two different compounds (PCBs and PBDEs). Accordingly, these applications have shown that the developed model is versatile in terms of applicability to various chemicals and different sites. The results and discussions of two applications are explained below.

The application of FTHP model to Lake Michigan sediment data has demonstrated that the calibration of the newly developed model yield satisfactory results, which were comparable or better than the water column calibration results of LM2 model for developed as part of the LMMBP. FTHP model results demonstrated that settling, resuspension, and biodegradation are important processes controlling PCB fate and transport in Lake Michigan sediments. Comparative evaluation of model forecasts indicated that toxicity reduction and decrease of amount of higher homolog groups can be realised by the scenario of DA20+DA18 – bioaugmentation of LM sediments with *dehalococcoides sp.* CBDB1 and phylotype DEH10. This study also emphasizes the importance of congener specific modeling of PCBs as well as incorporation of anaerobic dechlorination into modeling contaminated sediments.

The application of FTHP model to San Francisco bay sediments has indicated that settling, resuspension, and biodegradation are the important processes controlling PBDE fate and transport in San Francisco bay sediments. During trial of various scenarios, extra debromination pathways for which microcosm data could not be obtained were also incorporated into the model with assumed biodegradation rate constants. This bioaugmentation scenario using extra debromination pathways yield the best outcome in terms of reducing most of the bioaccumulative PBDE congeners from the sediments. A change in toxicity evaluation unfortunately could not be performed as TEF values for PBDE congeners are not yet present in the literature.

However, model enabled us to see that bioaccumulative congeners can be reduced via remediation of sediment using bioaugmentation. This study shows the importance of biodegradation in a fate and transport model for family of hydrophobic compounds such as PBDEs when many reactions can take place, changing the congener profiles and their persistence. Use of such models can help monitor and plan remediation efforts focused on decreasing the concentration as well as risk associated with toxic compounds from contaminated sediments.

This study also investigated the estimation of  $k_m$  values. This research has identified that systematic and relatively simple estimation of  $k_m$  leads the way to better understanding fate and transport of individual congeners in the environment. For example, toxic PCB congeners being the mother or daughter of dechlorination reactions can be predicted, toxicity reduction could be made possible. By this way, mathematical fate and transport models can incorporate real  $k_m$  values rather than simplistic first-order degradation rates for total-PCBs. Overall, systematic identification and quantification of anaerobic dehalogenation pathways coupled with congener specific modeling can aid remediation efforts such that congener specific monitoring/enhancement of bioremediation could be possible for sediment-bound HOCs.



## CHAPTER 10

### RECOMMENDATIONS

As distinct from the literature, the present research explored, for the first time, the effects of biodegradation with products in sediment considering F&T processes. Therefore, further studies are recommended to enhance the power of FTHP model:

- In sediment of shallow water, PBDEs can undergo photolytic degradation. In such a case, ADM model can also be performed by using photolytic debromination pathways of polybrominated diphenyl ethers.
- Preparation of microcosm with relevant field study will provide better estimation for  $k_m$  to use in FTHP model. For example, in FTHP model, biodegradation rate constant input to Lake Michigan was from BH microcosm sediment data. If the microcosm sediment taken from Lake Michigan is used for  $k_m$  estimation, this will enhance the application and remediation.
- In PBDE application, one of the challenge is the unknown physicochemical properties of some congeners such as  $K_{ow}$  and solubility. Therefore, EPISUITE was used in this study. Further studies are recommended for PBDE application of FTHP model after these values are studied in the literature.



## REFERENCES

- Abramowicz, D. A. (1995). Aerobic and anaerobic PCB biodegradation in the environment. In *Environmental Health Perspectives* (Vol. 103, pp. 97–99).
- Adrian, L., Dudková, V., Demnerová, K., & Bedard, D. L. (2009). “Dehalococcoides” sp. strain CBDB1 extensively dechlorinates the commercial polychlorinated biphenyl mixture Aroclor 1260. *Applied and Environmental Microbiology*, 75(13), 4516–24.
- Ahlborg, U., Becking, G., Birnbaum, L., Brouwer, A., Derks, H., Feeley, M., ... Yrjänheikki, E. (1994). Toxic equivalency factors for dioxin-like PCBs. *Chemosphere*, 28(6), 1049–1067.
- Allan, I. J., & Stegemann, J. A. (2007). Modelling of pollutant fate and behaviour in bed sediments. In D. Barcelo & M. Petrovic (Eds.), *Sustainable Management of Sediment Resources: Sediment Quality and Impact Assessment of Pollutants* (pp. 263–294). Amsterdam: Elsevier.
- Ambrose, R. B., Hill, S. I., & Mulkey, L. A. (1983). *User’s Manual for the Chemical Transport and Fate Model TOXIWASP Version 1*. EPA-600/3-837005. Athens, GA. Retrieved from <http://nepis.epa.gov/>
- Ambrose, R. B., Wool, T. A., Connolly, J. P., & Schanz, R. W. (1988). *WASP4, A Hydrodynamic and Water Quality Model- Model Theory, User’s Manual, and Programmer’s Guide*. EPA-600/3-87/039. Athens, GA.
- ATSDR. (2004). Toxicological profile for polybrominated biphenyl and polybrominated diphenyl ethers. Retrieved September 1, 2015, from <http://www.atsdr.cdc.gov/toxprofiles/tp68.pdf>
- Ballschmiter, K., & Zell, M. (1980). Analysis of Polychlorinated Biphenyls ( PCB ) by Glass Capillary Gas Chromatography. *Fresenius J Anal Chem*, 31(302), 20–31.

- Bedard, D. L. (2001). Microbial dechlorination of PCBs in aquatic sediments. In L. W. Robertson & L. G. Hansen (Eds.), *PCBs: Recent Advances in Environmental Toxicology and Health Effects* (pp. 27–33). Kentucky: The University Press of Kentucky.
- Bedard, D. L. (2003). Polychlorinated Biphenyls in Aquatic Sediments: Environmental Fate and Outlook for Biological Treatment. In M. M. Haggblom & I. D. Bossert (Eds.), *Dehalogenation: Microbial Processes and Environmental Applications* (pp. 443–465). Kluwer Academic Publishers.
- Bedard, D. L., Pohl, E. A., Bailey, J. J., & Murphy, A. J. A. (2005). Characterization of the PCB substrate range of microbial dechlorination process LP. *Environmental Science & Technology*, *39*(17), 6831–6838.
- Bedard, D. L., & Quensen III, J. F. (1995). Microbial reductive dechlorination of polychlorinated biphenyls. In L. Y. Young & C. Cerniglia (Eds.), *Microbial Transformation and Degradation of Toxic Organic Chemicals* (pp. 127–216). New York: Wiley-Liss Inc.
- Bedard, D. L., Unterman, R., Bopp, L. H., Brennan, M. J., Haberl, M. L., & Johnson, C. (1986). Rapid assay for screening and characterizing microorganisms for the ability to degrade polychlorinated biphenyls. *Applied and Environmental Microbiology*, *51*(4), 761–8.
- Blauenstein, M. (2007). *Modeling the Environmental Fate of Polybrominated Diphenyl Ethers in Lake Thun*. MS Thesis, Department of Environmental Science, Swiss Federal Institute of Technology Zurich, ETH Zurich.
- Bogdal, C., Scheringer, M., Schmid, P., Blauenstein, M., Kohler, M., & Hungerbuhler, K. (2010). Levels, fluxes and time trends of persistent organic pollutants in Lake Thun, Switzerland: Combining trace analysis and multimedia modeling. *Science of the Total Environment*, *408*(17), 3654–3663.
- Boyer, J. M., Chapra, S. C., Ruiz, C. E., & Dortch, M. S. (1994). *RECOVERY, A Mathematical Model to Predict the Temporal Response of Surface Water to Contaminated Sediments*, Technical Report W-94-4. Vicksburg, Mississippi.



Retrieved from <http://el.erdc.usace.army.mil/elmodels/pdf/w-94-4.pdf>

- Breivik, K., Sweetman, A., Pacyna, J. M., & Jones, K. C. (2002). Towards a global historical emission inventory for selected PCB congeners — a mass balance approach: 1. Global production and consumption. *Science of the Total Environment*, 290(1-3), 181–198.
- Breivik, K., Sweetman, A., Pacyna, J. M., & Jones, K. C. (2007). Towards a global historical emission inventory for selected PCB congeners - A mass balance approach. 3. An update. *Science of the Total Environment*, 377(2-3), 296–307.
- Brown, J. F. J., Bedard, D. L., Brennan, M. J., Carnahan, J. C., Feng, H., & Wagner, R. E. (1987). Polychlorinated biphenyl dechlorination in aquatic sediments. *Science*, 236, 709–712.
- Brown, J. F. J., Wagner, R. E., Feng, H., Bedard, D. L., Carnahan, J. C., & May, R. J. (1984). Environmental degradation of PCBs. *Environ. Toxicol. Chem.*, 6, 579–593.
- Burns, L. ., Cline, D. M., & Lassiter, R. R. (1982). *Exposure Analysis Modeling System (EXAMS): Users Manual and System Documentation*. EPA 600/3/82/023. Athens, GA.
- Bzdusek, P. A. (2005). *PCB or PAH Sources and Degradation in Aquatic Sediments Determined By Positive Matrix Factorization*. PhD Dissertation, Department of Civil Engineering and Mechanics, University of Wisconsin-Milwaukee, Wisconsin, Milwaukee.
- Bzdusek, P. A., Christensen, E. R., Lee, C. M., Pakdeesusuk, U., & Freedman, D. L. (2006). PCB congeners and dechlorination in sediments of Lake Hartwell, South Carolina, determined from cores collected in 1987 and 1998. *Environmental Science & Technology*, 40(1), 109–119.
- Bzdusek, P. A., Lu, J. H., & Christensen, E. R. (2006). PCB congeners and dechlorination in sediments of Sheboygan River, Wisconsin, determined by matrix factorization. *Environmental Science & Technology*, 40(1), 120–129.

- Caffrey, J. M. (1995). Spatial and Seasonal Patterns in Sediment Nitrogen Remineralization and Ammonium Concentrations in San-Francisco Bay, California. *Estuaries*, 18(1B), 219–233. Retrieved from <Go to ISI>://WOS:A1995RD90000003
- Chamkha, A. J. (2007). Numerical Modeling of Contaminant Transport with Spatially-Dependent Dispersion and Non-Linear Chemical Reaction. *Nonlinear Analysis: Modelling and Control*, 12(3), 329–343.
- Chapra, S. C. (1997). *Surface Water-Quality Modeling*. New York: Waveland Press inc.
- Chapra, S. C., & Reckhow, K. H. (1983). *Approaches for Lake Management, Vol. 2: Mechanistic Modeling*. Butterworth, Woburn, MA: Ann Arbor Science.
- Chen-Charpentier, B. M., & Kojouharov, H. V. (2008). Mathematical modeling of bioremediation of trichloroethylene in aquifers. *Computers and Mathematics with Applications*, 56(3), 645–656.
- Cho, Y. C., Sokol, R. C., Frohnhoefer, R. C., & Rhee, G. Y. (2003). Reductive Dechlorination of polychlorinated biphenyls: threshold concentration and dechlorination kinetics of individual congeners in Aroclor 1248. *Environmental Science and Technology*, 37(24), 5651–5656.
- Choe, K.-Y., Gill, G. a., Lehman, R. D., Han, S., Heim, W. a., & Coale, K. H. (2004). Sediment-water exchange of total mercury and monomethyl mercury in the San Francisco Bay Delta. *Limnology and Oceanography*, 49(5), 1512–1527.
- Commandeur, L. C. M., van Eyseren, H. E., Opmeer, M. R., Govers, H. a. J., & Parsons, J. R. (1995). Biodegradation Kinetics of Highly Chlorinated Biphenyls by *Alcaligenes* sp. JB1 in an Aerobic Continuous Culture System. *Environmental Science & Technology*, 29(12), 3038–3043.
- Connolly, J. P., Zahakos, H. A., Benaman, J., Ziegler, C. K., Rhea, J. R., & Russell, K. (2000). A model of PCB fate in the Upper Hudson River. *Environmental Science and Technology*, 34(19), 4076–4087.

- Cutter, L. a., Watts, J. E. M., Sowers, K. R., & May, H. D. (2001). Identification of a microorganism that links its growth to the reductive dechlorination of 2,3,5,6-chlorobiphenyl. *Environmental Microbiology*, 3(11), 699–709.
- Davis, J. A. (2004). The long-term fate of polychlorinated biphenyls in San Francisco Bay, USA. *Environmental Toxicology*, 23(10), 2396–2409.
- De Wit, C. a. (2002). An overview of brominated flame retardants in the environment. *Chemosphere*, 46(5), 583–624.
- Demirtepe, H. (2012). *Modeling Anaerobic Dechlorination of Polychlorinated Biphenyls*. MS Thesis, Department of Environmental Engineering, Middle East Technical University, Ankara, Turkey.
- Demirtepe, H., Kjellerup, B., Sowers, K. R., & Imamoglu, I. (2015). Evaluation of PCB dechlorination pathways in anaerobic sediment microcosms using an anaerobic dechlorination model. *Journal of Hazardous Materials*, 296, 120–127.
- Dercova, K., Vrana, B., & Balaz, S. (1998). Evaporation and elimination of PCBs during degradation by *Pseudomonas stutzeri*. *Toxicological and Environmental Chemistry*, 66(1-4), 11–16. Retrieved from <http://www.scopus.com/inward/record.url?eid=2-s2.0-0031946142&partnerID=40&md5=1d85b9790491d8a9a8172409e9bd819b>
- Dercova, K., Vrana, B., & Balaz, S. (1999). A kinetic distribution model of evaporation, biosorption and biodegradation of polychlorinated biphenyls (PCBs) in the suspension of *Pseudomonas stutzeri*. *Chemosphere*, 38(6), 1391–1400.
- Di Toro, D. M., Fitzpatrick, J. J., & Thomann, R. V. (1982). *Water Quality Analysis Simulation Program (WASP) and Model Verification Program (MVP) - Documentation*. Westwood, N.J.
- Ding, C., Chow, W. L., & He, J. (2013). Isolation of *Acetobacterium* sp. strain AG, which reductively debrominates octa- and pentabrominated diphenyl ether technical mixtures. *Applied and Environmental Microbiology*, 79(4), 1110–7.
- Dunnivant, F. M., & Anders, E. (2006). *A Basic Introduction to Pollutant Fate and*

*Transport: An Integrated Approach with Chemistry, Modeling, Risk Assessment, and Environmental Legislation*. New Jersey: A John Wiley and Sons, Inc.

Endicott, D. D., Richardson, W. L., & Rossmann, R. (2006). Part 1 Introduction Chapter 2 . PCBs Modeling Overview. In R. Rossmann (Ed.), *Results of the Lake Michigan Mass Balance Project: Polychlorinated Biphenyls Modeling Report* (pp. 16–25). Grosse Ile, Michigan. EPA-600/R-04/167: USEPA. Retrieved from [http://www.epa.gov/med/grosseile\\_site/LMMBP/lmmbp-pcb-report/lmmbp-pcb-report.pdf](http://www.epa.gov/med/grosseile_site/LMMBP/lmmbp-pcb-report/lmmbp-pcb-report.pdf)

Fagervold, S. K., May, H. D., & Sowers, K. R. (2007). Microbial reductive dechlorination of aroclor 1260 in Baltimore harbor sediment microcosms is catalyzed by three phylotypes within the phylum Chloroflexi. *Applied and Environmental Microbiology*, 73(9), 3009–18. Retrieved from <http://www.pubmedcentral.nih.gov/articlerender.fcgi?artid=1892865&tool=pmc-entrez&rendertype=abstract>

Fagervold, S. K., Watts, J. E. M., May, H. D., & Sowers, K. R. (2005). Sequential Reductive Dechlorination of meta-Chlorinated Polychlorinated Biphenyl Congeners in Sediment Microcosms by Two Different Chloroflexi Phylotypes. *Applied and Environmental Microbiology*, 71(12), 8085–8090.

Fagervold, S. K., Watts, J. E. M., May, H. D., & Sowers, K. R. (2011). Effects of bioaugmentation on indigenous PCB dechlorinating activity in sediment microcosms. *Water Research*, 45, 3899–3907.

Farley, K. J., Wands, J. R., Damiani, D. R., & Cooney, T. (1999). Transport, fate and bioaccumulation of PCBs in the Lower Hudson River. Retrieved December 19, 2013, from <http://rucore.libraries.rutgers.edu/rutgers-lib/35226/>

Fennell, D. E., Nijenhuis, I., Wilson, S. F., Zinder, S. H., & Haggblom, M. M. (2004). Strain 195 Reductively Dechlorinates Diverse Chlorinated Aromatic Pollutants. *Environmental Science & Technology*, 38, 2075–2081.

Frame, G. M., Cochran, J. W., & Bøwadt, S. S. (1996). Complete PCB congener distributions for 17 aroclor mixtures determined by 3 HRGC systems optimized

- for comprehensive, quantitative, congener-specific analysis. *Journal of High Resolution Chromatography*, 19(12), 657–668.
- Gerecke, A. C., Hartmann, P. C., Heeb, N. V., Kohler, H.-P. E., Giger, W., Schmid, P., ... Kohler, M. (2005). Anaerobic degradation of decabromodiphenyl ether. *Environmental Science & Technology*, 39(4), 1078–83.
- Gouin, T., & Harner, T. (2003). Modelling the environmental fate of the polybrominated diphenyl ethers. *Environment International*, 29(6), 717–724.
- Gouin, T., Mackay, D., Webster, E., & Wania, F. (2000). Screening chemicals for persistence in the environment. *Environmental Science & Technology*, 34(5), 881–884.
- Greene, R. W., Di Toro, D. M., Farley, K. J., Phillips, K. L., & Tomey, C. (2013). Modeling water column partitioning of polychlorinated biphenyls to natural organic matter and black carbon. *Environ. Sci. Technol.*, 47, 6408–6414.
- Hale, R. C., Alaei, M., Manchester-Neesvig, J. B., Stapleton, H. M., & Ikononou, M. G. (2003). Polybrominated diphenyl ether flame retardants in the North American environment. *Environment International*, 29, 771–779.
- He, J., Robrock, K. R., & Alvarez-Cohen, L. (2006). Microbial reductive debromination of polybrominated diphenyl ethers (PBDEs). *Environmental Science and Technology*, 40(14), 4429–4434.
- Henry, T. R., & DeVito, M. J. (2003). Non-Dioxin-Like PCBs: Effects and Consideration in Ecological Risk Assessment. Retrieved January 23, 2015, from <http://www.epa.gov/oswer/riskassessment/pdf/1340-erasc-003.pdf>
- House, W. A., Denison, F. H., Warwick, M. S., & Zhmud, B. V. (2000). Dissolution of silica and the development of concentration profiles in freshwater sediments. *Applied Geochemistry*, 15(4), 425–438.
- Huang, H. W., Chang, B. V., & Lee, C. C. (2014). Reductive debromination of decabromodiphenyl ether by anaerobic microbes from river sediment. *International Biodeterioration and Biodegradation*, 87, 60–65.

- Hughes, A. S., Vanbriesen, J. M., & Small, M. J. (2010). Identification of structural properties associated with polychlorinated biphenyl dechlorination processes. *Environmental Science & Technology*, *44*, 2842–2848.
- Hughes, A. S., VanBriesen, J. M., & Small, M. J. (2015). Impacts of PCB analytical interpretation uncertainties on dechlorination assessment and remedial decisions. *Chemosphere*, *133*, 61–67. Retrieved from <http://linkinghub.elsevier.com/retrieve/pii/S0045653515002969>
- Imamoglu, I. (2001). *PCB Sources and Degredation in River Sediments Determined by Receptor Modeling*. PhD. Dissertation, Department of Civil Engineering and Mechanics, University of Wisconsin-Milwaukee, Wisconsin, Milwaukee.
- Imamoglu, I., Li, K., & Christensen, E. R. (2002). Modeling polychlorinated biphenyl congener patterns and dechlorination in dated sediments from the Ashtabula River, Ohio, USA. *Environmental Toxicology and Chemistry*, *21*(11), 2283–2291.
- Imamoglu, I., Li, K., Christensen, E. R., & McMullin, J. K. (2004). Sources and dechlorination of polychlorinated biphenyl congeners in the sediments of Fox River, Wisconsin. *Environmental Science & Technology*, *38*(9), 2574–83. Retrieved from <http://www.ncbi.nlm.nih.gov/pubmed/15180053>
- Johnson, G. W., Quensen, J. F., Chiarenzelli, J. R., & Hamilton, C. (2005). Polychlorinated Biphenyls. In R. D. Morrison & B. L. Murphy (Eds.), *Environmental Forensics: Contaminant Specific Guide*.
- Karcher, S. C. (2005). *Statistical Method For Polychlorinated Biphenyl Dechlorination Modeling and Pathway Analysis*. Carnegie Mellon University.
- Karcher, S. C., Small, M. J., & VanBriesen, J. M. (2004). Statistical method to evaluate the occurrence of PCB transformations in river sediments with application to Hudson River data. *Environmental Science & Technology*, *38*(24), 6760–6. Retrieved from <http://www.ncbi.nlm.nih.gov/pubmed/15669337>
- Karcher, S. C., Vanbriesen, J. M., & Small, M. J. (2007). Numerical Method to Elucidate Likely Target Positions Polychlorinated Biphenyl Dechlorination,

(March), 278–286.

La Guardia, M. J., Hale, R. C., & Harvey, E. (2006). Detailed polybrominated diphenyl ether (PBDE) congener composition of the widely used penta-, octa-, and deca-PBDE technical flame-retardant mixtures. *Environmental Science and Technology*, 40(20), 6247–6254.

Lassen, C., Soren, L., & Andersen, L. I. (1999). *Brominated Flame Retardants - Substance Flow Analysis and Assessment of Alternatives*. *Environmental Project Nr. 494 1999*. Retrieved from <http://www.indymedia.org/media/2009/07/926988.pdf>

Li, A., Rockne, K. J., Sturchio, N. C., Mills, W. J., Song, W., Ford, J. C., & Buckley, D. R. (2006). *Chronology of pbde air deposition in the great lakes from sedimentary records*. *Great Lake Atmospheric Deposition Program Office Air and Radiation Division USEPA Region V*. Chicago, IL. Retrieved from <http://anli.people.uic.edu/Final2.pdf>

Lick, W. (2009). *Sediment and Contaminant Transport in Surface Waters*. London: Taylor & Francis Group.

LimnoTech. (2007). *PCB TMDL Model for the Potomac River Estuary. Final Report on Hydrodynamic/Salinity and PCB Transport and Fate Models* (Vol. EPA Contra). Duxbury, MA.

Locat, J., Therrien, R., & Dueri, S. (2003). Simulation of the migration of dissolved contaminants through a subaqueous capping layer: model development and application for As migration. *Journal of Environmental Engineering and Science*, 2(3), 213–226.

Lombard, N. J., Ghosh, U., Kjellerup, B. V., & Sowers, K. R. (2014). Kinetics and threshold level of 2,3,4,5-tetrachlorobiphenyl dechlorination by an organohalide respiring bacterium. *Environmental Science and Technology*, 48(8), 4353–4360.

Mackay, D., Shiu, W. Y., Ma, K., & Lee, S. C. (2006). *Properties and Environmental Fate Second Edition Introduction and Hydrocarbons*. *Chemphyschem A European Journal Of Chemical Physics And Physical Chemistry* (Vol. III).

Retrieved from <http://www.crcnetbase.com/doi/book/10.1201/9781420044393>

- Martinez, W. L., Martinez, A. R., & Crc, H. (2002). Computational Statistics Handbook with Matlab. *New York*, 65(1), 616.
- May, H. D., Cutter, L. a, Miller, G. S., Milliken, C. E., Watts, J. E. M., & Sowers, K. R. (2006). Stimulatory and inhibitory effects of organohalides on the dehalogenating activities of PCB-dechlorinating bacterium o-17. *Environmental Science & Technology*, 40(18), 5704–9. Retrieved from <http://www.ncbi.nlm.nih.gov/pubmed/17007129>
- Meysman, F. J. R., Middelburg, J. J., Herman, P. M. J., & Heip, C. H. R. (2003). Reactive transport in surface sediments. I. Model complexity and software quality. *Computers & Geosciences*, 29(3), 291–300.
- Mucci, A., Boudreau, B., & Guignard, C. (2003). Diagenetic mobility of trace elements in sediments covered by a flash flood deposit: Mn, Fe and As. *Applied Geochemistry*, 18(7), 1011–1026.
- NRCC. (2002). Bioavailability of Contaminants in Soils and Sediments. In *Processes, Tools, and Applications by National Research Council Committee*. Washington: National Academy Press.
- Oram, J., Davis, J. A., & Leatherbarrow, J. E. (2008). *A Model of Long-Term PCB Fate in San Francisco Bay: Model Formulation, Calibration, and Uncertainty Analysis (v2.1)*. RMP Contribution NN, San Francisco Estuary Institute, Oakland, CA. Retrieved from [http://legacy.sfei.org/rmp/contam\\_fate\\_meetings/1-15-08/04-Forecast\\_Document\\_010808\\_v3.pdf](http://legacy.sfei.org/rmp/contam_fate_meetings/1-15-08/04-Forecast_Document_010808_v3.pdf)
- Oram, J., McKee, L. J., Werme, C. E., Connor, M. S., Oros, D. R., Grace, R., & Rodigari, F. (2008). A mass budget of polybrominated diphenyl ethers in San Francisco Bay, CA. *Environment International*, 34, 1137–1147.
- Palermo, M. R., Maynard, S., Miller, J., & Reible, D. D. (1998). *Guidance for in-situ subaqueous capping of contaminated sediments*. EPA905-B96-004. Chicago, IL.
- Parsons, J., Segarra, M. J. B., Cornelissen, G., Gustafsson, O., Grotenhuis, T., Harms,



- H., Etxeberria, O. S. (2007). Characterisation of contaminants in sediments-effects of bioavailability on impact. In *Sustainable Management of Sediment Resources: Sediment Quality and Impact Assessment of Pollutants* (pp. 35–60). Amsterdam: Elsevier.
- Petrovic, M., Eljarrat, E., Diez, S., Kowalewska, G., & Barcelo, D. (2007). *Sustainable Management of Sediment Resources: Sediment Quality and Impact Assessment of Pollutants*. Amsterdam, The Netherlands: Elsevier.
- POPs. (2008). The 12 POPs under the Stockholm Convention. Retrieved May 24, 2015, from <http://www.pops.int/%5C/documents/pops/default.htm>
- Qi, Y. (2003). *PCB Volatilization from Sediments*. University of Cincinnati.
- Quensen III J., F., & Tiedje, J. M. (1997). Evaluation of PCB dechlorination in sediments. In D. Sheehan (Ed.), *Methods in Biotechnology* (pp. 257–273). Totawa, NJ: Humana Press Inc.
- Ramaswami, A., Milford, J. B., & Small, M. J. (2005). Overview of Numerical Methods in Environmental Engineering. In *Integrated Environmental Modeling: Pollutant Transport, Fate, and Risk in the Environment* (pp. 206–238). Hoboken, New Jersey: John Wiley & Sons, Inc.
- Robrock, K. R., Korytár, P., & Alvarez-Cohen, L. (2008). Pathways for the anaerobic microbial debromination of polybrominated diphenyl ethers. *Environmental Science & Technology*, 42(8), 2845–2852.
- Rodenburg, L. a., Meng, Q., Yee, D., & Greenfield, B. K. (2014). Evidence for photochemical and microbial debromination of polybrominated diphenyl ether flame retardants in San Francisco Bay sediment. *Chemosphere*, 106, 36–43.
- Rossmann, R. (2006). *Results of the Lake Michigan Mass Balance Project: Polychlorinated Biphenyls Modeling Report*. Michigan. Retrieved from [http://www.epa.gov/med/grosseile\\_site/LMMBP/lmmbp-pcb-report/lmmbp-pcb-report.pdf](http://www.epa.gov/med/grosseile_site/LMMBP/lmmbp-pcb-report/lmmbp-pcb-report.pdf)
- Rowe, M. D. (2009). Modeling contaminant behavior in lake superior: a comparison

of pcb.

- Ruiz, C. E., Aziz, N. M., & Schroeder, P. R. (2001). RECOVERY: A contaminated sediment-water interaction model. *Environmental Modeling and Assessment*, 6, 151–158.
- Russell, K. T., Rhea, J. R., Ku, W., Glaser, D., & Cepko, R. P. (2006). Use of Mathematical Models to Evaluate Management Options for Reducing PCB Bioaccumulation by Fish in Two Streams at The Neal's Landfill Site, Bloomington. *Water Environment Federation, WEFTEC*, 41(50), 3875–3889.
- Schafer, D., Kober, R., & Dahmke, A. (2003). Competing TCE and cis-DCE degradation kinetics by zero-valent iron - Experimental results and numerical simulation. *Journal of Contaminant Hydrology*, 65, 183–202.
- Schneider, A. R. (2005). *PCB Desorption From Resuspended Hudson River Sediment. Maryland, USA*. University of Maryland, College Park.
- Schnoor, J. L. (1996). *Environmental Modeling: Fate and Transport of Pollutants in Water, Air and Soil*. New York: John Wiley & Sons, Inc.
- SFEI. (2015). The Regional Monitoring Program for Water Quality in the San Francisco Bay (RMP) by the San Francisco Estuary Institute. Retrieved from <http://www.sfei.org/rmp>
- Shen, J. (2011). James River PCB TMDL Study: Numerical Modeling Approach. Retrieved November 20, 2013, from [www.deq.state.va.us/Portals/0/DEQ/Water/TMDL/PCB/jmspcbvim427.pdf](http://www.deq.state.va.us/Portals/0/DEQ/Water/TMDL/PCB/jmspcbvim427.pdf)
- Shen, J., Hong, B., Schugam, L., Zhao, Y., & White, J. (2012). Modeling of polychlorinated biphenyls (PCBs) in the Baltimore Harbor. *Ecological Modelling*, 242, 54–68. Retrieved from [http://apps.webofknowledge.com/full\\_record.do?product=UA&search\\_mode=GeneralSearch&qid=3&SID=3FQVwWLgunI8MxiDqVJ&page=1&doc=2](http://apps.webofknowledge.com/full_record.do?product=UA&search_mode=GeneralSearch&qid=3&SID=3FQVwWLgunI8MxiDqVJ&page=1&doc=2)
- Siebielska, I., & Sidelko, R. (2015). Polychlorinated biphenyl concentration changes in sewage sludge and organic municipal waste mixtures during composting and

- anaerobic digestion. *Chemosphere*, 126, 88–95. Retrieved from <http://www.sciencedirect.com/science/article/pii/S0045653514014799>
- Sinkkonen, S., & Paasivirta, J. (2000). Degradation half-life times of PCDDs, PCDFs and PCBs for environmental fate modeling. *Chemosphere*, 40(9-11), 943–949.
- Song, M., Luo, C., Li, F., Jiang, L., Wang, Y., Zhang, D., & Zhang, G. (2015). Anaerobic degradation of Polychlorinated Biphenyls (PCBs) and Polychlorinated Biphenyls Ethers (PBDEs), and microbial community dynamics of electronic waste-contaminated soil. *Science of The Total Environment*, 502, 426–433. Retrieved from <http://linkinghub.elsevier.com/retrieve/pii/S0048969714013679>
- Sowers, K. R., & May, H. D. (2013). In situ treatment of PCBs by anaerobic microbial dechlorination in aquatic sediment: are we there yet? *Current Opinion in Biotechnology*, 24, 482–488. Retrieved from <http://linkinghub.elsevier.com/retrieve/pii/S0958166912001590>
- Suk, N. S., & Fikslin, T. J. (2011). *Water quality model for carbon and PCB (polychlorinated biphenyl) homologs for Zones 2 - 6 of the Delaware River*. Delaware River Basin Commission. West Trenton, NJ.
- Sutton, R., Sedlak, M. D., Yee, D., Davis, J. a., Crane, D., Grace, R., & Arsem, N. (2015). Declines in Polybrominated Diphenyl Ether Contamination of San Francisco Bay following Production Phase-Outs and Bans. *Environmental Science & Technology*, 49(2), 777–784.
- Sutton, R., Sedlak, M., & Davis, J. (2014). *Polybrominated Diphenyl Ethers (PBDEs) in San Francisco Bay: A Summary of Occurrence and Trends*. RMP Contribution No. 713. San Francisco Estuary Institute, Richmond, California. 62pp.
- Tandlich, R. (2003). *Microbial PCB Degradation and Binding to soil components*. PhD. Dissertation, Agriculture and Applied Science, North Dakota State University, Fargo, North Dakota.
- Thomann, R. V., & Di Toro, D. M. (1984). *Physico-Chemical Model of Toxic Substances in the Great Lakes. Project Summary*. EPA-600/S3-84-050.

- Tokarz, J. A., Ahn, M. Y., Leng, J., Filley, T. R., & Nies, L. (2008). Reductive debromination of polybrominated diphenyl ethers in anaerobic sediment and a biomimetic system. *Environmental Science and Technology*, *42*(4), 1157–1164.
- Travis, B. J., & Rosenberg, N. D. (1997). Modeling in situ bioremediation of TCE at Savannah River: Effects of product toxicity and microbial interactions on TCE degradation. *Environmental Science and Technology*, *31*(11), 3093–3102.
- UNEP. (1999). *Guidelines for the Identification of PCBs and Materials Containing PCBs. First Issue.* Retrieved from <http://chm.pops.int/Implementation/PCBs/DocumentsPublications/tabid/665/Default.aspx>
- USEPA. (2010). An Exposure Assessment of Polybrominated Diphenyl Ethers. National Center for Environmental Assessment, Washington, DC; EPA/600/R-08/086F. Retrieved July 3, 2015, from <http://www.epa.gov/ncea>
- USEPA. (2013). Use of Dioxin TEFs in Calculating Dioxin TEQs at CERCLA and RCRA Sites. Retrieved September 29, 2015, from [http://www.epa.gov/superfund/health/contaminants/dioxin/pdfs/Use\\_of\\_Dioxin\\_TEFs\\_in\\_Calculating\\_Dioxin\\_TEQs\\_at\\_CERCLA\\_and\\_RCRA\\_Sites.pdf](http://www.epa.gov/superfund/health/contaminants/dioxin/pdfs/Use_of_Dioxin_TEFs_in_Calculating_Dioxin_TEQs_at_CERCLA_and_RCRA_Sites.pdf)
- USEPA. (2015). U.S. Environmental Protection Agency, Great Lakes National Program Office, Chicago, USA. Personal Communication. Retrieved from <http://www3.epa.gov/greatlakes/lmmb/results-pubs.html>
- Van den Berg, M., Birnbaum, L. S., Denison, M., De Vito, M., Farland, W., Feeley, M., Peterson, R. E. (2006). The 2005 World Health Organization reevaluation of human and mammalian toxic equivalency factors for dioxins and dioxin-like compounds. *Toxicological Sciences*, *93*(2), 223–241.
- van der Lee, J., De Windt, L., Lagneau, V., & Goblet, P. (2003). Module-oriented modeling of reactive transport with HYTEC. *Computers and Geosciences*, *29*(3), 265–275.
- Wei, H., Zou, Y., Li, A., Christensen, E. R., & Rockne, K. J. (2013). Photolytic debromination pathway of polybrominated diphenyl ethers in hexane by sunlight.

*Environmental Pollution*, 174, 194–200.

Weston solutions. (2004). *Model Calibration : Modeling Study of PCB Contamination in the Housatonic River. Appendix A Watershed Model Calibration*. DCN.GE-122304-ACMG. Pittsfield, Massachusetts.

WHO. (2003). Concise International Chemical Assessment Document 53: Hydrogen sulfide: Human health aspects. Retrieved December 23, 2013, from <http://www.who.int/ipcs/publications/cicad/en/cicad55.pdf>

Wu, Q. Z., Sowers, K. R., & May, H. D. (2000). Establishment of a polychlorinated biphenyl-dechlorinating microbial consortium, specific for doubly flanked chlorines, in a defined, sediment-free medium. *Applied and Environmental Microbiology*, 66(1), 49–53.

Wu, Q. Z., Watts, J. E. M., Sowers, K. R., & May, H. D. (2002). Identification of a bacterium that specifically catalyzes the reductive dechlorination of polychlorinated biphenyls with doubly flanked chlorines. *Applied and Environmental Microbiology*, 68(2), 807–812. Retrieved from <http://eutils.ncbi.nlm.nih.gov/entrez/eutils/elink.fcgi?dbfrom=pubmed&id=11823222&retmode=ref&cmd=prlinks>

Xu, Z., Wu, Y., & Yu, F. (2012). A Three-Dimensional Flow and Transport Modeling of an Aquifer Contaminated by Perchloroethylene Subject to Multi-PRB Remediation. *Transport in Porous Media*, 91, 319–337.

Yee, D., Bemis, B., Hammond, D., Heim, W., Jaffe, B., Rattonetti, A., & van Bergen, S. (2011). *Age estimates and pollutant concentrations of sediment cores from San Francisco Bay and Wetlands. A Technical Report of the Regional Monitoring Program: SFEI Contribution 652*. San Francisco Estuary Institute, Oakland, CA. 45pp + Appendices A, B and C.

Yu, S., & Semprini, L. (2004). Kinetics and modeling of reductive dechlorination at high PCE and TCE concentrations. *Biotechnology and Bioengineering*, 88(4), 451–64. Retrieved from <http://www.ncbi.nlm.nih.gov/pubmed/15384053>

Zanaroli, G., Balloi, A., Negroni, A., Borruso, L., Daffonchio, D., & Fava, F. (2012).

- A Chloroflexi bacterium dechlorinates polychlorinated biphenyls in marine sediments under in situ-like biogeochemical conditions. *Journal of Hazardous Materials*, 209-210, 449–457.
- Zanaroli, G., Balloi, A., Negroni, A., Daffonchio, D., Young, L. Y., & Fava, F. (2010). Characterization of the microbial community from the marine sediment of the Venice lagoon capable of reductive dechlorination of coplanar polychlorinated biphenyls (PCBs). *Journal of Hazardous Materials*, 178(1-3), 417–426.
- Zhang, X. (2006). Part 4 LM2 Toxic. Chapter 3. Model Description. In R. Rossmann (Ed.), (pp. 223–245). Grosse Ile, Michigan. EPA-600/R-04/167: USEPA. Retrieved from [http://www.epa.gov/med/grosseile\\_site/LMMBP/lmmbp-pcb-report/lmmbp-pcb-report.pdf](http://www.epa.gov/med/grosseile_site/LMMBP/lmmbp-pcb-report/lmmbp-pcb-report.pdf)
- Zhang, X., Rygwelski, K. R., & Rossmann, R. (2009). The Lake Michigan contaminant transport and fate model, LM2-toxic: Development, overview, and application. *Journal of Great Lakes Research*, 35(1), 128–136. Retrieved from [http://resolver.scholarsportal.info/resolve/03801330/v35i0001/128\\_tlmctamldoa](http://resolver.scholarsportal.info/resolve/03801330/v35i0001/128_tlmctamldoa)  
a
- Zhang, X., Rygwelski, K. R., Rossmann, R., Pauer, J. J., & Kreis, R. G. (2008). Model construct and calibration of an integrated water quality model (LM2-Toxic) for the Lake Michigan Mass Balance Project. *Ecological Modelling*, 219, 92–106.
- Zou, Y., Christensen, E. R., Zheng, W., Wei, H., & Li, A. (2014). Estimating stepwise debromination pathways of polybrominated diphenyl ethers with an analogue Markov Chain Monte Carlo algorithm. *Chemosphere*, 114, 187–194. Retrieved from <http://linkinghub.elsevier.com/retrieve/pii/S0045653514005827>

## APPENDIX A

### LIST OF CONGENERS

Table A.1 List of PCB congeners

#	Structure	#	Structure	#	Structure	#	Structure	#	Structure
<b>MonoCB</b>		41	234-2	84	236-23	<b>HexaCB</b>		<b>HeptaCB</b>	
1	2-	42	23-24	85	234-24	128	234-234	170	2345-234
2	3-	43	235-2	86	2345-2	129	2345-23	171	2346-234
3	4-	44	23-25	87	234-25	130	234-235	172	2345-235
<b>DiCB</b>		45	236-2	88	2346-2	131	2346-23	173	23456-23
4	2-2	46	23-26	89	234-26	132	234-236	174	2345-236
5	23-	47	24-24	90	235-24	133	235-235	175	2346-235
6	2-3	48	245-2	91	236-24	134	2356-23	176	2346-236
7	24-	49	24-25	92	235-25	135	235-236	177	2356-234
8	2-4	50	246-2	93	2356-2	136	236-236	178	2356-235
9	25-	51	24-26	94	235-26	137	2345-24	179	2356-236
10	26-	52	25-25	95	236-25	138	234-245	180	2345-245
11	3-3	53	25-26	96	236-26	139	2346-24	181	23456-24
12	34-	54	26-26	97	245-23	140	234-246	182	2345-246
13	3-4	55	234-3	98	246-23	141	2345-25	183	2346-245
14	35-	56	23-34	99	245-24	142	23456-2	184	2346-246
15	4-4	57	235-3	100	246-24	143	2345-26	185	23456-25
<b>TriCB</b>		58	23-35	101	245-25	144	2346-25	186	23456-26
16	23-2	59	236-3	102	245-26	145	2346-26	187	2356-245
17	24-2	60	234-4	103	246-25	146	235-245	188	2356-246
18	25-2	61	2345-	104	246-26	147	2356-24	189	2345-345
19	26-2	62	2346-	105	234-34	148	235-246	190	23456-34
20	23-3	63	235-4	106	2345-3	149	236-245	191	2346-345
21	234-	64	236-4	107	234-35	150	236-246	192	23456-35
22	23-4	65	2356-	108	2346-3	151	2356-25	193	2356-345
23	235-	66	24-34	109	235-34	152	2356-26	<b>OctaCB</b>	
24	236-	67	245-3	110	236-34	153	245-245	194	2345-2345
25	24-3	68	24-35	111	235-35	154	245-246	195	23456-234
26	25-3	69	246-3	112	2356-3	155	246-246	196	2345-2346
27	26-3	70	25-34	113	236-35	156	2345-34	197	2346-2346
28	24-4	71	26-34	114	2345-4	157	234-345	198	23456-235
29	245-	72	25-35	115	2346-4	158	2346-34	199	2345-2356
30	246-	73	26-35	116	23456-	159	2345-35	200	23456-236
31	25-4	74	245-4	117	2356-4	160	23456-3	201	2346-2356
32	26-4	75	246-4	118	245-34	161	2346-35	202	2356-2356
33	34-2	76	345-2	119	246-34	162	235-345	203	23456-245
34	35-2	77	34-34	120	245-35	163	2356-34	204	23456-246
35	34-3	78	345-3	121	246-35	164	236-345	205	23456-345
36	35-3	79	34-35	122	345-23	165	2356-35	<b>NonaCB</b>	
37	34-4	80	35-35	123	345-24	166	23456-4	206	23456-2345
38	345-	81	345-4	124	345-25	167	245-345	207	23456-2346
39	35-4	<b>PentaCB</b>		125	345-26	168	246-345	208	23456-2356
<b>TetraCB</b>		82	234-23	126	345-34	169	345-345	<b>DecaCB</b>	
40	23-23	83	235-23	127	345-35			209	23456-23456

Table A.2 List of most commonly studied PBDE congeners (USEPA, 2010)

BDE congener number	Chemical formula	BDE congener number	Chemical formula
<b>I. MonoBDE</b>		BDE 118	2,3',4,4',5-BDE
BDE 3	4-BDE	BDE 119	2,3',4,4',6-BDE
<b>II. DiBDE</b>		BDE 126	3,3',4,4',5-BDE
BDE 7	2,4-BDE	BDE 138	2,2',3,4,4',5'-BDE
BDE 8	2,4'-BDE	BDE 140	2,2',3,4,4',6-BDE
BDE 11	3,3'-BDE	<b>VI. HexaBDE</b>	
BDE 12	2,6-BDE	BDE 153	2,2',4,4',5,5'-BDE
BDE 13	3,4'-BDE	BDE 154	2,2',4,4',5,6'-BDE
BDE 15	4,4'-BDE	BDE 155	2,2',4,4',6,6'-BDE
<b>III. TriBDE</b>		BDE 166	2,3,4,4',5,6-BDE
BDE 17	2,2',4-BDE	<b>VII. HeptaBDE</b>	
BDE 25	2,3',4-BDE	BDE 181	2,2',3,4,4',5,6-BDE
BDE 28	2,4,4'-BDE	BDE 183	2,2',3,4,4',5',6-BDE
BDE 30	2,4,6-BDE	BDE 190	2,3,3',4,4',5,6-BDE
BDE 32	2,4',6-BDE	<b>VIII. OctaBDE</b>	
BDE 33	2',3,4-BDE	BDE 196	2,2',3,3',4,4',5',6-BDE
BDE 35	3,3',4-BDE	BDE 197	2,2',3,3',4,4',6,6'-BDE
BDE 37	3,4,4'-BDE	BDE 203	2,2',3,4,4',5,5',6-BDE
<b>IV. TetraBDE</b>		<b>IX. NonaBDE</b>	
BDE 47	2,2',4,4'-BDE	BDE 206	2,2',3,3',4,4',5,5',6-BDE
BDE 49	2,2',4,5'-BDE	BDE 207	2,2',3,3',4,4',5,6,6'-BDE
BDE 66	2,3',4,4'-BDE	BDE 208	2,2',3,3',4,5,5',6,6'-BDE
BDE 71	2,3',4',6-BDE	<b>X. DecaBDE</b>	
BDE 75	2,4,4',6-BDE	BDE 209	2,2',3,3',4,4',5,5',6,6'-BDE
BDE 77	3,3',4,4'-BDE		
<b>V. PentaBDE</b>			
BDE 85	2,2',3,4,4'-BDE		
BDE 99	2,2',4,4',5-BDE		
BDE 100	2,2',4,4',6-BDE		
BDE 105	2,3,3',4,4'-BDE		
BDE 116	2,3,4,5,6-BDE		



## APPENDIX B

### LIST AND NAMES OF MOST COMMONLY STUDIED PBDE CONGENERS

Table B.1 Technical flame-retardant (Penta- Octa- and Deca-PBDEs) compositions  
(%, w/w) (La Guardia et al., 2006)

IUPAC	Compound	Penta-PBDE			Octa-PBDE		Deca-PBDE
		DE-71(1)	Bromkal 70-5DE(2)	Bromkal 70-5DE(3)	Bromkal 79-8DE(3)	Bromkal 79-8DE(4)	
BDE-17	2,2',4-tri-BDE	0.04	0.022	t	nd	na	nr
BDE-28	2,4,4'-tri-BDE	0.37	0.11	t	nd	na	nr
BDE-42	2,2',3,4'-tetra-BDE	0.02	na	nd	nd	na	nr
BDE-47	2,2',4,4'-tetra-BDE	33	37	M	nd	na	nr
BDE-48	2,2',4,5-tetra-BDE	0.05	na	nd	nd	na	nr
BDE-49	2,2',4,5'-tetra-BDE	0.77	na	o	nd	na	nr
BDE-51	2,2',4,6'-tetra-BDE	0.02	nd	nd	nd	na	nr
BDE-66	2,3',4,4'-tetra-BDE	1.02	0.22	t	nd	na	nr
BDE-74	2,4,4',4',5-tetra-BDE	na	na	o	nd	na	nr
BDE-85	2,2',3',3',4,4'-penta-BDE	3.18	1.6	m	nd	na	nr
BDE-91	2,2',3,3,4',6-penta-BDE	0.07	na	na	na	na	nr
BDE-97	2,2',3',3',4,5-penta-BDE	na	na	o*	nd	na	nr
BDE-99	2,2',4,4',4,4',5-penta-BDE	42.5	35	M	nd	na	nr
BDE-100	2,2',4,4',4,4',6-penta-BDE	10.9	6.8	m	nd	na	nr
BDE-101	2,2',4,5,5',4,5,5'-penta-BDE	na	na	o	nd	na	nr
BDE-102	2,2',4,5,6',4,5,6'-penta-BDE	0.13	na	nd	nd	na	nr
BDE-118	2,3',4,4',4,4',5-penta-BDE	na	na	o*	nd	na	nr
BDE-119	2,3',4,4',4,4',6-penta-BDE	0.002	nd	nd	nd	na	nr
BDE-138	2,2',3,4,4',3,4,4',5'-hexa-BDE	0.24	0.41	t	nd	na	nr
BDE-139	2,2',3,4,4',3,4,4',6-hexa-BDE	0.16	na	o	nd	na	nr
BDE-140	2,2',3,4,4',3,4,4',6'-hexa-BDE	nd	na	o	nd	na	nr
BDE-153	2,2',4,4',4,4',5,5'-hexa-BDE	3.75	3.9	m	nd	na	nr
BDE-154	2,2',4,4',4,4',5,6'-hexa-BDE	3	2.5	m	nd	na	nr
BDE-155	2,2',4,4',4,4',6,6'-hexa-BDE	0.32	na	o	nd	na	nr
BDE-156	2,3,3',3',4,4',5-hexa-BDE	nd	na	nd	nd	na	nr
BDE-173	2,2',3,3',4,3,3',4,5,6-hepta-BDE	na	na	nd	o*	na	nr
BDE-181	2,2',3,4,4',3,4,4',5,6-hepta-BDE	na	na	nd	o	na	nr
BDE-183	2,2',3,4,4',3,4,4',5',6-hepta-BDE	0.02	nd	t	M	d	nr
BDE-190	2,3,3',4,4',4,4',5,6-hepta-BDE	na	nd	nd	o	na	nr
BDE-191	2,3,3',4,4',4,4',5',6-hepta-BDE	na	na	nd	o*	na	nr
BDE-196	2,2',3,3',3,3',4,4',5,6'-octa-BDE	na	na	na	m	d	nr
BDE-197	2,2',3,3',3,3',4,4',6,6'-octa-BDE	na	na	na	M	d	nr
BDE-203	2,2',3,4,4',3,4,4',5,5',6-octa-BDE	na	na	nd	m	d	nr
BDE-204	2,2',3,4,4',3,4,4',5,6,6'-octa-BDE	na	na	nd	t	d**	nr
BDE-205	2,3,3',4,4',4,4',5,5',6-octa-BDE	na	na	nd	o	na	nr
BDE-206	2,2',3,3',3,3',4,4',5,5',6-nona-BDE	na	na	nd	m	d	nr
BDE-207	2,2',3,3',3,3',4,4',5,6,6'-nona-BDE	na	na	nd	M	d	≤3***
BDE-208	2,2',3,3',3,3',4,5,5',6,6'-nona-BDE	na	na	nd	m	d	
BDE-209	deca-BDE	na	na	nd	M	d	≥97

na=not analyzed, nd=not detected, nr=not reported, d=detected, (M=major, m=minor, t=trace and o=other congeners) \*=co-elude, \*\*=identified as

BDE-204 in reference Korytár, et al. 2005. \*\*\*=includes trace amounts of octa-PBDEs



## APPENDIX C

### MASS BALANCE EQUATIONS AND MECHANISMS OF THE MODELS REVIEWED IN THE LITERATURE

Table C.1 Recovery Model (Boyer et al., 1994 and Ruiz et al., 2000)

Items	Explanation
<b>Mass Balance Equations for Sediment Layer</b>	
Mass Balance for mixed sediment layer	$V_m \frac{dc_m}{dt} = -k_m V_m c_m + v_s A_w F_{pw} c_w - v_r A_m c_m - v_b A_m c_m$ $-v_d A_m (F_{dw} c_w - F_{dp} c_m) + v_d A_m (F_{dp} c_s(0) - F_{dp} c_m) \quad *$
Mass Balance for deep sediment	$\frac{\partial c_s}{\partial t} = \varphi F_{dp} D_s \frac{\partial^2 c_s}{\partial z^2} - v_b \frac{\partial c_s}{\partial z} - k_s c_s = F_{dps} D_s \frac{\partial^2 c_s}{\partial z^2} - v_b \frac{\partial c_s}{\partial z} - k_s c_s$
<b>Media, Dimension and Boundaries</b>	
Media	Water, mixed, and deep sediments in lakes, embankments, harbors, estuaries, and ocean parcels as long as the assumption is of a completely mixed water body
Dimension	1D
Boundary	IC: at $t=0$ , $C_s=C_{s0}$ ( $z_m < z < L$ ) and IC: at $t=0$ , $c_s=0$ ( $L < z < \infty$ ) BC 1: at $z=z_m$ $J=J_m$ and BC 2: at $z=\infty$ $dc_s/dz=0$
<b>Numeric Solution</b>	
Numeric Solutions	Adaptive-step-size, Runge Kutta 4 <sup>th</sup> for ODEs, Crank Nicholson for PDEs
<b>Transport Processes and Reactions</b>	
Transport	Burial, porewater diffusion, resuspension, settling and bioturbation
Reaction	Sorption (Kd) (linear reversible sorption), degradation
<b>Parameter Estimation</b>	
Partitioning-linear sorption: Particulate fraction of contaminant in the <b>water</b>	$F_{pw} = \frac{K_{dw} S_w}{1 + K_{dw} S_w} = \frac{\text{Mass of A (Particulate form)}}{\text{Mass of A (Dissolved form)} + \text{Mass of A (Particulate form)}}$
Partitioning-linear sorption: Dissolved fraction of contaminant in the <b>water</b>	$F_{dw} = 1 - F_{pw} = \frac{1}{1 + K_{dw} S_w} = \frac{\text{Mass of A (Dissolved form)}}{\text{Mass of A (Dissolved form)} + \text{Mass of A (Particulate form)}}$
Partitioning-linear sorption: Dissolved fraction of contaminant in the <b>pore water</b>	$F_{dp} = \frac{1}{\varphi + K_{ds}(1-\varphi)_p} = \frac{\text{Mass of A (Dissolved form)}}{\text{Mass of A (Dissolved form)} + \text{Mass of A (Particulate form)}}$
Partitioning coefficient	$K_d = 0.617 f_{oc} K_{ow}$
Mass transfer coefficient for diffusive sediment-water exchange	$v_d = \frac{\varphi D_s}{z'}$
Molecular Diffusivity	$D_s = m \varphi^2$
Solid mass balance to predict one of velocities	$0 = v_s A_w s_w - (v_r + v_b) A_m (1 - \varphi)_p$
Biodegradation	First order decay

\*:  $v_d A_m (F_{dw} c_w - F_{dpm} c_m / \varphi_m) + v_d A_m (F_{dps} c_s(0) / \varphi_s - F_{dpm} c_m / \varphi_m)$

Table C.2 TOXIWASP Model (Ambrose et al., 1983)

Items	Explanation
<b>Mass Balance Equations for Sediment Layer</b>	
Mass Balance for diffusion/dispersion and pore water transport of dissolved chemical between bed and overlying water column	$\frac{\partial c_p}{\partial t} = \frac{\partial}{\partial y} (D^b \frac{\partial c_p}{\partial y}) - \frac{\partial (u_p c_p)}{\partial y} - R_s - K$
Mass Balance for sediment bound transport (settling and resuspension) of particulate chemical between bed and overlying water column	$\frac{\partial c_b}{\partial t} = \frac{\partial}{\partial y} (D^{bs} \frac{\partial c_b}{\partial y}) - \frac{w_s c_b}{L_s} + R_s - K$
Sediment Mass balance	$\frac{\partial c_2}{\partial t} = u \frac{\partial c_2}{\partial x} + \frac{\partial}{\partial x} (E \frac{\partial c_2}{\partial x}) + \frac{w_2}{V} + S_2$
Deposition-Scour-Pore water diffusion-Direct Sorption Exchange with Bed Sediment-Percolation (+Infiltration)-Degradation	$V_4 \frac{dc_{14}}{dt} = \frac{w_{d3} c_{23} c_{13} a_{23}}{L_{W3} c_{23}} - \frac{w_{s4} c_{24} c_{14} a_{24}}{L_{b4} c_{24}} - D_{3-4}^b A_{3-4} \left( \frac{c_{14} a_{14} - c_{13} a_{13}}{L_{3-4}} \right) - D_{3-4}^b A_{3-4} f_{34} \frac{c_{24}}{\phi_4} \left( \frac{c_{14} a_{24}}{c_{24}} - \frac{c_{13} a_{23}}{c_{23}} \right) - u_{p4} A \left( \frac{c_{14} a_{14}}{\phi_4} \text{ or } \frac{c_{14} a_{14}}{\phi_4} \right) - \left[ \sum_{k=1}^3 k_{bac} C_{bac} \alpha_{14} \right]$
<b>Media, Dimension and Boundaries</b>	
Media	Surface water, surface sediment and bed sediment in streams, lakes, reservoirs, estuaries, and coastal waters.
Dimension	1D, 2D or 3D
Boundary	Ambrose et al. (1983), p.59
<b>Numeric Solution</b>	
Numeric Solutions	Explicit backward difference (completely mixed compartmentalized models with finite difference solutions to the set of time variable, ordinary differential equations)
<b>Transport Processes and Reactions</b>	
Transport	Pore water diffusion, burial, erosion, deposition, dispersion, percolation
Reaction	Kinetic degradation/transformation(hydrolysis, biodegradation, oxidation, photolysis and volatilization) sorption
<b>Parameter Estimation</b>	
Partitioning- sorption: Dissolved fraction of contaminant in the water	$C_T = C(\alpha_1 + \alpha_2 + \alpha_3) \quad C_1 = C \alpha_1, \quad C_W = \frac{C \alpha_1}{\phi} \quad \alpha_1 = \frac{1}{1 + K_{p2}(\frac{S}{\phi}) + K_{p3}(\frac{B}{\phi})}$
Partitioning- sorption: Sorbed fraction of contaminant on sediment	$C_2 = C \alpha_2, \quad C_S = \frac{C \alpha_2}{S} \quad \alpha_2 = \frac{1 K_{p2}(\frac{S}{\phi})}{1 + K_{p2}(\frac{S}{\phi}) + K_{p3}(\frac{B}{\phi})}$
Partitioning- sorption: Sorbed fraction of contaminant onto biological phase	$C_3 = C \alpha_3 \quad C_{bio} = \frac{C \alpha_3}{B} \quad \alpha_3 = \frac{K_{p3}(\frac{B}{\phi})}{1 + K_{p2}(\frac{S}{\phi}) + K_{p3}(\frac{B}{\phi})}$
Net rate of chemical transfer bw dissolved and sorbed state	$R_s = S(k_s C_w' - k_d C_s')$
Sorption desorption rate	$KT = \frac{SCALB * D^b A_s}{BVOL * L_c} \times \frac{1 + KPB * S'}{KPB * S'}$
Net exchange of sediment-Erosion	$S_2 = \frac{w_s S_b}{L_b} - \frac{w_d S_w}{L_w}$
Transformation and Biodegradation term	$\frac{dc}{dt} = \sum_{j=1}^n K_j C$
Microbial degradation (2 <sup>nd</sup> order)	$R_{bac} = k_{bac} C_{bac} C$

Table C.3 LM-2 Model

Items	Explanation
<b>Mass Balance Equations for Sediment Layer</b>	
Mass Balance for sediment layer	$\frac{dC_j}{dt} = \sum_i^n R_{ij}(C_i - C_j) + S_{sw,j} + S_{b,j} + S_{k,j}$
<b>Media, Dimension and Boundaries</b>	
Media	Lake water and surficial sediment
Dimension	1D
Boundary	No information was given in the reference
<b>Numeric Solution</b>	
Numeric Solutions	(completely mixed compartmentalized models with finite difference solutions to the set of time variable, ordinary differential equations)
<b>Transport Processes and Reactions</b>	
Transport	Pore water diffusion, burial, settling and resuspension
Reaction	Kinetic degradation/transformation(hydrolysis, biodegradation, oxidation, photolysis and volatilization), sorption
Dimension	1D
Boundary	No information was given in the reference
Bulk Dispersion/Diffusion Coefficient	$R_{ij} = \frac{E_{ij}A}{\Delta x_{ij}}$
Vertical exchange coefficient	$v_t = \frac{v \cdot (\frac{dT_t}{dt})}{A_t \cdot (T_u - T_l)} \quad E_t = v_t \cdot z_t$
Resuspension rate of <b>Carbon:PDC</b> in surficial sediment	for water depth >100m $v_r = \alpha(W - W_{cr})$ for water depth <100m $\bar{v}_r = \frac{v_s C_w - v_b C_s - k_{ds} z C_s}{C_s}$
<b>Parameter Estimation</b>	
Phase partitioning coefficients and total PCB concentration	$K_{DOC} = \frac{C_{DOC}}{[DOC]C_d} \quad K'_{POC} = \frac{C_{POC}}{[POC]C_d}$ $C_T = C_d + C_{DOC} + C_{POC} \quad C_t = C_d(1 + K_{DOC}[DOC] + K'_{POC}[POC])$
Three phase PCB Partitioning	$\frac{[POC]C_{d,\alpha}}{C_{POC}} = \frac{K_{DOC}}{K'_{POC}}[DOC] + \frac{1}{K'_{POC}}$
Two phase PCB Partitioning (bound to POC and dissolved+ bound to DOC)	$K'_{POC} = \frac{C_{POC}}{[POC]C_{d,\alpha}} \quad C_s^a = C_s^b \rho (1 - \phi) 10^3$
Decay rates for <b>Carbon: BIC, PDC, and DOC</b> (in water and sediment)	$k_{d,solid} = \left( \frac{\hat{k}_{d,solid} C_{solid}}{k_{1/2,solid} + C_{solid}} \right) \theta^{T-20} \quad k_{ds,solid} = \bar{k}_{ds,solid} \theta^{T-20}$

Table C.4 PMHR Model (Farley et al., 1999)

Items	Explanation
<b>Mass Balance Equations for Sediment Layer</b>	
Mass Balance for surface sediment layer	$V_{sed} \frac{dC_{sed_i}}{dt} = w_s A_s m_i \Gamma_i - w_u A_s m_{sed_i} \Gamma_{sed_i} - w_b A_s m_{sed_i} \Gamma_{sed_i} - k'_f A_s [C_{dis+DOC_{sed_i}} - C_{dis+DOC_i}] - k_{sed_i} V_{sed_i} C_{dis_{sed_i}}$
<b>Media, Dimension and Boundaries</b>	
Media	River water, surface sediment and biota
Dimension	1D
Boundary	No information was given in the reference
<b>Numeric Solution</b>	
Numeric Solutions	No information was given in the reference
<b>Transport Processes and Reactions</b>	
Transport	Burial, porewater diffusion, resuspension, settling
Reaction	Sorption, degradation, bioaccumulation
<b>Parameter Estimation</b>	
Sorption considering phytoplankton	$K_d = \frac{a_{phyto/oc} K_{oc}}{1 + (\frac{k_d}{k_u}) a_{phyto/oc} K_{oc}} f_{oc} = \frac{POC\ conc}{SS\ or\ Sediment\ conc} a_{DOC} K_{ow}$
the equilibrium partitioning relationships to solids and DOC, and the total mass conservation equation	$K_d = \Gamma / C_{dis}$ $K_{DOC} = (C_{DOC}/DOC)/C_{dis} \quad C = \varphi C_{dis} + \varphi C_{DOC} + \Gamma m$
Biodegradation	First order
Media	River water, surface sediment and biota

Table C.5 WASP4 Model (Ambrose et al., 1988)

Items	Explanation
<b>Mass Balance Equations for Sediment Layer</b>	
Mass Balance for water column and benthos	$\frac{\Delta(V_j C_j)}{\Delta t} = \sum_i (-Q_{ij} C_{ij}) + \sum_i (-Q_{p_{ij}} C_{ij} f_{Dj}) + \sum_i \sum_s (-w_{sij} A_{ij} C_j f_{sj}) + \sum_i (R_{ij} \Delta C_{ij})$ $+ \sum_i \left( R_{p_{ij}} \left( \frac{f_{Dj} C_j}{n_j} - \frac{f_{Di} C_i}{n_i} \right) \right) + \sum_L w_{Lj} + \sum_N w_{Nj} + \sum_B Q_{j0} C_{Bj} + \sum_K \sum_C (V_j S_{Kc_j})$
<b>Media, Dimension and Boundaries</b>	
Media	Water and sediments in lakes, estuaries, and rivers
Dimension	1D, 2D or 3D
Boundary	No information was given in the reference
<b>Numeric Solution</b>	
Numeric Solutions	Finite difference solutions: Explicit backward difference
<b>Transport Processes and Reactions</b>	
Transport	Water column and pore water advection, solids transport, Water column and pore water dispersion, point, nonpoint and boundary loads
Reaction	Kinetic transformations
<b>Parameter Estimation</b>	
Pore Water Advection into/out of the bed, Dispersion Exchange between segments and Pore Water Diffusion	$\frac{\partial M_i}{\partial t} = Q_{ij} f_{Dj} / n_i \quad \frac{\partial M_i}{\partial t} = \frac{E_{ij}(t) A_{ij}}{L_{cij}} (C_j - C_i) \quad \frac{\partial M_i}{\partial t} = \frac{E_{ij}(t) A_{ij} n_{ij}}{L_{cij} n_{ij}} (f_{Dj} C_j / n_j - f_{Di} C_i / n_i)$
Partitioning fractions	$f_s = \frac{C'_s M_s}{C} = \frac{K_{ps} M'_s}{1 + K_{pB} B' + \sum_s K_{ps} M'_s} \quad f_B = \frac{C'_B B}{C} = \frac{K_{pB} B'}{1 + K_{pB} B' + \sum_s K_{ps} M'_s}$ $f_D = \frac{C'_w n}{C} = \frac{1}{1 + K_{pB} B' + \sum_s K_{ps} M'_s}$
Koc estimation (a0=log0.6 and a1=log1)	$\log K_{oc} = a_0 + a_1 \log K_{ow} \quad K_{pB} = \frac{C_B/n}{B' C'_w} = \frac{C'_B}{C'_w} = 1.0 K_{oc}$
Equilibrium sorption to solid	$K_{ps0} = \frac{C_s/n}{M'_s C'_w} = \frac{C'_s}{C'_w} = f_{oc} K_{oc} \quad K_{ps} = \frac{K_{ps0}}{1 + M_s K_{ps0} / \theta_x}$
Equilibrium sorption to DOC	$K_{pB} = \frac{C_B/n}{B' C'_w} = \frac{C'_B}{C'_w} = 1.0 K_{oc}$
Maximum Stable step size for $\Delta t$	$\Delta t_{max} = \text{Min} \left( \frac{V_j}{\sum_i (\Delta Q_{ij}) + \sum_i (R_{ij}) + \sum_k (S_{jk} V_j / C_j)} \right)$
Net Sediment Flux Rate	$w_{BS} = A_{ij} (w_{Ri} S_i - w_{Dj} S_j)$
Biodegradation rate estimations	Table 4.9
Biodegradation	First or second order

Table C.6 Mass Balance Equations for surface sediment layer

Explanation	References
$V_2 \frac{dC_2}{dt} = k_2 V_2 C_2 - v_s A F_{p1} C_1 - v_r A C_2 - v_b A C_2 - v_d A [F_{d1} C_1 - F_{d2} C_2]$	Chapra, 1997 p.708
$V_s \frac{dC_{Ts}}{dt} = w_a A f_p C_T - w_{rs} A f_{ps} C_{Ts} + K_L A \left( \frac{f_p C_T}{\varphi} - \frac{f_{ds} C_{Ts}}{\varphi_s} \right) - w_s A C_{Ts} - K_s V_s C_{Ts}$	Thomann and DiToro, 1984
$V_{s,H} \frac{dC_s}{dt} = v_{s,H} A f_{sH} C_H - v_{r,s} A f_{sS} C_s - v_b A f_{sS} C_s - K_f A_d \left[ (f_{dS} - f_{bS}) \frac{C_s}{n_s} - (f_{dH} - f_{bH}) C_H \right]$	MICHTOX: Endicott et al., 2005
$\frac{\partial C_s}{\partial t} = -v_z \frac{\partial C_s}{\partial z} + D_s \frac{\partial^2 C_s}{\partial z^2} + r_{sorp} + r_{reac} + S(C)_{source} \quad r_{sorp} = \left( \frac{1-\epsilon}{\epsilon} \right) \rho_s \left( \frac{3}{R_p} \right) k_f (C_s - C_s^*)$ <p>reac:0 and S(C)source:0 and reac:0 and S(C)source:0</p>	Qi, 2003



## APPENDIX D

### INPUT AND OUTPUT OF THE PATHWAY FUNCTION FOR PCBs AND PBDEs

Table D.1 Input of the Pathway Function for PCBs

1.Flanked Any(3+4+5)*		2. Flanked Meta or Flanked Para(3+5)*		3. Flanked Meta*		4.Flanked Ortho*		5.Flanked Para*	
23	2	23	2	23	2	23	3	34	3
34	4	34	4	34	4	234	34	234	23
234	24	234	24	234	24	235	35	345	35
235	25	235	25	235	25	2345	345	245	25
236	26	236	26	236	26	2356	235	2345	235
345	34	345	34	345	34	23456	2345	2346	236
2345	245	2345	245	2345	245			23456	2356
2345	234	2345	234	2345	234				
2346	246	2346	246	2346	246				
2356	236	2356	236	2356	236				
23456	2346	23456	2346	23456	2346				
23	3	34	3						
234	34	234	23						
235	35	345	35						
2345	345	245	25						
2356	235	2345	235						
23456	2345	2346	236						
34	3	23456	2356						
234	23								
345	35								
245	25								
2345	235								
2346	236								
23456	2356								

Table D.1 (continued)

6. Meta Any *		7. Ortho Any *		8. Para Any *		9. Flanked or meta(1+6) *		10. Flanked or para(1+8) *		11. Double Flanked para-any	
3		2		4		23	2	23	2	345	35
23	2	23	3	24	2	34	4	34	4	2345	235
25	2	24	4	34	3	234	24	234	24	23456	2356
34	4	25	2	234	23	235	25	235	25		
35	3	26	2	345	35	236	26	236	26		
234	24	234	34	245	25	345	34	345	34		
235	25	235	35	246	26	2345	245	2345	245		
236	23	236	23	2345	235	2345	234	2345	234		
236	26	245	45	2346	236	2346	246	2346	246		
345	34	246	24	23456	2356	2356	236	2356	236		
2345	245	2345	345			23456	2346	23456	2346		
2345	234	2346	234			23	3	23	3		
2346	246	2356	235			234	34	234	34		
2356	236	23456	2345			235	35	235	35		
23456	2346					2345	345	2345	345		
						2356	356	2356	356		
						23456	2345	23456	2345		
						34	3	34	3		
						234	23	234	23		
						345	35	345	35		
						245	25	245	25		
						2345	235	2345	235		
						2346	236	2346	236		
						23456	2356	23456	2356		
						3	4	4	4		
						25	2	24	2		
						35	3	246	26		
						235	23				

Table D.1 (continued)

12.Double Flanked meta-any	13.Doubly Flanked para or doubly flanked meta	14. Singly Flanked para or singly flanked meta	15.doubly flanked meta and para+singly flanked meta+para	16.Microorganism o-17
234	345	23	234	2356
2345	2345	235	2345	235
2346	23456	236	2345	234
2356	234	245	2346	2345
23456	2345	2356	2356	2346
	2346	34	23456	23456
	2356	345	345	245
	23456	234	23	245
	245	245	25	
	34	3	26	
	2346	236	24	
			236	
			4	
			23	
			34	
			345	
			234	
			25	
			26	
			24	
			236	
			4	
			23	
			24	
			25	
			26	
			34	
			35	
			236	
			246	
			345	
			2-2	
			26-2	
			26-26	
			2356-26	
			23456-26	
			2356-2356	



Table D.2 Output of the Pathway Function for PCBs

No. of Pathways: 371												No. of Pathways: 281															
1. Flanked Any(3+4+5)*												2. Flanked Meta or Flanked Para(3+5)*															
m	d	m	d	m	d	m	d	m	d	m	d	m	d	m	d	m	d	m	d	m	d						
5	1	65	23	106	57	129	122	152	94	173	134	189	167	205	190	1	83	43	119	75	153	101	176	150	196	183	
16	4	65	24	106	67	130	83	153	103	173	142	189	156	205	191	16	4	83	44	120	72	154	103	177	132	197	176
16	6	66	25	106	78	130	87	154	103	174	132	190	158	205	192	20	6	84	46	122	56	156	106	177	134	199	174
20	6	66	28	107	68	130	90	156	105	174	135	190	163	205	193	21	5	85	42	124	70	156	106	177	147	199	177
20	11	67	26	107	79	130	107	156	106	174	143	191	158	206	194	21	7	85	47	124	72	156	106	178	147	199	178
21	5	70	26	108	59	130	109	156	109	174	149	191	161	206	195	22	8	86	41	126	77	156	114	178	151	199	187
21	7	70	31	109	57	131	84	156	114	174	164	191	164	206	196	23	9	86	43	126	78	156	118	179	152	200	176
22	8	71	27	109	63	131	88	156	118	175	135	192	159	206	199	24	10	86	48	126	79	157	105	179	152	200	179
23	9	71	32	109	70	131	108	156	126	175	144	192	161	206	203	29	9	87	44	126	81	157	107	180	138	200	186
23	14	74	31	109	79	132	84	157	105	175	148	192	165	206	205	33	6	87	49	127	79	157	122	180	141	201	176
24	10	77	35	110	59	132	91	157	107	175	161	193	163	207	196	33	8	88	50	127	80	158	108	180	146	201	179
29	9	77	37	110	64	132	110	157	122	176	136	193	164	207	197	35	11	90	49	128	85	158	110	180	153	202	179
33	6	78	35	110	71	133	92	157	126	176	145	193	165	207	200	37	15	91	51	129	83	158	115	181	139	203	183
33	8	81	37	111	72	133	111	158	108	176	150	194	170	207	201	37	14	92	52	129	86	158	119	181	147	203	185
35	11	83	43	111	80	134	83	158	110	177	130	194	172	208	199	40	16	94	53	129	97	159	107	182	148	203	187
37	15	83	44	112	57	134	84	158	115	177	132	194	180	208	200	41	16	95	53	130	97	159	111	182	148	205	190
38	14	83	57	112	59	134	112	159	107	177	147	195	170	208	202	42	17	97	44	130	87	159	120	183	144	205	191
40	20	84	59	114	60	135	94	159	111	177	163	195	171	209	206	43	18	99	49	131	88	163	110	183	145	205	193
41	16	85	42	114	63	135	95	159	120	178	135	195	173	209	207	46	18	101	52	131	88	163	112	185	144	206	195
41	17	85	47	114	74	135	113	159	127	178	135	195	181	209	208	48	18	102	53	132	84	163	117	185	151	206	196
41	31	85	66	114	81	138	87	161	113	178	151	195	181	209	208	48	18	105	55	132	91	164	110	186	145	206	199
42	17	86	41	115	64	138	97	163	109	178	165	195	190	209	209	55	20	105	56	133	92	164	113	186	145	206	203
42	25	86	43	115	75	138	99	163	110	179	135	196	171	209	209	55	25	105	60	134	84	165	113	187	149	207	197
43	18	86	48	116	61	138	118	163	112	179	136	196	174	209	209	56	20	105	66	134	93	167	118	187	151	207	200
43	34	87	44	116	62	139	91	163	117	179	152	196	175	209	209	56	22	106	55	135	94	167	120	189	156	207	201
44	18	87	49	116	65	139	100	164	110	180	138	196	182	209	209	56	33	106	57	135	95	167	124	189	157	208	200
44	26	87	70	117	63	141	87	164	113	180	141	196	183	209	209	57	26	106	67	138	87	170	128	189	159	208	201
46	19	88	50	117	64	141	92	165	111	180	146	196	191	209	209	59	27	107	68	138	87	170	129	189	167	208	202
46	27	90	49	118	67	141	101	165	113	180	153	197	176	209	209	60	22	108	59	138	99	170	130	190	158	209	207
48	18	90	68	118	70	141	124	167	118	180	167	199	172	209	209	60	28	109	57	139	91	170	138	190	163	209	208
55	20	91	51	118	74	142	86	167	120	181	139	199	174	209	209	61	21	109	63	139	100	171	131	191	158	209	208
55	25	92	52	119	75	142	88	167	124	181	147	199	177	209	209	61	23	109	70	141	87	171	132	191	161	209	208
55	35	92	72	120	72	142	93	170	128	182	148	199	178	209	209	61	29	110	59	141	92	171	139	191	164	209	208
56	20	93	43	122	56	143	94	170	129	182	154	199	187	209	209	62	24	110	64	141	101	172	130	192	161	209	208
56	22	94	53	122	78	143	102	170	130	183	144	199	193	209	209	63	31	110	71	142	88	172	133	192	165	209	208
56	33	94	73	124	70	144	95	170	138	183	149	200	174	209	209	64	32	111	72	142	88	172	133	192	165	209	208
56	35	95	53	124	72	144	103	170	156	183	154	200	176	209	209	65	24	112	59	143	94	172	141	193	163	209	208
57	26	95	44	126	77	145	104	170	157	185	141	200	179	209	209	65	25	113	73	143	102	173	131	193	165	209	208
59	27	97	48	126	78	146	92	171	131	185	144	200	186	209	209	66	28	114	60	144	95	173	134	194	170	209	208
60	22	97	67	126	79	146	101	171	132	185	151	201	175	209	209	67	26	114	63	144	100	173	142	194	172	209	208
60	28	99	49	126	81	146	120	171	139	186	143	201	179	209	209	70	26	114	74	145	104	174	132	194	180	209	208
60	37	101	52	127	79	147	90	171	158	186	145	201	179	209	209	70	31	115	64	146	92	174	135	195	171	209	208
61	21	102	53	127	80	147	91	172	130	186	152	202	178	209	209	71	27	115	75	146	101	174	143	195	173	209	208
61	23	105	55	128	85	148	103	172	133	187	146	202	179	209	209	71	32	116	62	147	91	174	143	195	173	209	208
61	29	105	56	128	105	149	95	172	141	187	149	203	180	209	209	74	31	116	65	148	103	175	144	195	181	209	208
61	36	105	60	129	83	149	102	172	146	187	151	203	183	209	209	77	35	117	64	149	95	175	144	196	171	209	208
62	24	105	66	129	86	150	104	172	159	189	156	203	185	209	209	78	37	118	67	149	102	175	144	196	174	209	208
63	31	105	77	129	97	151	129	173	129	189	157	203	187	209	209	78	35	118	70	150	104	176	146	196	175	209	208
64	32	106	55	129	106	151	95	173	131	189	159	205	189	209	209	81	37	118	74	151	95	176	145	196	182	209	208

Table D.2 (continued)

No. of Pathways: 170												No. of Pathways: 90												No. of Pathways: 111												No. of Pathways: 229											
3. Flanked Meta*												4. Flanked Ortho*												5. Flanked Para*												6. Meta Any*											
m	d	m	d	m	d	m	d	m	d	m	d	m	d	m	d	m	d	m	d	m	d	m	d	m	d	m	d	m	d	m	d	m	d	m	d	m	d	m	d	m	d	m	d	m	d		
5	1	107	68	158	115	196	171	16	6	152	94	5	143	94	200	179	1	70	31	113	59	156	118	190	158																						
16	4	109	63	158	119	196	182	20	11	156	126	29	9	144	95	201	179	6	70	33	113	73	157	105	191	158																					
20	6	109	70	159	107	196	183	23	14	157	126	33	6	146	92	203	185	9	71	32	114	60	158	115	192	161																					
21	7	110	64	159	120	199	174	40	20	159	127	35	11	149	95	203	187	16	72	26	114	74	158	119	193	163																					
22	8	110	71	163	110	199	177	41	33	163	109	38	14	153	101	205	192	18	72	34	115	75	159	106	193	164																					
23	9	111	72	163	117	199	187	42	25	165	111	41	16	154	103	205	193	20	73	27	116	62	159	107	194	170																					
24	10	112	59	164	110	200	176	43	34	170	156	48	18	156	106	206	199	20	77	37	117	64	159	120	194	180																					
33	8	113	73	166	113	200	186	44	26	170	157	55	20	156	109	207	200	21	78	35	118	74	161	108	195	171																					
37	15	114	60	167	118	201	176	46	27	171	158	56	20	157	107	207	201	22	78	38	119	75	163	110	195	181																					
40	16	114	74	170	128	202	179	55	35	172	159	60	22	157	122	208	202	23	79	35	120	67	163	117	196	171																					
41	17	115	75	170	138	203	183	56	35	173	129	61	23	158	108	209	208	23	81	37	122	56	164	110	196	182																					
42	17	116	62	171	139	205	190	60	37	174	164	62	24	158	110	209	208	24	10	83	40	124	70	165	112	196	183																				
43	18	117	64	172	130	205	191	61	38	175	161	66	25	159	111			25	7	83	43	126	77	165	113	199	174																				
44	18	118	74	172	141	206	195	65	23	177	130	67	26	161	113			26	6	83	44	126	81	167	118	199	177																				
46	19	119	75	172	146	206	196	83	57	177	163	70	26	163	112			26	6	84	46	127	78	170	128	199	187																				
55	25	122	56	173	131	206	203	84	59	178	133	71	27	164	113			27	10	85	47	127	79	170	138	200	176																				
56	22	124	70	173	142	207	197	85	66	178	165	74	31	167	120			31	8	86	41	128	85	171	139	200	186																				
57	33	126	77	174	132	208	200	87	70	179	135	77	35	167	124			33	8	86	48	129	86	172	129	201	176																				
59	27	127	79	174	149	209	207	92	72	185	141	86	43	170	130			37	15	87	49	130	87	172	141	203	183																				
60	26	128	85	175	144			93	43	186	143	87	44	171	131			40	16	88	50	130	90	172	146	205	190																				
61	21	129	86	175	148			94	73	187	146	97	44	171	132			41	17	90	42	131	88	173	151	205	191																				
61	21	129	97	176	145			97	67	190	156	99	49	172	133			42	17	90	49	132	91	173	142	206	195																				
63	31	130	87	176	150			105	77	192	159	101	52	173	134			43	16	91	51	133	83	174	132	206	196																				
64	32	130	90	177	132			106	78	194	189	102	53	174	135			44	18	92	43	133	92	174	143	206	203																				
65	24	131	88	177	147			107	79	195	170	105	55	175	135			44	16	92	44	134	84	174	149	207	197																				
66	28	132	91	178	135			109	79	195	190	105	56	176	136			44	18	92	52	134	93	175	131	208	200																				
70	31	133	92	178	151			111	80	196	191	106	57	177	136			46	19	94	46	135	84	175	144	208	201																				
71	32	134	84	179	136			112	57	199	172	108	59	180	141			49	17	94	53	135	94	175	148	209	207																				
77	37	134	93	179	152			114	81	199	193	109	57	180	146			52	18	95	53	135	95	176	145																						
78	35	135	94	180	138			116	61	200	174	110	59	181	147			53	19	97	48	138	99	176	150																						
81	37	135	95	180	153			117	63	201	175	114	63	182	148			55	21	101	48	139	100	177	132																						
83	43	138	99	181	139			122	78	202	178	115	64	183	144			55	25	103	50	141	86	177	147																						
83	44	139	100	182	154			128	105	203	180	116	65	183	149			56	22	105	60	141	87	178	134																						
84	46	141	87	183	154			129	106	205	189	118	67	185	151			56	31	105	66	141	101	178	135																						
85	47	141	101	185	144			129	122	206	194	118	70	186	152			57	20	106	55	142	88	178	151																						
86	41	142	88	186	145			130	107	206	205	120	72	187	151			57	23	106	61	143	102	179	136																						
86	48	143	102	187	149			130	109	207	196	124	72	189	159			57	26	106	67	144	88	179	152																						
87	49	144	103	189	156			131	108	208	199	126	78	190	163			59	24	107	55	144	103	180	138																						
88	50	145	104	189	157			132	110	209	206	126	79	191	161			59	27	107	68	145	104	180	138																						
90	49	146	101	189	167			133	111	209	206	127	80	191	164			60	28	108	62	146	97	181	139																						
91	51	147	91	190	158			134	83	210	176	129	83	192	165			61	21	109	56	146	101	182	154																						
92	52	148	103	191	158			134	112	210	176	130	83	192	165			61	29	109	63	147	91	183	154																						
94	53	149	102	192	161			135	113	210	177	131	84	194	172			63	22	109	70	148	103	185	142																						
95	53	150	104	193	163			138	118	211	178	132	84	195	173			63	31	110	64	149	102	185	144																						
97	48	151	95	193	164			141	124	212	179	138	87	195	177			64	32	110	71	150	104	186	145																						
105	60	156	105	194	170			142	186	213	180	138	97	196	174			65	24	111	57	151	93	187	149																						
105	66	156	114	194	180			146	120	214	181	139	91	196	175			66	28	111	72	151	95	188	156																						
106	55	156	118	195	171			147	90	214	181	141	92	197	176			67	29	112	59	156	105	189	157																						
106	67	157	105	195	181			151	92	215	182	142	93	199	178			68	25	112	65	156	114	189	167																						

Table D.2 (continued)

No. of Pathways: 193												No. of Pathways: 150												Pathways No:413											
7. Ortho Any*												8. Para Any*												9. Flanked or meta(1+6)*											
m	d	m	d	m	d	m	d	m	d	m	d	m	d	m	d	m	d	m	d	m	d	m	d	m	d	m	d	m	d	m	d	m	d		
4	1	66	37	122	78	174	129	7	1	101	52	161	113	5	1	55	35	85	66	110	64	131	108	156	114	174	143	191	161	206	203				
9	1	70	33	128	105	174	164	8	1	102	53	163	112	6	1	56	20	86	41	110	71	132	84	156	118	174	149	191	164	206	205				
10	1	71	33	129	106	175	165	17	4	103	53	164	113	9	1	56	22	86	43	111	72	132	84	156	118	174	149	191	164	206	196				
16	5	72	34	129	122	175	161	21	5	104	54	167	120	16	4	56	33	86	48	111	72	132	110	157	105	175	131	192	161	207	197				
16	6	73	34	130	107	176	131	22	5	105	55	167	124	16	6	56	35	87	41	111	80	133	83	157	107	175	135	192	165	207	200				
17	7	75	28	130	109	176	132	25	6	105	56	170	129	18	4	57	20	87	44	112	59	133	92	157	122	175	144	193	163	207	201				
17	8	83	57	131	108	177	130	28	7	106	57	170	130	20	5	57	23	87	49	112	65	133	111	157	126	175	148	193	164	208	199				
18	4	84	40	132	110	177	163	28	8	108	59	171	131	20	6	57	26	87	70	113	59	134	84	158	108	175	141	193	165	208	200				
18	9	84	59	133	111	178	133	29	9	109	59	171	132	20	11	59	24	88	50	113	73	134	93	158	110	176	136	194	170	208	201				
19	4	85	60	134	83	178	165	31	9	110	59	172	133	21	5	59	27	90	42	114	60	134	112	158	115	176	136	194	172	208	202				
19	10	85	66	134	112	179	134	32	10	114	61	173	134	21	7	60	22	90	49	114	63	135	84	158	119	176	150	194	180	209	206				
20	11	86	61	135	83	179	135	33	6	114	63	174	135	22	8	60	28	90	68	114	74	135	94	159	106	177	132	194	189	209	207				
23	14	87	41	135	113	180	167	35	11	115	62	175	135	23	8	60	37	91	51	114	81	135	95	159	107	177	134	195	170	209	208				
24	5	87	70	136	84	183	138	38	14	115	64	176	136	23	9	61	21	92	43	115	64	135	113	159	111	177	147	195	171						
26	6	88	41	138	118	185	141	41	16	116	65	177	134	23	14	61	23	92	44	115	75	138	87	159	120	177	163	195	173						
27	6	88	62	139	85	185	142	42	16	117	65	180	141	24	10	61	29	92	52	116	61	138	87	159	127	178	134	195	177						
28	15	90	63	139	115	186	142	47	17	118	67	180	146	25	7	61	38	92	72	116	62	138	99	161	108	178	135	195	181						
31	8	90	68	141	86	186	143	48	18	118	70	181	142	26	6	62	24	94	46	116	65	138	118	161	113	178	151	195	190						
32	8	91	42	141	124	187	146	49	18	119	71	181	147	26	9	63	22	94	53	117	64	139	91	163	110	178	165	196	171						
34	14	91	64	142	86	190	156	50	19	120	72	182	143	27	10	63	31	94	73	118	67	139	100	163	112	179	136	196	174						
40	20	92	43	142	116	191	157	51	19	124	72	182	148	29	9	64	32	95	53	118	70	141	86	163	117	179	152	196	175						
41	21	92	72	143	86	192	159	55	20	126	78	183	144	31	8	65	24	97	44	118	74	141	87	164	110	180	138	196	182						
41	33	93	43	144	87	194	189	56	20	126	79	183	149	33	6	66	25	97	48	119	75	141	92	164	113	180	141	196	183						
42	22	93	65	144	88	195	170	60	21	127	80	185	151	33	8	66	28	97	67	120	67	141	101	165	112	180	146	196	191						
42	25	94	43	145	88	195	190	60	22	129	83	186	152	34	6	67	26	99	49	120	72	141	124	165	113	180	153	197	176						
43	23	94	73	146	120	196	170	61	23	130	83	187	151	35	11	67	29	101	48	122	56	142	86	167	118	180	167	199	174						
43	34	95	44	147	90	196	191	62	24	131	84	189	159	37	15	68	25	101	52	122	78	142	88	167	120	181	139	199	177						
44	16	97	67	147	117	197	171	63	23	132	84	190	163	38	14	70	26	102	53	124	70	142	93	167	124	181	147	199	178						
44	26	99	74	148	90	199	172	64	24	138	87	191	161	40	16	70	31	103	50	124	72	143	94	170	128	182	148	199	187						
46	16	100	47	149	97	199	193	66	25	138	97	191	164	40	20	70	33	105	55	126	77	143	102	170	129	182	154	199	193						
46	27	100	75	150	91	200	173	66	33	139	88	192	163	41	16	71	27	105	56	126	78	144	88	170	130	183	144	200	174						
47	28	101	48	151	92	200	174	67	26	139	91	193	165	41	17	71	32	105	60	126	79	144	95	170	138	183	149	200	176						
48	29	102	48	151	93	201	175	68	34	141	92	194	172	41	33	72	26	105	66	126	81	144	103	170	156	183	154	200	179						
49	17	103	49	152	93	201	177	70	26	142	94	195	173	42	17	72	34	105	77	127	78	145	104	170	157	185	141	200	186						
49	31	103	50	152	94	202	178	71	27	143	94	195	177	42	25	73	27	106	57	127	79	146	92	171	131	185	142	201	176						
50	17	104	50	154	99	203	180	74	29	144	95	196	174	43	16	74	31	106	57	127	80	146	97	171	132	185	144	201	179						
51	17	104	51	156	126	205	189	74	31	146	95	196	175	43	18	77	35	106	61	128	85	146	101	171	139	185	151	202	179						
51	32	105	77	157	126	206	194	75	32	147	93	197	176	43	34	77	37	106	67	128	85	146	120	171	158	186	143	203	180						
52	18	106	78	158	105	206	205	77	35	148	94	199	178	44	16	78	35	106	78	129	86	148	103	172	130	186	145	203	183						
53	18	107	79	159	127	207	195	81	38	149	95	200	179	44	18	78	38	107	55	129	86	148	103	172	130	186	152	203	185						
53	19	108	55	161	107	207	196	85	41	153	101	201	179	44	26	79	35	107	68	129	97	149	95	172	133	187	149	203	187						
54	19	109	79	163	109	208	199	85	42	154	102	201	185	46	19	81	37	107	79	129	106	149	102	172	141	187	151	205	189						
55	35	110	56	164	122	209	206	86	43	154	103	203	187	46	27	83	40	108	59	129	122	150	104	172	146	189	156	205	190						
56	35	111	80	165	111			87	44	156	106	205	192	48	18	83	43	108	62	130	132	151	93	172	145	189	157	205	191						
59	20	112	57	170	156			90	43	156	109	205	193	49	17	83	44	109	56	130	87	151	95	173	129	189	159	205	192						
60	37	114	81	170	157			97	44	157	107	206	199	52	18	83	57	109	57	130	90	153	101	173	131	189	167	205	193						
61	38	115	60	171	128			99	48	157	122	207	200	53	19	84	46	109	63	130	107	154	103	173	134	190	158	206	194						
62	21	116	61	171	158			99	49	158	108	207	201	55	20	84	59	109	70	130	109	156	105	173	142	190	158	206	195						
64	22	117	63	172	159			100	50	158	110	208	202	55	21	85	42	109	79	131	84	156	106	174	132	190	163	206	196						
65	23	119	66	173	129			100	51	159	111	209	208	55	25	85	47	110	59	131	88	156	109	174	135	191	158	206	199						

Table D.2 (continued)

No. of Pathways: 393												No. of Pathways: 44												No. of Pathways: 60												No. of Pathways: 104											
10. Flanked or para(4+8)*												11. Double flanked para-any												12. Double flanked meta-any												13. Doubly flanked para or doubly flanked meta											
m	d	m	d	m	d	m	d	m	d	m	d	m	d	m	d	m	d	m	d	m	d	m	d	m	d	m	d	m	d	m	d	m	d	m	d	m	d	m	d	m	d						
5	1	56	33	88	50	115	64	138	97	161	113	180	138	196	175	38	14	21	7	196	183	21	7	172	132	172	132	208	201																		
7	1	56	35	90	43	115	75	138	99	163	110	180	141	196	182	61	23	41	17	199	187	38	14	172	146	172	146	208	202																		
8	1	57	26	90	49	116	61	138	118	163	112	180	146	196	183	86	43	55	23	200	176	41	17	173	131	173	131	209	207																		
16	4	59	27	90	68	116	62	139	88	163	117	180	153	196	191	106	57	60	28	203	183	55	25	173	134	173	134	209	208																		
16	6	60	21	91	51	116	65	139	91	164	110	180	167	197	176	114	63	61	29	205	191	60	28	174	135	174	135																				
17	4	60	22	92	52	117	64	139	100	164	113	181	139	199	174	116	65	85	47	206	196	61	23	174	149																						
20	6	60	28	92	72	117	65	141	87	165	113	181	142	199	177	124	72	86	48	207	197	85	47	176	150																						
20	11	60	37	94	53	118	67	141	92	167	118	181	147	199	178	126	79	87	49	207	197	85	47	177	147																						
21	5	61	21	94	73	118	70	141	101	167	120	182	143	199	187	127	80	88	50	208	201	86	43	177	147																						
21	7	61	23	95	53	118	74	141	124	167	124	182	148	199	193	129	83	105	66	209	207	86	48	180	146																						
22	5	61	29	97	44	119	71	142	86	170	128	182	154	200	174	141	92	106	67	209	207	87	49	180	153																						
22	8	61	38	97	48	119	75	142	88	170	129	183	144	200	176	142	93	107	68	209	207	88	50	181	139																						
23	9	62	24	97	67	120	72	142	93	170	130	183	149	200	179	143	94	114	74	209	207	88	50	181	139																						
23	14	63	23	99	48	122	56	143	94	170	136	183	154	200	186	156	109	115	75	209	207	88	50	181	139																						
24	10	63	31	99	49	122	78	143	102	170	158	185	141	201	176	157	107	115	75	209	207	88	50	181	139																						
25	6	64	24	100	50	124	70	144	95	170	157	185	144	201	179	159	111	128	85	209	207	106	67	182	148																						
28	7	64	32	100	51	124	72	144	103	171	131	185	151	202	179	164	113	129	97	209	207	107	68	183	154																						
28	8	65	24	101	52	126	77	145	104	171	132	186	143	203	180	167	120	130	90	209	207	114	74	185	151																						
29	9	66	25	102	53	126	78	146	92	171	139	186	145	203	183	170	130	132	91	209	207	115	75	186	145																						
31	9	66	28	103	53	126	79	146	101	171	158	186	152	203	185	172	133	138	99	209	207	116	62	186	145																						
32	10	66	33	104	54	126	81	146	120	172	130	187	149	203	187	173	134	139	100	209	207	116	65	186	145																						
33	6	67	26	105	55	127	79	147	91	172	133	187	151	205	189	174	135	141	101	209	207	124	72	189	167																						
33	8	68	34	105	56	127	80	147	93	172	141	189	156	205	190	180	146	142	88	209	207	126	79	190	158																						
35	11	70	26	105	60	128	85	148	94	172	146	189	157	205	191	181	147	143	102	209	207	127	80	190	163																						
37	15	70	31	105	66	128	105	148	103	172	159	189	159	205	192	182	148	144	103	209	207	128	85	191	161																						
38	14	71	27	105	77	129	83	149	95	173	129	189	167	205	193	185	151	145	104	209	207	129	83	192	161																						
40	16	71	32	106	55	129	86	149	102	173	131	190	156	206	194	186	152	156	118	209	207	129	83	192	165																						
40	20	74	29	106	57	129	97	150	104	173	134	190	158	206	195	189	159	158	119	209	207	130	90	193	165																						
41	16	74	31	106	67	129	106	151	95	173	142	190	163	206	196	190	163	159	120	209	207	132	91	194	172																						
41	17	75	31	106	78	129	122	153	101	174	132	191	158	206	196	191	161	170	138	209	207	138	99	194	180																						
41	33	77	35	107	68	130	83	154	102	174	135	191	161	206	203	192	169	171	139	209	207	139	100	195	171																						
42	16	77	37	107	79	130	87	154	103	174	143	191	164	206	203	193	165	172	146	209	207	141	92	195	177																						
42	17	78	35	108	59	130	90	156	105	174	149	192	159	207	196	194	172	173	131	209	207	141	101	195	181																						
42	25	81	37	109	57	130	107	156	106	174	164	192	161	207	197	195	177	174	149	209	207	142	88	196	175																						
43	18	81	38	109	63	130	109	156	109	175	135	192	165	207	200	199	175	175	148	209	207	142	93	196	182																						
43	34	83	43	109	70	131	84	156	114	175	144	193	163	207	201	199	178	176	150	209	207	143	94	196	183																						
44	18	83	44	109	79	131	88	156	118	175	148	193	164	208	199	200	179	177	147	209	207	143	102	199	178																						
44	26	83	57	110	59	131	108	156	126	175	161	193	165	208	200	203	187	180	153	209	207	144	103	199	187																						
46	19	84	46	110	64	132	84	157	105	176	136	194	170	208	201	205	192	181	139	209	207	145	104	200	176																						
46	27	84	59	110	71	132	91	157	107	176	145	194	172	208	202	205	193	182	154	209	207	156	109	200	179																						
47	17	85	41	111	72	132	110	157	122	176	150	194	180	209	206	206	199	183	154	209	207	156	118	203	187																						
48	18	85	42	111	80	133	92	157	126	177	132	194	189	209	207	207	201	185	144	209	207	157	107	203	187																						
49	18	85	47	112	59	133	111	158	108	177	147	195	170	209	208	208	202	186	145	209	207	158	119	205	191																						
50	19	85	66	113	73	134	84	158	110	177	134	195	171	209	208	209	209	189	167	209	207	159	111	205	192																						
51	19	86	41	114	60	134	93	158	115	177	135	195	173	209	208	209	209	190	158	209	207	159	120	205	193																						
55	20	86	43	114	61	134	112	158	119	178	135	195	177	209	208	209	209	192	161	209	207	164	113	206	196																						
55	25	86	48	114	63	135	94	159	107	178	151	195	181	209	206	206	206	194	180	209	207	167	120	206	199																						
55	35	87	44	114	74	135	95	159	111	178	165	195	190	209	206	206	206	195	190	209	207	170	130	206	203																						
56	20	87	49	114	81	135	113	159	120	179	136	196	171	209	206	206	206	196	191	209	207	170	138	207	197																						
56	22	87	70	115	62	138	87	159	127	179	152	196	174	209	206	206	206	196	191	209	207	171	139	207	201																						



Table D.2 (continued)

No. of Pathways: 179										No. of Pathways: 283										No. of Pathways: 48			
14. Singly Flanked para or singly flanked meta										15. Doubly flanked meta and para+singly flanked meta+para										16. Microorganism o-			
m	d	m	d	m	d	m	d	m	d	m	d	m	d	m	d	m	d	m	d	m	d	m	d
5	1	87	44	134	84	178	135	16	4	117	64	146	101	175	135	196	174	21	7				
16	4	90	49	134	93	178	151	16	4	35	118	66	147	91	175	144	174	23	21				
20	6	91	51	135	94	179	136	20	6	37	118	67	148	103	175	148	196	29	7				
21	5	92	52	135	95	179	152	21	5	83	43	70	149	91	176	136	183	29	9				
22	8	94	53	138	85	180	141	21	7	83	44	74	149	95	176	145	197	61	29				
23	9	95	53	138	87	183	139	22	8	84	46	74	149	102	176	150	199	65	23				
24	10	97	42	138	97	183	144	23	9	85	42	75	149	104	177	132	199	128	85				
29	7	97	44	139	91	183	149	24	10	85	47	72	151	104	177	134	199	130	90				
29	9	97	48	144	95	187	147	29	7	86	43	72	151	95	177	147	200	176	130				
33	6	99	47	146	90	187	149	29	9	86	48	70	153	101	178	135	200	179	133				
33	8	99	49	146	92	187	151	33	6	87	44	72	154	100	178	151	200	186	138				
35	11	101	49	146	101	189	156	33	8	87	49	77	154	103	179	136	201	176	138				
37	15	101	52	147	91	191	158	35	11	88	50	78	156	106	179	152	201	179	138				
40	16	102	51	148	103	191	164	37	15	90	49	79	156	109	180	141	202	179	146				
41	16	102	53	149	91	193	163	38	14	91	51	81	156	114	180	146	203	181	146				
42	17	105	55	149	95	193	164	40	16	92	52	79	156	118	180	153	203	181	146				
43	18	105	56	149	102	195	173	41	16	94	53	80	157	105	181	153	203	185	153				
44	18	105	60	150	104	196	174	41	17	95	53	85	157	107	181	147	203	187	153				
46	19	108	59	151	95	197	176	42	17	97	42	83	157	122	182	148	205	190	170				
48	17	109	57	153	99	199	174	43	18	97	44	86	158	108	182	154	205	191	171				
48	18	109	63	153	101	200	186	44	18	97	48	86	158	110	183	139	205	192	172				
55	20	109	70	154	100	201	176	46	19	99	47	83	158	115	183	144	205	193	172				
56	20	110	59	154	103	201	179	48	17	99	49	87	158	119	183	149	206	196	175				
56	22	110	64	156	106	202	179	48	18	101	49	90	159	111	183	154	206	199	175				
56	33	110	71	156	114	203	181	55	20	101	52	84	159	120	185	144	206	203	177				
57	26	111	72	157	105	203	185	55	23	102	51	88	161	113	185	151	207	197	177				
59	27	112	59	157	122	205	190	56	20	102	53	84	163	110	186	145	207	200	178				
60	22	113	73	158	108	207	200	56	22	105	55	91	163	112	186	152	207	201	178				
62	24	115	64	158	110	208	200	56	33	105	56	92	163	117	187	147	208	200	180				
63	31	117	64	158	115	208	200	57	26	105	60	84	164	110	187	149	208	201	180				
64	32	118	66	161	113	209	200	59	27	105	66	93	164	113	187	151	208	202	183				
65	24	118	66	163	110	210	200	60	22	106	57	94	165	113	189	156	209	207	183				
66	25	118	70	163	112	210	200	60	28	106	67	135	165	118	189	159	209	207	183				
66	28	118	74	163	117	210	200	61	23	107	68	138	167	120	189	167	209	207	183				
67	25	119	75	164	110	211	200	61	29	108	59	138	167	120	189	167	209	207	183				
67	26	120	68	165	113	211	200	62	24	109	57	138	167	124	190	158	209	208	187				
70	26	120	72	167	118	212	200	63	31	109	57	138	167	129	190	163	209	208	187				
70	31	122	56	167	124	212	200	64	32	109	63	138	167	130	191	158	209	208	187				
71	27	124	70	170	129	213	200	64	32	109	70	139	161	138	191	158	209	208	187				
71	32	126	77	171	131	213	200	65	24	110	59	139	161	131	191	164	209	207	183				
74	28	126	78	171	132	213	200	66	25	110	64	141	161	132	192	161	209	207	183				
74	31	126	81	172	141	213	200	66	28	110	71	141	161	139	192	165	209	207	183				
74	31	126	81	172	141	213	200	67	23	111	72	142	161	133	193	163	209	207	183				
77	35	127	79	173	142	214	200	67	26	111	72	142	161	133	193	163	209	207	183				
77	37	129	86	174	143	214	200	70	26	112	59	142	161	141	193	164	209	207	183				
78	35	130	83	175	135	215	200	70	31	114	73	143	161	146	193	165	209	207	183				
81	37	130	87	175	144	215	200	71	27	114	74	144	161	144	194	180	209	207	183				
83	43	131	84	176	144	215	200	71	32	115	64	144	161	142	195	171	209	207	183				
83	44	131	88	176	145	215	200	74	28	115	75	145	161	142	195	171	209	207	183				
84	46	132	84	177	145	215	200	74	31	116	62	146	161	143	195	173	209	207	183				
85	42	133	92	177	134	215	200	77	35	116	65	146	161	149	195	181	209	207	183				

Table D.2 (continued)

17. Microorganism DFI			18. Microorganism DEH10			19. Microorganism SF1			20. Microorganism CBDB1			21. Microorganism Deh. m. 195			22. Microorganism SF2			23. DEH10+SF1			24. o17+DF1			25. DEH10+SF1+o17+DF1			
m	d		m	d		m	d		m	d		m	d		m	d		m	d		m	d		m	d		
21	7		49	53		21	7		100	100		188	75		50	151		135	94		21	21		7	21		
38	14		99	47	68	29	9	141	92	195	181	115	50	151	183	154	92	135	94	21	21	7	21	21	7	21	7
41	17		101	49	91	33	6	142	88	196	175	116	75	183			154	149	102	29	29	7	29	29	7	29	7
61	23		102	51	92	35	11	142	93	199	178	116	62	183				174	149	29	29	9	29	29	9	29	9
86	43		132	91	130	38	14	143	94	200	176	139	100	100				180	146	61	61	23	61	61	23	61	23
88	50		138	99	147	41	17	144	103	200	179	142	88	88				180	153	29	29	61	29	29	61	29	61
128	85		146	90	154	48	18	145	104	203	183	142	93	93						128	85	128	85	128	85	128	85
138	99		151	95	170	55	25	146	92	203	185	144	103	103						138	85	138	85	138	85	138	85
143	94		153	99	170	56	20	149	95	203	187	145	104	104						138	87	138	87	138	87	138	87
145	104				187	60	28	153	101	205	191	158	119	119						138	99	138	99	138	99	138	99
157	107					61	23	154	103	205	192	173	131	131						170	170	170	170	170	170	170	170
167	120					66	25	156	106	205	193	173	134	134						170	171	171	171	171	171	171	171
170	130					67	26	157	107	206	196	176	148	148						180	180	180	180	180	180	180	180
171	139					70	26	157	107	206	199	176	150	150						180	180	180	180	180	180	180	180
180	146					71	27	158	108	207	197	181	139	139						180	180	180	180	180	180	180	180
183	154					74	31	158	119	207	201	181	147	147						180	180	180	180	180	180	180	180
189	159					77	35	159	111	208	201	183	154	154						183	183	183	183	183	183	183	183
191	161					85	47	164	113	208	202	185	144	144						183	183	183	183	183	183	183	183
194	172					86	43	167	120	209	207	185	151	151						194	194	194	194	194	194	194	194
195	181					87	44	167	124	209	208	186	145	145						194	194	194	194	194	194	194	194
196	175					87	49	170	130			186	152	152						195	195	195	195	195	195	195	195
196	182					88	50	171	139			190	158	158						196	196	196	196	196	196	196	196
205	192					97	44	172	133			192	163	163						196	196	196	196	196	196	196	196
						99	49	173	131			192	161	161						203	203	203	203	203	203	203	203
						101	52	173	134			195	171	171						203	203	203	203	203	203	203	203
						102	53	174	135			195	171	171						206	206	206	206	206	206	206	206
						105	55	175	148			196	182	182						206	206	206	206	206	206	206	206
						105	66	176	150			196	182	182						206	206	206	206	206	206	206	206
						106	57	177	147			200	176	176						206	206	206	206	206	206	206	206
						107	68	180	141			200	179	179						206	206	206	206	206	206	206	206
						109	57	180	146			203	183	183						206	206	206	206	206	206	206	206
						114	63	181	139			203	187	187						206	206	206	206	206	206	206	206
						115	75	181	147			205	191	191						206	206	206	206	206	206	206	206
						116	62	182	148			205	193	193						206	206	206	206	206	206	206	206
						116	65	183	144			206	196	196						206	206	206	206	206	206	206	206
						118	67	183	154			206	199	199						206	206	206	206	206	206	206	206
						118	70	185	144			207	197	197						206	206	206	206	206	206	206	206
						120	72	185	151			207	201	201						206	206	206	206	206	206	206	206
						124	72	186	145			208	201	201						206	206	206	206	206	206	206	206
						126	78	186	152			208	202	202						206	206	206	206	206	206	206	206
						126	79	189	159			209	207	207						206	206	206	206	206	206	206	206
						127	80	190	158			209	207	207						206	206	206	206	206	206	206	206
						128	85	190	163			209	208	208						206	206	206	206	206	206	206	206
						129	83	191	161			209	208	208						206	206	206	206	206	206	206	206
						130	83	192	161			209	208	208						206	206	206	206	206	206	206	206
						130	90	192	165			209	208	208						206	206	206	206	206	206	206	206
						132	84	193	165			209	208	208						206	206	206	206	206	206	206	206
						132	91	194	172			209	208	208						206	206	206	206	206	206	206	206
						138	87	195	171			209	208	208						206	206	206	206	206	206	206	206
						138	99	195	177			209	208	208						206	206	206	206	206	206	206	206

m:mother, d: daughter

Table D.3 Input of the Pathway Function for PBDEs

1. Flanked Any(3+4+5)*	2. Flanked Meta or Flanked Para(3+5)*	3. Flanked Meta*	4. Flanked Ortho*	5. Flanked Para*
23	23	23	23	34
34	34	34	234	234
234	234	234	235	345
235	235	235	2345	245
236	236	236	2356	2345
345	345	345	23456	2346
2345	2345	2345		23456
2346	2346	2346		2356
2356	2356	2356		
23456	23456	23456		
23	34			
234	234			
235	345			
2345	245			
2356	2345			
23456	2346			
34	3			
234	23			
345	35			
245	25			
2345	235			
2346	2346			
23456	2356			

Table D.3 (continued)

6. Meta Any*		7. Ortho Any*		8. Para Any*		9. Flanked or meta(1+6)*		10. Flanked or para(1+8)*		11. Double Flanked para-any	
3	2	4	23	4	23	2	23	2	23	2	345
23	23	24	34	2	34	4	34	4	34	4	2345
25	24	34	4	3	234	24	234	24	234	24	23456
34	25	234	2	23	235	25	235	25	235	25	
35	26	345	2	35	236	26	236	26	236	26	
234	234	245	34	25	345	34	345	34	345	34	
235	235	246	35	26	2345	245	2345	245	2345	245	
235	236	2345	23	235	2345	234	2345	234	2345	234	
236	245	2346	45	236	2346	246	2346	246	2346	246	
345	246	23456	24	2356	2356	236	2356	236	2356	236	
2345	2345	345	345	2356	23456	2346	23456	2346	23456	2346	
2345	2346	234	234		23	3	23	3	23	3	
2346	2356	2356	235		234	34	234	34	234	34	
2356	23456	23456	2345		235	35	235	35	235	35	
23456					2345	345	2345	345	2345	345	
						245	2356	356	2356	356	
						2345	2345	345	2345	345	
						2346	2346	356	2356	356	
						23456	23456	2345	23456	2345	
							34	3	34	3	
							234	23	234	23	
							345	35	345	35	
							245	25	245	25	
							2345	235	2345	235	
							2346	236	2346	236	
							23456	2356	23456	2356	
							3	4	3	4	
							25	2	24	2	
							35	3	246	26	
							235	23			



Table D.4 Output of the Pathway Function for PBDEs

Pathways No:5		Pathways No:1		Pathways No:4		Pathways No:1		Pathways No:0		Pathways No:1		Pathways No:1		Pathways No:1		Pathways No:1	
<b>1.Flanked Any(3+4+5)*</b>		<b>2. Flanked Meta or Flanked Para(3+5)*</b>		<b>3. Flanked Meta*</b>		<b>4.Flanked Ortho*</b>		<b>5.Flanked Para*</b>		<b>6.Meta Any*</b>		<b>7. Ortho Any*</b>					
m	d	m	d	m	d	m	d	m	d	m	d	m	d	m	d	m	d
99	47	183	154	99	47	183	153			183	154	47	28			100	47
153	99			153	99							154	99			154	99
154	100			154	100												
183	153			183	154												
183	154																
<b>8. Para Any*</b>		<b>9. Flanked or meta(1+6)*</b>		<b>10. Flanked or para(1+8)*</b>		<b>11.Double Flanked para-any</b>		<b>12.Double Flanked meta-any</b>		<b>13.Doubly Flanked para or doubly flanked meta</b>		<b>14. Singly Flanked para or singly flanked meta</b>					
m	d	m	d	m	d	m	d	m	d	m	d	m	d	m	d	m	d
		183	154	183	154			183	154	183	154	183	154	99	47	153	99
														154	100	154	100
<b>15. Doubly flanked meta and para+singly flanked</b>		<b>16. Tokarzetal2008 with biometrics</b>		<b>17. Tokarzetal2008 without biometrics</b>		<b>18. Huangetal_2014</b>		<b>19. Robrocketal_2008</b>		<b>20.Ding et al 2013_penta</b>		<b>21.Ding et al 2013_octa</b>					
m	d	m	d	m	d	m	d	m	d	m	d	m	d	m	d	m	d
99	47	47	28	47	28	47	28	47	28	47	28	47	28	183	153	183	154
153	99	99	47	100	47	100	47	99	47	99	47	99	47	183	154	183	154
154	100	153	99	154	99	154	99	153	99	153	99	153	99				
183	154	154	99	154	100	154	100	183	153	183	153	183	153				
		183	154	183	154	183	154	183	154	183	154	183	154				

m:mother, d: daughter

**APPENDIX E**

**RESULTS OF ADM FOR BH SEDIMENT MICROCOSMS  
CONTAMINATED BY PCBs**

Table E.1 Numbers of samples and shuffles in each sample run by ADM

D. Activity No	1.BH			2.BH+SFI+DEH10 (SFI+DEH10)			3.BH+017+DF1 (o17+DF1)			4.BH+all (SFI+DEH10+ o17+DF1)			Total # of Shuffles	n <sup>a</sup>
	t0-t100	t100-t200	t200-t300	t0-t100	t100-t200	t200-t300	t0-t100	t100-t200	t200-t300	t0-t100	t100-t200	t200-t300		
5	2	0	0	0	0	0	1	0	0	0	0	1	4	3
11	0	62	100	65	32	81	100	0	16	0	63	50	569	9
12	1	0	19	0	0	4	0	0	0	0	0	2	26	4
13	2	0	0	1	0	0	1	0	0	0	0	1	5	3
16	100	100	100	100	100	100	100	0	100	100	100	100	1100	11
17	100	100	100	100	100	100	100	100	100	100	100	100	1200	12
18	100	7	53	22	0	51	100	38	100	50	11	100	632	11
19	100	40	36	68	7	82	100	17	20	76	0	82	628	11
20	2	0	0	0	0	0	0	0	0	0	0	0	2	1
21	100	25	100	42	0	44	0	46	33	38	0	38	466	9
22	100	100	100	100	100	100	100	100	100	100	100	100	1200	12
23	100	100	100	100	100	100	100	100	100	100	100	100	1200	12

<sup>a</sup>: number of samples run by ADM for corresponding activity



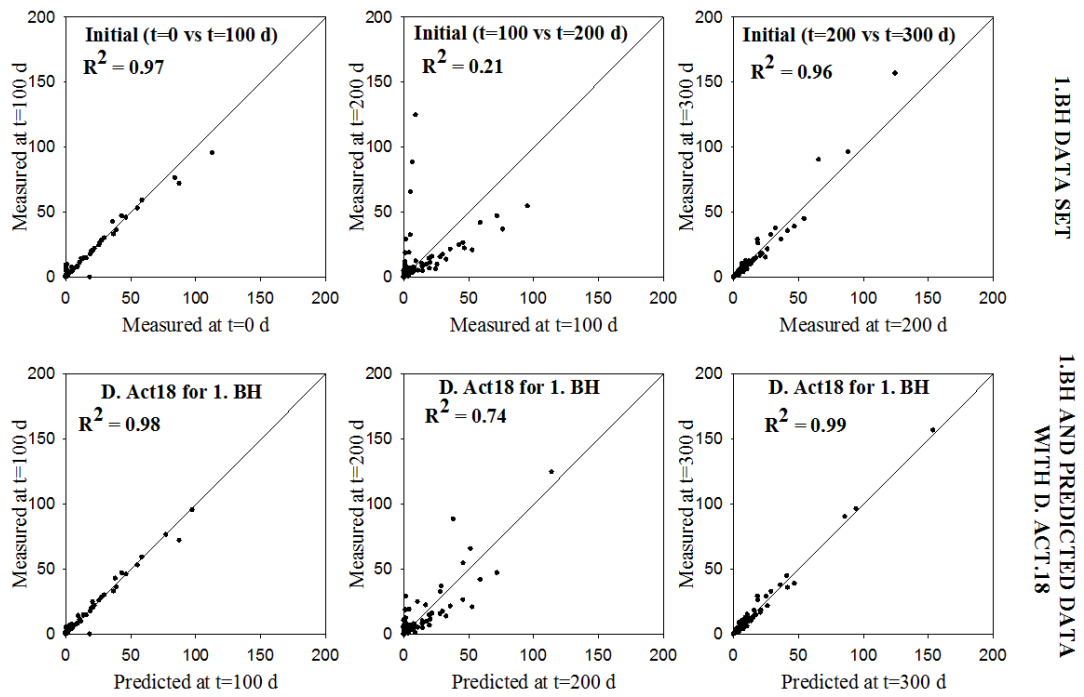


Figure E.1 Comparison of scatter plot of (first row) the PCB profiles of Data set 1.BH for days, t0 vs. t100, t100 vs. t200 and t200 vs. t300 and (second row) prediction profiles at days 100, 200 and 300 for DA 18 (Activity of DEH10) by ADM

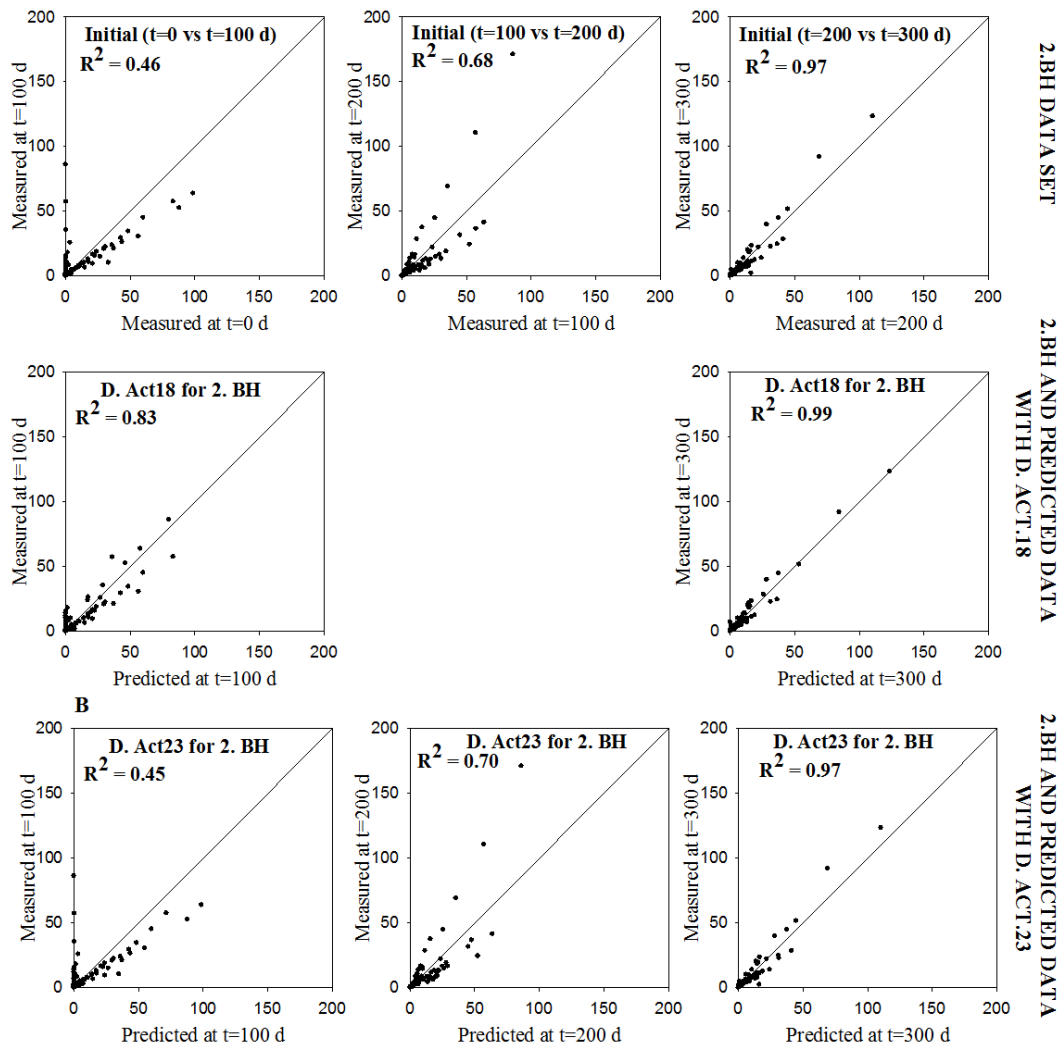


Figure E.2 Comparison of scatter plot of (first row) the PCB profiles of Data set 2.BH for days , t0 vs. t100, t100 vs. t200 and t200 vs. t300, (second row) prediction profiles at days 100 and 300 for DA 18 (Activity of DEH10) by ADM and (third row) prediction profiles at days 100, 200 and 300 for DA 23 (Activity of DEH10+SF1) by ADM

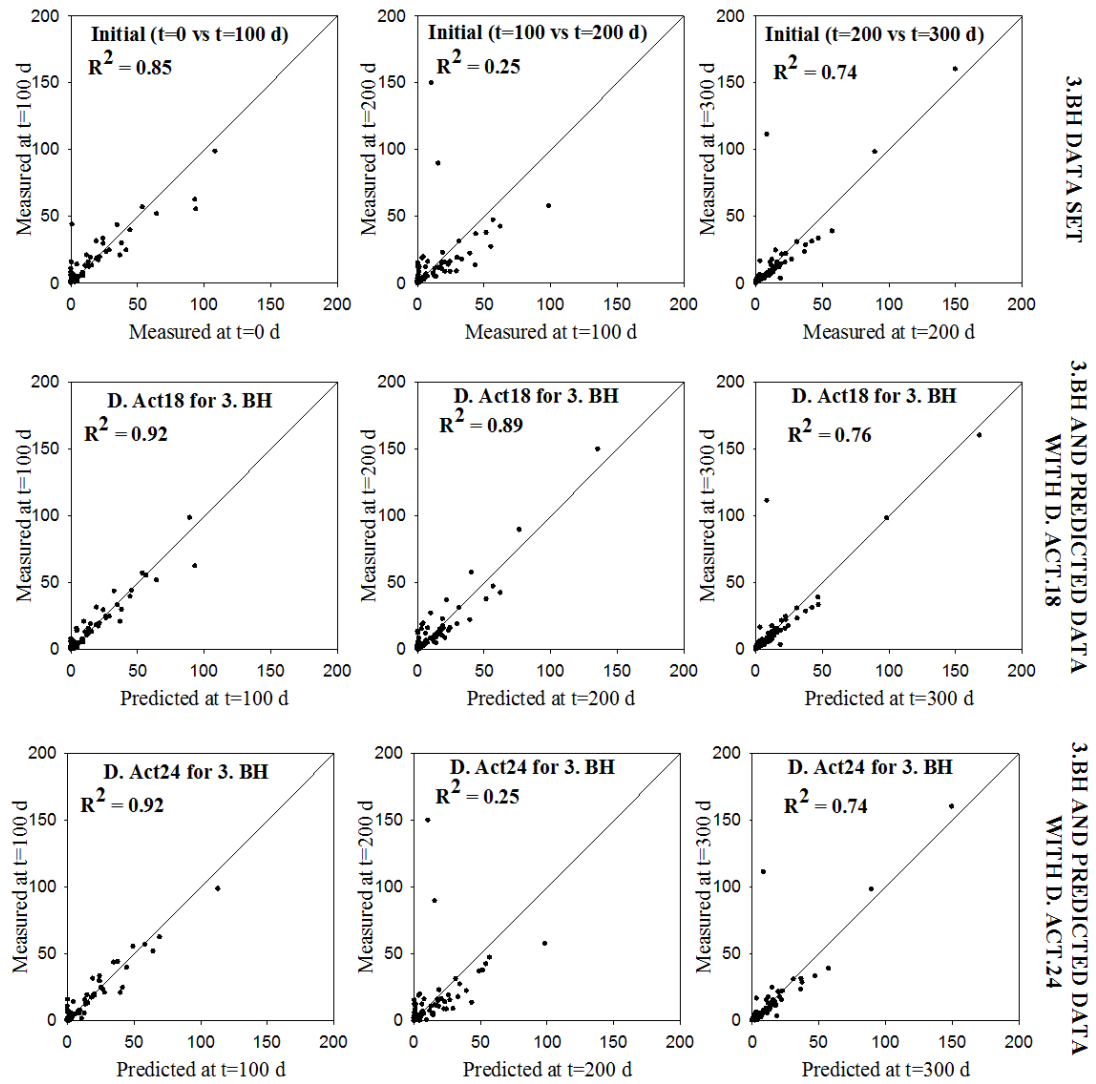


Figure E.3 Comparison of scatter plot of (first row) the PCB profiles of Data set 3.BH for days , t0 vs. t100, t100 vs. t200 and t200 vs. t300, (second row) prediction profiles at days 100, 200 and 300 for DA 18 (Activity of DEH10) by ADM and (third row) prediction profiles at days 100, 200 and 300 for DA 24 (Activity of o17+DF1) by ADM

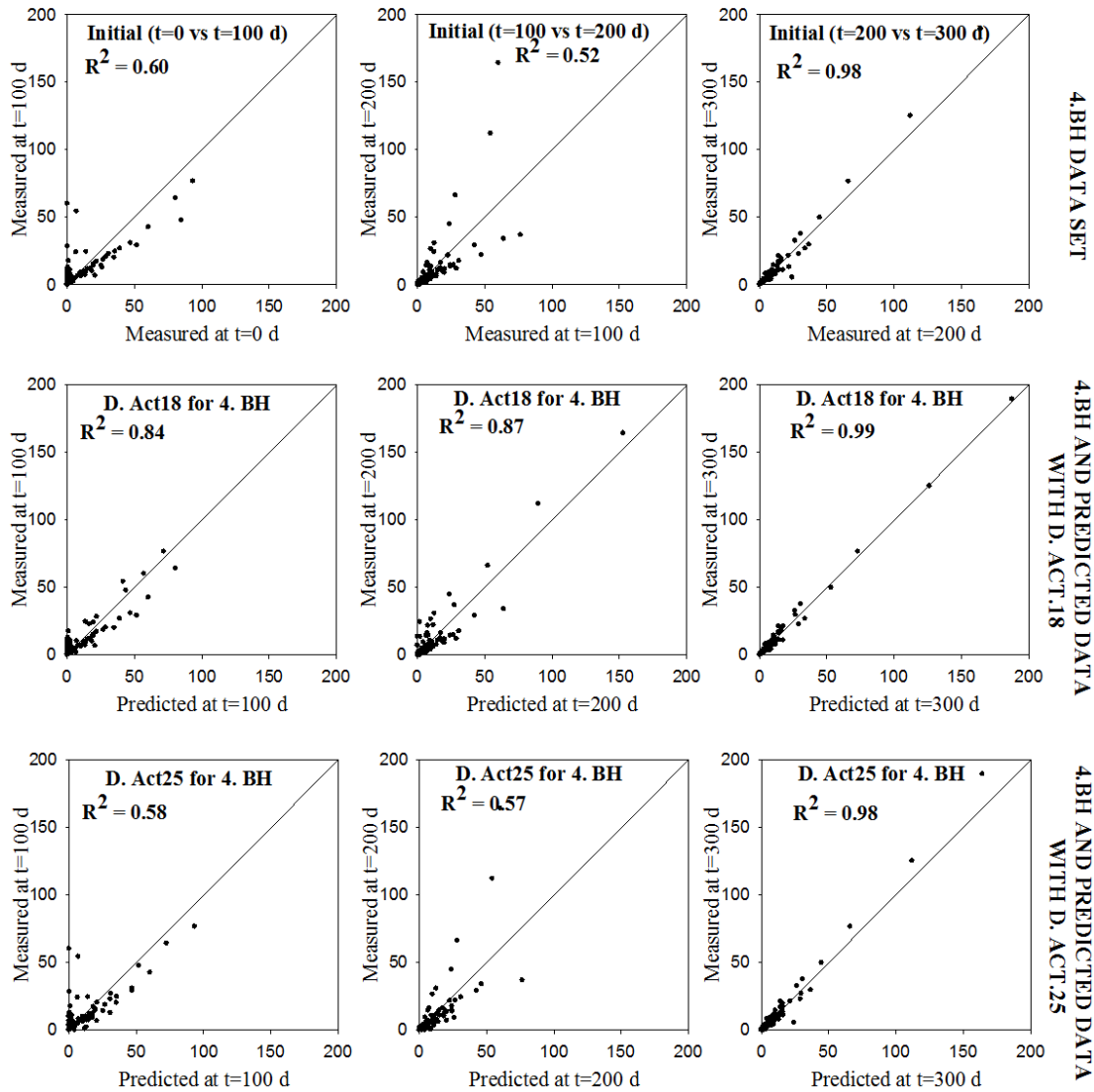


Figure E.4 Comparison of scatter plot of (first row) the PCB profiles of Data set 4.BH for days , t0 vs. t100, t100 vs. t200 and t200 vs. t300, (second row) prediction profiles at days 100, 200 and 300 for DA 18 (Activity of DEH10) by ADM and (third row) prediction profiles at days 100, 200 and 300 for DA 25 (Activity of Deh10+SF1+o17+DF1) by ADM

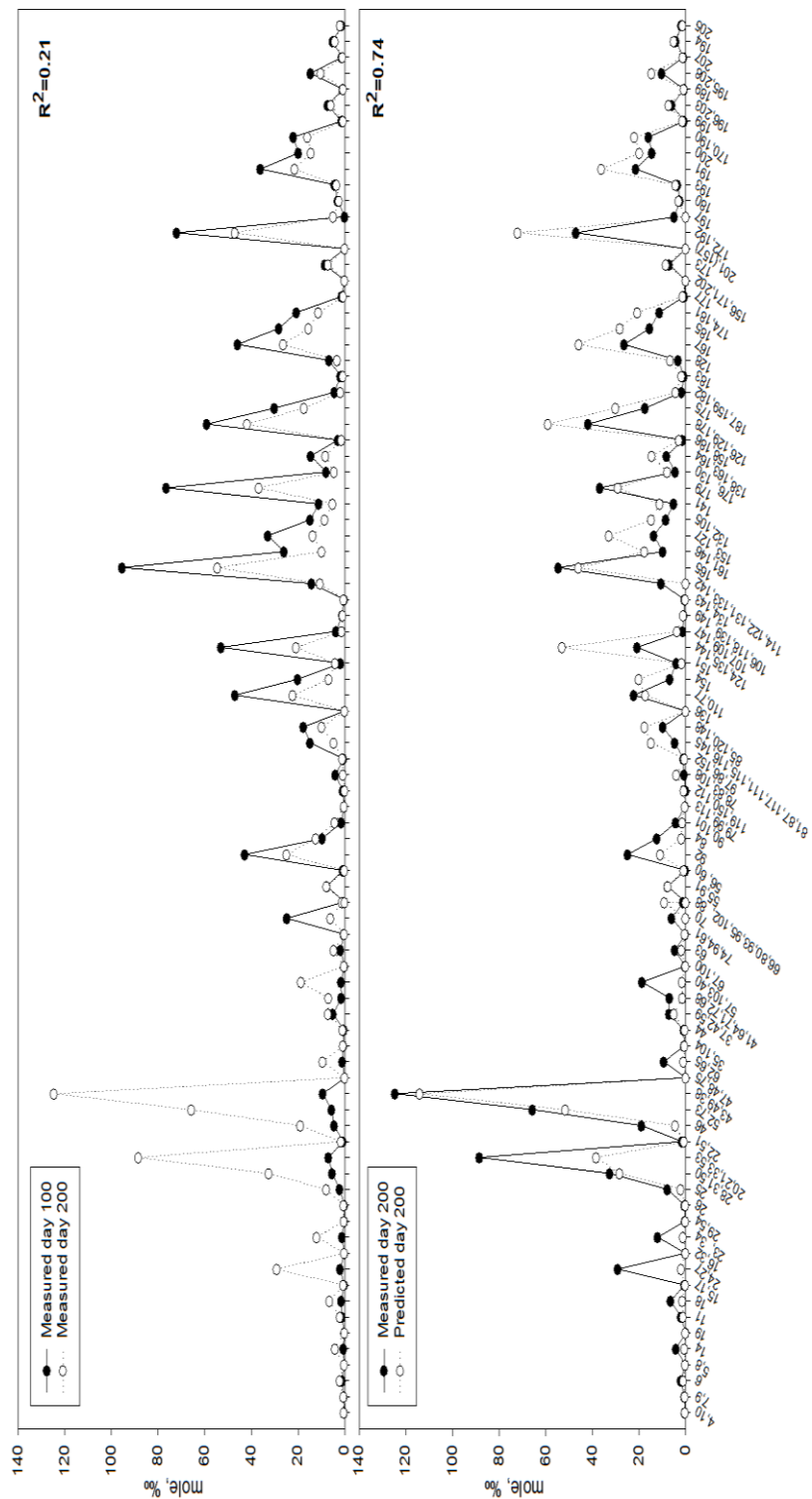


Figure E.5 PCB congener profiles of Data Set 1.BH: Graph above is measured day 100 vs. 100, Graph below is day 200 measured vs. predicted by the model for D. Act. 18

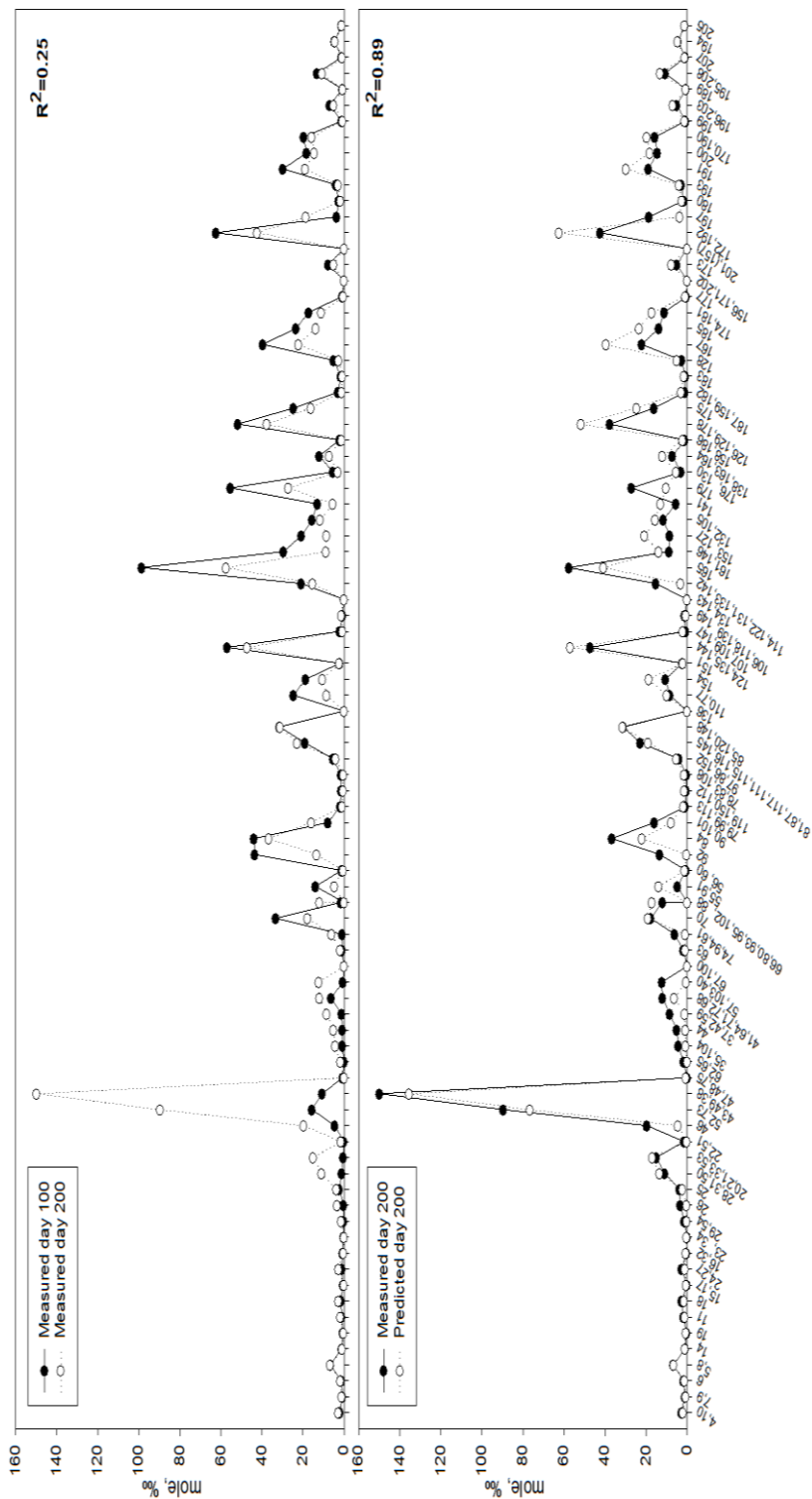


Figure E.6 PCB congener profiles of Data Set 3.BH: Graph above is measured day 100 vs. 200, Graph below is day 200 measured vs. predicted by the model for D. Act. 18

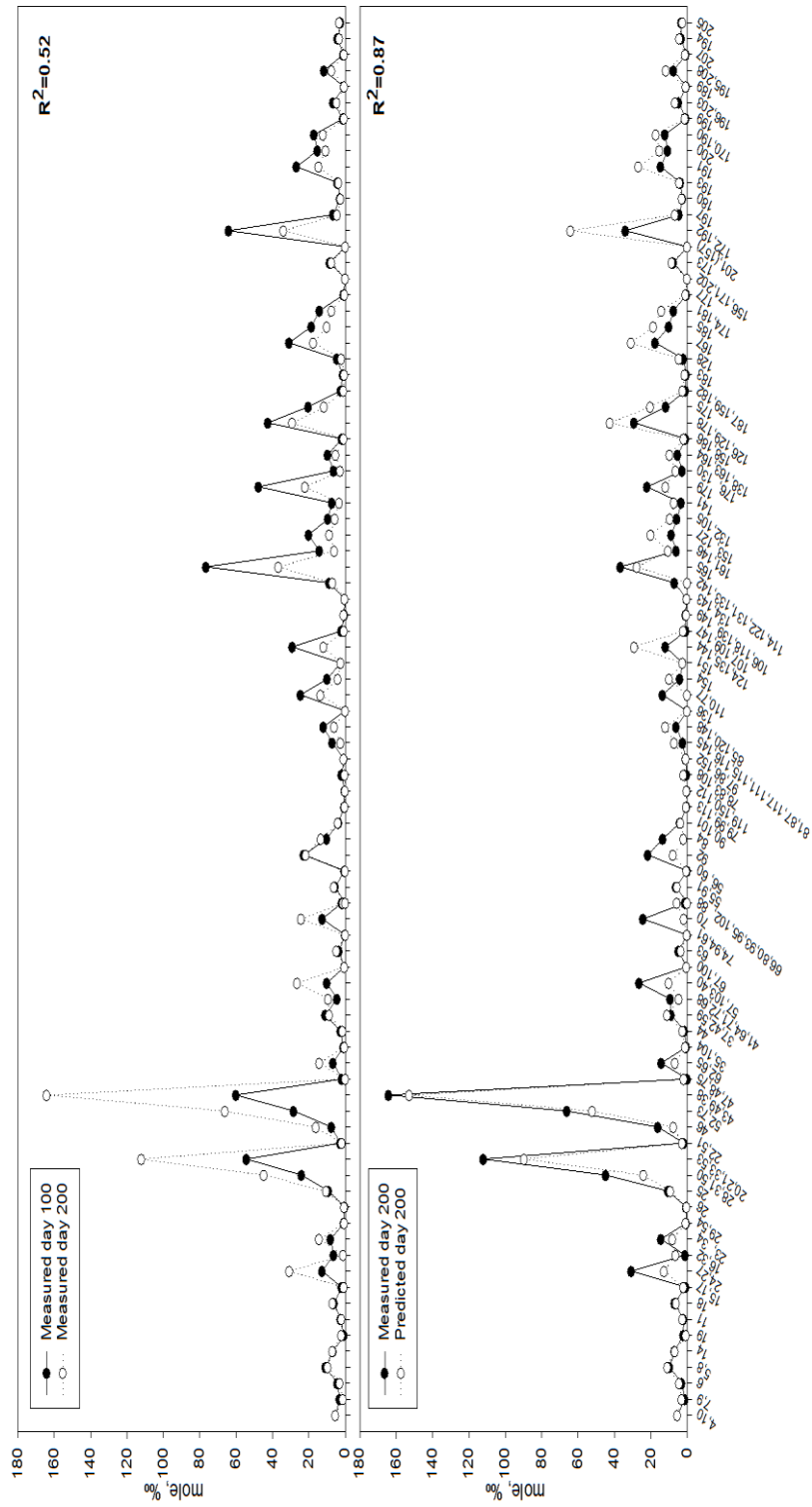


Figure E.7 PCB congener profiles of Data Set 4.BH: Graph above is measured day 100 vs. 200, Graph below is day 200 measured vs. predicted by the model for DA 18

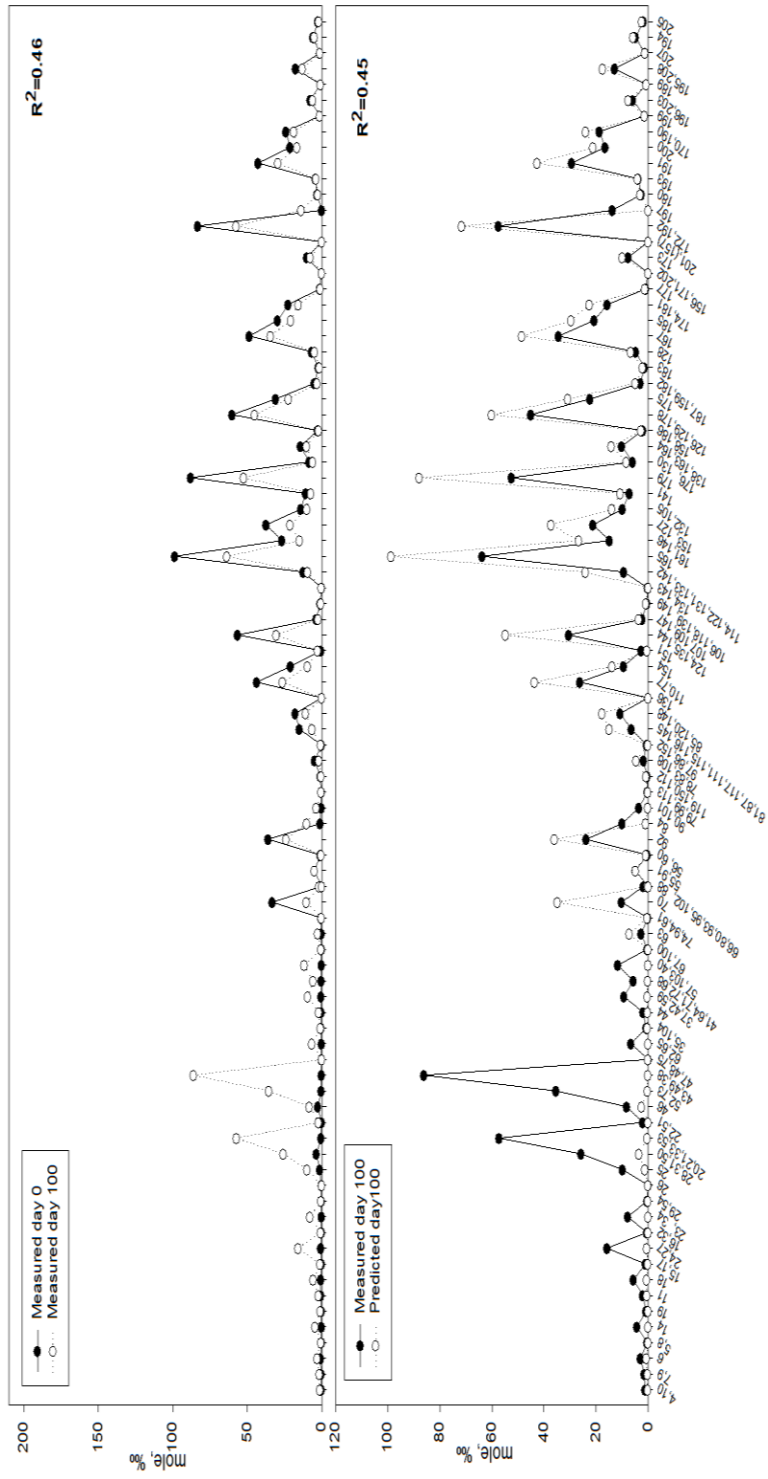


Figure E.8 PCB congener profiles of Data Set 2.BH: Graph above is measured day 0 vs. 100, Graph below is day 100 measured vs. predicted by the model for DA 23



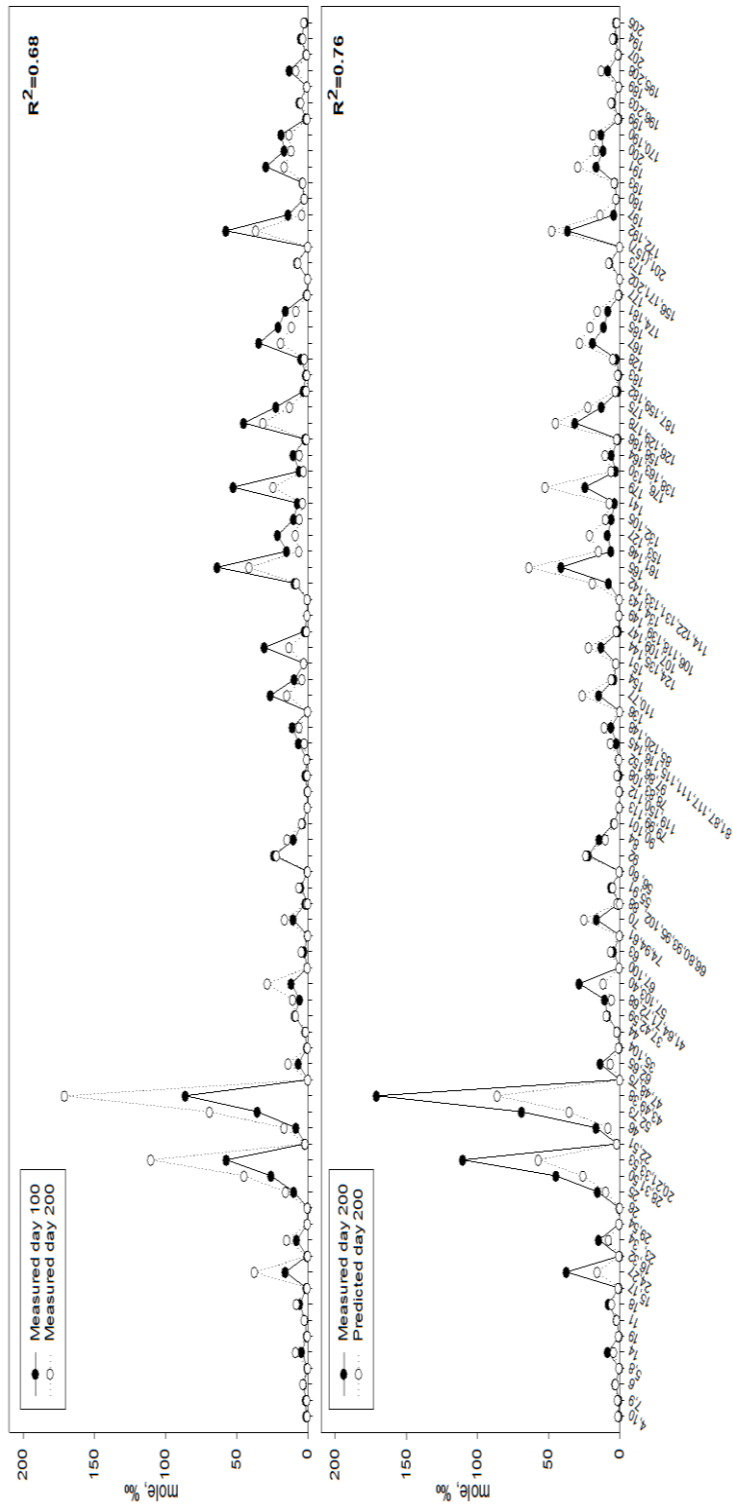
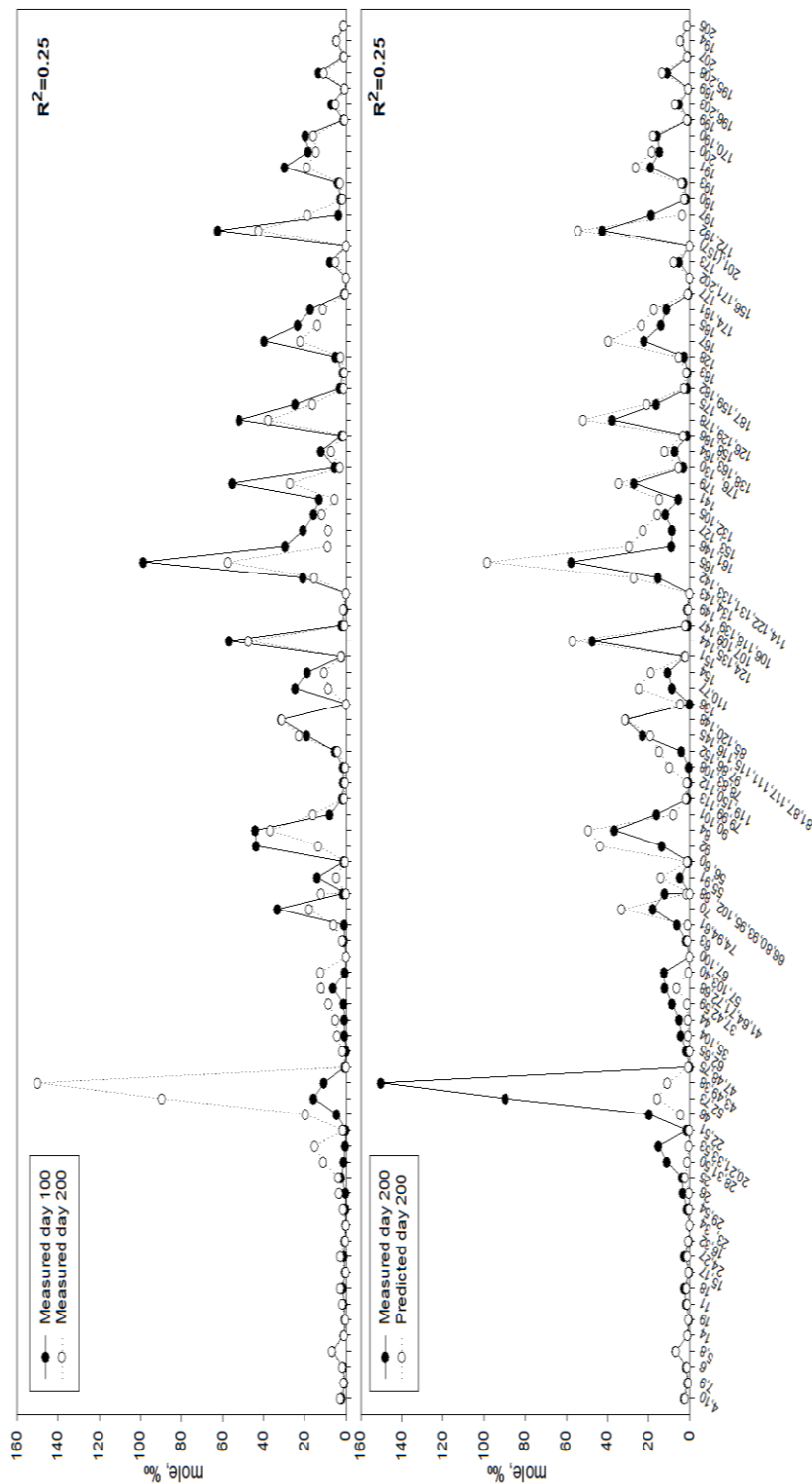


Figure E.9 PCB congener profiles of Data Set 2.BH: Graph above is measured day 100 vs. 200, Graph below is day 200 measured vs. predicted by the model for DA 23



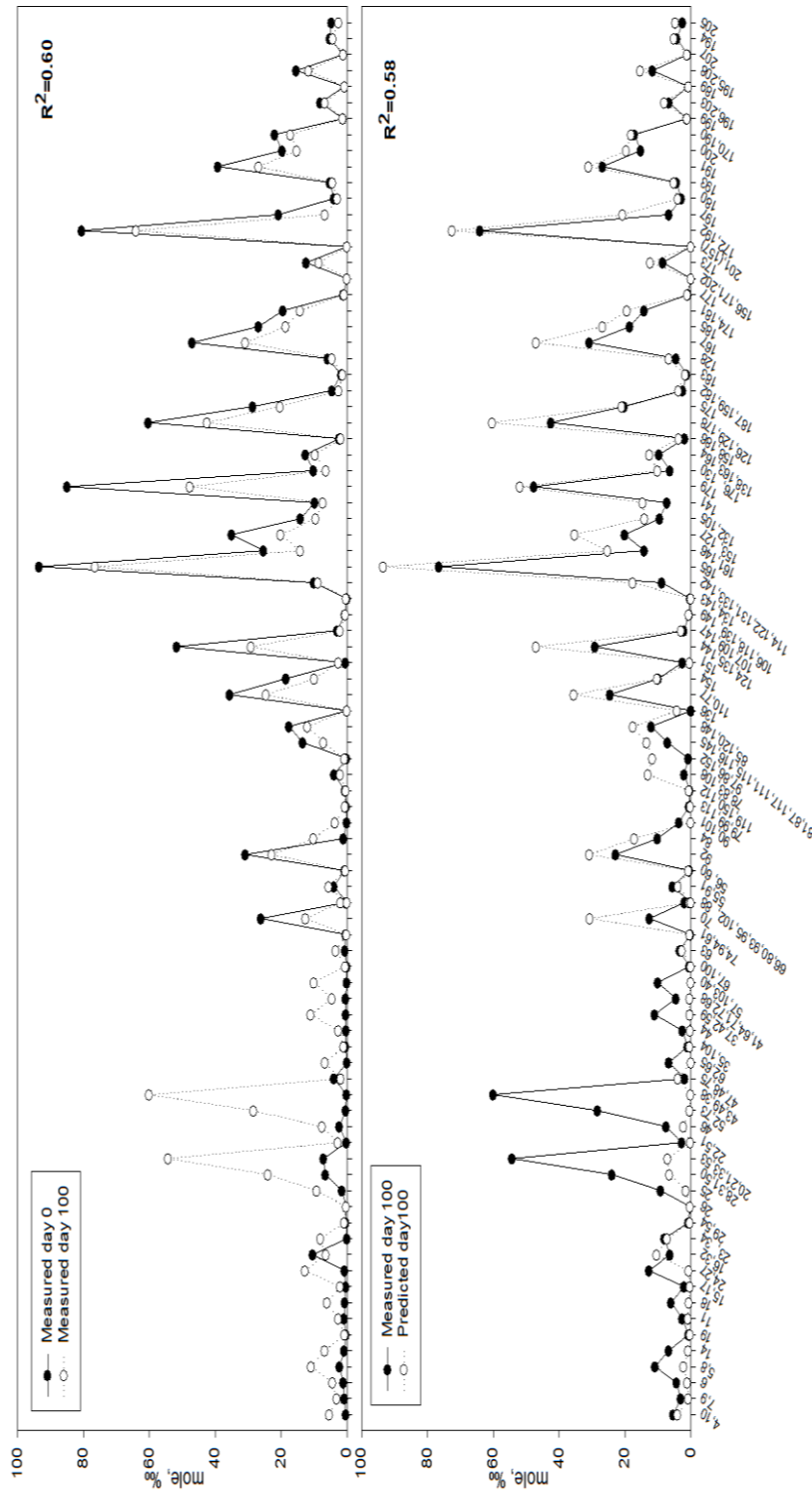
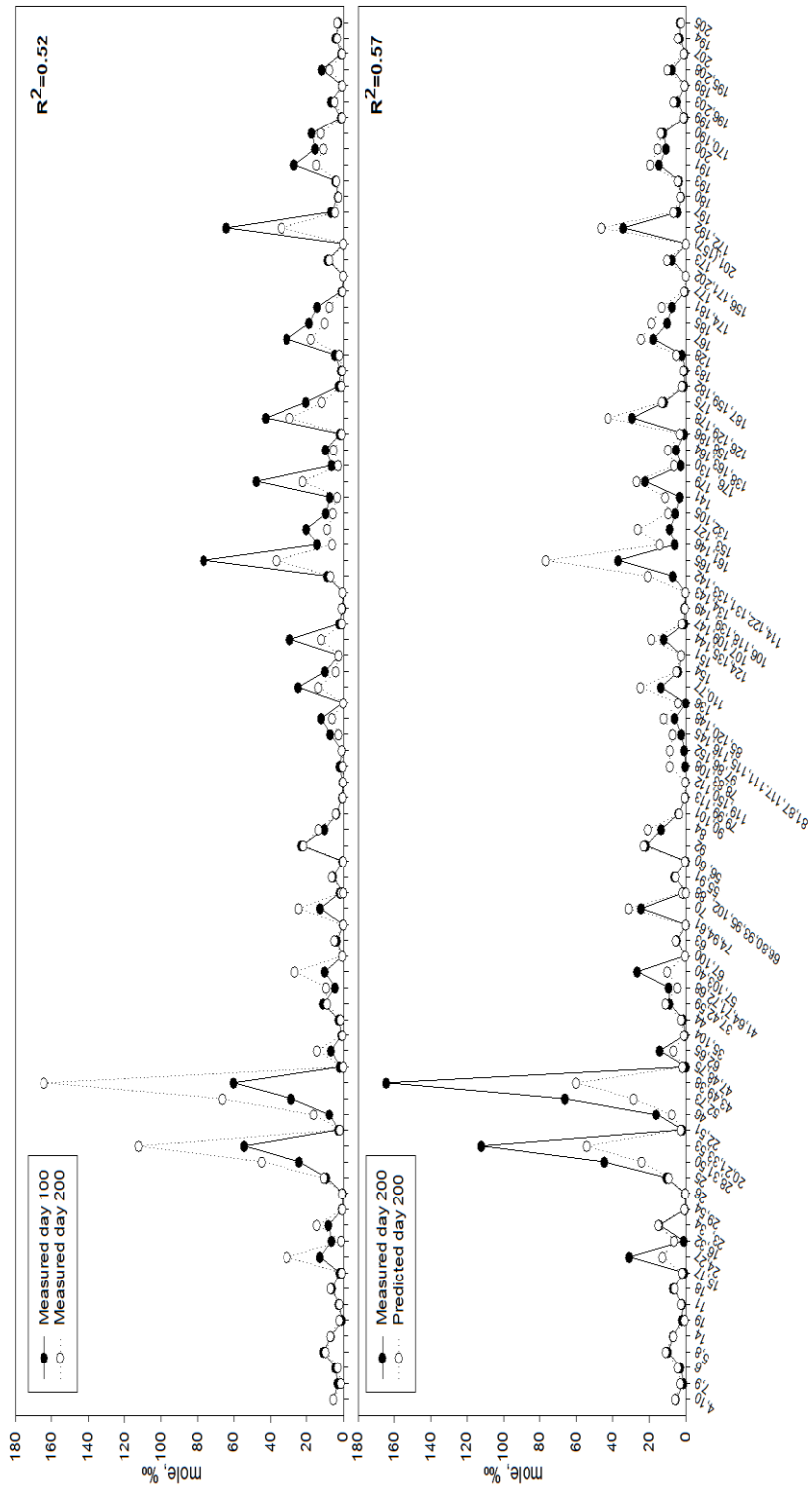


Figure E.11 PCB congener profiles of Data Set 4.BH: Graph above is measured day 0 vs. 100, Graph below is day 100 measured vs. predicted by the model for DA 25



## APPENDIX F

### RESULTS OF FTHP MODEL FOR LAKE MICHIGAN SEDIMENTS CONTAMINATED BY PCBs

Table F.1  $k_m$  values estimated by ADM for DA18, DA25, DA19, DA13 and DA20

Congener IUPAC No		$k_m$ values of DA18 estimated by ADM			
Mother	Daughter	Min	Med	Max	Avg±SD
66	33	0	0.0034	0.0266	0.005±0.0047
101	49	0.0001	0.0071	0.0531	0.009±0.0122
138/163	99	0.0006	0.0056	0.0215	0.0053±0.0044
105/132/153	99	0.0010	0.0027	0.0111	0.0032±0.0021
146	101	0.0018	0.0053	0.1234	0.0184±0.0354
151	66	0	0.0045	0.1290	0.0068±0.0165

Table F.1 (*Continued*)

Congener IUPAC No		$k_m$ values of DA25 estimated by ADM			
Mother	Daughter	Min	Med	Max	Avg±SD
138/163	85	0	0.0018	0.0031	0.002±32.9808
138/163	81	0	0.0014	0.0029	0.0017±45.4477
138/163	87	0	0.0014	0.0029	0.0017±45.4477
138/163	99	0	0.0022	0.0076	0.0026±22.8106
118	66	0	0.0014	0.0108	0.0014±0
170/190	66	0	0.0014	0.0108	0.0014±0
180	146	0	0.0013	0.0024	0.0013±10.1275
180	105/132/153	0.0004	0.0014	0.0025	0.0015±7.726

Table F.1 (Continued)

Congener IUPAC No		$k_m$ values of DA19 estimated by ADM			
Mother	Daughter	Min	Med	Max	Avg±SD
101	49	0.0006	0.0071	0.3652	0.0155±0.0509
84/92	52	0	0.0062	0.0281	0.0066±0.0073
170/190	138/163	0	0	0	0±0
182/187	118	0	0.0002	0.0013	0.0003±0.0004
182/187	123/149	0	0.0002	0.0013	0.0003±0.0004

Table F.1 (Continued)

Congener IUPAC No		$k_m$ values of DA13 estimated by ADM			
Mother	Daughter	Min	Med	Max	Avg±SD
56/60	28/31	0	0	0	0±0
81	49	0	0.0105	0.1119	0.0466±0.0576
87	49	0	0.0105	0.1119	0.0466±0.0576
66	28/31	0.002	0.0033	0.0137	0.0057±0.0047
105/132/163	66	0	0	0.0001	0±0
105/132/163	66	0	0.0011	0.002	0.0012±0.0007
138/163	99	0.0007	0.0021	0.0057	0.0024±0.002
182/187	81	0.0006	0.0016	0.0019	0.0013±0.0005
182/187	87	0.0006	0.0016	0.0019	0.0013±0.0005
182/187	85	0	0.0004	0.002	0.0007±0.0009
170/190	138/163	0	0	0.0005	0.0002±0.0002
180	146	0.0008	0.0009	0.0016	0.0012±0.0003
180	105/132/153	0	0.0001	0.0015	0.0004±0.0006

Table F.1 (Continued)

Congener IUPAC No		$k_m$ values of DA20 estimated by ADM			
Mother	Daughter	Min	Med	Max	Avg±SD
56/60	33	0	0	0	0±0
56/60	28/31	0	0	0	0±0
70/76	26	0	0.0076	0.0152	0.0076±0.0107
74	28/31	0	0	0	0±0
81	44	0	0	0.0001	0±0.0001
81	49	0.0042	0.0051	0.006	0.0051±0.0013
87	44	0	0	0.0001	0±0.0001
87	49	0.0042	0.0051	0.006	0.0051±0.0013
66	28/31	0.0005	0.0005	0.0005	0.0005±0
99	49	0	0.0013	0.0025	0.0013±0.0018
101	52	0.0008	0.0009	0.0009	0.0009±0.0001
66	33	0.0021	0.0023	0.0026	0.0023±0.0004
105/132/153	66	0	0	0	0±0
118	70	0	0.0001	0.0001	0.0001±0.0001
123/149	70	0	0.0001	0.0001	0.0001±0.0001
118	66	0	0	0	0±0
123/149	66	0	0.0001	0.0001	0.0001±0.0001
105/132/153	84/92	0	0	0	0±0
138/163	81	0.0003	0.0005	0.0007	0.0005±0.0003
138/163	87	0.0003	0.0005	0.0007	0.0005±0.0003
138/163	99	0.0009	0.001	0.0012	0.001±0.0002
170/190	138/163	0.0005	0.0006	0.0007	0.0006±0.0001
180	146	0.0011	0.0011	0.0011	0.0011±0
182/187	85	0	0	0	0±0
182/187	81	0.0004	0.0004	0.0005	0.0004±0.0001
182/187	87	0.0004	0.0004	0.0005	0.0004±0.0001
146	84/92	0.0016	0.0023	0.003	0.0023±0.001

Table F.2 Trials for calibration of PCB congeners in Lake Michigan sediment

Congener IUPAC No	No Deg Term (S)		$v_s=0.75$ m/d(50%)		$v_s=2.25$ m/d(150%)		$v_b$ m/d(50%)		$v_b$ m/d(150%)		$K_d$ with min values (log $K_{ow}$ min)		$K_d$ with max values (log $K_{ow}$ max)	
	R <sup>2</sup>	RMSE	R <sup>2</sup>	RMSE	R <sup>2</sup>	RMSE	R <sup>2</sup>	RMSE	R <sup>2</sup>	RMSE	R <sup>2</sup>	RMSE	R <sup>2</sup>	RMSE
16	0.45	12.18	0.45	13.28	0.44	11.37	0.45	12.18	0.45	12.18	0.45	12.08	0.45	12.22
26	0.80	16.06	<b>0.81</b>	17.38	0.80	15.12	0.80	16.06	0.80	16.06	0.80	15.98	0.80	16.10
28/31	0.81	242.49	0.81	264.43	0.81	226.93	0.81	242.49	0.81	242.49	0.81	240.66	0.81	248.08
33	0.73	47.17	0.73	50.14	0.72	45.27	0.73	47.17	0.73	47.17	0.73	46.83	0.73	47.90
44	0.56	46.29	<b>0.57</b>	48.87	0.56	46.52	0.56	46.29	0.56	46.29	0.56	46.08	0.56	51.22
49	0.79	38.18	0.79	42.28	0.78	35.38	0.79	38.18	0.79	38.18	0.79	37.75	0.79	40.41
52	0.74	63.72	<b>0.75</b>	70.70	0.74	59.58	0.74	63.72	0.74	63.72	0.74	61.59	0.74	66.91
56/60	0.83	92.43	<b>0.84</b>	108.87	0.83	81.27	0.83	92.43	0.83	92.43	0.83	91.51	0.83	125.23
66	0.76	195.68	0.76	219.72	0.75	182.67	0.76	195.68	0.76	195.68	0.76	194.59	0.76	196.96
70/76	0.79	89.48	<b>0.80</b>	102.02	0.79	82.37	0.79	89.48	0.79	89.48	0.79	88.57	0.79	91.51
74	0.87	53.74	0.87	60.98	0.87	48.29	0.87	53.74	0.87	53.74	0.87	53.56	0.87	56.67
81	0.78	3.82	0.78	4.55	0.78	3.27	0.78	3.82	0.78	3.82	0.78	3.74	0.78	4.04
84/92	0.68	91.33	0.68	99.41	0.68	84.39	0.68	91.33	0.68	91.33	0.68	78.87	0.68	187.94
85	0.37	23.28	0.37	24.20	0.36	24.49	0.37	23.28	0.37	23.28	0.37	23.44	0.37	23.27
87	0.83	28.48	<b>0.84</b>	33.45	0.83	24.73	0.83	28.48	0.83	28.48	0.83	25.72	0.83	36.52
99	0.53	32.10	<b>0.54</b>	32.82	0.53	31.48	0.53	32.10	0.53	32.10	0.53	29.04	0.53	85.26
101	0.62	40.95	0.62	47.87	0.62	38.89	0.62	40.95	0.62	40.95	0.62	39.34	0.62	69.10
118	0.41	53.87	<b>0.42</b>	60.74	0.41	52.60	0.41	53.87	0.41	53.87	0.41	52.52	0.41	75.84
123/149	0.16	23.32	0.16	24.52	0.16	23.36	0.16	23.32	0.16	23.32	0.16	23.28	0.16	30.71
105/132/153	0.20	68.53	<b>0.21</b>	74.35	0.20	68.94	0.20	68.53	0.20	68.53	0.20	68.95	0.20	108.38
151	0.17	6.02	<b>0.18</b>	5.92	0.17	6.67	0.17	6.02	0.17	6.02	0.17	6.08	0.17	6.17
138/163	0.51	151.97	0.51	161.30	0.51	144.00	0.51	151.97	0.51	151.97	0.51	129.39	0.51	286.68
170/190	0.29	16.46	0.29	18.89	0.29	15.29	0.29	16.46	0.29	16.46	0.29	16.04	0.29	17.49
180	0.09	34.90	0.09	37.87	0.09	34.56	0.09	34.90	0.09	34.90	0.09	34.50	0.09	35.28
182/187	0.00	12.68	0.00	12.74	0.00	12.66	0.00	12.68	0.00	12.68	0.00	12.99	0.00	13.59
195/208	0.05	6.23	0.05	6.06	0.05	6.42	0.05	6.23	0.05	6.23	0.05	6.51	0.05	6.01
146	0.21	14.58	0.21	15.24	0.21	14.09	0.21	14.58	0.21	14.58	0.21	13.66	0.21	16.45
∑ PCBs	0.73	1227.19	0.73	1426.542	0.73	1093.428	0.73	1227.192	0.73	1227.192	0.73	1155.692	0.73	1671.731
Min	0.00		0.00		0.00		0.00		0.00		0.00		0.00	
Max	0.87		0.87		0.87		0.87		0.87		0.87		0.87	
Average	0.53		0.53		0.53		0.53		0.53		0.53		0.53	
Std	0.28		0.28		0.28		0.28		0.28		0.28		0.28	



Table F.2 (continued)

Congener No	DAI8 <sub>min</sub>		DAI8 <sub>median</sub>		DAI8 <sub>max</sub>		v <sub>g</sub> =0.75 m/d and DAI8 <sub>min</sub>		v <sub>g</sub> =0.75 m/d and DAI8 <sub>min</sub> *0.1		v <sub>g</sub> =0.75 m/d and DAI8 <sub>max</sub>		v <sub>g</sub> =0.75 m/d and DAI8 <sub>median</sub>	
	R <sup>2</sup>	RMSE	R <sup>2</sup>	RMSE	R <sup>2</sup>	RMSE	R <sup>2</sup>	RMSE	R <sup>2</sup>	RMSE	R <sup>2</sup>	RMSE	R <sup>2</sup>	RMSE
16	0.45	12.18	0.45	12.18	0.45	12.18	0.45	13.28	0.45	13.28	0.45	13.28	0.45	13.28
26	0.80	16.06	0.80	16.06	0.80	16.06	<b>0.81</b>	17.38	<b>0.81</b>	17.38	<b>0.81</b>	17.38	<b>0.81</b>	17.38
28/31	0.81	242.49	0.81	242.49	0.81	242.49	0.81	264.43	0.81	264.43	0.81	264.43	0.81	264.43
33	0.73	47.17	<u>0.57</u>	376.22	0.73	563.59	0.73	50.14	<u>0.67</u>	426.93	0.73	426.93	<u>0.03</u>	610.29
44	0.56	46.29	0.56	46.29	0.56	46.29	<b>0.57</b>	48.87	<b>0.57</b>	48.87	<b>0.57</b>	48.87	<b>0.57</b>	48.87
49	0.79	44.17	<u>0.57</u>	197.96	<u>0.00</u>	270.78	0.79	50.08	<u>0.56</u>	222.32	0.79	222.32	<u>0.03</u>	290.85
52	0.74	63.72	0.74	63.72	0.74	63.72	<b>0.75</b>	70.70	<b>0.75</b>	70.70	<b>0.75</b>	70.70	<b>0.75</b>	70.70
56/60	0.83	92.43	0.83	92.43	0.83	92.43	<b>0.84</b>	108.87	<b>0.84</b>	108.87	<b>0.84</b>	108.87	<b>0.84</b>	108.87
66	0.76	195.68	<u>0.66</u>	340.15	<u>0.12</u>	602.10	0.76	219.72	<u>0.67</u>	333.90	0.76	333.90	<u>0.12</u>	601.46
70/76	0.79	89.48	0.79	89.48	0.79	89.48	<b>0.80</b>	102.02	<b>0.80</b>	102.02	<b>0.80</b>	102.02	<b>0.80</b>	102.02
74	0.87	53.74	0.87	53.74	0.87	53.74	0.87	60.98	0.87	60.98	0.87	60.98	0.87	60.98
81	0.78	3.82	0.78	3.82	0.78	3.82	0.78	4.55	0.78	4.55	0.78	4.55	0.78	4.55
84/92	0.68	91.33	0.68	91.33	0.68	91.33	0.68	99.41	0.68	99.41	0.68	99.41	0.68	99.41
85	0.37	23.28	0.37	23.28	0.37	23.28	0.37	24.20	0.37	24.20	0.37	24.20	0.37	24.20
87	0.83	28.48	0.83	28.48	0.83	28.48	<b>0.84</b>	33.45	<b>0.84</b>	33.45	<b>0.84</b>	33.45	<b>0.84</b>	33.45
99	<u>0.52</u>	242.12	<u>0.43</u>	549.89	<u>0.15</u>	723.65	<u>0.52</u>	263.80	<u>0.52</u>	263.80	<u>0.52</u>	263.80	<u>0.17</u>	757.09
101	<b>0.65</b>	47.29	<u>0.49</u>	143.93	<u>0.10</u>	220.33	<u>0.57</u>	58.00	<u>0.57</u>	58.00	<u>0.50</u>	144.04	<u>0.10</u>	220.53
118	0.41	53.87	0.41	53.87	0.41	53.87	<b>0.42</b>	60.74	<b>0.42</b>	60.74	<b>0.42</b>	60.74	<b>0.42</b>	60.74
123/149	0.16	23.32	0.16	23.32	0.16	23.32	0.16	24.52	0.16	24.52	0.16	24.52	0.16	24.52
105/132/153	0.20	131.52	<u>0.18</u>	213.38	<u>0.08</u>	296.56	0.20	123.82	0.20	123.82	0.20	123.82	<u>0.08</u>	297.17
151	0.17	6.02	<u>0.13</u>	21.80	<u>0.00</u>	32.95	<b>0.18</b>	5.92	<b>0.18</b>	5.92	<b>0.18</b>	5.92	<b>0.00</b>	32.96
138/163	<u>0.50</u>	95.81	<u>0.45</u>	222.81	<u>0.22</u>	326.46	0.51	96.78	0.51	96.78	0.51	96.78	<u>0.22</u>	328.16
170/190	0.29	16.46	0.29	16.46	0.29	16.46	0.29	18.89	0.29	18.89	0.29	18.89	0.29	18.89
180	0.09	34.90	0.09	34.90	0.09	34.90	0.09	37.87	0.09	37.87	0.09	37.87	0.09	37.87
182/187	0.00	12.68	0.00	12.68	0.00	12.68	0.00	12.74	0.00	12.74	0.00	12.74	0.00	12.74
195/208	0.05	6.23	0.05	6.23	0.05	6.23	0.05	6.06	0.05	6.06	0.05	6.06	0.05	6.06
146	<u>0.19</u>	23.03	<u>0.14</u>	34.28	<u>0.00</u>	53.73	<u>0.19</u>	23.34	<u>0.19</u>	23.34	<u>0.14</u>	34.85	<u>0.00</u>	53.79
∑PCBs	0.73	1227.229	0.73	1227.731	0.73	1228.088	0.73	1426.59	0.73	1426.59	0.73	1427.35	<b>0.74</b>	1429.98
Min	0.00		0.00		0.00		0.00		0.00		0.00		0.00	
Max	0.87		0.87		0.87		0.87		0.87		0.87		0.87	
Average	0.53		0.49		0.39		0.53		0.53		0.50		0.39	
Std	0.28		0.28		0.33		0.28		0.28		0.28		0.33	

Bold and underlined numbers : maximum increase according to value in No degradation case, Italic and underlined numbers decrease according to value in No degradation case.

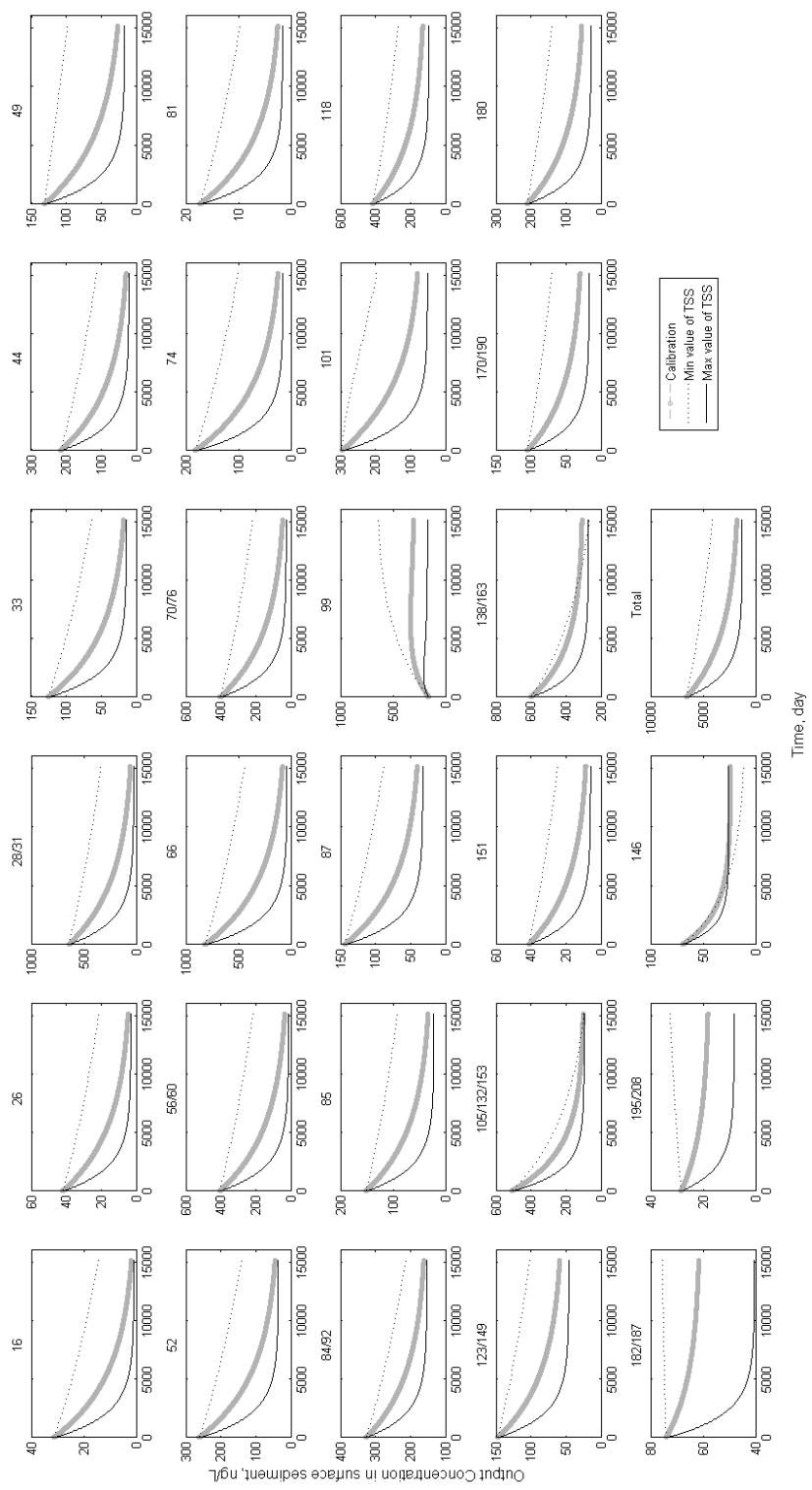


Figure F.1 Sensitivity Analysis of PCB congeners in Lake Michigan sediment: TSS Comparison

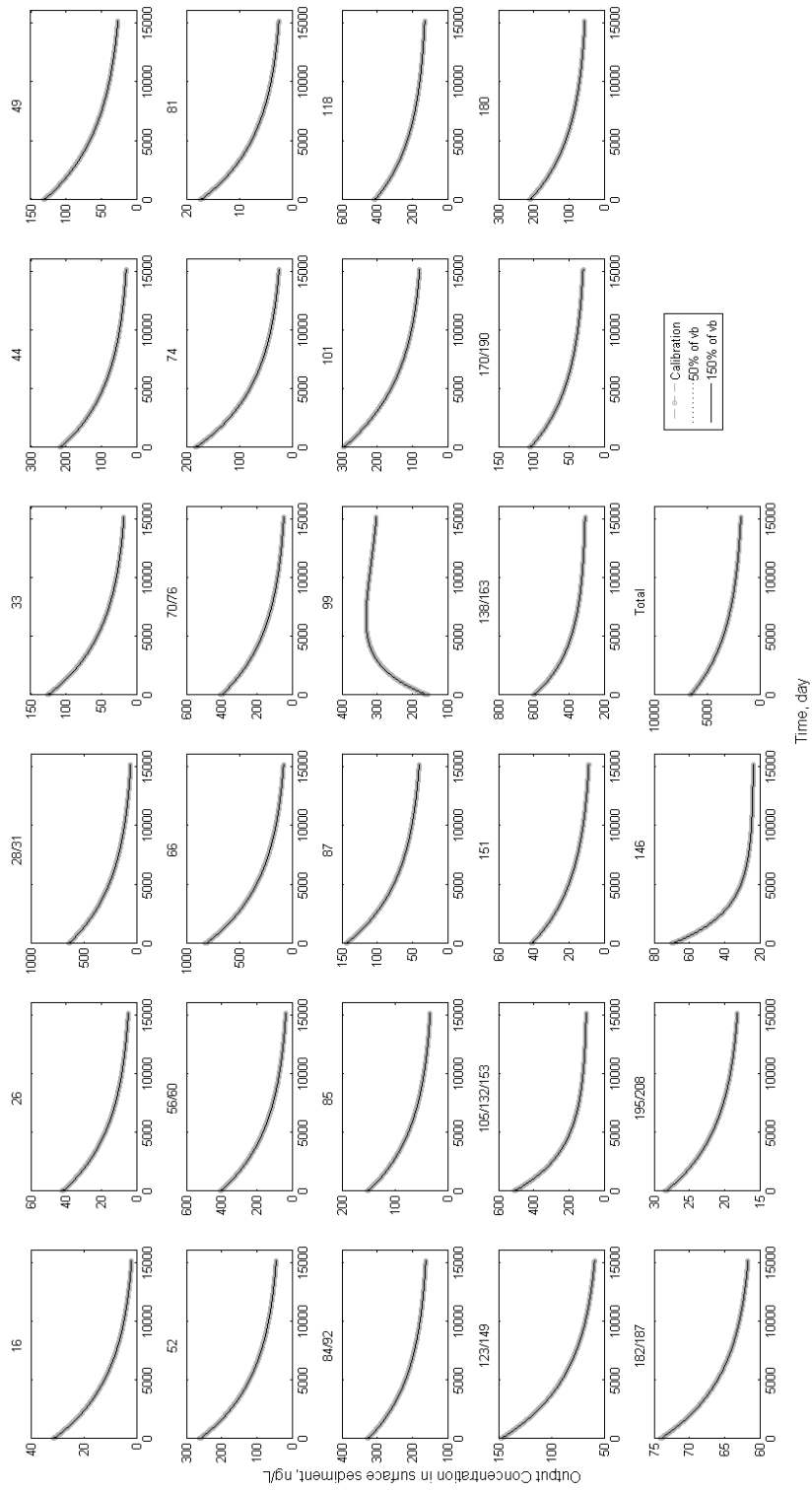


Figure F.2 Sensitivity Analysis of PCB congeners in Lake Michigan sediment:  $v_b$  Comparison

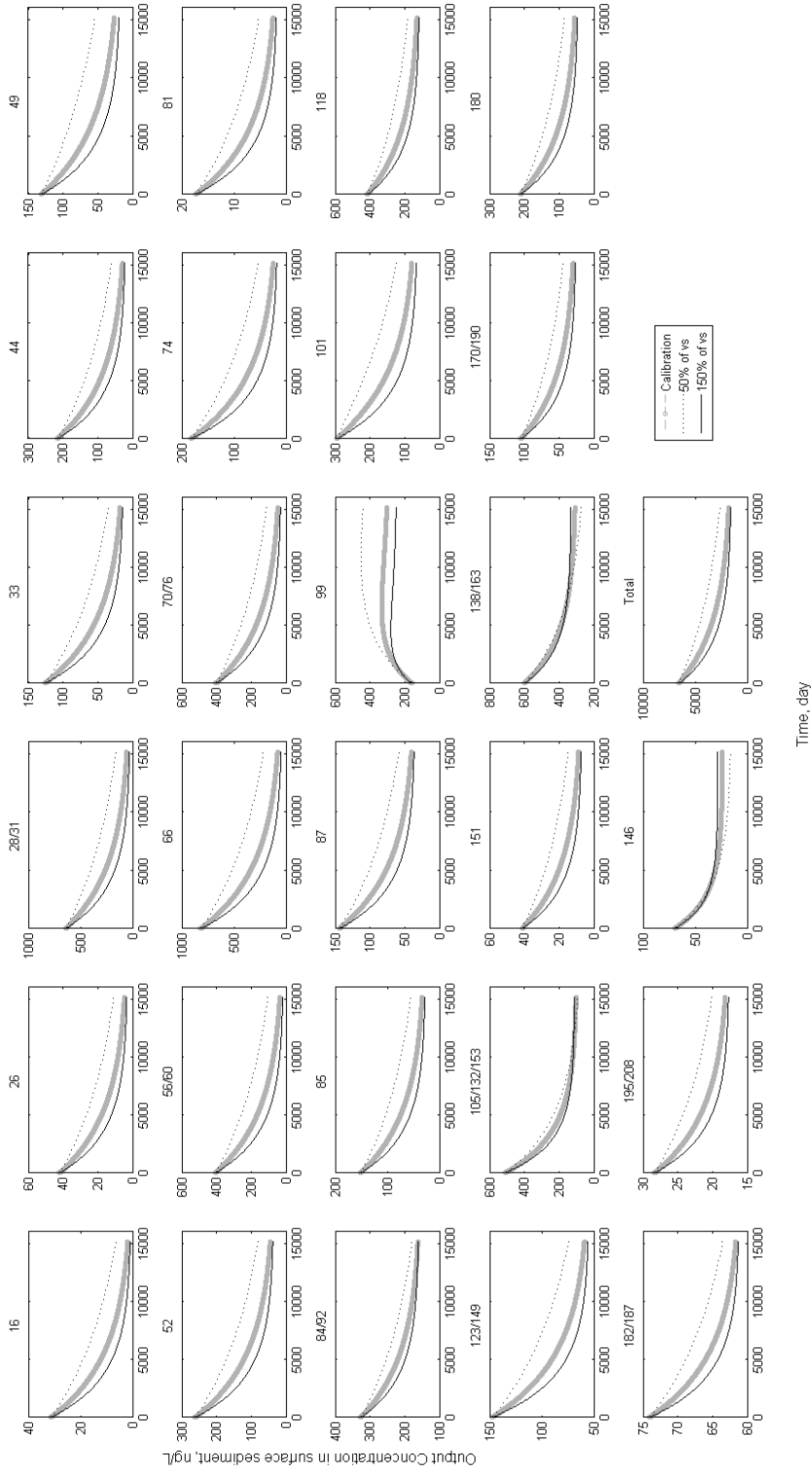


Figure F.3 Sensitivity Analysis of PCB congeners in Lake Michigan sediment:  $v_s$  Comparison

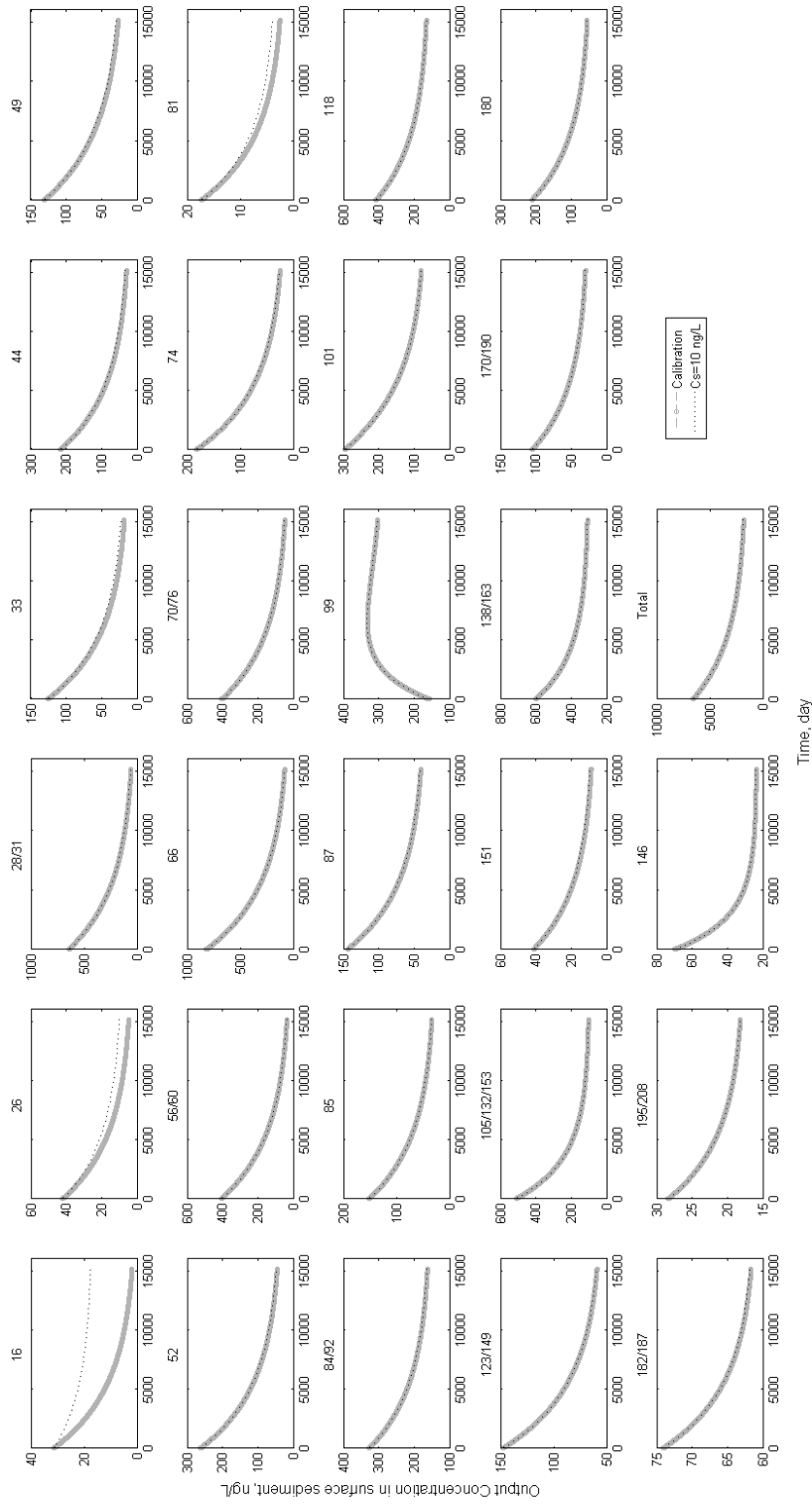


Figure F.4 Sensitivity Analysis of PCB congeners in Lake Michigan sediment:  $C_s$  Comparison

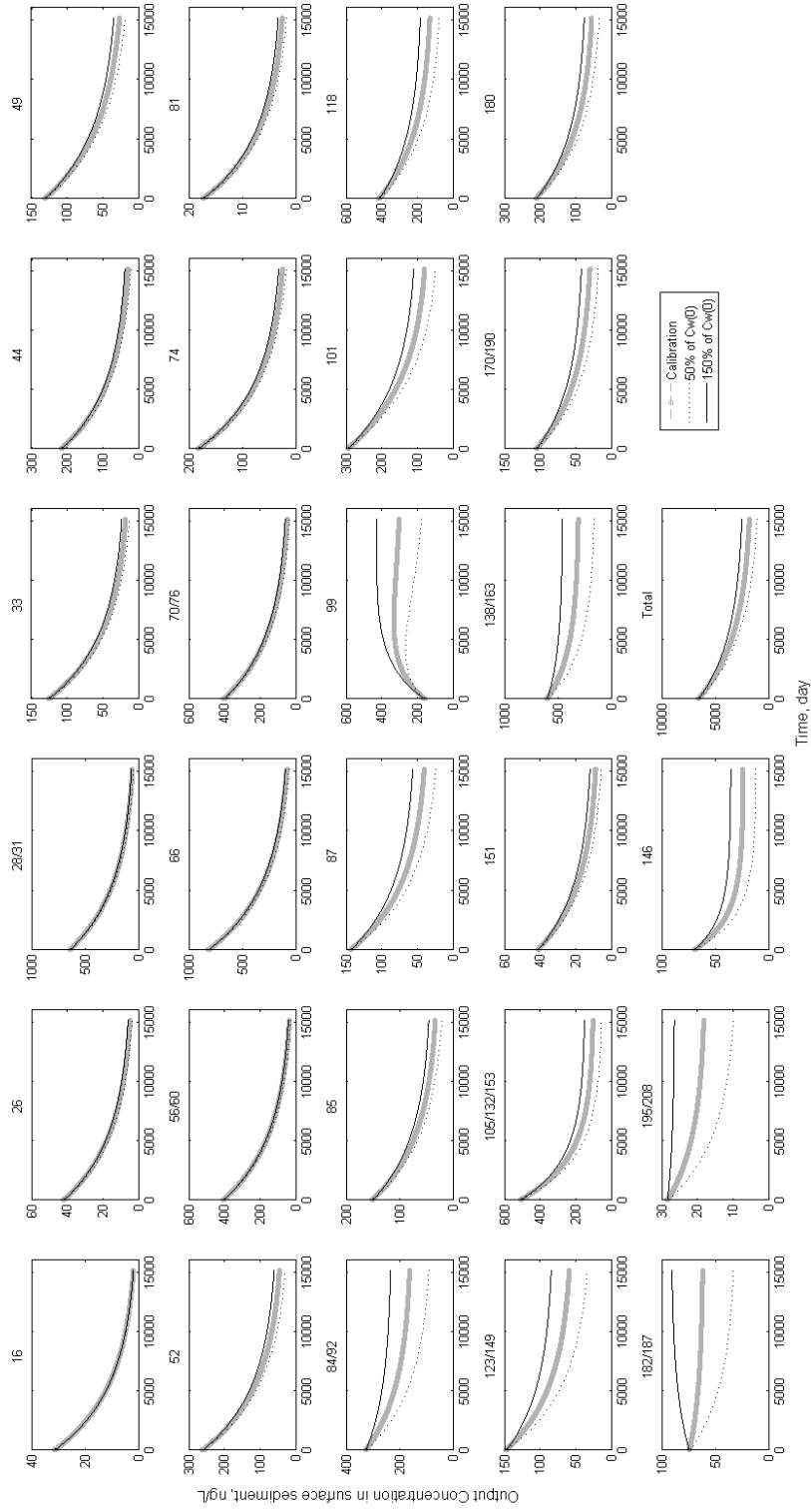


Figure F.5 Sensitivity Analysis of PCB congeners in Lake Michigan sediment:  $C_w$  Comparison

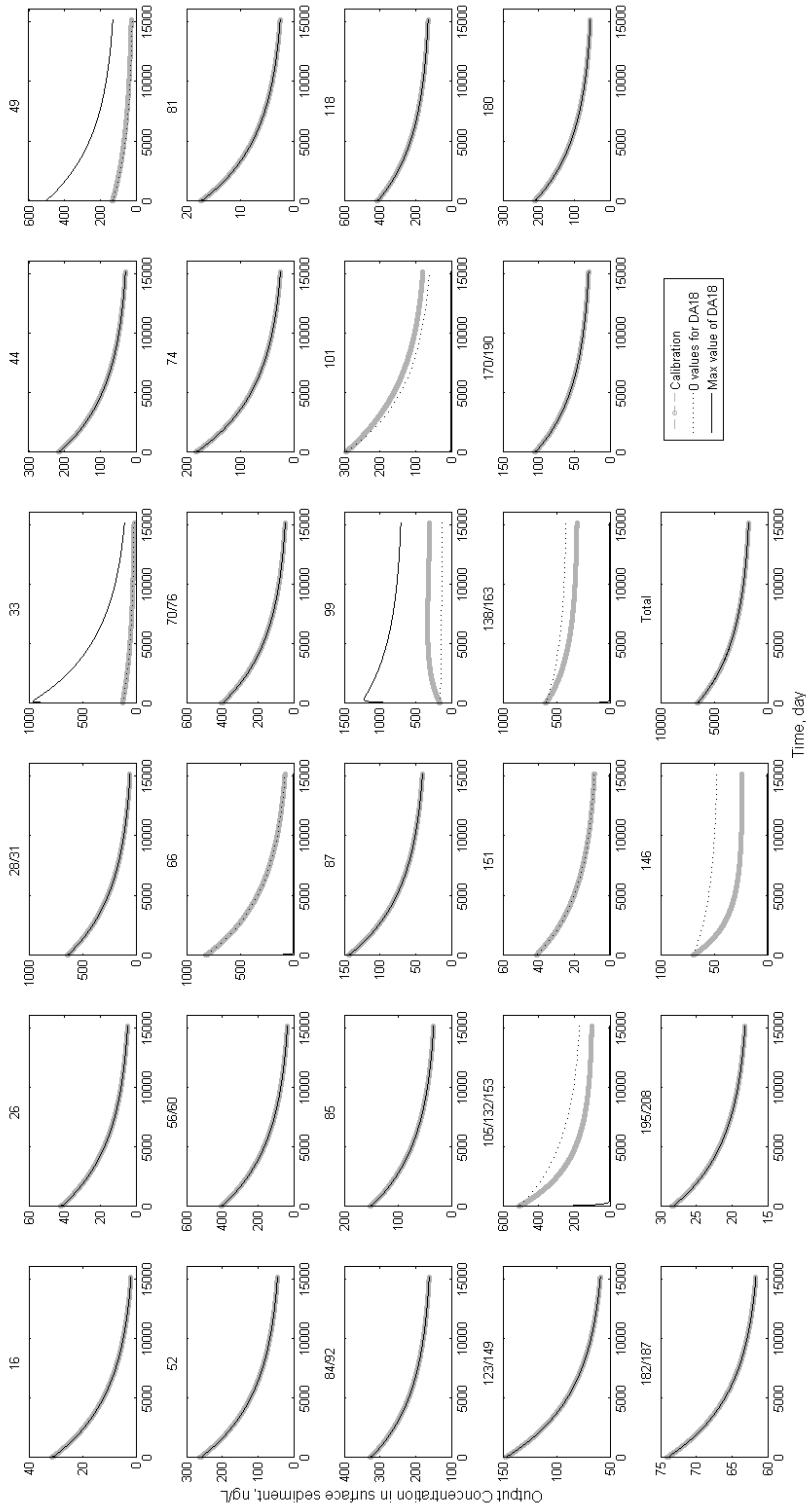


Figure F.6 Sensitivity Analysis of PCB congeners in Lake Michigan sediment: DA18 Comparison

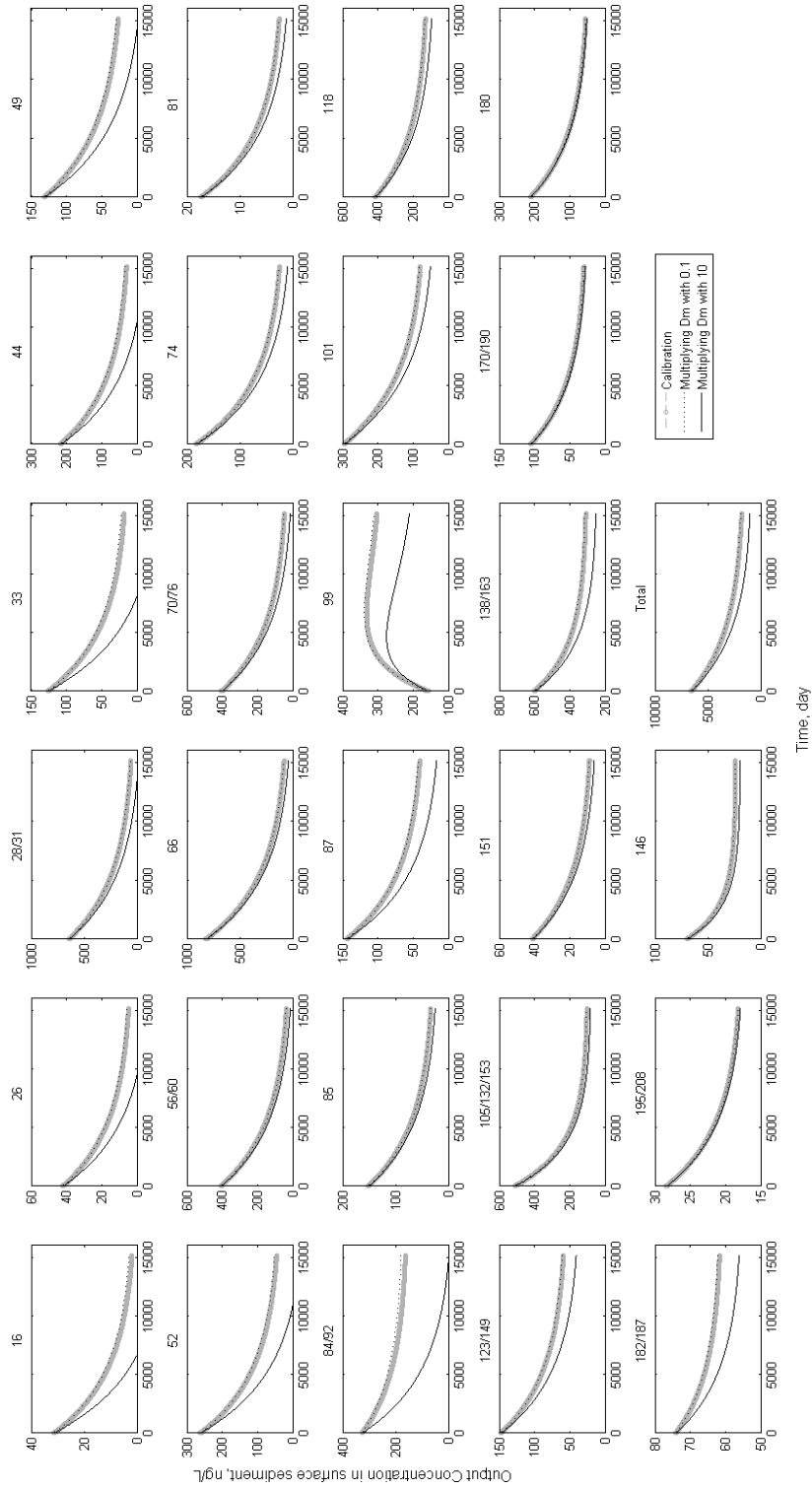


Figure F.7 Sensitivity Analysis of PCB congeners in Lake Michigan sediment: Diffusion Comparison



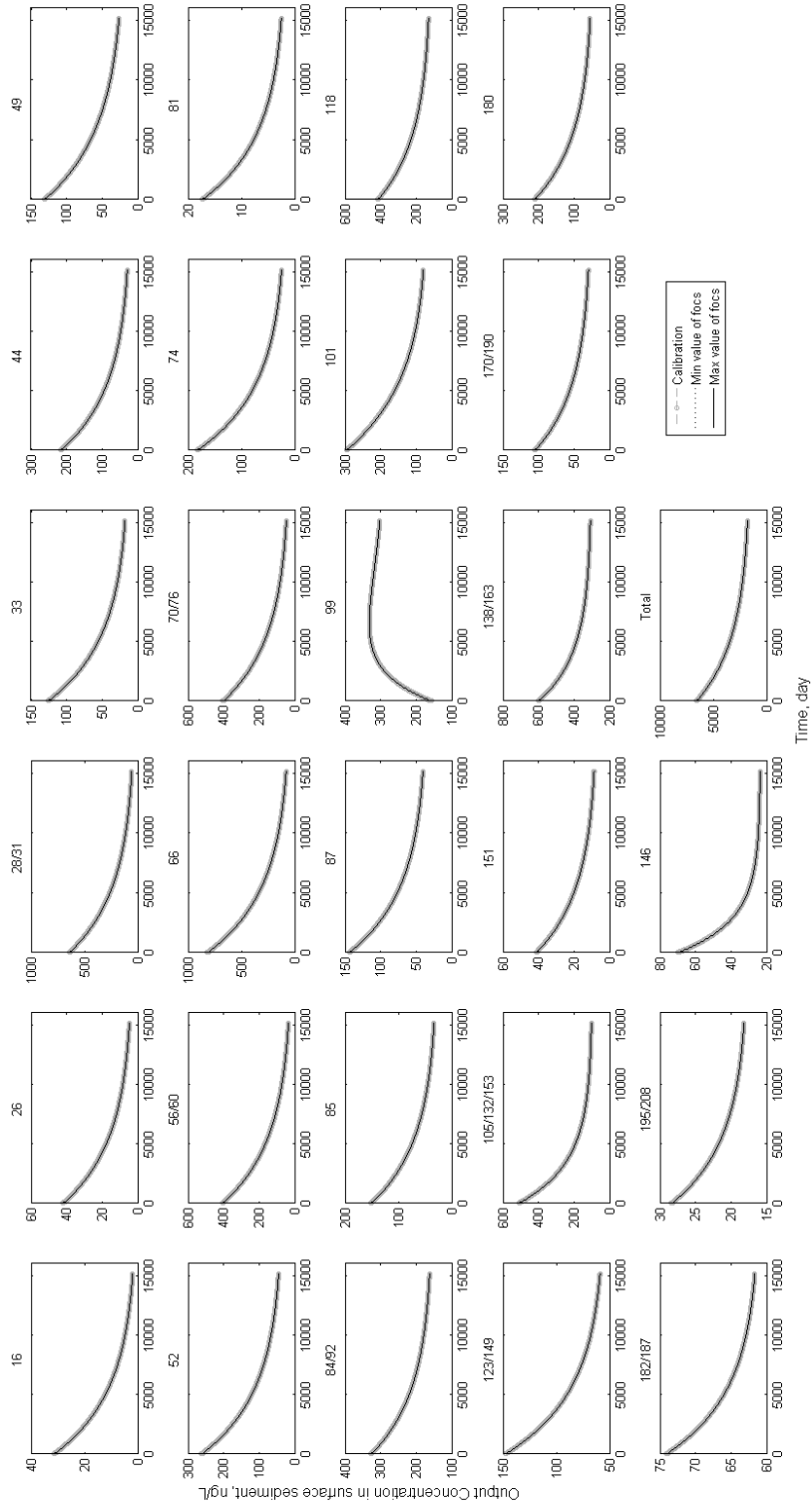


Figure F.8 Sensitivity Analysis of PCB congeners in Lake Michigan sediment:  $f_{ocs}$  Comparison

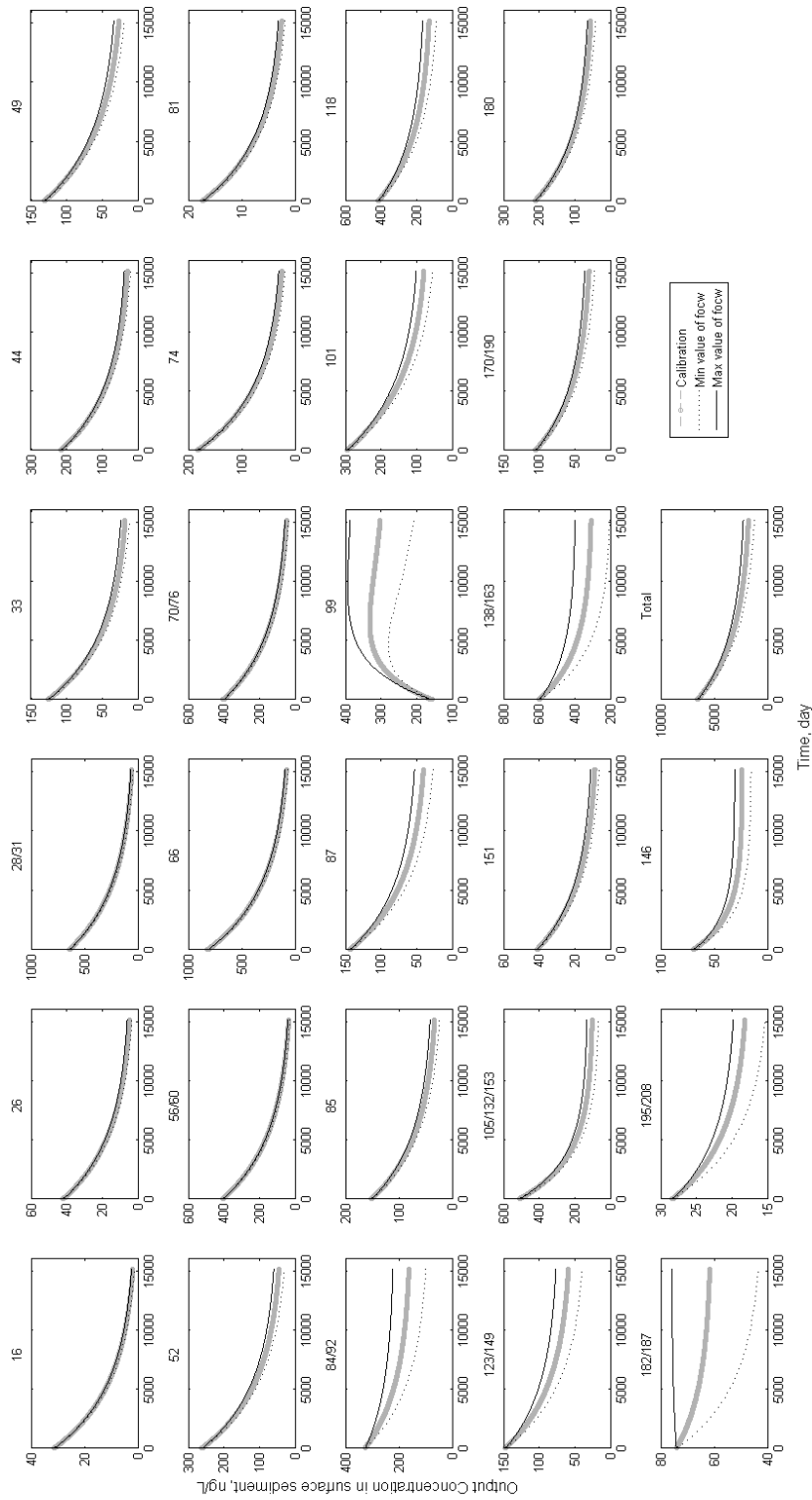


Figure F.9 Sensitivity Analysis of PCB congeners in Lake Michigan sediment:  $f_{0cw}$  Comparison

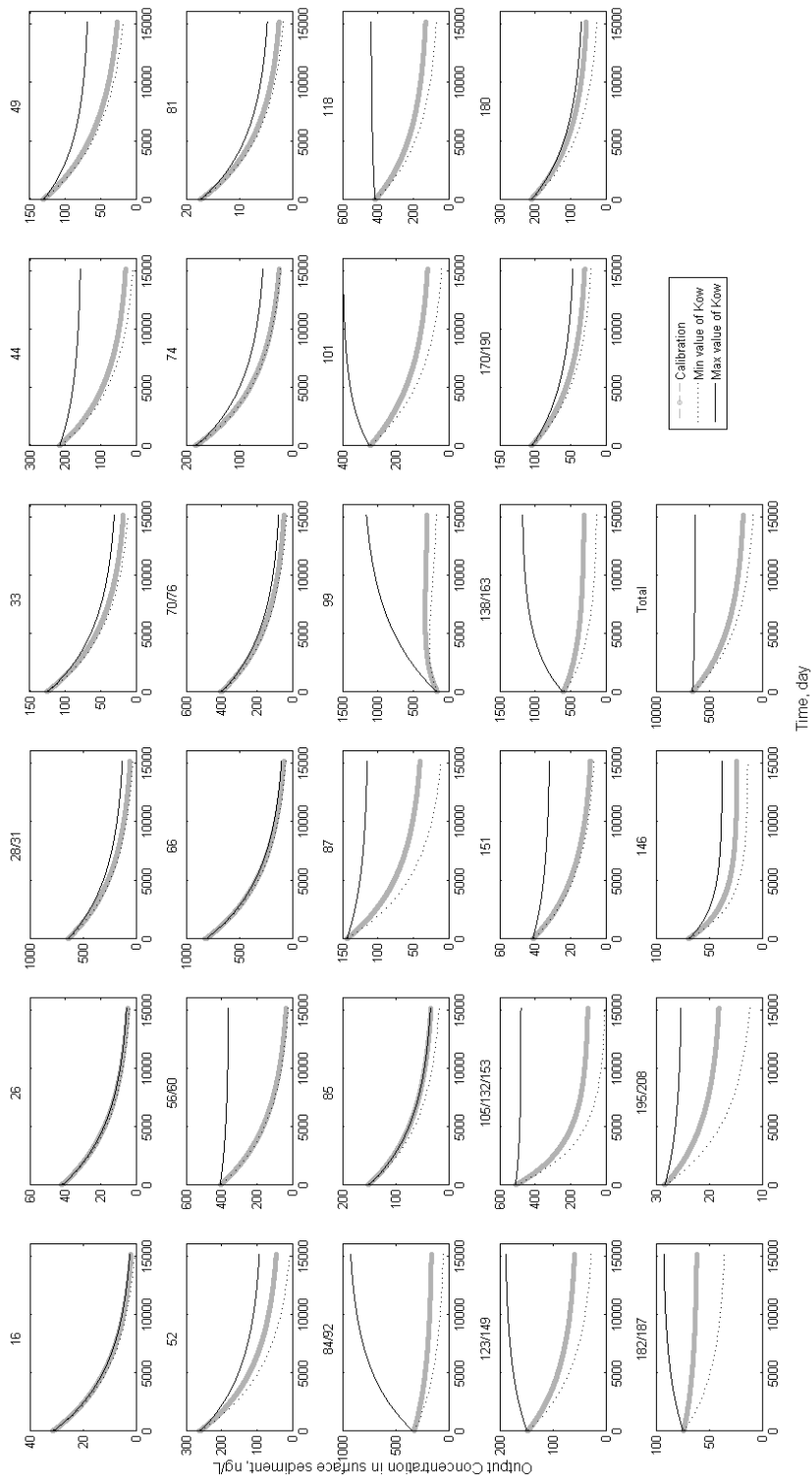


Figure F.10 Sensitivity Analysis of PCB congeners in Lake Michigan sediment:  $K_{ow}$  Comparison

Table F.3 Min, Max, Mean and Variance of 7 Parameters for Uncertainty Analysis

Parameters	Distribution	Lower Limit	Upper Limit	Mean	Variance
TSS, mg/L	Lognormal	0.2	2.41	0.942	0.162
$v_s$ , m/day	Uniform	0.2	1.5		
$f_{ocw}$	Uniform	0.039	0.09		

Table F.3 (Continued)

Congener IUPAC No		$k_m$ =Lognormal			
Mother	Daughter	Min	Max	Avg	Variance
66	33			$10^{-20}$	$8.7 \times 10^{-41}$
101	49			$10^{-5}$	$1.85 \times 10^{-10}$
138/163	99			$6.1 \times 10^{-5}$	$2.50 \times 10^{-10}$
105/132/153	99			0.00010	$4.69 \times 10^{-9}$
146	101			0.00018	$1.22 \times 10^{-7}$
151	66			$10^{-20}$	$5.95 \times 10^{-40}$

Table F.3 (Continued)

Congener IUPAC No	C <sub>w</sub> avg	Lognormal variance	LogK <sub>ow</sub> avg	Lognormal variance	D <sub>m</sub> avg	Lognormal variance
<b>16</b>	0.00190	0.00000	5.06	0.21	0.5714x10 <sup>5</sup>	0.00000
<b>26</b>	0.00167	0.00000	5.68	0.01	0.5714x10 <sup>5</sup>	0.00000
<b>28/31</b>	0.01156	0.00003	5.72	0.11	0.5714x10 <sup>5</sup>	0.00000
<b>33</b>	0.00711	0.00000	5.75	0.03	0.5714x10 <sup>5</sup>	0.00000
<b>44</b>	0.00867	0.00001	5.84	0.20	0.5471x10 <sup>5</sup>	0.00000
<b>49</b>	0.00469	0.00000	6.03	0.06	0.5471x10 <sup>5</sup>	0.00000
<b>52</b>	0.01156	0.00001	5.79	0.29	0.5471x10 <sup>5</sup>	0.00000
<b>56/60</b>	0.00385	0.00001	6.05	0.22	0.5471x10 <sup>5</sup>	0.00000
<b>66</b>	0.00725	0.00011	6.10	0.04	0.5471x10 <sup>5</sup>	0.00000
<b>70/76</b>	0.00595	0.00001	6.09	0.04	0.5471x10 <sup>5</sup>	0.00000
<b>74</b>	0.00268	0.00000	6.34	0.09	0.5471x10 <sup>5</sup>	0.00000
<b>81</b>	0.00024	0.00000	6.30	0.05	0.5471x10 <sup>5</sup>	0.00000
<b>84/92</b>	0.03038	0.00030	6.24	0.17	0.5228x10 <sup>5</sup>	0.00000
<b>85</b>	0.00165	0.00000	6.44	0.06	0.5228x10 <sup>5</sup>	0.00000
<b>87</b>	0.00447	0.00000	6.29	0.11	0.5228x10 <sup>5</sup>	0.00000
<b>99</b>	0.01285	0.00005	6.64	0.16	0.5228x10 <sup>5</sup>	0.00000
<b>101</b>	0.00498	0.00000	6.40	0.42	0.5228x10 <sup>5</sup>	0.00000
<b>118</b>	0.00711	0.00003	6.70	0.11	0.5228x10 <sup>5</sup>	0.00000
<b>123/149</b>	0.00371	0.00000	6.60	0.08	0.51065x10 <sup>5</sup>	0.00000
<b>105/132/153</b>	0.00650	0.00004	6.81	0.32	0.5066x10 <sup>5</sup>	0.00000
<b>151</b>	0.00055	0.00000	6.62	0.09	0.4985x10 <sup>5</sup>	0.00000
<b>138/163</b>	0.01663	0.00000	6.92	0.11	0.4985x10 <sup>5</sup>	0.00000
<b>170/190</b>	0.00067	0.00000	7.12	0.03	0.4742x10 <sup>5</sup>	0.00000
<b>180</b>	0.00101	0.00000	7.10	0.07	0.4742x10 <sup>5</sup>	0.00000
<b>182/187</b>	0.00156	0.00000	7.06	0.03	0.4742x10 <sup>5</sup>	0.00000
<b>195/208</b>	0.00020	0.00000	7.89	0.21	0.43775x10 <sup>5</sup>	0.00000
<b>146</b>	0.00181	0.00000	6.85	0.03	0.4985x10 <sup>5</sup>	0.00000

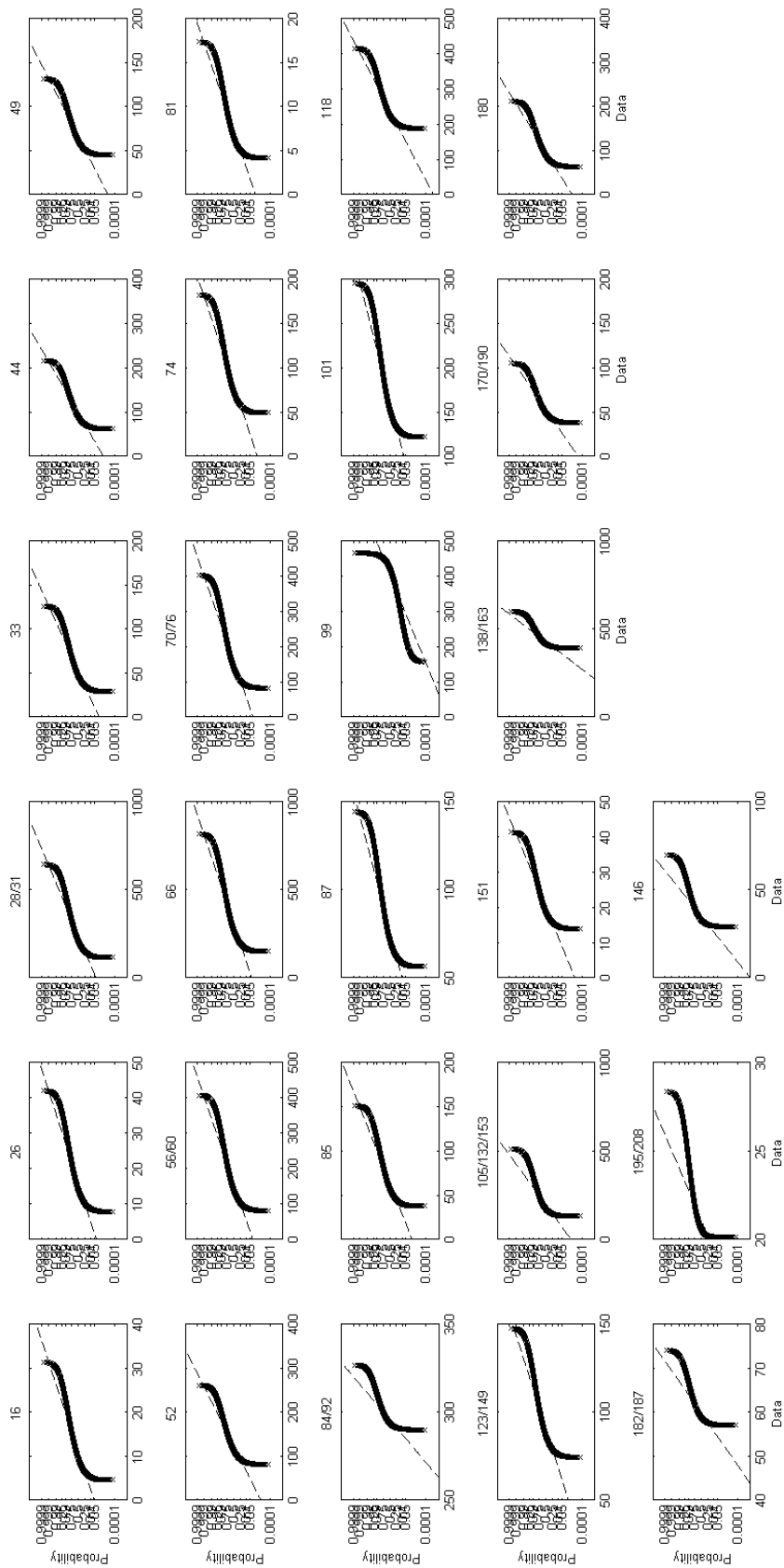


Figure F.11 Probability Graph for Normal Distribution of Uncertainty Analysis of Lake Michigan at 20-year

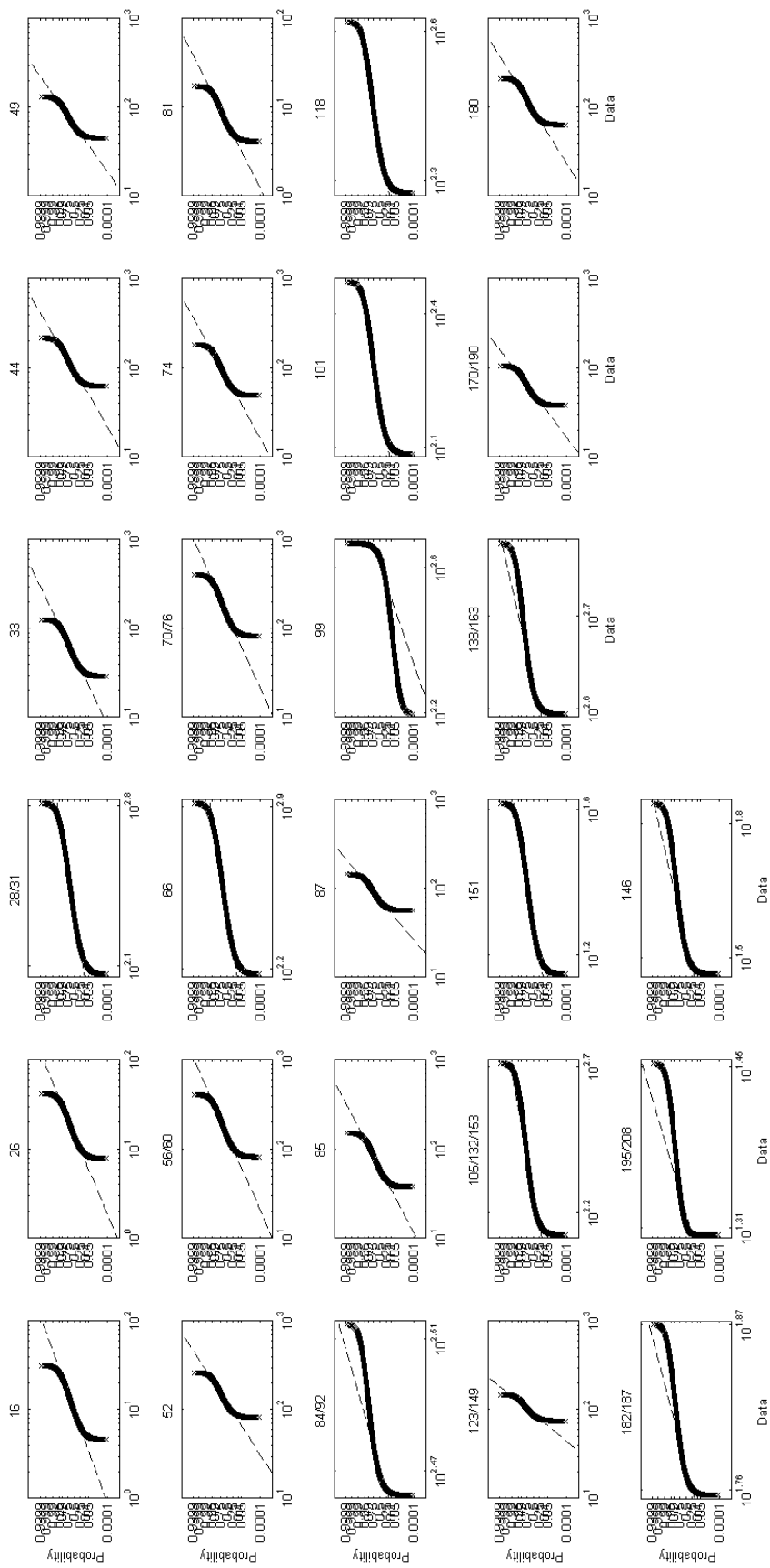


Figure F.12 Probability Graph for Lognormal Distribution of Uncertainty Analysis of Lake Michigan at 20 year

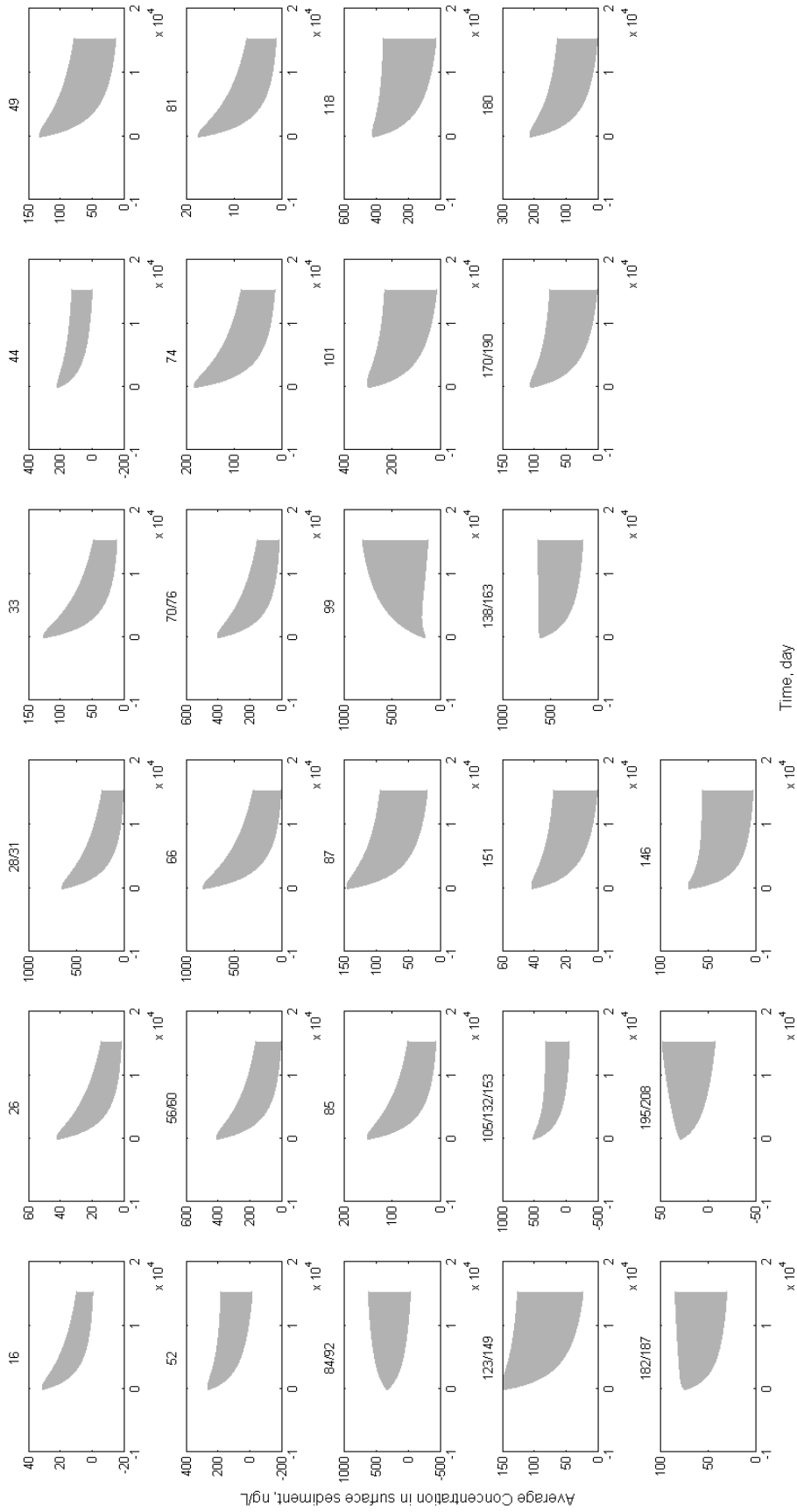


Figure F. 13 Mean and Standard Deviation of Output Concentration of Each Congener for 1000 runs by MC Simulation



## **APPENDIX G**

### **RESULTS OF FTHP MODEL FOR SAN FRANCISCO BAY SEDIMENTS CONTAMINATED BY PBDEs**

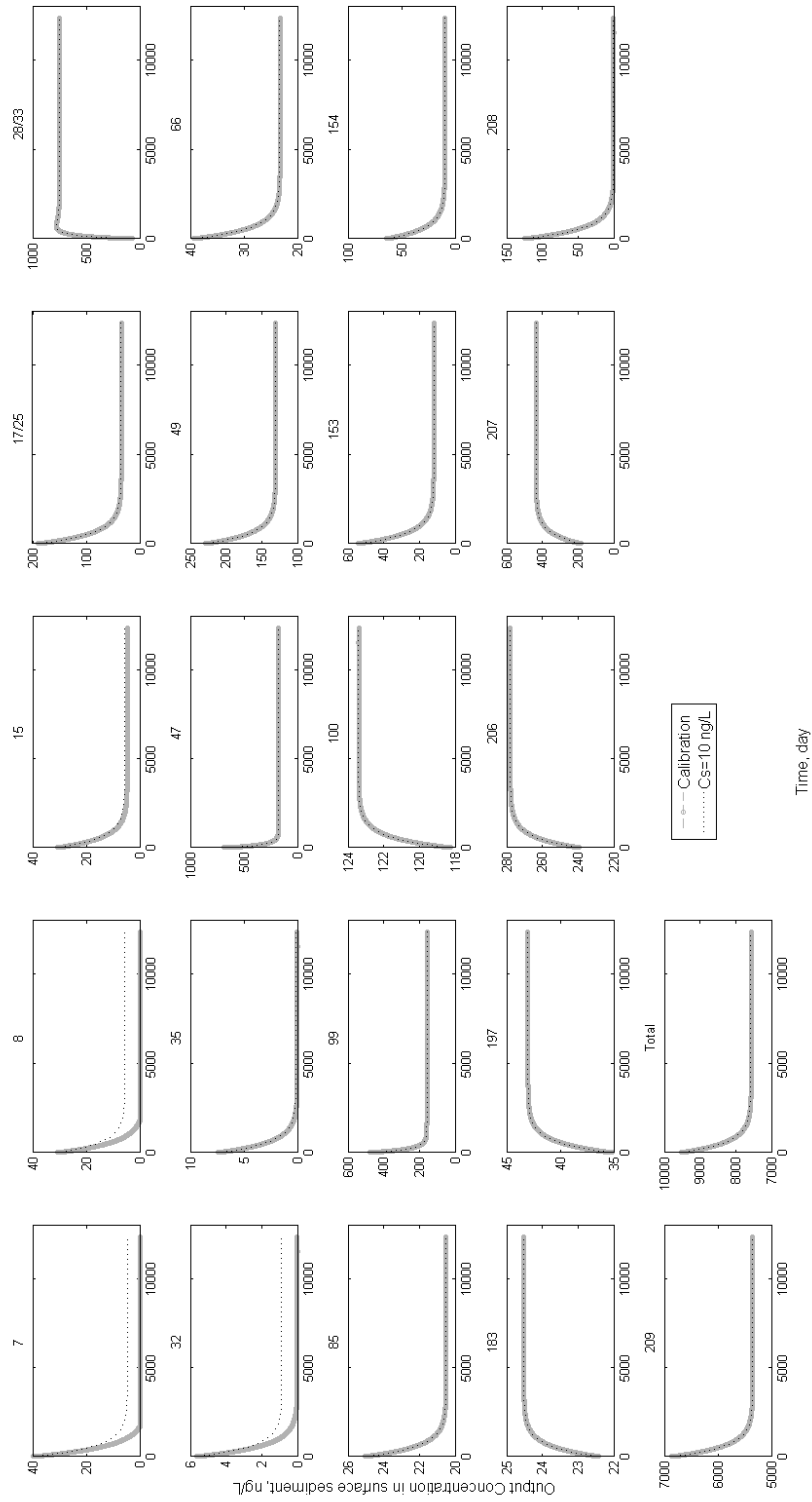
Table G.1 Trials for calibration of PBDE congeners in Lake Michigan sediment

Congener No	No Deg Term (S)		$v_b=0.5$ m/d(50%)		$v_b=1.5$ m/d(150%)		$v_b=0.00000097$ m/d		$v_b=0.00000291$ , m/d		$K_d$ with min values ( $\log K_{ow}-1$ )		$K_d$ with max values ( $\log K_{ow}+1$ )		Dehalogenations of 8 paths with $k_{max}$ J	
	R2	RMSE	R2	RMSE	R2	RMSE	R2	RMSE	R2	RMSE	R2	RMSE	R2	RMSE	R2	RMSE
7	0.07	22.51	0.02	21.47	0.11	22.51	0.07	22.51	0.07	22.51	0.08	22.63	0.06	13.77	0.07	22.51
8	0.00	19.80	0.00	18.35	0.02	19.87	0.00	19.80	0.00	19.80	0.01	20.01	0.00	14.16	0.00	19.80
15	0.16	11.13	0.09	10.61	0.23	10.85	0.16	11.13	0.16	11.13	0.17	14.11	0.16	14.59	0.16	11.13
17/25	0.09	75.15	0.05	69.68	0.14	74.52	0.09	75.15	0.09	75.15	0.10	98.03	0.09	89.81	0.09	75.15
28/33	0.41	19.49	0.33	17.61	0.49	19.66	0.41	19.49	0.41	19.49	0.42	25.80	0.41	24.61	0.69	722.26
32	0.68	1.47	0.59	1.16	0.73	1.66	0.68	1.47	0.68	1.47	0.68	1.47	0.68	1.47	0.68	1.47
35	0.43	2.35	0.33	2.23	0.50	2.44	0.43	2.35	0.43	2.35	0.43	2.35	0.43	2.35	0.43	2.35
47	0.38	310.80	0.32	322.79	0.45	306.25	0.38	310.80	0.38	310.80	0.38	198.26	0.38	564.00	0.69	137.22
49	0.34	72.38	0.24	83.74	0.43	66.66	0.34	72.38	0.34	72.38	0.34	71.38	0.34	124.95	0.34	72.38
66	0.53	14.94	0.43	17.03	0.63	13.99	0.53	14.94	0.53	14.94	0.53	9.63	0.53	25.59	0.53	14.94
85	0.90	14.46	0.84	15.19	0.94	14.20	0.90	14.46	0.90	14.46	0.90	2.94	0.90	14.96	0.90	14.46
99	0.52	253.74	0.45	262.98	0.60	250.38	0.52	253.74	0.52	253.74	0.52	209.92	0.52	435.67	0.81	68.08
100	0.56	101.83	0.48	95.87	0.64	104.21	0.56	101.83	0.56	101.83	0.56	98.95	0.56	113.01	0.45	70.43
153	0.75	45.25	0.69	42.49	0.80	46.29	0.75	45.25	0.75	45.25	0.75	45.25	0.75	45.94	0.79	11.30
154	0.59	49.26	0.50	48.03	0.68	49.76	0.59	49.26	0.59	49.26	0.59	49.32	0.59	49.33	0.68	14.09
183	0.85	20.93	0.78	20.13	0.90	21.23	0.85	20.93	0.85	20.93	0.85	20.96	0.85	20.96	0.85	18.23
197	0.94	31.88	0.96	30.60	0.90	32.30	0.94	31.88	0.94	31.88	0.94	31.88	0.94	31.89	0.94	31.88
206	0.53	190.30	0.43	183.65	0.63	192.97	0.53	190.30	0.53	190.30	0.53	190.30	0.53	190.31	0.53	190.30
207	0.60	305.15	0.50	262.02	0.68	321.17	0.60	305.15	0.60	305.15	0.60	299.75	0.60	305.10	0.60	305.15
208	0.75	23.96	0.66	29.21	0.82	23.50	0.75	23.96	0.75	23.96	0.75	23.96	0.75	23.96	0.75	23.96
209	0.44	3600.03	0.35	3845.29	0.52	3492.68	0.44	3600.03	0.44	3600.03	0.44	2126.37	0.44	3565.27	0.44	3600.03
$\Sigma$ PBDEs	0.45	4903.87	0.37	5186.61	0.54	4783.44	0.45	4903.87	0.45	4903.87	0.45	2960.38	0.45	5539.53	0.45	4904.31
Min	0.00		0.00		0.02		0.00		0.00		0.01		0.00		0.00	
Max	0.94		0.96		0.94		0.94		0.94		0.94		0.94		0.94	
Average	0.50		0.43		0.56		0.50		0.50		0.50		0.50		0.54	
Std	0.27		0.27		0.27		0.27		0.27		0.27		0.27		0.28	

Table G.1 (continued)

Congener No	Dehalogenations of 8 paths with kmax_II		Dehalogenations of 8 paths with kmedian_I		Dehalogenations of 8 paths with kmedian_II		Dehalogenations of 8 paths with kmax_I		v <sub>g</sub> =1.5 m/d(150%)		v <sub>g</sub> =1.5 Dehalogenations of 8 paths with kmax_II		v <sub>g</sub> =1.5 m/d(150%)		v <sub>g</sub> =1.5 Dehalogenations of 8 paths with kmedian_I		v <sub>g</sub> =1.5 m/d(150%)		v <sub>g</sub> =1.5 Dehalogenations of 8 paths with kmedian_III			
	R2	RMSE	R2	RMSE	R2	RMSE	R2	RMSE	R2	RMSE	R2	RMSE	R2	RMSE	R2	RMSE	R2	RMSE	R2	RMSE	R2	RMSE
7	0.07	22.51	0.07	22.51	0.07	22.51	0.11	22.51	0.11	22.51	0.11	22.51	0.11	22.51	0.11	22.51	0.11	22.51	0.11	22.51	0.11	22.51
8	0.00	19.80	0.00	19.80	0.00	19.80	0.02	19.87	0.02	19.87	0.02	19.87	0.02	19.87	0.02	19.87	0.02	19.87	0.02	19.87	0.02	19.87
15	0.16	11.13	0.16	11.13	0.16	11.13	0.23	10.85	0.23	10.85	0.23	10.85	0.23	10.85	0.23	10.85	0.23	10.85	0.23	10.85	0.23	10.85
17/25	0.09	75.15	0.09	75.15	0.09	75.15	0.14	74.52	0.14	74.52	0.14	74.52	0.14	74.52	0.14	74.52	0.14	74.52	0.14	74.52	0.14	74.52
28/33	<b>0.69</b>	734.15	<b>0.63</b>	393.50	<b>0.61</b>	464.33	<b>0.69</b>	625.69	<b>0.69</b>	625.69	<b>0.69</b>	625.69	<b>0.69</b>	625.69	<b>0.69</b>	625.69	<b>0.69</b>	625.69	<b>0.69</b>	625.69	<b>0.69</b>	625.69
32	0.68	1.47	0.68	1.47	0.68	1.47	0.73	1.66	0.73	1.66	0.73	1.66	0.73	1.66	0.73	1.66	0.73	1.66	0.73	1.66	0.73	1.66
35	0.43	2.35	0.43	2.35	0.43	2.35	0.50	2.44	0.50	2.44	0.50	2.44	0.50	2.44	0.50	2.44	0.50	2.44	0.50	2.44	0.50	2.44
47	<b>0.70</b>	142.10	<b>0.53</b>	148.96	<b>0.43</b>	181.44	<b>0.71</b>	117.91	<b>0.72</b>	121.66	<b>0.58</b>	155.62	<b>0.43</b>	66.66	<b>0.49</b>	195.39	<b>0.43</b>	66.66	<b>0.49</b>	195.39	<b>0.43</b>	66.66
49	0.34	72.38	0.34	72.38	0.34	72.38	0.43	66.66	0.43	66.66	0.43	66.66	0.43	66.66	0.43	66.66	0.43	66.66	0.43	66.66	0.43	66.66
66	0.53	14.94	0.53	14.94	0.53	14.94	0.63	13.99	0.63	13.99	0.63	13.99	0.63	13.99	0.63	13.99	0.63	13.99	0.63	13.99	0.63	13.99
85	0.90	14.46	0.90	14.46	0.90	14.46	0.94	14.20	0.94	14.20	0.94	14.20	0.94	14.20	0.94	14.20	0.94	14.20	0.94	14.20	0.94	14.20
99	<b>0.81</b>	68.08	<b>0.66</b>	114.74	<b>0.77</b>	75.16	<b>0.83</b>	74.13	<b>0.83</b>	74.13	<b>0.83</b>	74.13	<b>0.83</b>	74.13	<b>0.83</b>	74.13	<b>0.83</b>	74.13	<b>0.83</b>	74.13	<b>0.83</b>	74.13
100	<u>0.45</u>	70.43	0.56	101.83	0.56	52.99	<b>0.64</b>	83.53	<b>0.64</b>	83.53	<b>0.64</b>	83.53	<b>0.64</b>	83.53	<b>0.64</b>	83.53	<b>0.64</b>	83.53	<b>0.64</b>	83.53	<b>0.64</b>	83.53
153	<b>0.79</b>	11.30	0.75	44.82	0.75	44.82	<b>0.80</b>	7.51	<b>0.80</b>	7.51	<b>0.80</b>	7.51	<b>0.80</b>	7.51	<b>0.80</b>	7.51	<b>0.80</b>	7.51	<b>0.80</b>	7.51	<b>0.80</b>	7.51
154	<b>0.68</b>	14.09	0.59	49.40	0.59	42.16	<b>0.68</b>	12.55	<b>0.68</b>	12.55	<b>0.68</b>	12.55	<b>0.68</b>	12.55	<b>0.68</b>	12.55	<b>0.68</b>	12.55	<b>0.68</b>	12.55	<b>0.68</b>	12.55
183	0.85	18.23	0.85	20.79	0.85	20.72	0.85	20.72	0.85	20.72	0.85	20.72	0.85	20.72	0.85	20.72	0.85	20.72	0.85	20.72	0.85	20.72
197	0.94	31.88	0.94	31.88	0.94	31.88	0.90	32.30	0.90	32.30	0.90	32.30	0.90	32.30	0.90	32.30	0.90	32.30	0.90	32.30	0.90	32.30
206	0.53	190.30	0.53	190.30	0.53	190.30	0.63	192.97	0.63	192.97	0.63	192.97	0.63	192.97	0.63	192.97	0.63	192.97	0.63	192.97	0.63	192.97
207	0.60	305.15	0.60	305.15	0.60	305.15	0.68	321.17	0.68	321.17	0.68	321.17	0.68	321.17	0.68	321.17	0.68	321.17	0.68	321.17	0.68	321.17
208	0.75	23.96	0.75	23.96	0.75	23.96	0.82	23.50	0.82	23.50	0.82	23.50	0.82	23.50	0.82	23.50	0.82	23.50	0.82	23.50	0.82	23.50
209	0.44	3600.03	0.44	3600.03	0.44	3600.03	0.52	3492.68	0.52	3492.68	0.52	3492.68	0.52	3492.68	0.52	3492.68	0.52	3492.68	0.52	3492.68	0.52	3492.68
ΣPBDEs	0.45	4904.34	0.45	4903.93	0.45	4903.96	0.54	4783.74	0.54	4783.74	0.54	4783.74	0.54	4783.74	0.54	4783.74	0.54	4783.74	0.54	4783.74	0.54	4783.74
Min	0.00		0.00		0.00		0.02		0.02		0.02		0.02		0.02		0.02		0.02		0.02	
Max	0.94		0.94		0.94		0.94		0.94		0.94		0.94		0.94		0.94		0.94		0.94	
Average	<b>0.54</b>		<b>0.53</b>		<b>0.52</b>		<b>0.60</b>		<b>0.60</b>		<b>0.58</b>		<b>0.58</b>		<b>0.58</b>		<b>0.58</b>		<b>0.58</b>		<b>0.58</b>	
Std	<b>0.28</b>		0.27		0.27		0.27		0.27		0.27		0.27		0.27		0.27		0.27		0.27	

Bold and underlined numbers : maximum increase according to value in No degradation case, Italic and underlined numbers decrease according to value in No degradation case.



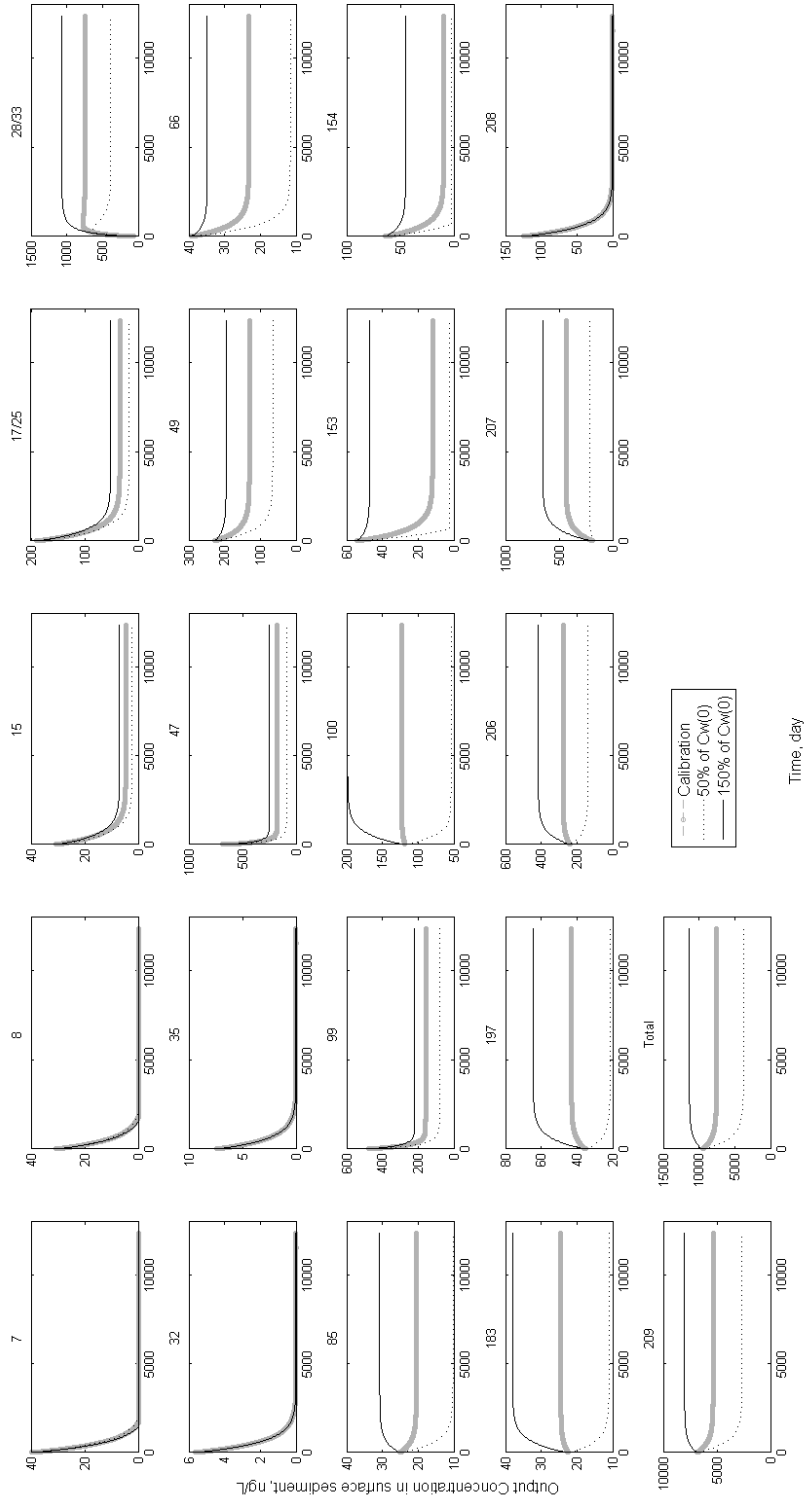


Figure G.2 Sensitivity Analysis of PBDE congeners in SF Bay sediment:  $C_w$  Comparison

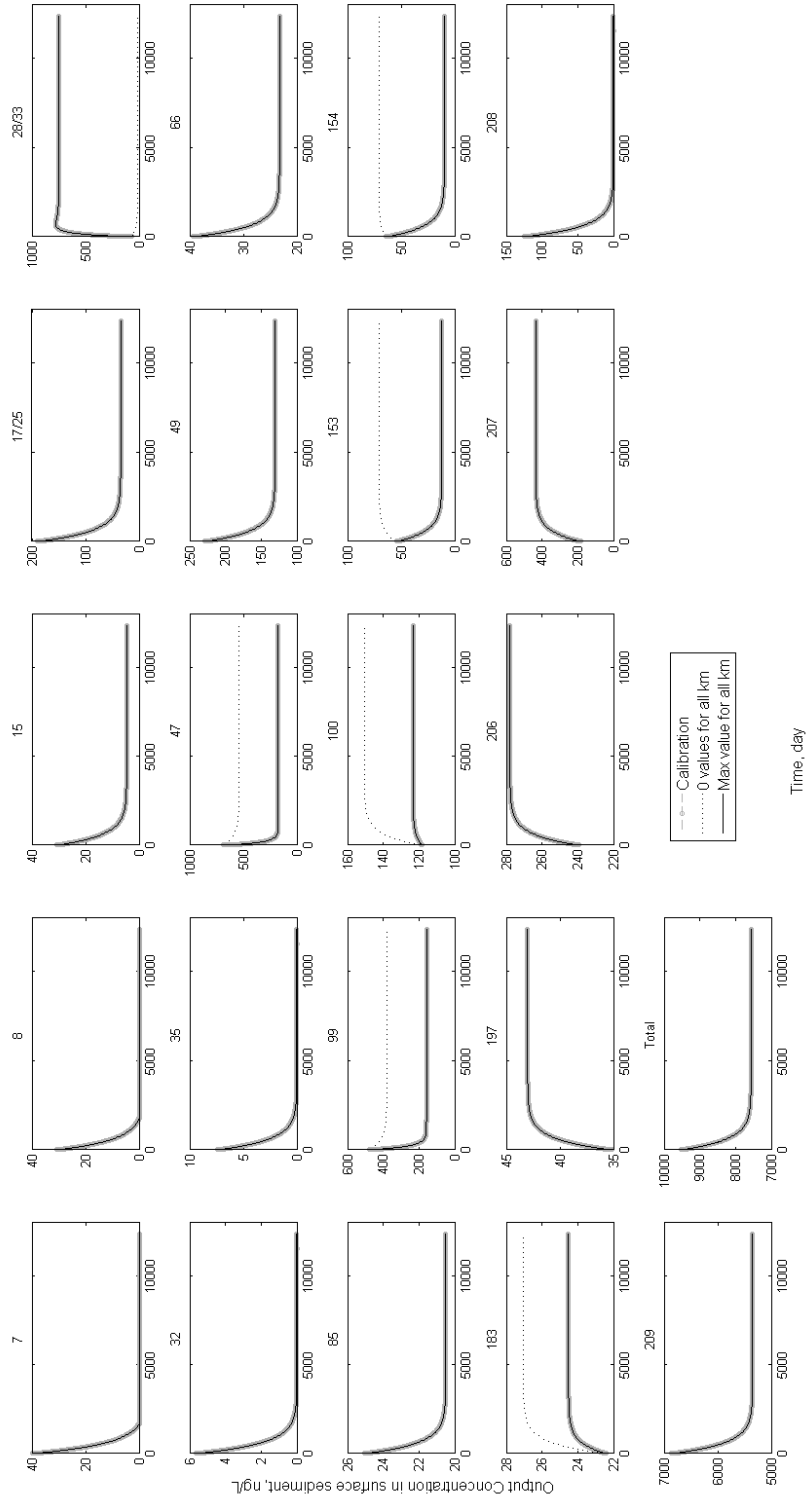


Figure G.3 Sensitivity Analysis of PBDE congeners in SF Bay sediment:  $k_m$  Comparison

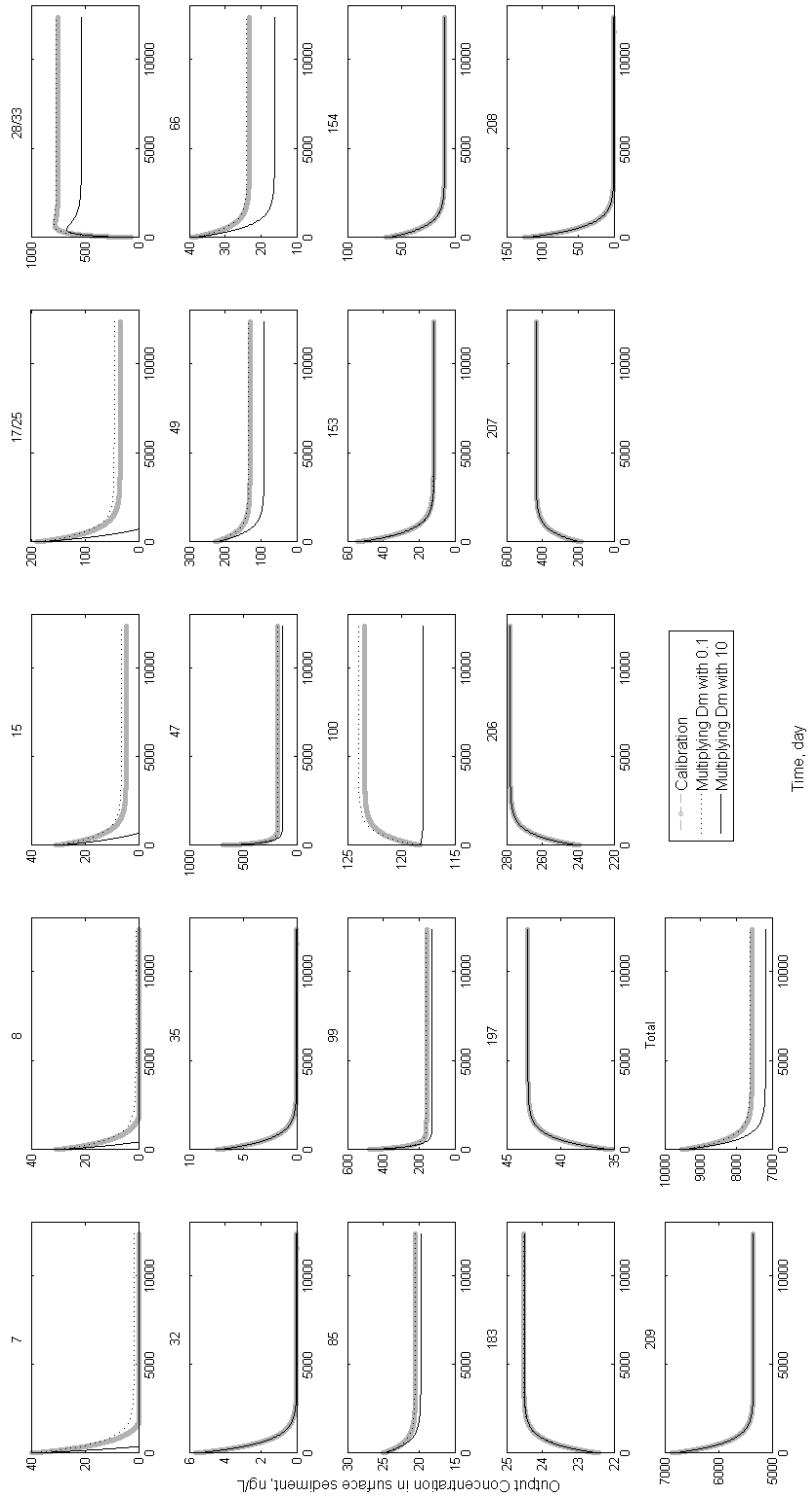


Figure G.4 Sensitivity Analysis of PBDE congeners in SF Bay sediment:  $D_m$  Comparison

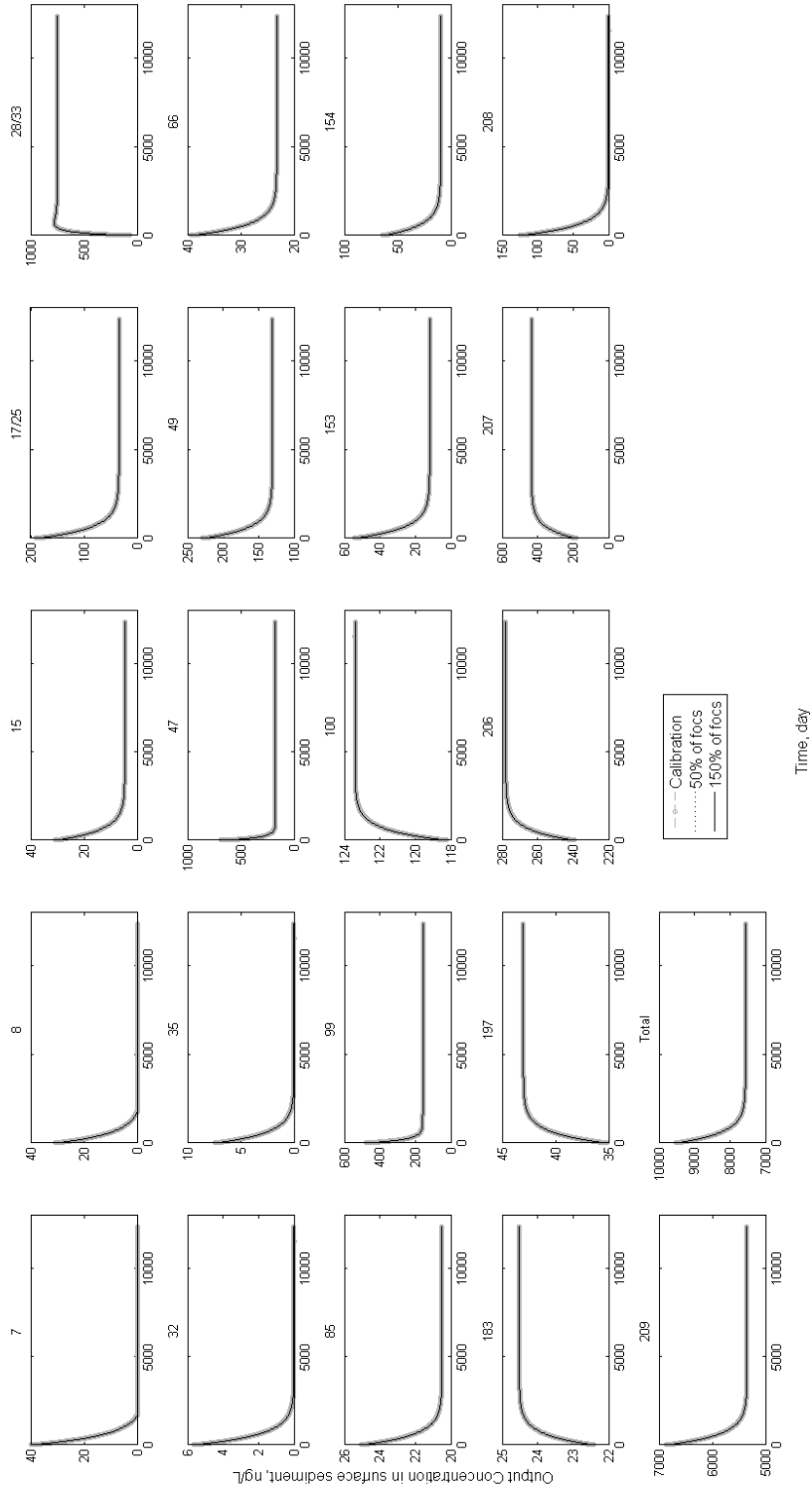


Figure G.5 Sensitivity Analysis of PBDE congeners in SF Bay sediment:  $f_{ocs}$  Comparison



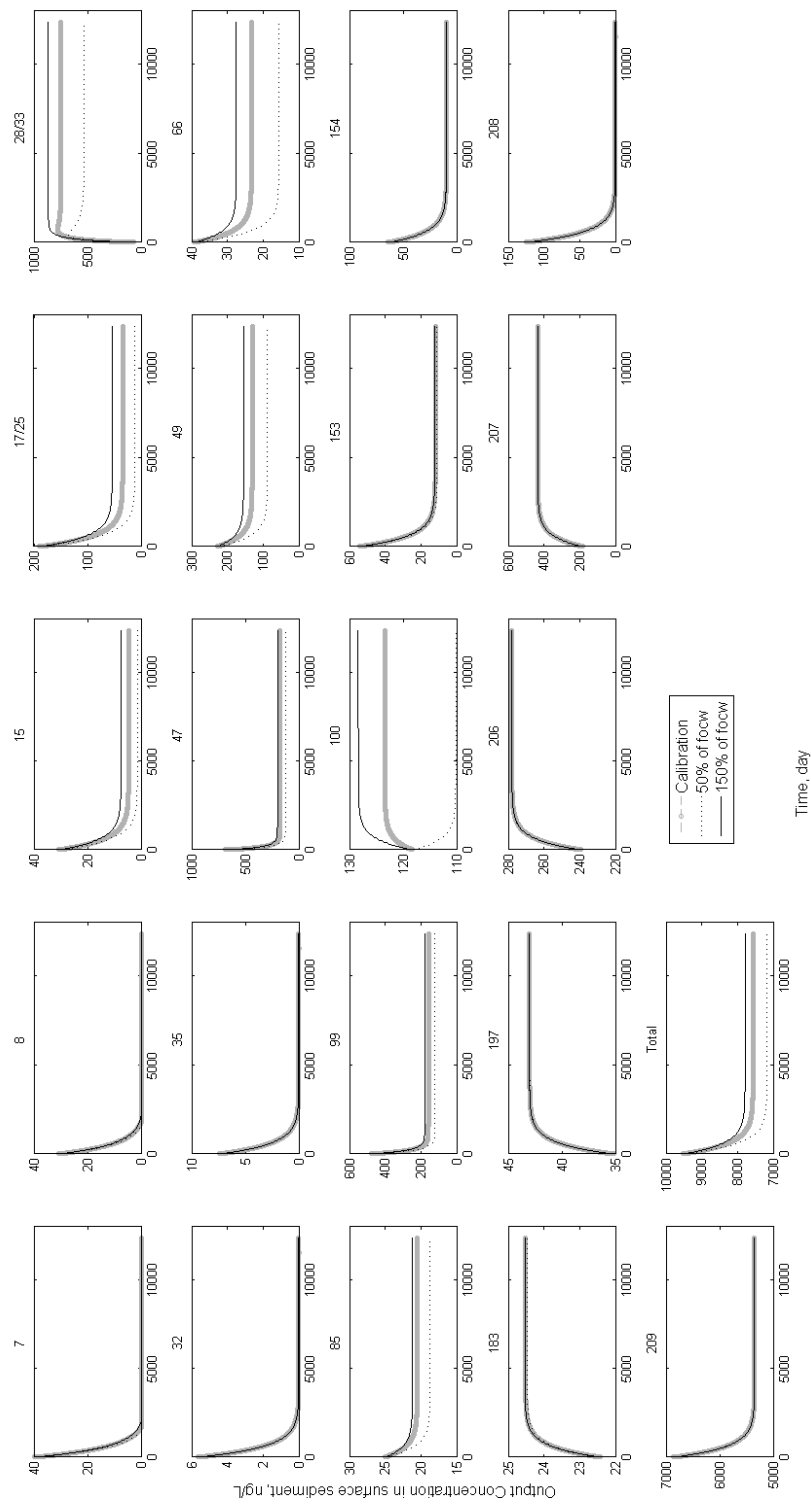


Figure G.6 Sensitivity Analysis of PBDE congeners in SF Bay sediment:  $f_{ocw}$  Comparison

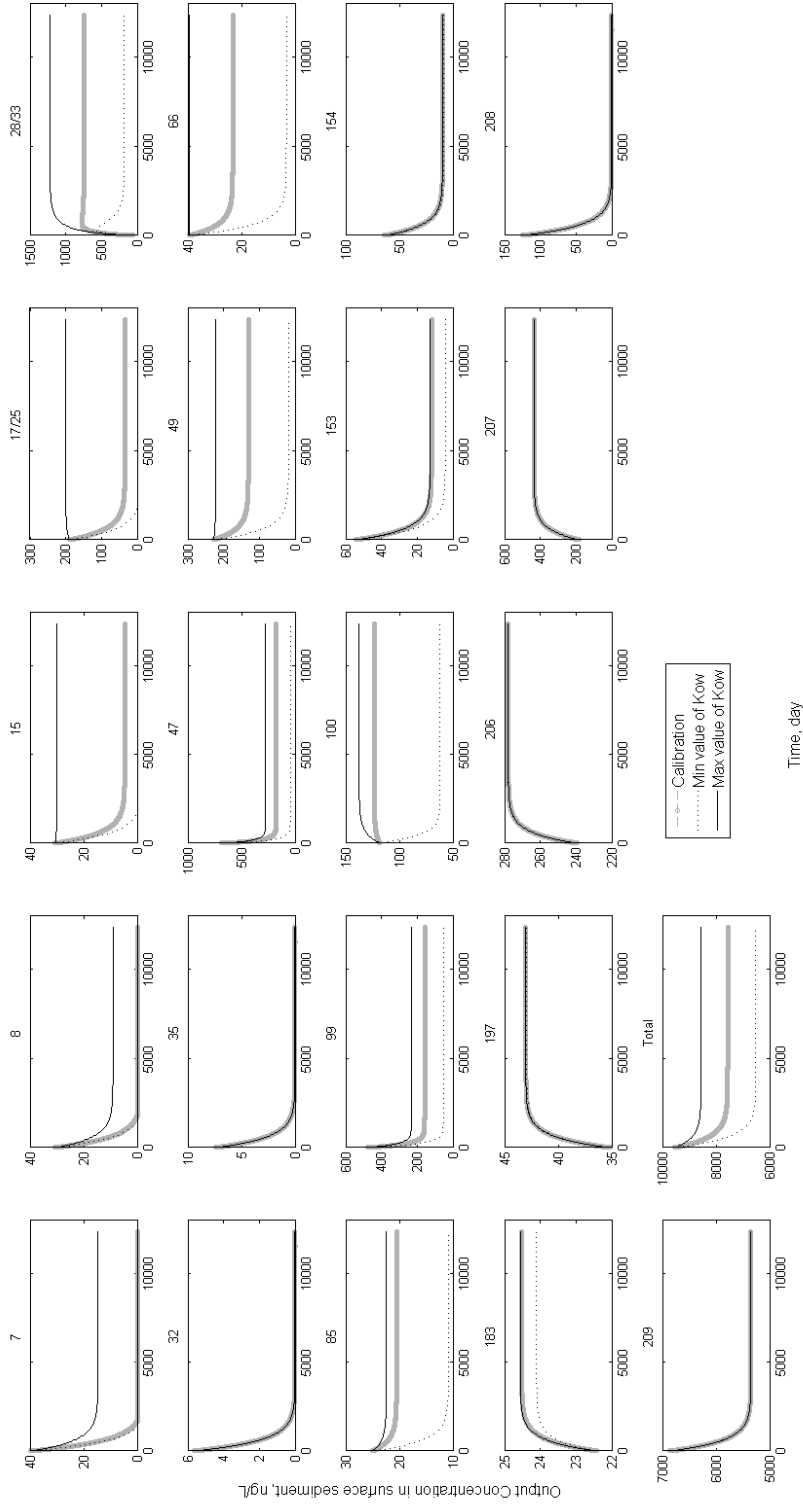


Figure G.7 Sensitivity Analysis of PBDE congeners in SF Bay sediment:  $K_{ow}$  Comparison

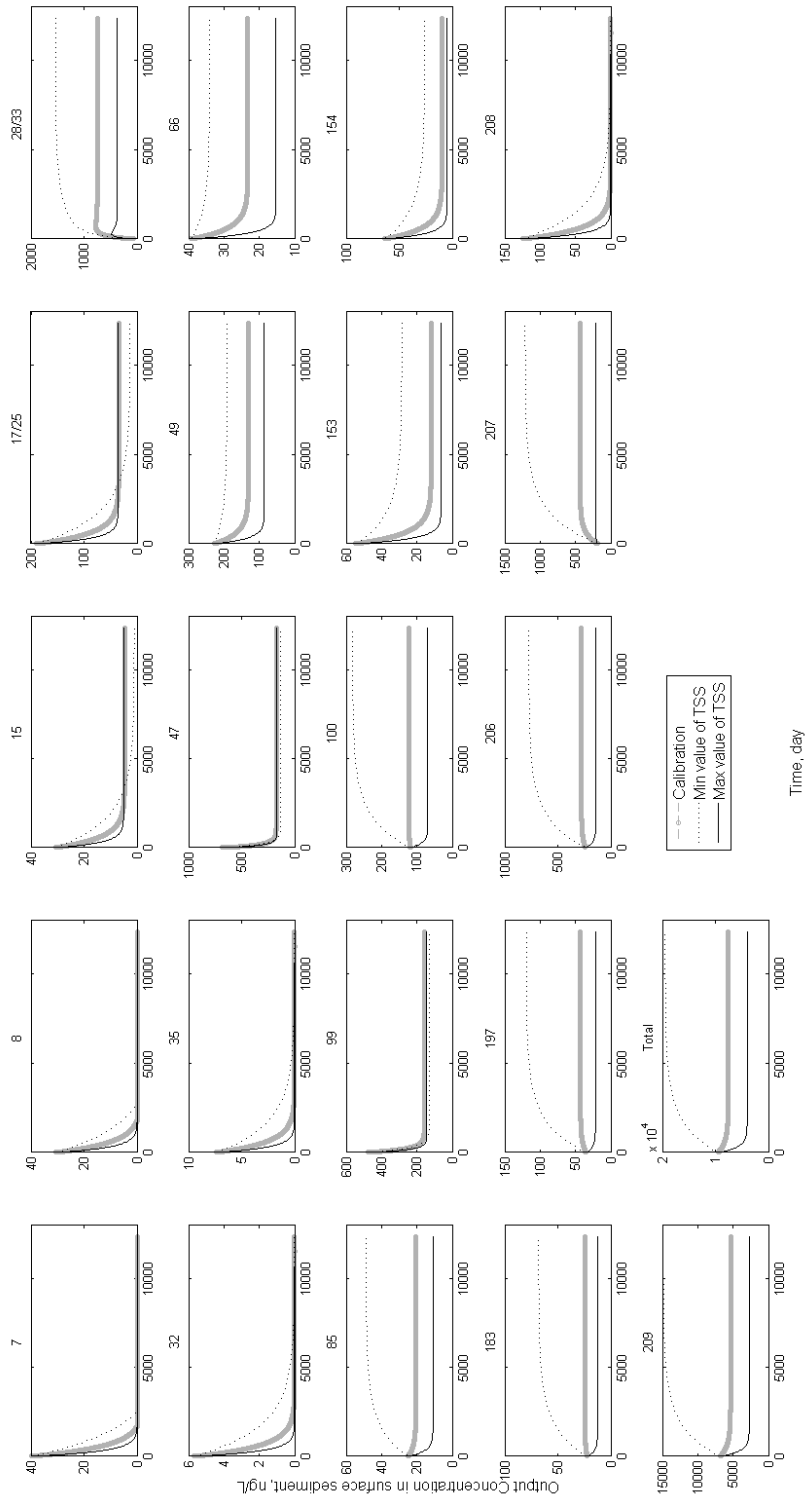


Figure G.8 Sensitivity Analysis of PBDE congeners in SF Bay sediment: TSS Comparison

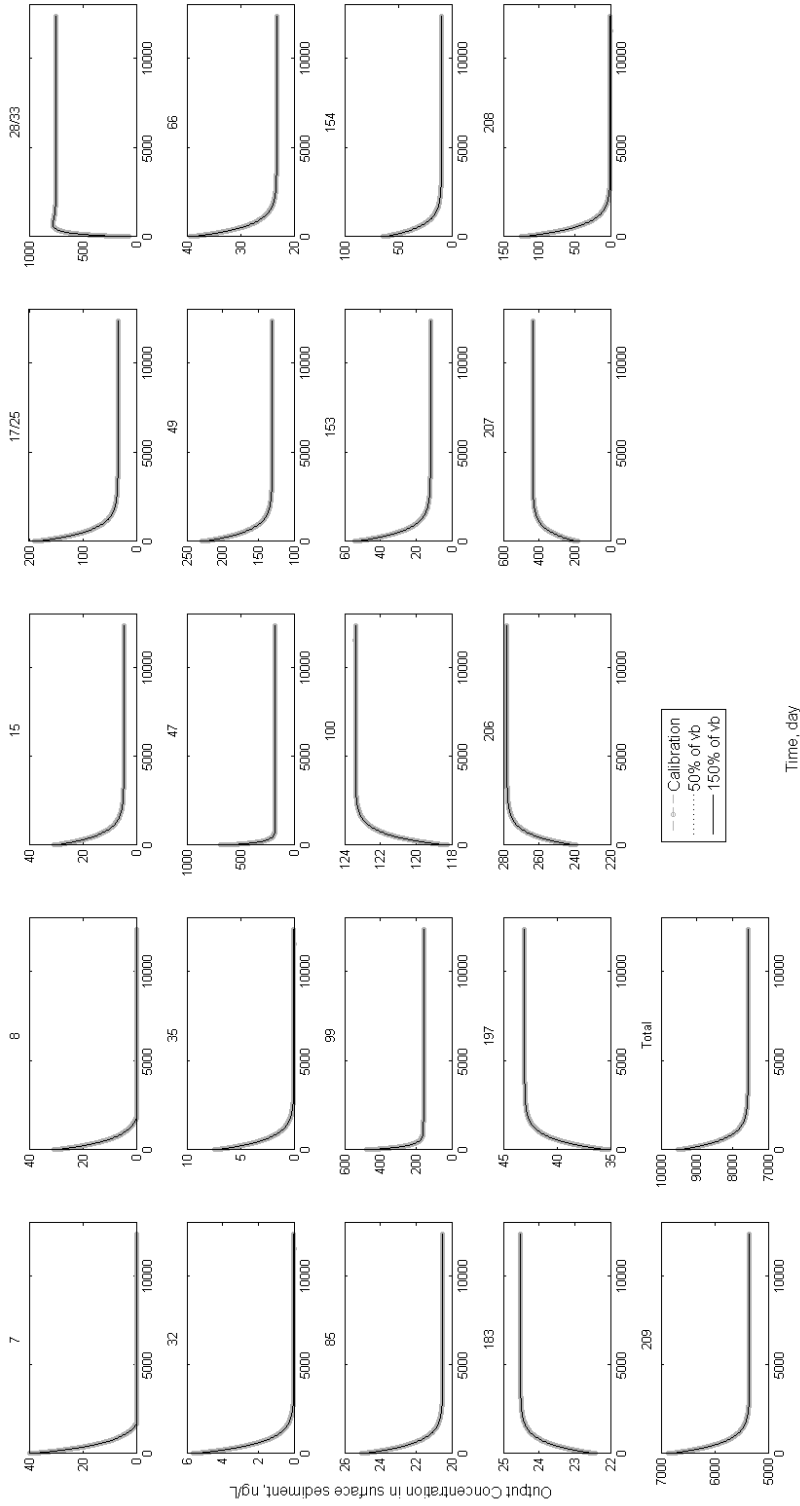


Figure G.9 Sensitivity Analysis of PBDE congeners in SF Bay sediment:  $v_b$  Comparison

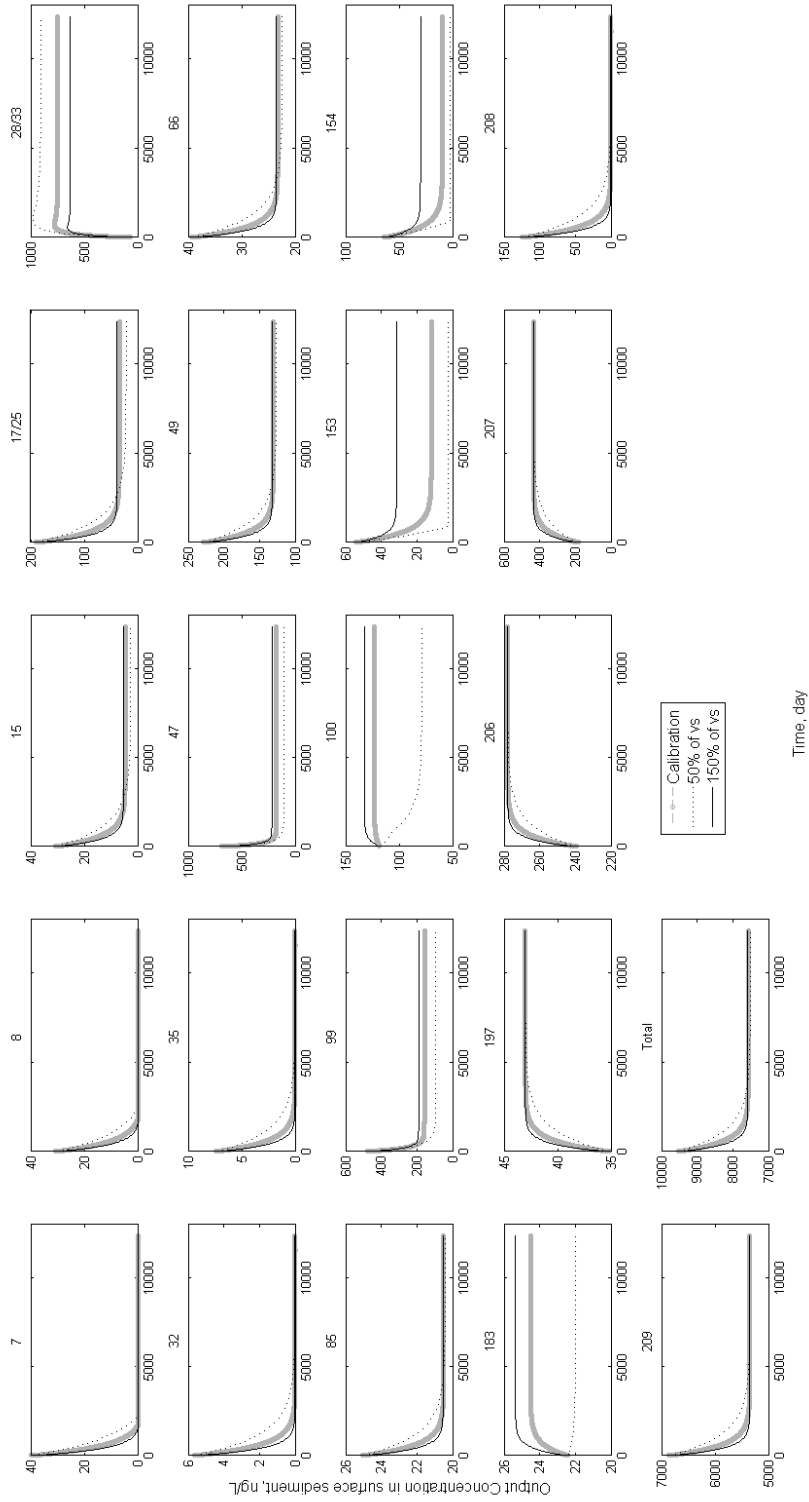


Figure G.10 Sensitivity Analysis of PBDE congeners in SF Bay sediment:  $v_s$  Comparison

Table G.2 Min, Max, Mean and Variance of 7 Parameters for Uncertainty Analysis

Parameters	Distribution	Lower Limit	Upper Limit	Mean	Variance
TSS, mg/L	Lognormal			37.67	350.97
f <sub>ocw</sub>	Uniform	0.005	0.015		

Table G.2 (Continued)

Congener IUPAC No		k <sub>m</sub> =Lognormal			
Mother	Daughter	Min	Max	Avg	Variance
47	28/33			0.007	0.000058
99	47			0.003	0.000012
100	47			0.001	0.000002
153	99			0.024	0.002
154	99			0.018	0.001
154	100			0.008	0.00007
183	153			0.003	0.00002
183	154			0.017	0.001

Table G.2 (Continued)

Congener IUPAC No	Cw avg	Lognormal variance	LogKow avg	Lognormal variance
<b>7</b>	0.006	0.9 x10 <sup>9</sup>	4.99	0.0006
<b>8</b>	0.004	0.3 x10 <sup>9</sup>	4.99	0.0006
<b>15</b>	0.003	0.2 x10 <sup>9</sup>	5.83	0.0008
<b>17/25</b>	0.019	8.7 x10 <sup>9</sup>	5.88	0.0009
<b>28/33</b>	0.005	0.6 x10 <sup>9</sup>	5.88	0.0009
<b>32</b>	0	0	5.88	0.0009
<b>35</b>	0	0	6.72	0.0011
<b>47</b>	0.056	78.7 x10 <sup>9</sup>	6.77	0.0011
<b>49</b>	0.014	4.6 x10 <sup>9</sup>	6.77	0.0011
<b>66</b>	0.002	0.1 x10 <sup>9</sup>	6.77	0.0011
<b>85</b>	0.001	41 x10 <sup>12</sup>	7.66	0.0015
<b>99</b>	0.037	33.7 x10 <sup>9</sup>	6.84	0.0012
<b>100</b>	0.009	2.2 x10 <sup>9</sup>	7.66	0.0015
<b>153</b>	0.004	0.4 x10 <sup>9</sup>	8.55	0.0018
<b>154</b>	0.004	0.4 x10 <sup>9</sup>	9.55	0.0023
<b>183</b>	0.002	0.1 x10 <sup>9</sup>	9.44	0.0022
<b>197</b>	0.002	0.1 x10 <sup>9</sup>	10.33	0.0027
<b>206</b>	0.016	6.2 x10 <sup>9</sup>	11.22	0.0031
<b>207</b>	0.025	15.1 x10 <sup>9</sup>	11.22	0.0031
<b>208</b>	0	0	11.22	0.0031
<b>209</b>	0.302	2280 x10 <sup>9</sup>	12.11	0.0037

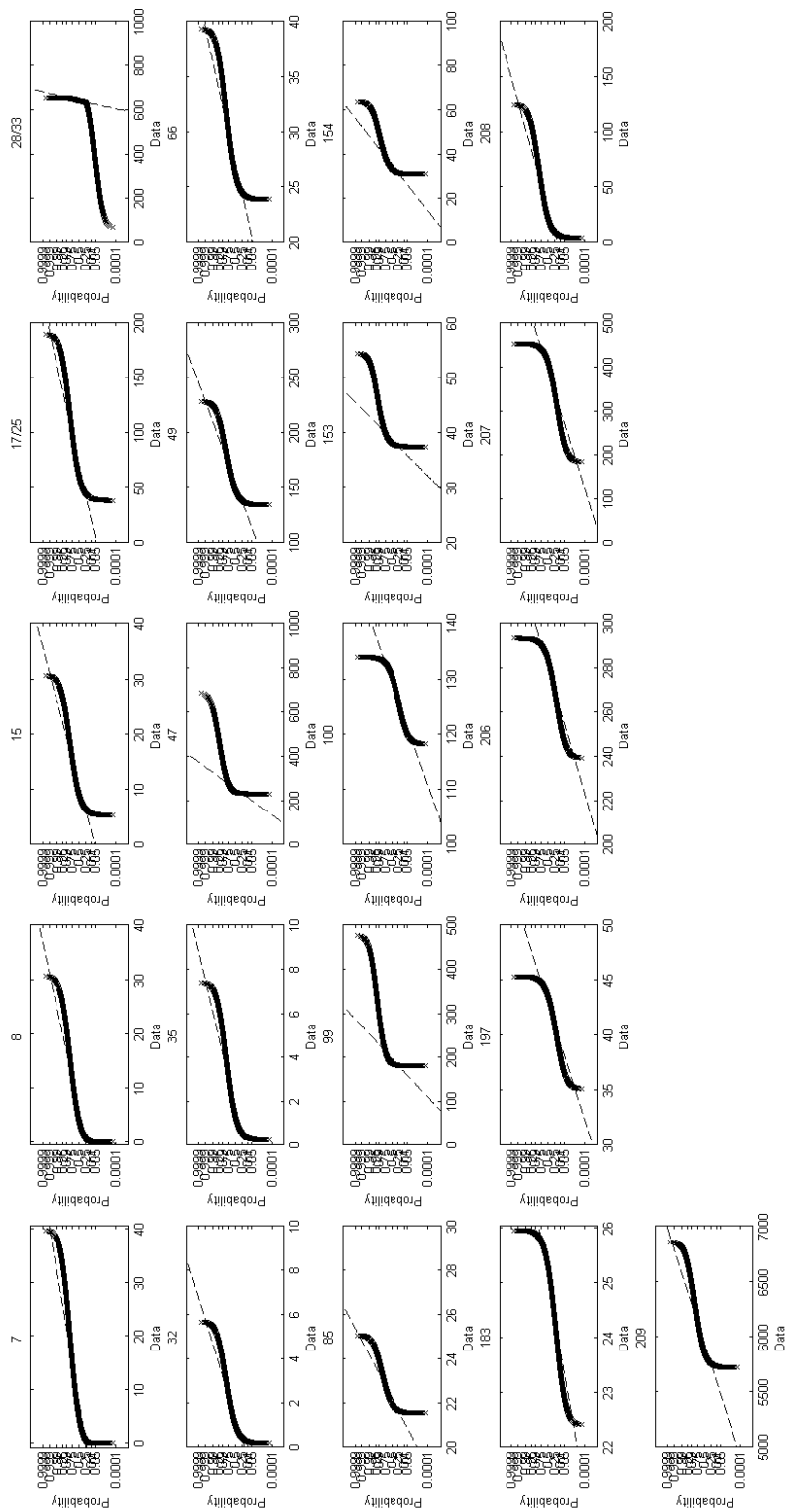


Figure G.11 Probability Graph for Normal Distribution of Uncertainty Analysis of Lake Michigan at 20-year



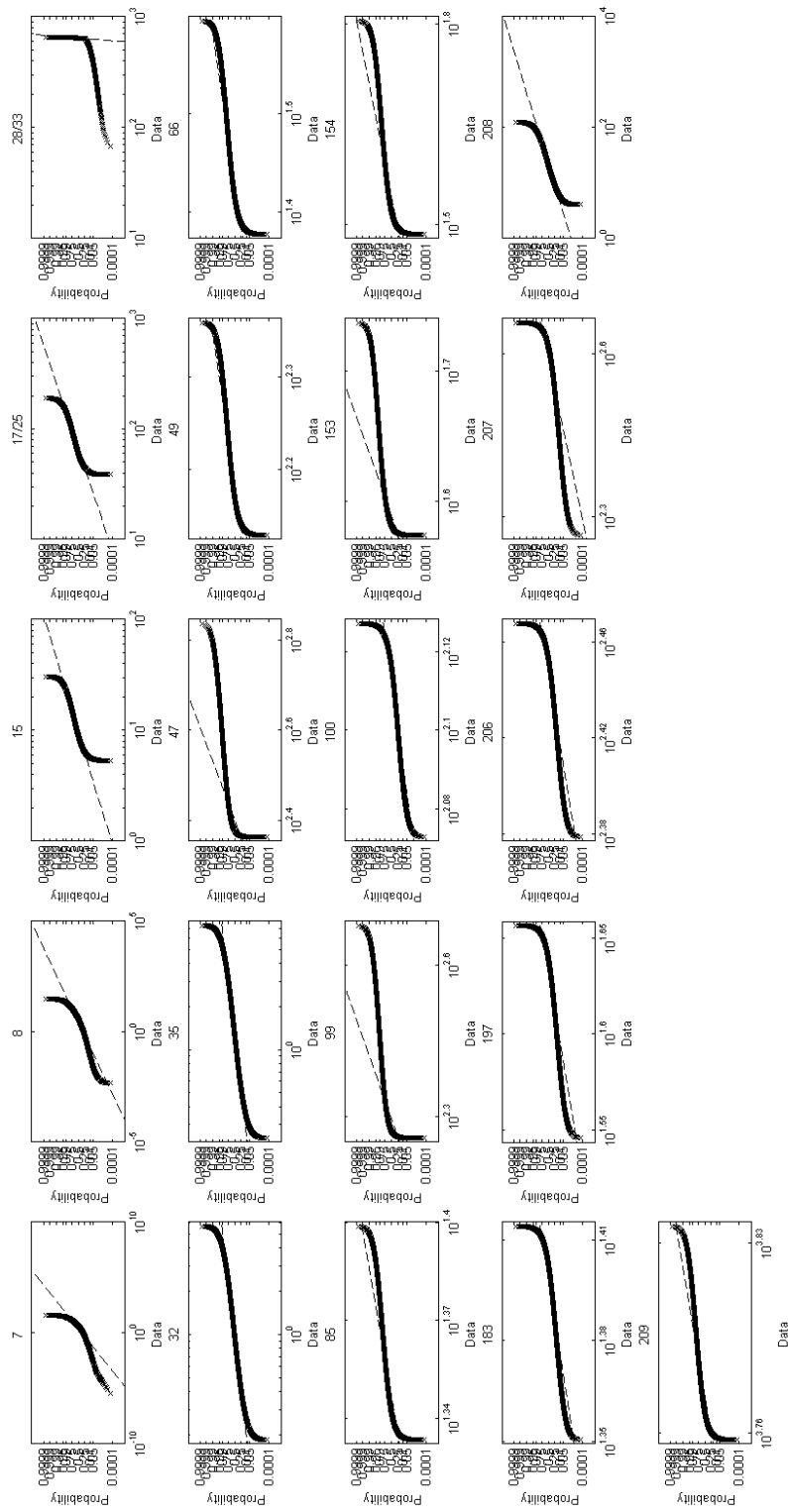


Figure G.12 Probability Graph for Lognormal Distribution of Uncertainty Analysis of Lake Michigan at 20-year

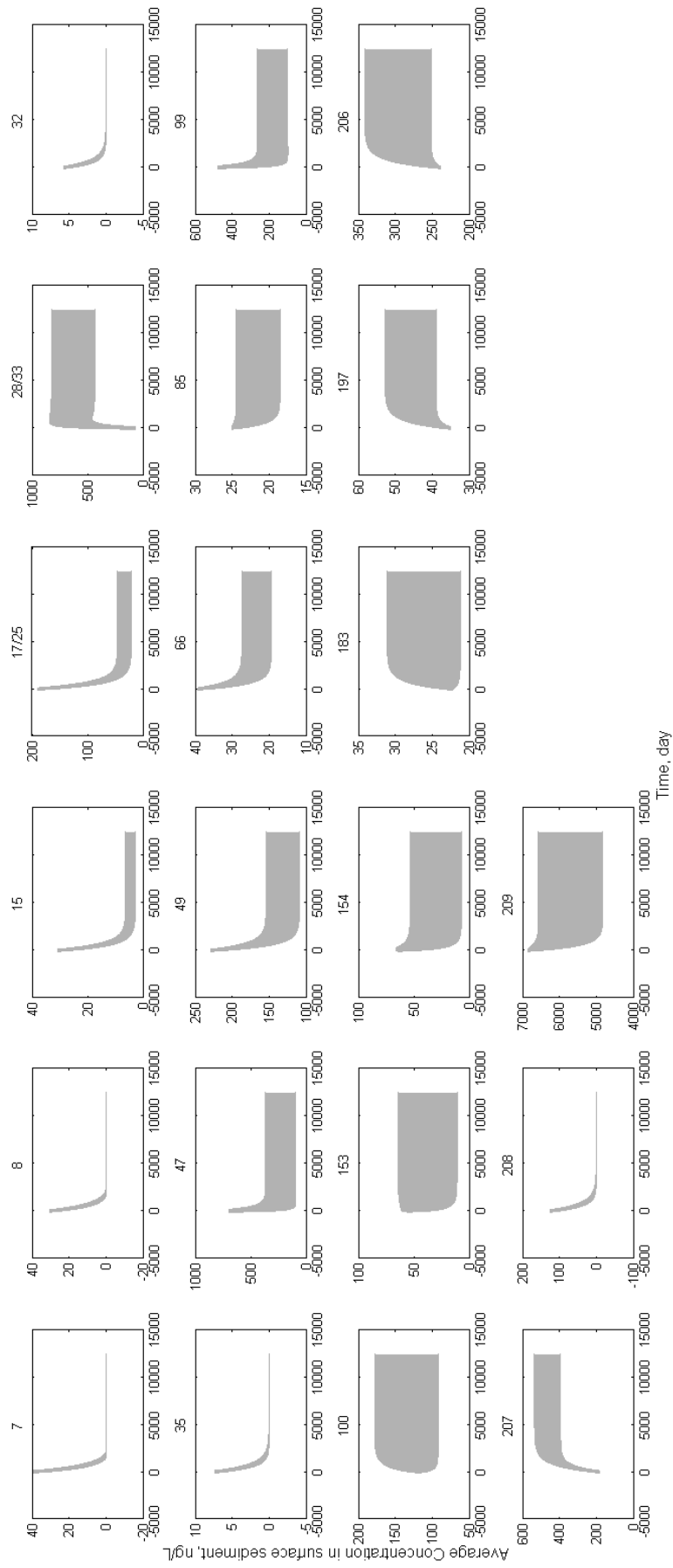


Figure G.13 Mean and Standard Deviation of Output Concentration of Each Congener for 1000 runs by MC Simulation

Table G.3  $k_m$  values for possible pathways used for the last scenario

Congener IUPAC No			Congener IUPAC No		
Mother	Daughter	$k_m$	Mother	Daughter	$k_m$
47	28/33	0.0072	<b>206</b>	<b>197</b>	<b>0.0010</b>
99	47	0.0035	<b>153</b>	<b>100</b>	<b>0.0160</b>
100	47	0.0010	<b>85</b>	<b>66</b>	<b>0.0020</b>
153	99	0.0241	<b>99</b>	<b>66</b>	<b>0.0020</b>
154	99	0.0180	<b>99</b>	<b>49</b>	<b>0.0020</b>
154	100	0.0080	<b>66</b>	<b>28/33</b>	<b>0.0070</b>
183	153	0.0026	<b>49</b>	<b>28/33</b>	<b>0.0070</b>
183	154	0.0173	<b>49</b>	<b>17/25</b>	<b>0.0070</b>
<b>209</b>	<b>208</b>	<b>0.0010</b>	<b>47</b>	<b>17/25</b>	<b>0.0070</b>
<b>209</b>	<b>207</b>	<b>0.0010</b>	<b>28/33</b>	<b>15</b>	<b>0.0070</b>
<b>209</b>	<b>206</b>	<b>0.0010</b>	<b>28/33</b>	<b>7</b>	<b>0.0070</b>

**Bold:** The pathways assumed for the last scenario



## CURRICULUM VITAE

### PERSONAL INFORMATION

Surname, Name: Karakaş, Filiz

Marital Status: Married

Email: [karakas\\_filiz@yahoo.com](mailto:karakas_filiz@yahoo.com)

Web: <https://tr.linkedin.com/in/filiz-karakas-37b51630>

Web: [https://www.researchgate.net/profile/Filiz\\_Karakas](https://www.researchgate.net/profile/Filiz_Karakas)

### EDUCATION

Degree	Institution	Year of Graduation
MSc	Middle East Technical University, Environmental Engineering	2010
BSc	Middle East Technical University, Environmental Engineering	2007

### WORK EXPERIENCE

Year	Place	Enrollment
2010- Present	Middle East Technical University, Environmental Engineering	Research Assistant
2013	Türkiye Teknoloji Geliştirme Vakfı (TTGV), Ankara	Expert Consultant
2008-2010	T&T Environment and Technologies, Ankara	Environmental Engineer
2005 Summer	CETSAN Ltd Co. Preparation of EIA Reports, Ankara	Intern Engineering Student
2004 Summer	ASKI – Ankara Water and Sewer Administration, Ankara	Intern Engineering Student
2003-2004	Marmara University Environmental Engineering, İstanbul	Student Assistant in General Chemistry Lab

## PUBLICATIONS

### Journal Papers

1. Karakas, F., Imamoglu, I. (2016). Estimation of biodegradation rate constants of PCB dechlorination reactions using an anaerobic dehalogenation model. *Journal of Hazardous Materials*. (Submitted).
2. Karakas F., Gedik K., Imamoglu I. (2016) PMF dynamics in fingerprinting: A comparative study of PMF2 and EPA-PMF3 for source apportionment of sediment PCBs. *Environmental Pollution*. (Submitted).
3. Kaya D., Karakas F., Sanin F.D., Imamoglu I. (2015). PCBs In Sludge: Development Of A Practical Extraction Procedure and Its Application In An Urban WWTP. *Water Environment Research*, 87(2), 145-151.
4. Karakas F., Gedik K., Imamoglu I. (2013) Apportionment of PCB sources near a transformer maintenance and repair facility in Ankara, Turkey. *Bulletin of Environmental Contamination and Toxicology*, 91(2), 141-147.
5. Gedik K., Demircioglu F., Imamoglu I. (2010) Spatial distribution and source apportionment of PCBs in sediments around İzmit industrial complexes, Turkey. *Chemosphere*, 81(8), 992-999.
6. Imamoglu I., Gedik K., Demircioglu F., Akduman N. (2009) Türkiye'nin poliklorlu bifeniller kaynaklı kirlilik durumuyla ilgili çalışmalar, *Cevre Bilim ve Teknoloji*, 3(2), 15-38.

### Conference Papers

1. Filiz Karakaş, Kadir Gedik, İpek İmamoğlu. Investigation of Polychlorinated Biphenyl Pollution In Lake Eymir By Using Positive Matrix Factorization Model. Environmental System Modeling Session: Environmental

Management, 10<sup>th</sup> Ulusal Çevre Mühendisliği Kongresi, 12-14 September 2013, Hacettepe University, Ankara, Turkey,377-381. (*in Turkish*)

2. Devrim Kaya, Filiz Karakaş, F.Dilek Sanin, Ipek Imamoglu. PCBs in Biosolids: Monitoring In a Large Urban WWTP Using a Newly Developed Practical Extraction Procedure. Session: Success Stories and Lessons Learned, 27th Annual Residuals and Biosolids Conference Highlights Emerging Opportunities for Sustainable Resource Recovery, 5-8 May 2013, Kentucky, Tennessee, USA.
3. Karakas F, Imamoglu I. An exploration of the use of PMF for the investigation of PCB sources and fate in the aquatic environment. Division of Environmental Chemistry, Receptor Modeling for Source Apportionment and Degradation Assessment of Organic Chemicals in the Aquatic Environment, ACS 242nd National Meeting, August 28 - September 1, 2011, Denver, Colorado, USA.
4. Demircioglu F, Gedik K, Imamoglu I. Investigation of the Fate of Polichlorinated Biphenyls Vicinity of Lake Eymir, VI. Türkiye’de Çevre Kirlenmesi Öncelikleri Sempozyumu (ÇEVKOS VI), 28-29 Mayıs 2009, Gebze Yüksek Teknoloji Enstitüsü, Kocaeli, Turkey s.76-80. (*in Turkish*)
5. Imamoglu I, Gedik K, Demircioglu F. Investigation of anaerobic dechlorination in PCB-contaminated sediments. Tenth International In Situ and On-Site Bioremediation Symposium, 5-8 May 2009, Baltimore, Maryland, USA.